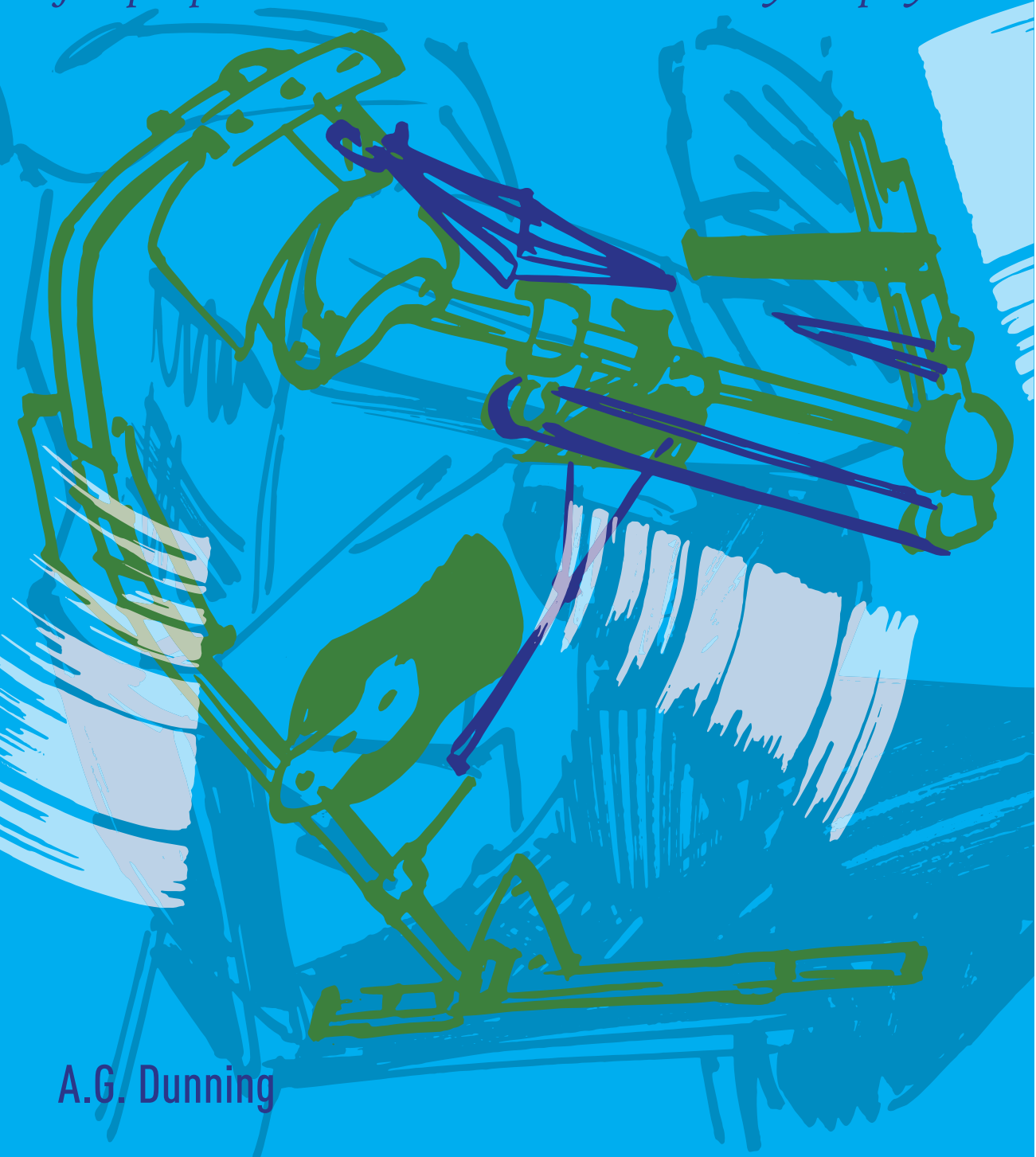


SLENDER SPRING SYSTEMS

for a close-to-body arm support

for people with Duchenne muscular dystrophy



A.G. Dunning

SLENDER SPRING SYSTEMS

FOR A CLOSE-TO-BODY DYNAMIC ARM SUPPORT
FOR PEOPLE WITH DUCHENNE MUSCULAR DYSTROPHY

SLENDER SPRING SYSTEMS

FOR A CLOSE-TO-BODY DYNAMIC ARM SUPPORT
FOR PEOPLE WITH DUCHENNE MUSCULAR DYSTROPHY

Proefschrift

ter verkrijging van de graad van doctor
aan de Technische Universiteit Delft,
op gezag van de Rector Magnificus prof. ir. K.C.A.M. Luyben,
voorzitter van het College voor Promoties,
in het openbaar te verdedigen op vrijdag 22 april 2016 om 12:30 uur

door

Alje Geert DUNNING

Master of Science in Mechanical Engineering
geboren te Noordoostpolder, Nederland.

This dissertation has been approved by the

promotor: prof. dr. ir. J.L. Herder

copromotor: dr. ir. D.H. Plettenburg

Composition of the doctoral committee:

Rector Magnificus

Prof. dr. ir. J.L. Herder

Dr. ir. D.H. Plettenburg

Prof. dr. ir. H.F.J.M. Koopman

chairman

Delft University of Technology

Delft University of Technology

University of Twente

Independent members:

Prof.dr. ir. R.H.M. Goossens

Prof.dr. ir. H. van der Kooij

Prof.dr. C.K. van der Sluis

Dr. ir. T. Rahman

Delft University of Technology

Delft University of Technology

University Medical Center Groningen

A.I. duPont Children's Hospital, Wilmington, USA



This research is supported by the Dutch Technology Foundation STW, which is part of the Netherlands Organisation for Scientific Research (NWO) and partly funded by the Ministry of Economic Affairs (project number 11832).

Printed by: Ipskamp Drukkers

Cover: R.J. Oosterhuis, graphic artist

ISBN 978-94-6186-611-0

Copyright © 2016 by A.G. Dunning

Author email: a.g.dunning@tudelft.nl; gerarddunning@gmail.com.

All rights reserved. No part of the material protected by this copyright notice may be reproduced or utilized in any form or by any other means, electronic or mechanical, including photocopying, recording, or by any other information storage and retrieval system, without the prior permission of the author.

CONTENTS

Summary	xi
Samenvatting	xiii
Flextension A-Gear project	xvii
I INTRODUCTION AND BACKGROUND	1
1 Introduction	3
1.1 Background	3
1.2 Present dynamic arm supports	4
1.3 Research goal	4
1.4 Outline of this thesis	4
References	6
2 Background	7
2.1 Duchenne Muscular Dystrophy	8
2.2 Most important activities of daily living	9
2.3 Arm kinematics	9
References	12
3 A review of assistive devices for arm balancing	15
3.1 Introduction	17
3.2 Method	18
3.2.1 Search method	18
3.2.2 Classification and comparison	18
3.3 Results	19
3.4 Discussion	23
3.5 Conclusions	24
References	25
II EXPLORING CONCEPTS	29
4 Conceptual design	31
4.1 Constraints and requirements	32
4.1.1 Intended use	32
4.1.2 Requirements	32

4.2	Functional decomposition	34
4.3	Concept overview	35
4.4	Evaluation	38
4.4.1	Transferring forces	38
4.4.2	Gravity balancing	39
4.5	Final choice	40
	References	40
5	Bending beams for upper arm balance	41
5.1	Introduction	43
5.2	Analysis	43
5.2.1	Constraints and requirements	43
5.2.2	Goal function	44
5.3	Conceptual Design	44
5.3.1	Beams as a method for storing energy	44
5.3.2	Final concept	45
5.3.3	Simulation	45
5.3.4	Influence of variables on energy in the beam	45
5.4	Experimental evaluation of the concept.	48
5.5	Prototype	50
5.5.1	Prototype	50
5.5.2	3D behavior	50
5.6	Discussion	50
5.7	Conclusions.	52
	References	53
6	Design of a compact actuated compliant elbow joint	55
6.1	Introduction	57
6.2	Method	57
6.2.1	Classifications	57
6.2.2	Properties of shape-changing materials	58
6.2.3	Benchmark calculations and performance indicators	58
6.2.4	Case study: a compact active compliant elbow joint	60
6.3	Results	60
6.3.1	Overview from literature	60
6.3.2	Simplified models of two promising configurations	61
6.3.3	Case study	64
6.4	Discussion	65
6.5	Conclusions.	67
	References	68
II-A	Close-to-body spring systems	73
7	Technical analysis of spring configurations	75
7.1	Introduction	77
7.2	Method	78
7.2.1	Assumptions and limitations.	78

7.2.2	Derivation of stiffness matrix	78
7.3	Application and behavior	84
7.3.1	Example 1	84
7.3.2	Behavior Example 1	87
7.3.3	Example 2	89
7.3.4	Behavior in example 2	90
7.4	Discussion	93
7.5	Conclusions.	94
	References	94
8	3-springs configuration	97
8.1	Introduction	99
8.2	Method	100
8.3	Results	104
8.4	Discussion	104
8.5	Conclusions.	108
	Appendix.	109
	References	109
9	Evaluation and comparison of 5 spring configurations	111
9.1	Introduction	113
9.2	Method	114
9.2.1	Spring configurations	114
9.2.2	Experimental evaluation.	114
9.2.3	Tuning rules	118
9.3	Results	119
9.3.1	Experimental evaluation of the spring configurations	119
9.3.2	Tuning rules	123
9.4	Discussion	125
9.5	Conclusions.	129
	References	130
III	DESIGN AND APPLICATION	133
10	A-Gear Passive version 1	135
10.1	Introduction	137
10.2	Method	137
10.2.1	Experimental setup	137
10.2.2	Procedures.	137
10.2.3	Outcome measures	138
10.3	Results	139
10.4	Discussion	139
10.5	Conclusions.	142
	References	142

11 A-Gear Passive version 2	145
11.1 Introduction	147
11.2 Method	147
11.2.1 Design method.	147
11.2.2 Characterization method	148
11.2.3 Pilot validation method	149
11.3 Results	151
11.3.1 Design results	151
11.3.2 Characterization results: balancing error	154
11.3.3 Results pilot validation.	156
11.4 Discussion	158
11.5 Conclusions.	160
Appendix.	161
References	163
12 A-Gear Passive version 3	165
12.1 Introduction	167
12.2 Method	168
12.2.1 Subdividing springs in 2D	168
12.2.2 Subdividing springs in 3D	168
12.2.3 Design around the human body	169
12.3 Results	172
12.3.1 2-parallel-spring configuration	172
12.3.2 3-spring configuration	173
12.4 Discussion	173
12.5 Conclusions.	176
References	176
IV DISCUSSION AND CONCLUSIONS	179
13 Discussion and conclusions	181
13.1 Discussion	182
13.2 Conclusions.	185
V APPENDIXES	187
A Characteristics of rubber bands	189
A.1 Introduction	189
A.2 Experimental setup	189
A.3 Evaluation	190
A.4 Results	190
A.5 Discussion and conclusions.	190
References	191

B Shoulder arc mechanism	195
B.1 Introduction	195
B.2 Varying the arc angles.	195
B.3 Conclusions.	198
References	198
Contribution to each article	199
Acknowledgements	201
Curriculum Vitæ	203
List of Publications	205
Propositions	208

SUMMARY

THE goal of this dissertation is to develop a wearable, passive, dynamic arm support that provides users with Duchenne muscular dystrophy (DMD) with support to perform activities of daily living. The arm support needs to be inconspicuous and not stigmatizing, to encourage the users to participate in social activities. Ideally, the device fits underneath clothing.

The first sub-goal is to review the state-of-the-art in dynamic arm supports in detail. At the date of publication of the review (June 2013), 23 dynamic passive and active arm supports were found, from which only 4 were wearable. Most of the devices that were found use a parallelogram linkage structure. This structure limits the range of motion of the arm and has a large volume. None of the devices were inconspicuous and fitted underneath clothing. The detailed review to these devices concludes that a serial linkage from the trunk to the arm is required to make the device inconspicuous and underneath clothing. This linkage should have the same degrees of freedom (DoF) as the human arm (3 DoF at the shoulder, 1 DoF at the elbow). In addition, the use of a passive support implies smaller actuators in case an active support is needed. The knowledge from the review is taken into account when defining concepts for a close-to-body arm support (second sub-goal).

The focus of the concept elaboration was on compliant structures and on a linkage system with rubber springs. The compliant structure concept was elaborated with two designs. One design uses bending beams as spring elements to support the upper arm. With only two very slender bending beams the upper arm was balanced in a single plane. A proof-of-principle prototype showed that the device gives enough support, is very slender (4 times smaller than current arm supports), and is comfortable. A second design and proof-of-principle prototype showed support of the forearm with a compliant joint consisting of 4 bi-stable leaf springs. The compliant elbow joint has self-aligning capabilities and can be worn underneath clothing. Nevertheless, the forearm is only supported, against gravity, in a single plane.

Next to the compliant structure concept, a linkage system with rubber springs is elaborated as a concept for a close-to-body arm support. The focus is on slender and close-to-body spring configurations. Analysis and re-definition of the theory of designing spring configurations resulted in the ability to create designs with multiple serial links. The main accomplishment of re-defining the theory is that the locations of the attachment points of the springs could be calculated very intuitive. Next to that, the behavior of the spring configuration for varying the parameters in the configuration (locations of the attachment points or the spring stiffness) becomes more understandable.

In the process, different spring configurations were designed. One spring configuration uses 2 bi-articular springs from the trunk to the forearm, parallel to the upper arm. Some locations of the attachment points of the springs can be chosen freely, others are related to these chosen locations. Another design balances the complete arm with

3 springs. In this configuration, each location of the spring attachment can be chosen freely and close to the body. The required balancing quality can be obtained by adjusting the spring stiffnesses. The balancing quality can be adjusted very easily to the preference of the user during the day. A comparison of the balancing quality and tuning capabilities of different spring configurations showed that the 3-springs configuration is excellent to apply in a close-to-body arm support. This is mainly due to its easiness of achieving and tuning the required balancing quality, and due to the opportunity to locate the spring attachments close to the body.

The third sub-goal was to apply the developed spring configurations into prototypes that could be evaluated on patients with DMD. The first prototype was based on a parallelogram structure, parallel to the body, running from the upper legs and hip to the forearm of the user. This prototype shows the advantage of trunk motion capability. The range of motion of the user increases by 10%, compared to the use of a currently available arm support that is attached to the wheelchair. For reaching anteriorly the increase in range of motion is even 50%. The surface electromyography (sEMG) activity is similar. This trunk motion capability was considered as very important by the patients. Therefore, it was included in all the future prototypes as well. Nevertheless, the prototype also showed that the parallelogram structure next to the arm limited the range of motion of the arm. This is because the DoF of the prototype were not similar as the DoF of the human arm. For this reason, in the second prototype this structure was redesigned such that it follows the body contours of the user. This resulted in a kinematic structure with 3 DoF at the shoulder joint and 1 DoF at the elbow joint. The structure was combined with a 2-springs configuration (based on an existing theoretical model). Rubber bands were used as spring elements. The prototype was evaluated with DMD patients and shows good results on comfort, balancing quality (less than 6% error with respect to the required balancing force) and range of motion. The user is able to perform most of the important activities of daily living again (e.g., eating, drinking, table-top activities, reaching the face, scratch the head, reaching for high objects). A downside of this device was that the spring configuration is not inconspicuous. Due to limitations of the spring configuration it is not possible to position the device closer to the body. Therefore, the third prototype is developed with the focus to position the spring configuration closer to the body. The 3-springs configuration was applied in the prototype. The rubber springs were split into hollow spring structures that fit around the body. In combination with covers on specific places to provide safety, extra structures for sideways stabilization and anatomically shaped body interfaces for more comfort, the third version of the prototype fits within 30mm from the body. This design allows for further optimization to bring the device even closer to the body. With this result, a wearable passive dynamic arm support is developed that supports the user during activities of daily living and is not stigmatizing.

SAMENVATTING

HET doel van dit onderzoek is de ontwikkeling van een draagbare, passieve, dynamische armondersteuning die gebruikers met Duchenne spierdystrofie ondersteunt tijdens alledaagse handelingen. De armondersteuning moet onopvallend en niet stigmatiserend zijn om participatie in sociale activiteiten te bevorderen. Idealiter past de armondersteuning onder de kleding.

Het eerste sub-doel is om een overzicht te genereren van de reeds bestaande dynamische armondersteuning en deze tot in detail te onderzoeken. Tot de datum van publicatie van dit overzicht (juni 2013), gaat dit om totaal 23 passieve en actieve armondersteuning. Slechts 4 van deze ondersteuning is draagbaar. Veel van de gevonden armondersteuning maken gebruik van een parallellogram stangenmechanisme. Deze structuur limiteert het bewegingsbereik van de arm en heeft een groot volume. Geen van de armondersteuning is onopvallend en past onder de kleding. Het gedailleerde onderzoek naar deze ondersteuning levert op dat een seriëel stangenmechanisme (zonder parallellogram) van de romp naar de arm nodig is om het apparaat onopvallend en onder de kleding te maken. Dit mechanisme moet dezelfde vrijheidsgraden hebben als de menselijke arm (3 vrijheidsgraden bij de schouder en 1 bij de elleboog). Daarnaast blijkt dat het gebruik van een passieve armondersteuning kleinere actuatoren impliceert wanneer een actieve armondersteuning nodig is. De bevindingen uit dit onderzoek zijn meegenomen in het ontwerpen van concepten voor een armondersteuning die dicht bij het lichaam past (tweede sub-doel).

De focus van de conceptuele ontwerpen lag bij comliante (flexibele) structuren en bij een stangenmechanisme met rubber veren. De comliante structuur is onderzocht en uitgewerkt aan de hand van twee ontwerpen. Het eerste ontwerp gebruikt buigende balkjes als elastische elementen om de bovenarm te ondersteunen. Met slechts twee zeer slanke buigende balkjes wordt de bovenarm gebalanceerd in een enkel vlak. Met een prototype is aangetoond dat het apparaat genoeg ondersteuning biedt, zeer slank is (4 keer kleiner dan huidige armondersteuning) en comfortabel draagt. Met een tweede ontwerp is de onderarm gebalanceerd met een compliant scharnier bestaande uit 4 bi-stabiele bladveren. Het comliante scharnier heeft zelf-uitlijnende mogelijkheden en kan onder de kleding gedragen worden. Echter wordt de onderarm, tegen de zwaartekracht in, gebalanceerd in een enkel vlak.

Naast de comliante structuur is het stangenmechanisme met rubber veren verder onderzocht. Dit als een concept om toe te passen in een armondersteuning die dicht bij het lichaam past (lichaamsgebonden). De focus ligt hierin op zeer slanke lichaamsgebonden veerconfiguraties. Analyse en herdefiniëring van de theorie voor het ontwerpen van dit soort veerconfiguraties maakt het nu mogelijk om ontwerpen te maken met meerdere seriële stangen. Het belangrijkste resultaat van deze herdefiniëring is allereerst dat de locaties van de aanhechtingspunten van de veren berekend kunnen worden op een zeer gebruikersvriendelijke manier. Daarnaast is het gedrag van de veerconfigu-

ratie voor variërende parameters (locaties van aanhechtingspunten of de veerstijfheid) inzichtelijker geworden.

In het proces zijn verschillende veerconfiguraties ontworpen. Een van de ontwerpen gebruikt 2 bi-articulaire veren van de romp naar de onderarm, evenwijdig aan de bovenarm. Bepaalde locaties voor de aanhechtingspunten van de veren zijn vrij te kiezen. De andere locaties zijn gerelateerd aan de gekozen locaties. Een ander ontwerp laat met 3 veren de volledige arm balanceren. In deze configuratie is elk aanhechtingspunt van de veren vrij en dichtbij het lichaam te kiezen. De gewenste balanceerkwaliteit wordt bereikt door de veerstijfheid van de veren aan te passen. Deze kan eenvoudig worden aangepast naar de wensen van de gebruiker naar gelang zijn activiteiten gedurende de dag. Verschillende veerconfiguraties zijn met elkaar vergeleken op de balanceerkwaliteit en aanpassingsmogelijkheden. Hiermee is aangetoond dat de 3-veren-configuratie uitstekend is toe te passen in een lichaamsgebonden armondersteuning. Dit voornamelijk vanwege het gemak om de gewenste balanceerkwaliteit te bereiken en aan te passen. Daarnaast vanwege de mogelijkheid om de aanhechtingspunten van de veren vrij en dichtbij het lichaam te kiezen.

Het derde sub-doel is om de ontwikkelde veerconfiguraties te vertalen naar prototypes, die testbaar zijn voor patiënten met Duchenne. Het eerste prototype is gebaseerd op een parallellogram structuur, evenwijdig aan het lichaam vanaf de bovenbenen en heup tot aan de onderarm van de gebruiker. Dit prototype toont het voordeel van de mogelijkheid om de romp vrij te kunnen bewegen. Het bewegingsbereik van de gebruiker neemt toe met 10% in vergelijking met het gebruik van een armondersteuning die vast zit aan de rolstoel. Voor reiken naar voren neemt het bewegingsbereik zelf toe met 50%. De activiteit van de spieren blijft hierbij gelijk. De mogelijkheid om de romp te kunnen bewegen wordt door de patiënten dusdanig belangrijk ervaren, dat deze mogelijkheid in alle opvolgende prototypes is ingebouwd. Echter toonde dit prototype ook dat de parallellogram structuur naast de arm het bewegingsbereik van de arm limiteerde. Dit komt omdat de vrijheidsgraden in het mechanisme niet overeen kwamen met de vrijheidsgraden in de menselijke arm. In het tweede prototype is deze structuur daarom opnieuw ontworpen, op een zodanige manier dat de contouren van het menselijk lichaam worden gevolgd. Dit heeft geresulteert in een kinematische structuur met 3 vrijheidsgraden bij de schouder en 1 vrijheidsgraad bij de elleboog, gecombineerd met een 2-veren-configuratie (gebaseerd op een reeds ontwikkeld theoretisch model). De veren hierin zijn uitgevoerd als rubber elastieken. Evaluatie van dit prototype met Duchenne patiënten levert goede resultaten op voor comfort, balanceerkwaliteit (minder dan 6% fout ten opzichte van de gewenste balanceerkracht), en bewegingsbereik. Het is voor de gebruiker weer mogelijk geworden om veel alledaagse handelingen uit te voeren, zoals bijvoorbeeld eten, drinken, handelingen boven het tafelblad, naar het gezicht reiken, op het hoofd krabben en naar hoge objecten reiken. Deze armondersteuning kent als nadeel dat vooral de veerconfiguratie niet onopvallend is. Door beperkingen in de veerconfiguratie is het echter niet mogelijk deze dichter op het lichaam te positioneren. Een derde prototype is ontwikkeld om de veerconfiguratie dichter op het lichaam te krijgen. Hiertoe is de 3-veren-configuratie toegepast in het prototype. De rubber veren zijn gesplitst en gevormd tot holle veerstructuren die om het lichaam gebogen worden. In combinatie met afdekking op specifieke plaatsen om veiligheid te garanderen, extra struc-

tuur voor zijdelingse stabiliteit en anatomisch gevormde lichaamsinterfaces voor meer comfort past het derde prototype binnen 30mm van het lichaam. Dit ontwerp biedt de mogelijkheid tot verdere optimalisatie, zodat de structuur nog dichter naar het lichaam kan worden gebracht. Met dit resultaat is een draagbare passieve arondersteuning ontwikkeld die alledaagse activiteiten ondersteunt en niet stigmatiserend is.

FLEXTENSION A-GEAR PROJECT

THE Flextension consortium was founded as an initiative of the Dutch Duchenne Parent Project in 2009. Flextension has the goal to improve the quality of life of people with Duchenne muscular dystrophy by developing assistive devices. The consortium is a collaboration between various expertise centers in the Netherlands, shown in the figure on the next page.

The first project is the A-Gear project. The goal of the A-Gear project is to develop an inconspicuous dynamic arm support that can support people with Duchenne muscular dystrophy with their activities of daily living. The strategy of the project is to develop a Passive A-Gear arm support, with a slender spring system and that is able to support the arm without the use of actuation, and an Active A-Gear, where actuators and a control strategy gives additional support to the user.

From each expertise center, a PhD candidate is working on the A-Gear project. At the Radboud university medical center, the PhD candidate will perform research on the clinical aspects of the project., which contains analysis of the arm movements, the progress of Duchenne muscular dystrophy in time, and the clinical evaluation of the developed arm supports. The PhD candidate from Delft University of Technology will focus on the mechanical design of the Passive A-Gear and the development of slender spring systems for a close-to-body arm support. This part of the project is the content of this dissertation. At the VU university medical center, the PhD candidate will work on the design of the Passive and Active A-Gear, with a special focus on the actuation of the Active A-Gear. The University of Twente is expert in bio-signaling and biomechanics. The PhD candidate will focus on the sensory interface and control strategies that are needed to control the Active A-Gear.

This project is funded by the Technology Foundation STW, project 11832. Special thanks goes to the sponsors of the project: United Parent Projects Muscular Dystrophy, Prinses Beatrix Spierfonds, Spieren voor Spieren, Johanna Kinderfonds, Kinderrevalidatie Fonds Adriaanstichting, Focal Meditech, OIM Orthopedie, Ambroise, Intespring.



The Flexension consortium is a collaboration between various expertise centers in the Netherlands: VU university medical center, University of Twente, Delft University of Technology, Radboud university medical center.

I

INTRODUCTION AND BACKGROUND

1

INTRODUCTION

1.1. BACKGROUND

THINK of how much you use your arms during the day. The arms are used for many tasks. For example with getting out of bed, dressing and washing yourself, brushing your teeth, going to the toilet, working on the computer or writing or scratching your head. During the day your arms are continuously active. Arm usage is very important to perform activities of daily living (ADL).

People with Duchenne Muscular Dystrophy (DMD) gradually lose the ability to use their arms. DMD is one of the most common types of muscular dystrophy in children and young adults. Its prevalence is 1 in every 3500-5000 male births [1, 2] and is caused by a mutation of the X-chromosome. The progressive disease affects the larger and most proximal muscles (upper leg and upper arm) first. At a later stage, the smaller and distal muscles (fingers) are also affected. From an age of 10 years old, patients need a wheelchair, because the leg muscles are deteriorated too much. When the arm muscles start to deteriorate, they become more dependent on their caregivers.

Next to that, people with DMD often develop psychosocial problems because they are restricted in their participation in social activities [3, 4]. The life expectancy also increases due to medical treatment, and is around 30 years old nowadays [5]. Among these reasons, the preservation of functional abilities becomes increasingly important.

The solution to overcome arm muscle weakness is to use a dynamic arm support. 'Dynamic' in this context is a field-specific term and means that the device supports the arm during movements. Such a device helps the user to lift their arm. It compensates for the gravity of the arm, so the user does not have to generate the muscle strength needed to lift their arm. With such a device, they become more independent, and can participate in social activities again. In order to encourage them to use an arm support, the device needs to support the arm in its natural and complete range of motion. At the same time, the device should be inconspicuous and able to be worn underneath clothing [6, 7]. This decreases the stigmatizing effect.

1.2. PRESENT DYNAMIC ARM SUPPORTS

THE current state of the art of dynamic arm support is insufficient in terms of functionality and aesthetics. Most devices are highly stigmatizing and not close to the body, nor do they support the complete natural range of motion of the arm. The main reason for these limitations is the serial (parallelogram) structure of the devices that does not move parallel to the arm of the user (in Chapter 3, a more elaborate discussion is performed). While a larger device is acceptable for training activities, a wearable device is desired in ADL. People are more eager to use an arm support in social activities when the device is inconspicuous. Next to that, for intuitive use and a decrease of interferences with the environment, it is important that the device is close to the body.

1.3. RESEARCH GOAL

As described before, people with DMD have a limited arm function and are restricted to participate in social activities. Together with an increasing life expectancy, it is very important to regain the arm function to be able to do ADL again.

The aim of this project is to develop a wearable, passive dynamic arm support that provides the user with support during ADL and is inconspicuous. In the ideal case, it fits underneath clothing. The support in the complete natural range of motion will prevent that contractures (a physical abnormality) are formed in the joints due to disuse of the arm. Furthermore, the increasing usage of the arm will decelerate the progress of the disease [8]. When the device is not stigmatizing and fits underneath clothing, the user is encouraged to participate in social activities.

The main goal is divided into three sub-goals. First, (1) a review of the state of the art in dynamic arm supports is performed, in order to see what the opportunities and limitations of current technologies are. After that, the knowledge about the current arm supports and the requirements and wishes from people with DMD is taken into account to (2) define concepts for a close-to-body arm support, with the focus on slender spring systems that could be located close to the body. Different concepts for slender spring systems are elaborated and (3) build into prototypes, which are evaluated on people with DMD.

1.4. OUTLINE OF THIS THESIS

PART I continues with Chapter 2, in which background information is given about the physiology and progress of DMD, and about the most important ADL and arm kinematics of people with DMD. A review of the current state-of-the-art in dynamic arm supports is presented in Chapter 3. This chapter presents the limitations and opportunities of existing arm supports.

The boundary conditions, requirements and different concepts for a new type of close-to-body and inconspicuous arm support are explained in Part II. In Chapter 4, the constraints and requirements for the device, and a concept evaluation is presented. In the next chapters, several concepts for close-to-body solutions are elaborated in detail and applied in proof-of-principle prototypes. Chapter 5 shows a principle where the upper arm is balanced with very slender bending beams. In Chapter 6, a compliant elbow joint is designed that is actuated with shape-memory-alloy wires. This part ends with a

sub-part about close-to-body spring configurations based on normal springs (Sup-part II-A). In Chapter 7, the technical analysis to design a spring configuration to balance the arm is described, together with a proposed design for close-to-body spring configuration based on 2 springs parallel to the upper arm. Another close-to-body spring configuration based on 3 springs is proposed in Chapter 8. The different spring configurations are compared and evaluated in Chapter 9, in order to find a suitable solution for a spring configuration to apply in a close-to-body arm support.

Part III presents the prototypes that were developed based on the spring systems described in Part II-A. Chapter 10 shows the design and evaluation of an arm support that has unrestricted trunk motion to increase the range of motion of the user. It also shows the limitations of the current widely used parallelogram structure. In Chapter 11, the design is evolved into a new type of arm support with a more natural range of motion. Chapter 12 presents the final design of the close-to-body and inconspicuous arm support.

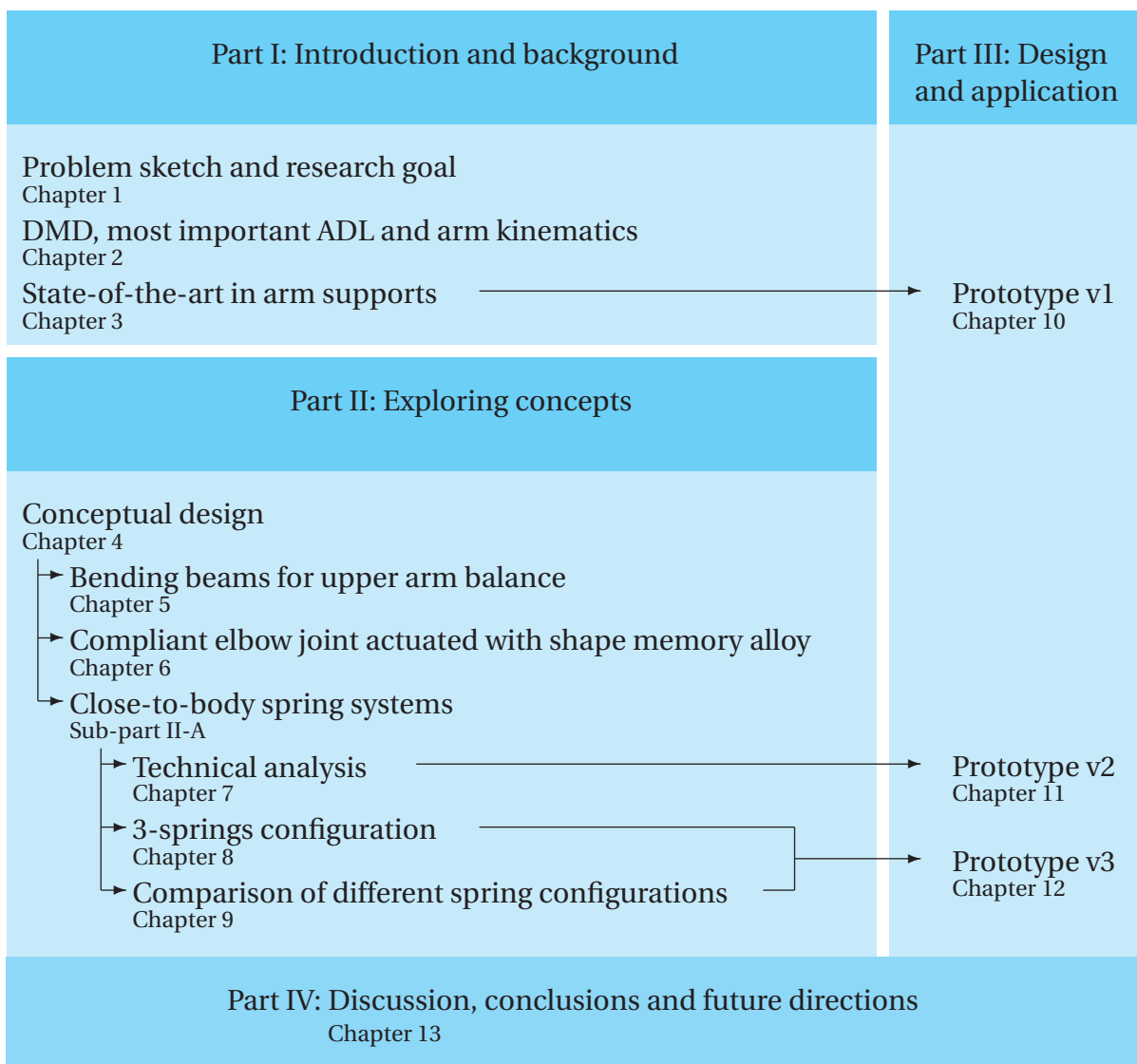


Figure 1.1: Visual outline of this thesis

REFERENCES

- [1] A. E. H. Emery, *Population frequencies of inherited neuromuscular diseases - a world survey*, Neuromuscular Disorders **I**, 19 (1991).
- [2] J. R. Mendell, C. Shilling, N. D. Leslie, K. M. Flanigan, R. Al-Dahhak, J. Gastier-Foster, K. Kneile, D. M. Dunn, B. Duval, A. Aoyagi, C. Hamil, M. Mahmoud, K. Roush, L. Bird, C. Rankin, H. Lilly, N. Street, R. Chandrasekar, and R. B. Weiss, *Evidence-based path to newborn screening for Duchenne muscular dystrophy*. Annals of neurology **71**, 304 (2012).
- [3] J. Rahbek, B. Werge, A. Madsen, J. Marquardt, B. Steffensen, and J. Jeppesen, *Adult life with Duchenne muscular dystrophy : Observations among an emerging and unforeseen patient population*, Pediatric Rehabilitation **8**, 17 (2005).
- [4] M. A. Grootenhuys, J. de Boone, and A. J. van der Kooi, *Living with muscular dystrophy: health related quality of life consequences for children and adults*, Health and quality of life outcomes **5**, 31 (2007).
- [5] M. Kohler, C. F. Clarenbach, C. Bahler, T. Brack, E. W. Russi, and K. E. Bloch, *Disability and survival in Duchenne muscular dystrophy*, Journal of Neurology, Neurosurgery & Psychiatry **80**, 320 (2009).
- [6] T. Rahman, W. Sample, R. Seliktar, M. Alexander, and M. Scavina, *A body-powered functional upper limb orthosis*, Journal of rehabilitation research and development **37**, 675 (2000).
- [7] A. Kumar and M. E. Phillips, *Use of powered mobile arm supports by people with neuromuscular conditions*. Journal of rehabilitation research and development **50**, 61 (2013).
- [8] M. Jansen, I. J. de Groot, N. van Alfen, and A. C. Geurts, *Physical training in boys with Duchenne Muscular Dystrophy: the protocol of the No Use is Disuse study*. BMC pediatrics **10**, 55 (2010).

2

BACKGROUND

This chapter provides background information on the physiology of Duchenne Muscular Dystrophy (DMD), the most important activities of daily living for DMD patients and the arm kinematics is given. In Section 2.1, the cause and progress of DMD is explained, next to the limitations DMD patients have. In Section 2.2, a list of 15 most important activities of daily living is given, which is based on a questionnaire among more than 200 patients worldwide. Section 2.3 explains how the arm can be simplified and modelled, and which reference frame is used to express the orientation of the arm. Next to that, the range of motion of the arm for different movements is shown.

2.1. DUCHENNE MUSCULAR DYSTROPHY

DUCHENNE Muscular Dystrophy (DMD) is a genetic disorder of the muscles. Due to an affected gene the dystrophin protein is missing. Due to the lack of this protein the muscles are fragile and muscle tissue slowly degenerates and is transformed into fat and scar tissue. The affected gene is located on the X-chromosome. This is the reason that mainly boys are affected by DMD. Girls have another X-chromosome, so they can compensate. The incidence of DMD is 1 in 3500-5000 male live births [1, 2].

DMD is a progressive disease (Fi. 2.1) that affects the largest and proximal muscles first. It starts with the large upper leg and upper arm muscles. In a later stage, the smaller and more distal muscles (e.g., fingers) are affected too. It is diagnosed at an age of 3-5 years old. Young children start to walk late, and fall often. At around 10 years old the children become wheelchair bound [3]. Walking is too difficult and too fatiguing. From this age they also have increased difficulty to use their arms. An extensive overview of limitations in activities is described in [4]. About an age of 20 years old, lifting the arm is impossible. From that age, the finger muscles and eventually also the heart muscle will not function well anymore. With the current medical treatment the life expectancy of DMD patients is about 30 years old [3].

Next to a limited arm functionality, they also experience increasing pain in their upper extremities [4]. Participation in social activities is also restricted when the disease progresses. Patients often have difficulties in performing work, playing sports or a hobby, or having a romantic relationship. This can be a huge problem and eventually result in social isolation [5].

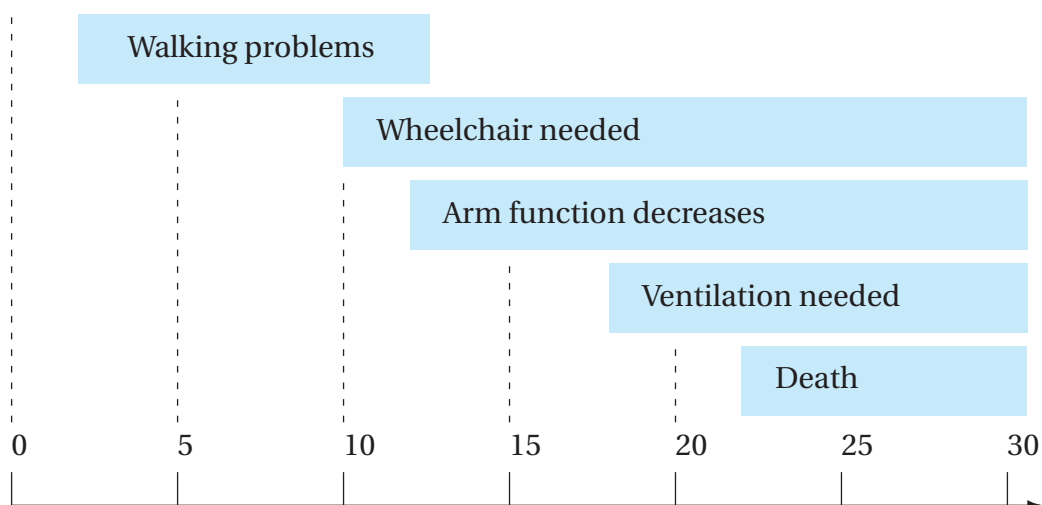


Figure 2.1: Timeline of the general progression of DMD in years, reproduced from [6].

2.2. MOST IMPORTANT ACTIVITIES OF DAILY LIVING

IN [4], 213 DMD patients were asked what for them the most important activities of daily living (ADL) are. A list of 15 activities is determined from what the say is important for them and which activities they experience the most limitations:

1. Eat
2. Drink
3. Use keyboard/mouse of computer
4. Use game controller
5. Open a packaging
6. Get dressed
7. Managing wheelchair
8. Wash body/face
9. Go to the toilet
10. Write
11. Read books
12. Lift heavy objects
13. Scratch head
14. Hug somebody
15. Reach for high objects

2.3. ARM KINEMATICS

THE human arm can make complex movements. The shoulder joint has 3 degrees of freedom (DoF). The upper arm can be moved for abduction/adduction, shoulder flexion/extension and lateral/medial shoulder rotation. The elbow joint has 1 DoF, for elbow flexion/extension. The lower arm has 1 extra DoF to rotate the wrist, pronation/supination. In total the human arm has 5 DoF. For this project pronation/supination in the lower arm is not considered into the design of the arm support, since this degrees of freedom is not affected by gravity and can also be considered as a degree of freedom of the wrist. Therefore only 4 DoF are taken into account.

The human arm can be simplified to a 2-link system, with a ball joint with 3 DoF at the shoulder, and a revolute joint (1DoF) at the elbow. The determination of the configuration of the human arm is sometimes difficult, because the angles for abduction/adduction and shoulder flexion/extension are hard to distinguish. Basically, those are the same movements, but in another plane. Therefore another reference frame is proposed in [7]. This reference frame describes the arm configuration in four angles: (1) the orientation of elevation plane (angle between the vertical plane through the upper arm and the frontal plane), (2) the elevation angle (angle between the upper arm and vertical axis through the shoulder), (3) the orientation of flexion plane (corresponding with shoulder rotation) and (4) the flexion angle (corresponding with elbow flexion/extension) (Fig. 2.2). In this dissertation this reference frame is used to express the configuration of the arm. In Fig. 2.3 the range of motion of the arm is shown for each angle in the reference frame [8–14]. The minimal angles that are needed to perform the most important ADL, the average angle that healthy subjects can perform and the passive angle that healthy subjects can reach with the help of an external guide are shown.

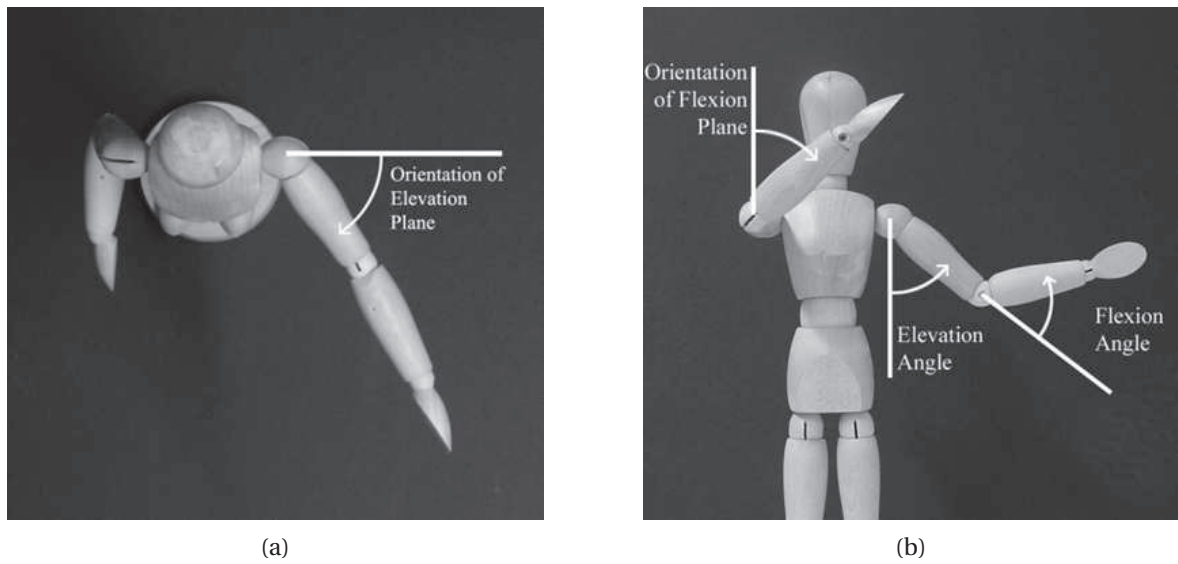


Figure 2.2: Reference frame of arm planes as used in this dissertation, extracted from [7] (with permission).

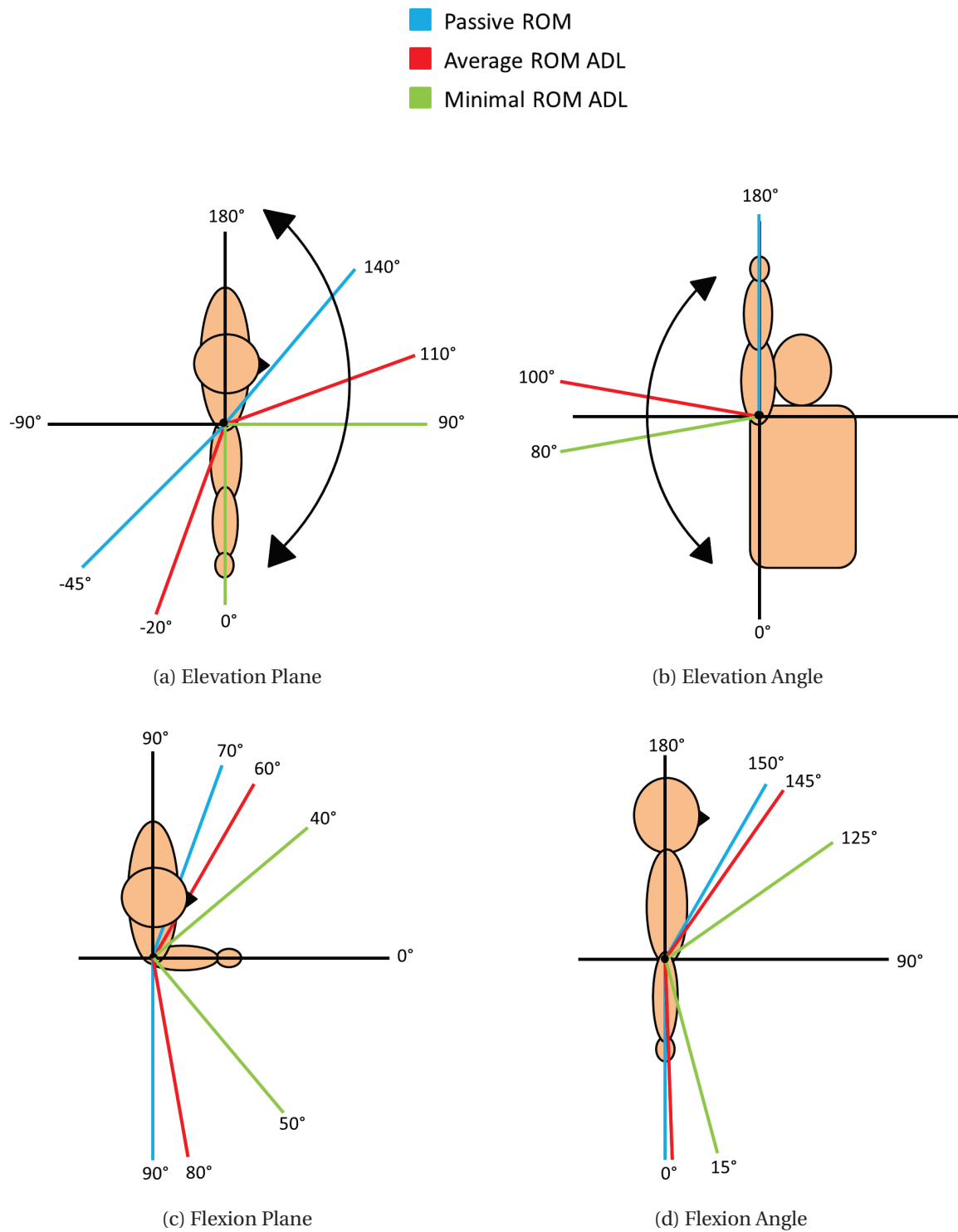


Figure 2.3: The minimal, average and passive range of motion of the arm of healthy subjects [8–14].

REFERENCES

- [1] A. E. H. Emery, *Population frequencies of inherited neuromuscular diseases - a world survey*, Neuromuscular Disorders **I**, 19 (1991).
- [2] J. R. Mendell, C. Shilling, N. D. Leslie, K. M. Flanigan, R. Al-Dahhak, J. Gastier-Foster, K. Kneile, D. M. Dunn, B. Duval, A. Aoyagi, C. Hamil, M. Mahmoud, K. Roush, L. Bird, C. Rankin, H. Lilly, N. Street, R. Chandrasekar, and R. B. Weiss, *Evidence-based path to newborn screening for Duchenne muscular dystrophy*. Annals of neurology **71**, 304 (2012).
- [3] M. Kohler, C. F. Clarenbach, C. Bahler, T. Brack, E. W. Russi, and K. E. Bloch, *Disability and survival in Duchenne muscular dystrophy*, Journal of Neurology, Neurosurgery & Psychiatry **80**, 320 (2009).
- [4] M. M. H. P. Janssen, A. Bergsma, A. C. H. Geurts, and I. J. M. de Groot, *Patterns of decline in upper limb function of boys and men with DMD: an international survey*, Journal of neurology **261**, 1269 (2014).
- [5] K. Bushby, R. Finkel, D. J. Birnkrant, L. E. Case, P. R. Clemens, L. Cripe, A. Kaul, K. Kinnett, C. McDonald, S. Pandya, J. Poysky, F. Shapiro, J. Tomezsko, and C. Constantin, *Diagnosis and management of Duchenne muscular dystrophy, part 2: implementation of multidisciplinary care*. Lancet neurology **9**, 177 (2010).
- [6] DMD Physiology, [https://kin450-neurophysiology.wikispaces.com/Duchenne+ Muscular+Dystrophy](https://kin450-neurophysiology.wikispaces.com/Duchenne+Muscular+Dystrophy), (2015).
- [7] L. F. Cardoso, S. Tomazio, and J. L. Herder, *Conceptual design of a passive arm orthosis*, ASME International Design Engineering Technical Conferences **5**, 747 (2002).
- [8] J. Aizawa, T. Masuda, T. Koyama, K. Nakamaru, K. Isozaki, A. Okawa, and S. Morita, *Three-dimensional motion of the upper extremity joints during various activities of daily living*. Journal of biomechanics **43**, 2915 (2010).
- [9] D. P. Romilly, C. Anglin, R. G. Gosine, C. Hershler, and S. U. Raschke, *A Functional Task Analysis and Motion Simulation for the Development of a Powered Upper-Limb Orthosis*, IEEE Transactions on Rehabilitation Engineering **2**, 119 (1994).
- [10] C. J. van Andel, N. Wolterbeek, C. A. M. Doorenbosch, D. H. E. J. Veeger, and J. Harlaar, *Complete 3D kinematics of upper extremity functional tasks*, Gait & posture **27**, 120 (2008).
- [11] J. Rosen, J. Perry, N. Manning, S. Burns, and B. Hannaford, *The human arm kinematics and dynamics during daily activities - toward a 7 DOF upper limb powered exoskeleton*, International Conference on Advanced Robotics , 532 (2005).
- [12] R. Safaee-Rad, E. Shwedyk, and A. O. Quanbury, *Three-dimensional measurement system for functional arm motion study*, Medical and Biological Engineering and Computing **28**, 569 (1990).

-
- [13] D. J. Magermans, E. K. J. Chadwick, H. E. J. Veeger, and F. C. T. van der Helm, *Requirements for upper extremity motions during activities of daily living*. *Clinical biomechanics* **20**, 591 (2005).
- [14] P. Raiss, O. Rettig, S. Wolf, M. Loew, and P. Kasten, *Range of motion of shoulder and elbow in activities of daily life in 3D motion analysis*, *Zeitschrift für Orthopädie und Unfallchirurgie* **145**, 493 (2007).

3

A REVIEW OF ASSISTIVE DEVICES FOR ARM BALANCING

Orinally appeared as:
A.G. Dunning, J.L. Herder,
A review of assistive devices for arm balancing,
IEEE International Conference on Rehabilitation Robotics, 6650485 (2013),
DOI:10.1109/ICORR.2013.6650485

As stated in the previous chapters, current arm supports are large and stigmatizing. In this chapter a review of the state-of-the-art of arm supports is presented. This review looks at the structure, balancing method, alignment with the body of the user, volume and range of motion of each device. This is done to gain more insight into the requirements and possibilities for a close-to-body arm support.

For consistent use of terminology, the word 'orthosis' (used in the original paper to refer to arm supports) is replaced here by 'arm support'.

ABSTRACT

DUE to neuromuscular disorders (e.g., Duchenne Muscular Dystrophy) people often lose muscle strength and become wheelchair bound. It is important to use muscles as much as possible. To allow this, and to increase independency of patients, an arm support can be used to perform activities of daily life. The arm support compensates for the gravity force of the arm, allowing people to perform movements with smaller muscle forces. This paper presents the state-of-the-art in passive and wearable active arm supports, and investigates how to proceed towards a suitable structure for a wearable passive arm support, that is able to balance the arm within its natural range of motion and is inconspicuous; in the ideal case it fits underneath the clothes. Existing devices were investigated with respect to the body interface, the volume, and the workspace. According to these evaluation metrics it is investigated to what extent the devices are wearable and inconspicuous. Furthermore, the balancing principle of the devices, the architecture, force transmission through the devices, and alignment with the body joints are investigated. It appears that there is only one wearable passive arm support presented in literature. This device can perform throughout the natural workspace of the arm, but is still too bulky to be inconspicuous. The other passive arm supports were conspicuous and mounted to the wheelchair. Except one, the wearable active arm supports were all conspicuous and heavy due to a large backpack to enclose the actuators. They also could not achieve the entire natural workspace of the human arm. A future design of an inconspicuous, wearable, passive arm support should stay close to the body, be comfortable to wear, and supports pronation and supination.

3.1. INTRODUCTION

PEOPLE with neuromuscular disorders often rely on assistive devices to perform Activities of Daily Living (ADL). Neuromuscular disorders (e.g., muscular dystrophy, spinal cord injuries or stroke) affect the muscles of the patient. The muscles deteriorate, contractures are formed due to the disuse of the arm, and eventually results in losing arm function.

One of the most common muscular dystrophies is Duchenne Muscular Dystrophy (DMD). DMD is caused by a mutation on the X-chromosome and has a prevalence of 1 for every 3500 male births [1]. DMD is characterized by progressive degeneration of the muscles. It starts with the most proximal muscles (e.g., upper legs, upper arms, shoulders), and proceeds to the more distal muscles of the human body (e.g., wrist, fingers). The disease affects the upper legs of the patient before they are 10 years old, and they will become confined to a wheelchair. When the upper arm muscles deteriorate, boys with DMD experience significant lack of muscle strength and can no longer perform ADL. Consequently, they become highly dependent on their caregivers. In addition, most people with DMD will develop severe psychological problems, due to restricted participation in society [2, 3].

To compensate for the muscle weakness and the impossibility of executing ADL, and to be able to participate in society, boys with DMD often depend on assistive devices. For example, a wheelchair is used to compensate for the loss of leg function. For the arm function, an arm support can be used to augment the muscle strength, to lift their arm again, and consequently become more independent. These devices should fulfill many requirements to encourage use in daily life and improve the quality of life. These requirements include aspects of comfort, easy donning and doffing, force transmission to the body, adjustable to the body, functionality, etc. Another important requirement is the aesthetics. One of the key assumptions for the project 'Flexextension', and also stated in [4], is that the users prefer an inconspicuous device that gives a natural support.

Much research on arm supports has been conducted in recent years. These devices can be categorized into three groups [5]: 1) robotic manipulators, 2) powered (active) arm supports and 3) non-powered (passive) arm supports. In the first group, several devices are developed and commercialized, including Jaco [6] and iARM [7]. These devices are intended for patients without any arm function. All these devices are heavy and very conspicuous, mounted to the wheelchair and act like an extra arm instead of supporting the arm of the user. While a larger device is acceptable for training activities, a wearable device is preferred for assistance in ADL [8].

A quick scan of previous research that presented the state-of-the-art for active [9] and passive assistive devices [10] showed that wearable passive arm supports are rare. In addition, only a few active supports are wearable, but these remain conspicuous.

To investigate the assumption that a critical design requirement of an arm support is inconspicuous, this study proceeds towards a suitable structure for a wearable passive arm support that is able to balance the arm within its natural range of motion and is inconspicuous; in the ideal case it fits underneath clothes. To achieve this goal, this study presents and discusses a review of the state-of-the-art in passive and wearable active upper limb assistive devices, to investigate the inconspicuousness and wearability of the devices. Therefore, it is proposed to look into three evaluation metrics: 1) the interface

points with the body, 2) the volume, and 3) the workspace of the devices. Additionally, this paper investigates the possibilities of combining the critical features of both passive and active arm supports into a wearable, inconspicuous passive support to improve the design of future arm supports.

3.2. METHOD

3.2.1. SEARCH METHOD

THIS study is separated into two parts. First, the state-of-the-art of passive arm supports is investigated. For this part, both wearable and non-wearable passive supports were considered. In this study, a passive arm support is defined as a device that can balance the arm fully passive for a certain range of motion. The balancing principle is decisive, meaning that even if the balancing force can be adjusted actively, it is still considered as a passive arm support.

Second, the active arm supports are investigated. After a quick scan of all the available active supports it was decided to choose for the wearable arm supports only. In this study, an active arm support is defined as a device that does not balance the arm, but dictates the movements of the arm using actuators. In this study, the arm is considered to be from the shoulder to the forearm, neglecting the wrist and the fingers.

After analyzing the topic and considering the constraints of this study, a search strategy was defined. Key subjects were determined and for each key subject a set of related keywords, including synonyms and related terms, were defined. The sets of keywords were used as search terms in the search engines Scopus [11] and Espacenet [12]. With Scopus, journal articles and conference proceedings were searched, while Espacenet was used to search for patents. In total six sets of keywords were used to define the key subjects: 1) arm support, 2) wearable, 3) structure, 4) static balancing, 5) adjusting force, and 6) actuation/control. An overview of the sets of keywords is shown in Table 3.1. To optimize and narrow the search results, different combinations of keywords were made. Cross-referencing is also an important step to find relevant articles. After an extensive search, the articles were assessed by reading the title and the figures, and if the article seemed relevant, the abstract was read.

3.2.2. CLASSIFICATION AND COMPARISON

It is important to define some constraints to formulate the design problem. To recapitulate, the goal is to proceed towards a suitable structure for a wearable, inconspicuous passive support that can balance the arm within the natural workspace and fits underneath clothing. For this study, it is stated that the device must fit within 20 mm from the body, to be inconspicuous and fits underneath clothing. Three evaluation metrics were proposed to investigate the inconspicuousness and wearability of existing devices.

The first evaluation metric is the body interface. For each arm support found in literature, it is determined which body part the device is attached to and to what extent the device is wearable.

The second evaluation metric quantifies the devices' volume to give insight on how inconspicuous the devices are. For each arm support, the volume within 20 mm from the skin around the whole arm, including the trunk, was calculated and compared with

Sets	Keywords
1. Arm support	Robot arm Orthosis, exoskeleton, assistive device, arm support Arm weakness, muscle weakness
2. Wearable	Wearable, portable, mobile Body-fitting, suit, harness
3. Structure	Human arm, bionic, upper extremity, upper limb
4. Static balancing	Static balancing, neutral equilibrium, zero stiffness, gravity compensation
5. Adjusting force	Manipulator Adjustable, variable force Control force
6. Actuation / control	Therapy assistant Rehabilitation Actuator, control

Table 3.1: Overview of the sets of keywords used in Scopus and Espacenet.

the available volume around the arm and trunk. Excess volume that does not fit within 20 mm from the skin was also calculated. The volume of each device was calculated in the position that the arm is lying on the arm rest (90 degrees flexion of the elbow). Note that all values that could not be identified in literature were estimated from figures and movies, based on anthropometric values [13].

Finally, the workspace is the third evaluation metric. The workspace is defined as the volume of space where the end-effector of the arm support can reach, measured along the horizontal x and y -axis, and the vertical z -axis (Fig. 3.3). This workspace was estimated or calculated and compared with the workspace of the center of gravity of the whole arm of a healthy child between 12-14 years, extracted from the DINED anthropometry database [13].

Furthermore, this study investigated the structure of the device, the architecture (serial or parallel), the balancing principle for passive devices, force transmission through the device, and the alignment with the body joints. It also investigated which degrees of freedom (DoF) are supported by the device. This could be 3 DoF in the shoulder (abduction/ adduction, flexion/extension, and rotation), and 2 DoF in the elbow (flexion/extension, and pronation/supination).

3.3. RESULTS

IN total, twelve passive arm supports and eleven wearable active devices were found in literature that are considered relevant. These devices were designed for assisting daily

life, but also for rehabilitation purposes. Below, a short description of the general findings of passive and active supports is given. After that, the results for the three evaluation metrics are shown.

Only one passive device is wearable [10]. The others are mounted to the wheelchair [14–17], [18–24]. Two points on the wheelchair are used to attach the device. One is behind the backseat of the wheelchair [14, 17, 19, 20, 22, 23] and the other is at the side [15, 16, 18, 24], where it replaces the armrest of the wheelchair.

All passive arm supports have a serial architecture, meaning that the base (i.e., wheelchair or trunk) is connected only to the forearm by a single chain of links. Most of them allow all of the defined degrees of freedom of the arm, except support of pronation and supination. This is only possible by movements of the bone with respect to the skin inside the support cup.

The arm is balanced with spring mechanisms. The spring mechanisms are constructed in combination with the arm to form an energy free system [25]. Several springs are used in the different mechanisms, varying from conventional helical springs [14, 16, 19, 21], constant torque springs [22], to rubber bands [10, 18, 20].

Some other noticeable features for passive arm supports were found in literature. Some devices only lift 75% of the weight of the arm, while 25% of the arm weight is supported by the shoulder [16, 23]. In some devices the upper arm and forearm were balanced independently [10, 17], offering an optimized balancing quality for different positions of the arm. It is also seen that some devices use a minimal construction at the elbow and forearm, to prevent interference with the table or other objects where the arm can rest [17].

The passive arm support with the largest volume within, and the smallest volume violating the prescribed available volume is the Wilmington Robotic Exoskeleton (WREX) [10]. Also, it is the only device that can be worn with a back brace. The structure is attached to the trunk and follows the arm closely along the shoulder to the forearm. With rubber bands the upper arm and forearm can be balanced independently.

Wearable active devices have the same kinematic architecture. They all run parallel to the arm from the trunk, via the shoulder to the forearm. Some devices use a mechanism to prevent misalignments with the body joints. For example, the use of a 3RRR spherical parallel shoulder mechanism [26], or a special 3-link shoulder mechanism allowing scapula motion [27]. In [28], a compliant soft-orthotic device is used to prevent misalignments.

In active arm supports, the actuators are locally at the joints [27], or stored in backpacks of large volume [29–32]. The forces from the actuators are transmitted to the joints with cables [28, 30, 32–34]. Since cables can only transfer tension forces, a combination of cables around the arm is used. In some devices pneumatic artificial muscles are used as actuators [29, 32, 34]. These are compliant and light-weight actuators, which can act and be placed in the same way as human muscles. The forces from the body are transferred to the structure through rigid links in the device.

In Fig. 3.1, a representation of the interface points of the arm support with the body or wheelchair is shown. In Fig. 3.1a, it is shown that all supports, except one, are mounted to the wheelchair. These devices are not wearable. They are all connected with the body at the forearm. Some devices have an extra cup to the elbow to prevent the

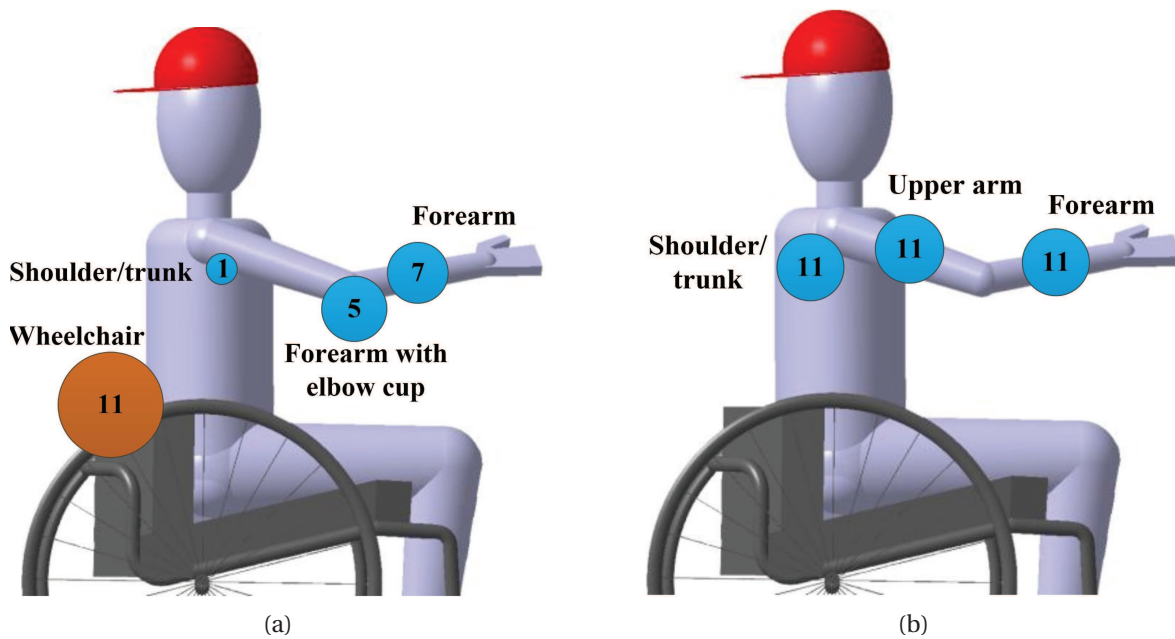


Figure 3.1: Representation of the interface points on the body or wheelchair for (a) passive and (b) active arm supports.

arm from falling out of the support cup during particular movements [15, 17–20, 22]. In Fig. 3.1b, the interface points of the wearable active support are shown. All devices are parallel to the arm, connected to the trunk, upper arm and forearm. In contrast to the only wearable passive device, which has a serial structure along the arm.

Fig. 3.2 shows the calculated volumes of the devices. The available volume within 20 mm from the body is approximately 0.01 m³. All passive arm supports use a small amount of volume within 20 mm from the body, but violate the prescribed available volume with a large amount of volume. The WREX scores the best on this metric. It exploits a lot of volume close to the body, and only a small amount is violating this available volume. Most active devices use a large amount of volume close to the body. However, compared to the passive supports, some devices violate the available volume with a relatively large amount of volume. This is mainly due to local actuators or a large structure on the back, where all the actuators are situated. Only in [28] a device is shown that stays close to the body. It should be mentioned that this device only supports shoulder abduction/adduction. If more DoF would be supported, the device needs more cables, which would increase the overall size.

In Fig. 3.3, the workspace of the arm supports can be seen. Data was not available for every device. The horizontal lines (blue, green, and red) represent the maximum and minimum boundaries of each axis (x, y, z, respectively). For five passive arm supports [14, 19, 21, 23, 24] the workspace is much larger than needed for the human arm. The WREX approaches the natural workspace of the arm very well. Other devices have difficulties to perform the upward movement for the natural range of motion of the human arm. The wearable active supports all have a smaller workspace than the human arm. Only the ABLE [30] reaches the complete workspace along the x and y-axis.

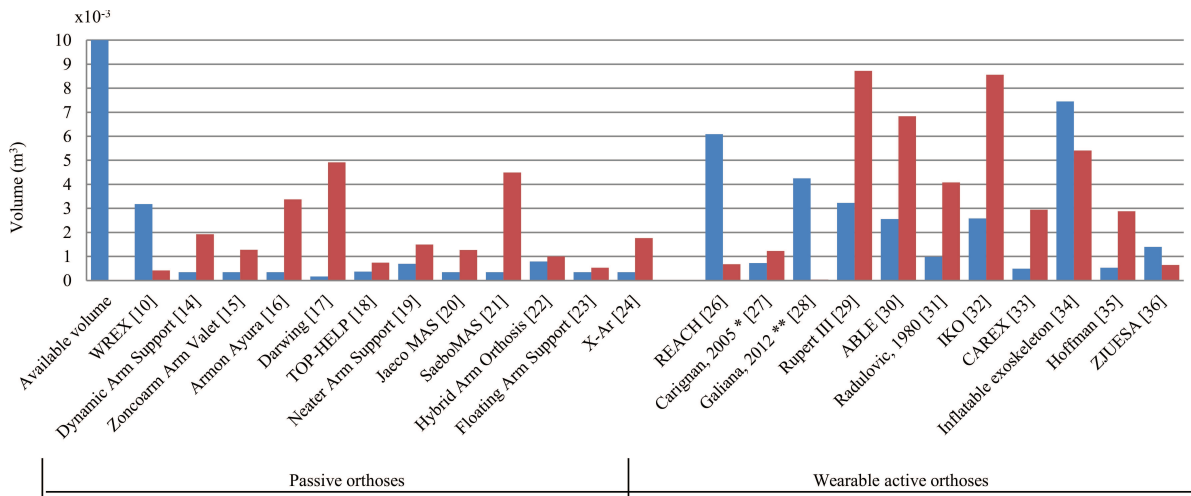


Figure 3.2: Volume of the devices within 20 mm from the body (blue) and violating 20 mm from the body (red). If the data was not available in the articles, the values were estimated based on figures and movies. *A torso structure was not mentioned in the article, so the volume is not taken into account. ** Only shoulder abduction/adduction is supported by this device.

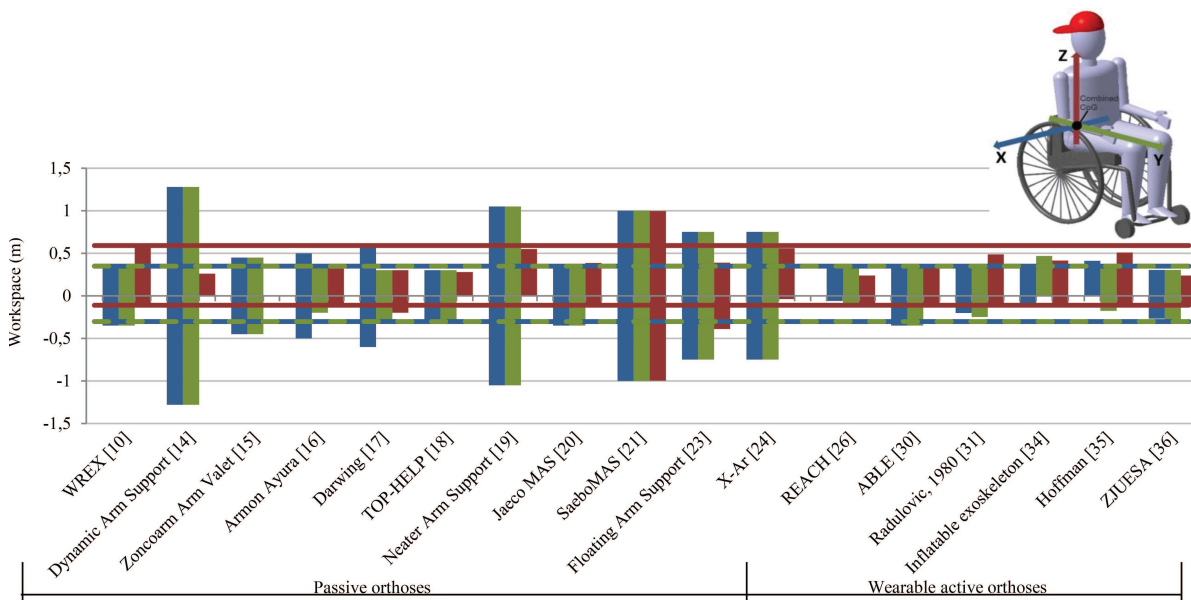


Figure 3.3: Workspace of the end-effector of the arm supports in x-direction (blue), y-direction (green) and z-direction (red). The horizontal lines (blue, green, and red) represent the maximum and minimum boundaries of each axis (x, y, z, respectively). If the data was not available in the articles, the values were estimated based on figures and movies.

3.4. DISCUSSION

THE results in Fig. 3.1 show that only one passive arm support is wearable. The others are connected to the wheelchair and also not close to the body. Some designs focused on the aesthetics, but in general they are not wearable underneath clothing, which makes them very conspicuous. All the passive supports use a serial linkage from the base (i.e., wheelchair or trunk) to the forearm. With such architecture, there are some positions of the arm where the device searches for the best position, which could mean that some links are positioned far from the body. This has to be kept in mind when designing a serial linkage that has to stay close to the body. The WREX has the best solution for this because it is designed to follow the arm contours. It moves parallel and as close to the arm as possible. In contrast to passive supports, all wearable active supports are connected to the trunk, upper arm and forearm. The devices stay closer to the body during movements, because they move parallel to the arm. But very good alignment with the body joints is needed to prevent singularities and injuries. This was already discussed by Schiele et al. [37], who stated that an ergonomic exoskeleton must not copy the human's kinematic structure to be robust to misalignments. The opinion of the authors is that the best way towards a wearable passive arm support with a natural workspace, is the design of a serial linkage connected to the trunk and the forearm that stays very close to the body.

Fig. 3.2 shows the volumes of the arm supports. Almost all passive devices utilize a small amount of volume within the 20 mm from the body. The serial linkages from the wheelchair to the forearm of the user were not designed in a way that will be close to the body. Not all devices were designed to be close to the body, but for the final goal of the project, exceeding the available volume represents a solution that is inconspicuous, heavy and not wearable. Only the WREX shows good results. Recall that the volumes were calculated for one position of the arm (lying on the arm rest). The volumes within and violating the available volume could change with different arm motions.

Comparing the passive with the wearable active devices, the active devices have relatively larger amounts of volume violating the proposed available volume. This is mainly due to the actuators that are placed in a large backpack. Although the parts connected to the arm approach the required volume, the backpack is conspicuous. This also adds weight on the back of the user that affects to wearability and user comfort. Moreover, since DMD patients are wheelchair bound, it is not possible to place such a large amount of volume on the back. Most of the devices with this structure use cables to transfer the forces from the actuators to the joints. Cable transmission implies high force capacity, high stiffness, and low inertia. However, there is also friction involved. This has to be minimized to apply such a structure for patients with very low muscle strength. With cable actuation, shear forces can be exerted on the user. The devices with local actuators at the limbs add weight along the extremities. This makes the limbs heavy, conspicuous and no natural movements are ensured.

Some interesting passive elbow supports were found in literature [38, 39]. These results were not taken into account because they did not support the whole arm. These devices were very close to the body and fit within the volume enclosed by 20 mm from the body, they could only perform flexion and extension of the elbow.

In Fig. 3.3, it can be seen that the serial linkages of the passive arm supports can

reach the workspace of the human arm along the horizontal x and y-axes. The full range of motion along the vertical z-axis is not supported in all devices. This can be justified because reaching above the shoulder is not required to complete many critical activities of daily life. Therefore, a design strategy could be to neglect the full vertical range of motion in future designs, focusing only on support of the most critical activities of daily life. There are three devices with a very large workspace [14, 19, 21]. The reason is unclear, because now all the material needed to reach the boundaries of the workspace has to go somewhere when the arm is close to the body. On the other hand, the active arm supports have smaller workspaces than the natural workspace of the human arm. The active devices are connected to the body at three points. That requires movements along the arm, but it also requires very good alignments with the body joints to prevent misalignment. These alignment difficulties affect the workspace of the device and the human arm and the comfort of wearing the device [37]. For future designs, a serial linkage that follows the arm contours with special joints at the shoulder and elbow that prevent misalignment with the body joints is proposed.

The passive arm supports use springs mechanisms to balance the arm in the combined centre of gravity of the upper and forearm. In this way, only one interface point with the arm is required. Besides the gravity compensation, the use of springs also introduces some small damping behaviour. This can have a positive effect on precision tasks, like writing and eating with a spoon. However, a perfect balancing quality has an unstable behaviour. There should be a trade-off between the perfect or near perfect balancing quality, where the user must have minimal muscle strength to overcome the remaining gravity force to move the structure.

There are two other remarks that can be made based on the results. First, only three arm supports support pronation and supination. This movement is important for many critical activities of daily life, for example eating and drinking. For future designs, it is proposed to include support for pronation and supination to achieve a more natural range of motion of the arm. Second, in two devices the upper arm and forearm were balanced independently. This could be very advantageous, because the balancing force of the arm differs through the entire workspace.

Finally, it should be mentioned again that this research focused only on the inconspicuousness and wearability of existing assistive devices. For future designs, other aspects (e.g., functionality, comfort, easy donning and doffing, etc.) should be taken into account. These aspects are of great importance to encourage the use of an arm support in daily life and improve the quality of life.

3.5. CONCLUSIONS

AN overview of the state-of-the-art of passive and wearable active arm supports has been presented. The wearability and inconspicuousness of the devices is investigated with respect to three evaluation metrics: 1) the body interface, 2) the volume, and 3) the workspace of the devices.

It is found that there are only 4 out of 23 devices that are wearable and have a relatively small amount of volume violating the available volume, which is enclosed by 20 mm from the arm and trunk. There is only one wearable passive arm support presented in literature that can perform within the entire natural workspace of the human arm. The

others are mounted to the wheelchair, rather bulky, and not inconspicuous. The passive devices have a serial structure from the forearm to the wheelchair or trunk. Wearable active devices are all attached to the trunk, upper arm and forearm. They have large structures to enclose the actuators. These are commonly positioned at the back of the user. These 'backpacks' are conspicuous, add weight to the user, and are not suitable to use when sitting in a wheelchair. Some passive devices support a larger workspace than the natural workspace of the human arm. Active devices have a smaller workspace than the human arm, because the parallel structures with three body interface points need alignment with the body joints to prevent misalignment. This affects the workspace of both the device and the arm.

For future designs of a wearable, inconspicuous arm support, a serial linkage from the trunk to the forearm is proposed. This device should be aligned and remain close to the body, without interfering with the body and causing user discomfort. The device should include a support for pronation and supination of the forearm. Independent balancing of the upper arm and forearm is advantageous. If the arm support needs actuation, remote actuators decrease the inertia of the moving limbs and can be placed out of sight.

REFERENCES

- [1] A. E. H. Emery, *Population frequencies of inherited neuromuscular diseases - a world survey*, *Neuromuscular Disorders* **1**, 19 (1991).
- [2] J. Rahbek, B. Werge, A. Madsen, J. Marquardt, B. Steffensen, and J. Jeppesen, *Adult life with Duchenne muscular dystrophy: Observations among an emerging and unforeseen patient population*, *Pediatric Rehabilitation* **8**, 17 (2005).
- [3] M. A. Grootenhuis, J. de Boone, and A. J. van der Kooi, *Living with muscular dystrophy: health related quality of life consequences for children and adults*, *Health and quality of life outcomes* **5**, 31 (2007).
- [4] T. Rahman, W. Sample, R. Seliktar, M. Alexander, and M. Scavina, *A body-powered functional upper limb orthosis*, *Journal of rehabilitation research and development* **37**, 675 (2000).
- [5] L. F. Cardoso, S. Tomazio, and J. L. Herder, *Conceptual design of a passive arm orthosis*, *ASME International Design Engineering Technical Conferences* **5**, 747 (2002).
- [6] Jaco of Focal Meditech, <http://www.focalmeditech.nl/index.php/home/75-personal-robot-jaco>, (2013).
- [7] iARM of Exact Dynamics, www.exactdynamics.nl, (2013).
- [8] E. A. Brackbill, Y. Mao, S. K. Agrawal, M. Annapragada, and V. N. Dubey, *Dynamics and control of a 4-dof wearable cable-driven upper arm exoskeleton*, *IEEE International Conference on Robotics and Automation*, 2300 (2009).
- [9] R. A. R. C. Gopura, K. Kiguchi, and D. S. V. Bandara, *A Brief Review on Upper Extremity Robotic Exoskeleton Systems*, *IEEE International Conference on Industrial and Information Systems* **8502**, 346 (2011).

- [10] T. Rahman, W. Sample, S. Jayakumar, M. M. King, J. Y. Wee, R. Seliktar, M. Alexander, M. Scavina, and A. Clark, *Passive exoskeletons for assisting limb movement*, Journal of rehabilitation research and development **43**, 583 (2006).
- [11] Scopus, www.scopus.com, (2013).
- [12] Espacenet, www.espacenet.com, (2013).
- [13] DINED, dined.io.tudelft.nl/dined/nl/ (2013).
- [14] G. Kramer, G. R. B. Romer, and H. J. A. Stuyt, *Design of a Dynamic Arm Support (DAS) for gravity compensation*, IEEE International Conference on Rehabilitation Robotics , 1042 (2007).
- [15] Arm Valet of ZoncoArm, www.zoncoarm.com, (2013).
- [16] J. L. Herder, *Development of a statically balanced arm support: ARMON*, IEEE International Conference on Rehabilitation Robotics , 281 (2005).
- [17] Darwing of Focal Meditech, www.darwing.nl, (2013).
- [18] TOP/HELP of Focal Meditech, www.focalmeditech.nl, (2013).
- [19] Arm Support of Neater Solutions, www.neater.co.uk, (2013).
- [20] Elevating MAS of Jaeco Orthopedics, www.jaecoorthopedic.com (2013).
- [21] MAS of Saebo, www.saebo.com, (2013).
- [22] N. K. S. Benjuya, *Hybrid Arm Orthosis*, Journal of Prosthetics and Orthotics **2**, 155 (1990).
- [23] J. Skorecki, *A "floating arm" support for wheel-chairs*, Annals of physical medicine **9**, 67 (1967).
- [24] X-Ar of Equipois, <http://www.equipoisinc.com/>, (2013).
- [25] J. L. Herder, *Energy-free systems: theory, conception, and design of statically balanced spring mechanisms* (dissertation, 2001) p. 268.
- [26] P. Bosscher and E. LaFay, *Haptic cobot exoskeleton: Concepts and mechanism design*, ASME International Design Engineering Technical Conferences , 1 (2006).
- [27] C. Carignan, M. Liszka, and S. Roderick, *Design of an arm exoskeleton with scapula motion for shoulder rehabilitation*, International Conference on Advanced Robotics , 524 (2005).
- [28] I. Galiana, F. K. L. Hammond III, R. D. Howe, and M. B. Popovic, *Wearable Soft Robotic Device for Post-Stroke Shoulder Rehabilitation: Identifying Misalignments*, IEEE International Conference on Industrial and Information Systems , 317 (2012).

- [29] T. G. Sugar, J. He, E. J. Koeneman, J. B. Koeneman, R. Herman, H. Huang, R. S. Schultz, D. E. Herring, J. Wanberg, S. Balasubramanian, P. Swenson, and J. a. Ward, *Design and control of RUPERT: a device for robotic upper extremity repetitive therapy*, IEEE transactions on neural systems and rehabilitation engineering **15**, 336 (2007).
- [30] P. Garrec, J. P. Friconneau, Y. Méasson, and Y. Perrot, *ABLE , an Innovative Transparent Exoskeleton for the Upper-Limb*, IEEE/RSJ International Conference on Intelligent Robots and Systems , 1483 (2008).
- [31] R. Radulovic, J. B. Piera, B. Cassagne, A. Grossiord, and G. Boruchowitsch, *The mobile arm support*, Prosthetics and orthotics international **4**, 101 (1980).
- [32] F. Martinez, I. Retolaza, A. Pujana-Arrese, A. Cenitagoya, J. Basurko, and J. Landaluze, *Design of a five actuated DoF upper limb exoskeleton oriented to workplace help*, IEEE RAS & EMBS International Conference on Biomedical Robotics and Biomechatronics , 169 (2008).
- [33] S. K. Agrawal, V. N. Dubey, J. Gangloff John J., E. Brackbill, Y. Mao, and V. Sangwan, *Design and Optimization of a Cable Driven Upper Arm Exoskeleton*, Journal of Medical Devices **3**, 1 (2009).
- [34] H. Kobayashi, A. Uchimura, Y. Isihida, T. Shiiba, K. Hiramatsu, M. Konami, T. Matsushita, and Y. Sato, *Development of a muscle suit for the upper body - Realization of abduction motion*, Advanced Robotics **18**, 497 (2004).
- [35] A. H. Hoffman, H. K. Ault, H. Toriumi, S. A. Smith, and C. Felice, *The Design and Kinematic Evaluation of a Passive Wearable Upper Extremity Orthosis*, Annual RESNA conference (2002).
- [36] Z. Jiafan, F. Hailun, D. Yiming, Z. Yu, Y. Canjun, and C. Ying, *Novel 6-DOF Wearable Exoskeleton Arm with Pneumatic Force-Feedback for Bilateral Teleoperation*, Chinese Journal of Mechanical Engineering **21**, 58 (2008).
- [37] A. Schiele, *Fundamentals of Ergonomic Exoskeleton Robots* (dissertation, 2008) p. 205.
- [38] D. H. Plettenburg, *The WILMER Elbow Orthosis*, IEEE International Conference on Rehabilitation Robotics (2007).
- [39] M. M. Wierzbicka and A. W. Wiegner, *Orthosis for Improvement of Arm Function in C5/C6 Tetraplegia*, Journal of Prosthetics and Orthotics **8**, 86 (1996).

II

EXPLORING CONCEPTS

4

CONCEPTUAL DESIGN

In the previous chapter, a review was presented on the state-of-the-art in arm supports. From that chapter, requirements, constraints and design ideas for a new type of arm support were proposed. In this chapter an overview of the defined constraints and requirements for a close-to-body arm support for people with DMD is presented (Section 4.1). Several concepts and an evaluation of those concepts are explained (Section 4.2 to 4.4). The constraints, requirements and concepts are defined in close collaboration with a multidisciplinary team, including DMD patients, project managers, physicians and developers of assistive devices.

4.1. CONSTRAINTS AND REQUIREMENTS

IN order to start the design of a close-to-body arm support it is needed to define constraints and requirements for the device. The constraints and requirements are defined in close collaboration with DMD patients, project managers, physicians and developers of assistive devices.

4.1.1. INTENDED USE

The arm support should be worn underneath clothing, and support the arm for the most important activities of daily life (Chapter 2.2). The passive arm support is intended for DMD patient of approximately 10-16 years old. At this age, all patients are wheelchair bound and are in the first stage of the disease. This means that they still have some muscle strength left to control the arm and to correct for some weight variations. The user wears the arm support for 12 hours a day.

4.1.2. REQUIREMENTS

The requirements are categorized into several sections. For each section a list of requirements is given, together with targets that are wished, planned or that must be reached in order to fulfill the requirement. Since this list is used as a guideline that is kept in mind during the design of concepts, many requirements are not quantified with values. It has to be noticed this is a not an exhaustive list and that the prototypes presented in this dissertation are not evaluated on the complete list of requirements.

FUNCTIONAL REQUIREMENTS

	Wish	Plan	Must	Unit
Increase arm's range of motion	also above the head (Fig. 2.3)	at least to shoulder level		
Adaptive for the stage of the disease		v		
Intuitive use, short learning period		< 1		hour
Possibility to go to the toilet or urinate in a bag			v	
Easy donning/doffing			max. 15	min
Redressing of body posture	v			
Sideways stabilization		v		
Support for the arms	2 arms	2 arms	1 arm	
Balancing force tuning during the day	v			
Customizable for anthropometry	by care-giver	by tool-maker		
Strong enough to withstand force in the structure			v	

COMFORT REQUIREMENTS

	Wish	Plan	Must	Unit
Low contact pressure at body interfaces		20 [1]	max. 30	mmHg
No collisions between device and user			v	
No obstruction of respiratory system			v	
Perspiration transport			v	

AESTHETICS REQUIREMENTS

	Wish	Plan	Must	Unit
Close-to-body	underneath clothing	max. 2 from body		cm
Visible parts look and feel good	v			

SAFETY REQUIREMENTS

	Wish	Plan	Must	Unit
No skin pinch			v	
Arm must not fall out of the device			v	
No sudden release of potential energy of springs			v	

MANUFACTURING REQUIREMENTS

	Wish	Plan	Must	Unit
Technical feasibility			v	
Easy to manufacture and assemble		max. 120		min

COMMERCIAL REQUIREMENTS

	Wish	Plan	Must	Unit
Reimbursement		v		
Cheaper or equal in price as current arm supports		v		

OTHER REQUIREMENTS

	Wish	Plan	Must	Unit
Compatible with lifting device or lifting by a person			v	
Possibility to extend with head/neck support		v		
Compatible with a PEG-probe			v	
Cleanable			v	
Silent	0	max. 30 (whispering)		dB
Possible to fit by orthopedic toolmaker			v	

4.2. FUNCTIONAL DECOMPOSITION

IN order to generate concepts, the functions of an arm support are determined. The main function is to support the arm of the user. This function is decomposed into several sub-functions. In Fig. 4.1, the functional decomposition is shown for a passive arm support. The arm support should transfer the forces to and from the body. The generated compensation force should be transferred to the arm of the user. This compensation force should always be aligned to the vertical direction of gravity. The forces and moments in the structure should be transferred to the fixed world, without being uncomfortable for the user. Next to that, the arm support should provide the motion freedom to be able to perform the required activities of daily living.

For each sub-function concepts can be generated. In the end, concepts for each sub-function can be combined into a concepts for a complete arm support. In this way, it is easier to generate concepts, and it also stimulates to think of out-of-the-box concept solutions. It stimulates to combine several (non-conventional) concepts with each other and to categorize concepts.

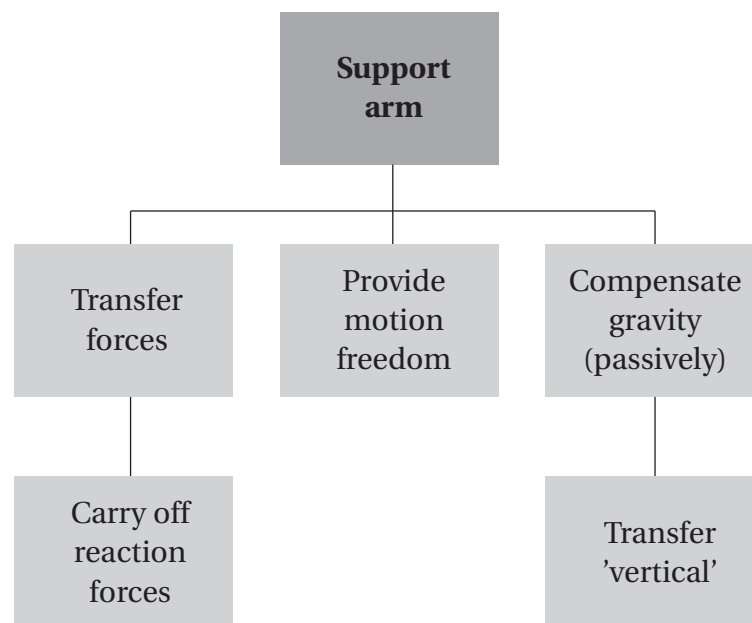


Figure 4.1: Functional decomposition of a passive arm support.

4.3. CONCEPT OVERVIEW

FOR many sub-functions concepts are generated. We did this in a brainstorm session with a multi-disciplinary team, including DMD patients, project managers, physicians and developers of assistive devices. In Fig. 4.2 a morphological overview of all the concepts is shown. The concepts are sorted according to the principle (first layer) and the type of each principle (second layer).

From the morphological overview the 5 most convenient combinations of concepts are determined. This is based on the knowledge and intuition of the multidisciplinary team. Below, each concept is briefly elaborated.

COMPLIANT STRUCTURE

In this concept, a body-shaped compliant structure/suit fits around the body of the user (Fig. 4.3). The structure consist of stiff parts and compliant parts. The joints and energy storage (gravity compensation) elements are included in the flexible structure, while the stiff structure gives some support and stability to the body. The elastic elements at the shoulder and elbow could be, for example, straw mechanisms.

GIRAFFE CONCEPT

This concept is based on the biomechanics of the neck of a giraffe. A ligament that runs along the complete neck, with branches to each vertebra, stores energy when the neck bends down and tends to pull the head back up. In this concept a rubber band will run along the arm, with branches to the upper arm and forearm (Fig. 4.4). The rubber bands are connected the shell structures to transfer the forces to the body. The structures do not have joints, but the joints of the human skeleton are used perform motion and transfer the forces.

SCALES WITH PNEUMATICS

The mechanical structure of this concepts is inspired by the scales of arthropods. The scales provide strength and stiffness close to the body. Conventional joints are aligned with the human joints. The gravity balancing could be provided in an active way, by pneumatic actuators (Fig. 4.5).

PARALLELOGRAMS

This concepts is based on the technique that is widely used in the state-of-the-art in arm supports (Chapter 3). A serial connection of parallelograms from the upper legs to the forearm transfers the forces from the arm to the seat of the wheelchair, and provide the range of motion that is required for the arm. Rubber springs inside the parallelograms provide the balancing force to balance the complete arm.

PULL DOLL

In this concept, the human skeletal is used as structure to transfer the forces. The balancing force could be provided by bowden cables that are connected to springs at the back or below the seat of the wheelchair. The bowden cables are included into a suit and can move the arm into various positions, like the pull doll toy.

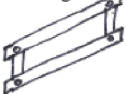
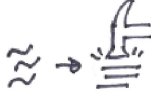
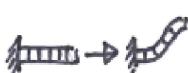
Compensate gravity (passively)	Principle	Temporarily fixed	Magnets	Springs					
	Type			Bending	Torsion			Axial	
	Concept	Pull-doll	Magnets in armrest	Elastic straw	Helical spring	Torsion spring	Spring+cam	Rubber bands	
									
	Principle	Damping	Aerodynamics			Weights			
	Type								
	Concept	Submerge in water	Air blower	Helicopter	Helium balloons	Rotational	Lift type with pulley		
									
Transfer forces	Principle	Through orthosis							
	Type	Compliant	Cables		Rigid		Flexible/ rigid		
	Concept	Compliant tree, leaf springs on joints	Pull doll/bowden	Hydrostats	Shell structures/ harness	Parallelogram rod mechanism	Nonnewtonian fluid	Vacuum or capacitive/ particles	
									
	Principle	To body					To world		
	Type								
	Concept	Use human skeleton	Upper leg cup	Suit	Varying support locations, depending on arm position	Vacuum	Fixed at wheelchair	Upper leg cup	
									

Figure 4.2: Morphological overview of concepts for the sub-functions of an arm support.

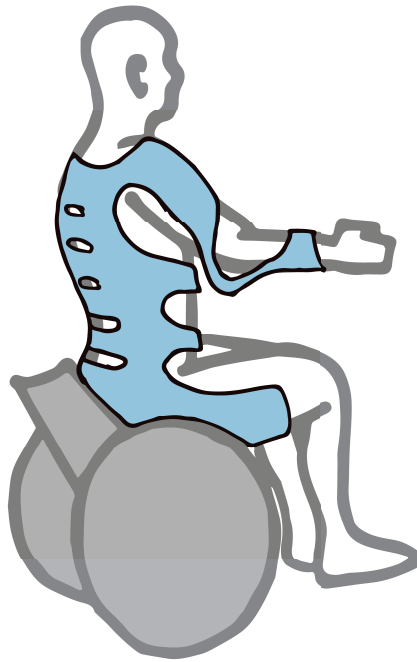


Figure 4.3: Concept for a compliant structure around the body.

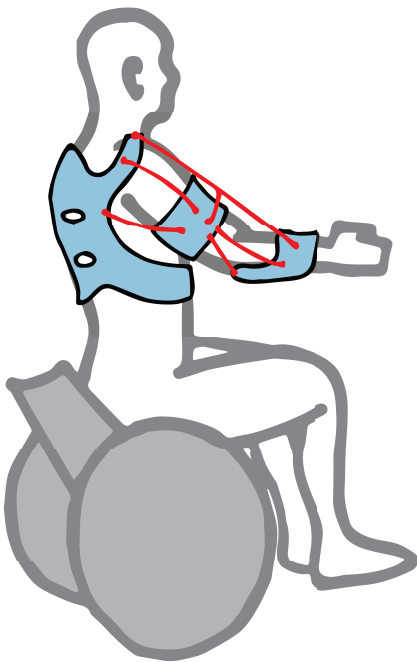


Figure 4.4: Concept that balances the arm with rubber branches (red) along the arm (like the neck of a giraffe).

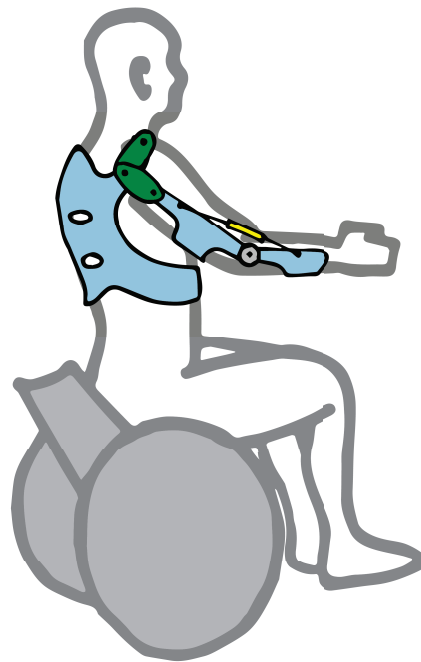


Figure 4.5: Concept of scales with pneumatic actuators (green: pneumatic vane actuators, yellow: pneumatic cylinder).

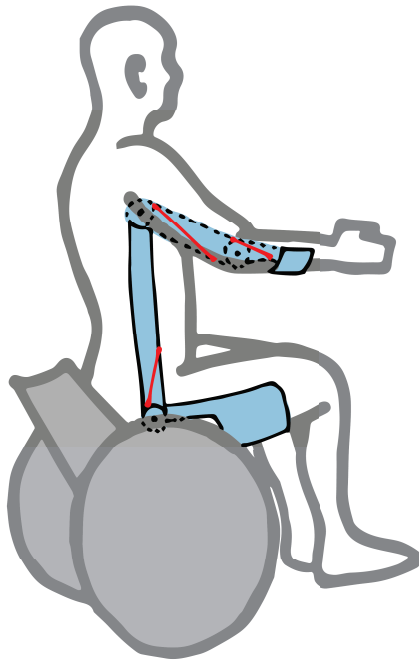


Figure 4.6: Concept with parallelograms from the upper legs to the forearm, with rubber bands inside to balance the arm (red).

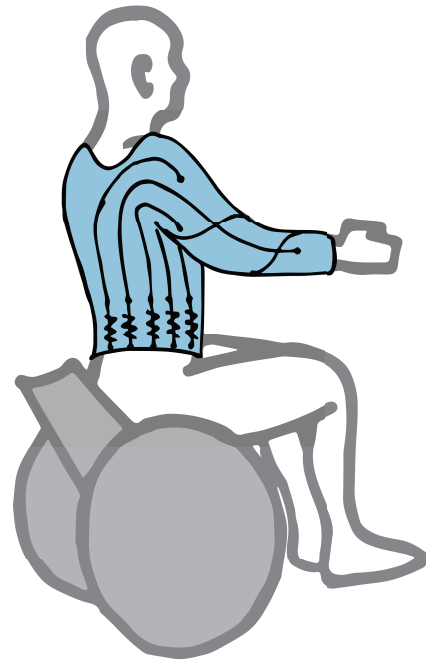


Figure 4.7: Concept of a suit with bowden cables running through it. The bowden cables are attached to springs, to create a balancing force.

4.4. EVALUATION

FOR the two main functions (transferring the forces and gravity balancing), the concepts were evaluated according to the most important requirements for these functions. In this section the evaluation is elaborated and the final choice of a concept for each function is made.

4.4.1. TRANSFERRING FORCES

The concepts for transferring the forces to the world that can be found in the five concepts that are explained in the previous section are: 1) a compliant structure, 2) a scale/shell structure, 3) a (parallelogram) linkage mechanism or 4) using the human skeleton. The most important requirements, together with the evaluation criteria are listed below. The scores for each requirement are 0 (insufficient), 1 (just sufficient), 2 (sufficient), 3 (good), 4 (ideal). Where possible, the requirements were evaluated according to values (mentioned with each requirement). Otherwise, the evaluation was based on the knowledge and interpretation of the expert.

- Close to body: 0 means '>10cm from body', 1 means '>5cm', 2 means '>3cm', 3 means '<3cm', 4 means '<2cm from body'.
- Technical feasibility: 0 means 'not available for many years', 1 means 'own research is needed', 2 means 'available within the time span of this project', 3 means 'currently available on the market, but adjustments are needed', 4 means 'currently available on the market and applicable as it is'.

	Av. weight factor	Compliant structure	Scales/shells	Linkage mechanism	Human skeleton	Ideal solution
Close to body	3.2	3.5	2.4	2.2	3.7	4
Technical feasibility	2.9	2.4	2.7	3.8	2.3	4
Ease of donning/doffing	2.5	2.3	2.2	2.8	2.4	4
Right conditions for static balance	2.3	2.5	2.4	3.8	1.4	4
Shear forces on user	3.3	2.7	2.6	3.1	1.6	4
Comfortable	2.9	2.9	1.9	2.4	2.9	4
Total score		68%	59%	74%	61%	100%

Table 4.1: Evaluation of the concepts for transferring forces to the world, according to the most important requirements for this function.

- Ease of donning/doffing: ranging from 0, meaning 'hard to don/dof and set up without an expert', to 4, meaning 'max. 2 actions are needed to don/dof'.
- Guarantees right conditions for static balance (e.g., transferring the vertical axis through the whole structure)
- Shear forces on user
- Comfortable

In Table 4.1, the evaluation of each concept according to each requirements is shown. The evaluation was done with the multidisciplinary team of experts. Each expert gave a weight factor (0-4) to each requirement and the scores on each requirement was multiplied with the weight factor. The final scores is shown as a percentage of the ideal solution.

4.4.2. GRAVITY BALANCING

The concepts for gravity balancing that can be found in the five concepts that are explained in the previous section are: 1) a compliant structure, 2) rubber branches (giraffe), 3) rubber bands, 4) metal springs or 5) using actuators. The most important requirements, together with the evaluation criteria are listed below. The evaluation was done in the same way as the evaluation of the concepts for transferring the forces to the world.

- Close to body: 0 means '>10cm from body', 1 means '>5cm', 2 means '>3cm', 3 means '<3cm', 4 means '<2cm from body'.

	Av. weight factor	Compliant structure	Rubber branches	Rubber bands	Metal springs	Actuators	Ideal solution
Close to body	2.9	2.7	2.5	2.5	2.0	1.6	4
Balancing quality	3.1	2.6	1.9	3.1	3.7	3.3	4
Service life	2.2	3.6	2.4	2.4	3.7	2.8	4
Comfortable	2.6	2.3	3.3	3.4	2.2	2.1	4
Total score		69%	64%	73%	71%	57%	100%

Table 4.2: Evaluation of the concepts for gravity balancing of the arm, according to the most important requirements for this function.

- Balancing quality: 0 means 'no balance', 1 means '<75% of the arm is balanced and tuning is impossible', 2 means '<75% of the arm is balanced, but tuning is possible', 3 means '<90% of the arm is balanced', 4 means '>95% of the arm is balanced'.
- Service life: 0 means '<1 week service life', 1 means '<1 month', 2 means '<3 months', 3 means '<1 year service life', 4 means 'infinite service life'.
- Comfortable

In Table 4.2, the average a weight factor and the final scores are shown.

4.5. FINAL CHOICE

THE most promising solutions for transferring the forces to the world are the use of a (parallelogram) linkage mechanism or a compliant structure. This should be combined with rubber bands, metal springs, or with a compliant structure to balance the arm. In the following chapters, several concepts for the use of compliant structures or linkage systems with rubber bands are elaborated.

REFERENCES

- [1] A. Schiele, *Fundamentals of Ergonomic Exoskeleton Robots* (dissertation, 2008) p. 205.

5

FEASIBILITY STUDY OF A BALANCED UPPER ARM SUPPORT BASED ON BENDING BEAMS

Orinally appeared as:

A.G. Dunning, J.L. Stroo, G. Radaelli, J.L. Herder,
Feasibility study of a balanced upper arm orthosis based on bending beams,
IEEE International Conference on Rehabilitation Robotics, 520 (2015),
DOI:10.1109/ICORR.2015.7281252

In the previous chapter, several concepts for gravity balancing of the arm and transferring forces to and from the body were shown. One of the concepts is the use of bending beams to replace normal or rubber (tension) springs. The advantage of this concept is that it places the springs on suitable locations, bringing the whole system closer to the body. In this chapter, this concept is elaborated in detail and a proof-of-principle prototype is designed and build to be evaluated on the body.

ABSTRACT

PEOPLE with neuromuscular diseases request an arm support close to the body for assistance with their arm movements. This paper proposes a concept for a passive arm support based on bending beams to support the eating movement and that is close to the body. Simulations resulted in the final configuration and dimensions of the beams, optimized to balance an arm. One Carbon-fiber-reinforced polymer beam with dimensions 0.22x0.0041x0.0027m at the medial side and one at the lateral side of the upper arm deliver the required energy for balancing the arm. Experimental evaluation of a prototype demonstrated the technical principle; more than 87% of the moment around the shoulder was balanced between 0 and 1.1rad. A second prototype was built for evaluation of the concept in relation to the body. The width of the elastic and structural elements was only 2x 7.5mm, which is more than four times smaller than in current arm supports. From this it was concluded that bending beams have the potential to make an arm support that is close to the body and can balance the arm in a single plane.

5.1. INTRODUCTION

PEOPLE with neuromuscular disorders have increasing difficulties to perform simple activities like eating, drinking and lifting objects. Duchenne Muscular Dystrophy (DMD) is the most common muscular dystrophy and affects 1 in 3500 male births [1]. The progressive degeneration of the muscles starts at the largest and most proximal muscles. As teenagers, the patients end up in a wheelchair and due to decreased arm function they become highly dependent on caregivers or assistive devices.

It is important for these adolescents that those supporting devices are unobtrusive and not stigmatizing [2, 3]. Furthermore, arm supports are supposed to assist activities of daily living (ADL). They should be comfortable and support the arm throughout its complete range of motion. The “Flexextension A-Gear project” is focusing on the development of a new type of arm support that fits underneath clothing.

In [4], 23 passive (non-powered) and active (powered) arm supports were compared and it was concluded that all of the devices are large and stigmatizing and/or do not support the complete range of motion of the arm. Only one device comes close to the body (WREX, Jaeco Orthopedic, USA), but this device does not fit underneath clothing and limits some movements of the arm.

The goal of this paper is to propose a concept for a balancing mechanism, so that the arm support can fit underneath clothing. In this paper, the focus is on balancing the upper arm during the eating movement, which is considered as the most essential activity to perform independently for people with DMD [5–7].

First, an analysis will be made on the design space and the requirements for the upper arm support (Section 5.2). Thereafter, a conceptual design of the balancing mechanism is described (Section 5.3). In Section 5.4, the conceptual design is converted into a proof-of-principle prototype, which is simulated and measured. Another prototype is presented in Section 5.5, which shows how close to the body it is. After a discussion of the results, the conclusion is drawn.

5.2. ANALYSIS

5.2.1. CONSTRAINTS AND REQUIREMENTS

THIS research only focuses on the eating movement of the upper arm. Therefore, the arm is simplified as a pendulum moving in a single plane, where the weight of the lower arm is considered as a point mass on the elbow. The center of mass (CoM) is calculated using anthropomorphic data [8]. This results in a mass of 3.84kg at a distance of 0.23m from the shoulder joint (S), which is considered as a perfect ball joint (Fig. 5.1). The upper arm should be able to rotate between 0rad (vertically pointing down) and 1.1rad to perform eating movements [9].

As mentioned in the introduction, an arm support should fulfill some important requirements to encourage the use by adolescents. The most important for this research is that the device needs to be inconspicuous. The ultimate goal is to fit the whole device within 20mm from the body. At the same time, it should give enough support during eating movement. Since it is important for the patients to keep using their muscles, a compensation of approximately 90% of the moment of the arm is considered as sufficient. Another important requirement is that the device should be comfortable for daily use.

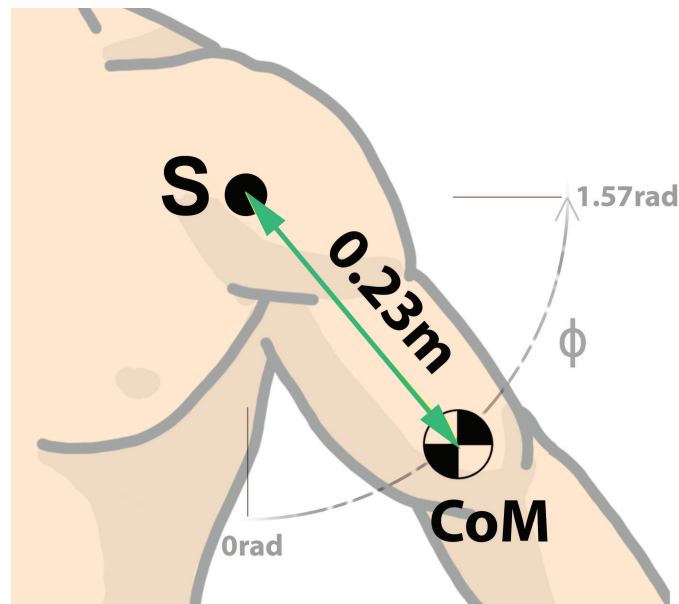


Figure 5.1: Representation of the arm as a simple pendulum rotating about the shoulder (S). The center of mass (CoM) is a combination of the mass of the upper arm and lower arm (considered as a point mass on the elbow).

5

Prerequisites for comfort are low shear forces and no obstructions of the sweat glands (e.g. in the axilla).

5.2.2. GOAL FUNCTION

The energy characteristic of the arm for a movement from 0rad to 1.57rad is shown in Fig. 5.2. The potential energy increases during elevation. To balance the arm, the total energy in the system should be constant throughout the movement. The goal function needs to be the exact opposite of the energy characteristic of the arm, meaning that energy is released during elevation.

5.3. CONCEPTUAL DESIGN

5.3.1. BEAMS AS A METHOD FOR STORING ENERGY

As shown in [4], the current balancing mechanisms for passive arm supports are all based on tension springs. Springs can only exert a pulling force. Therefore, an extra linkage is required to convert that pulling force to a supporting force on the arm without introducing shear forces on the skin.

However, compression springs can exert a pushing force. Consequently, no links are needed for the connection to the arm. Only a tension element like a wire suffices. A practical way to make a compact compression spring is the use of beams. Varying the initial shape of the beam can vary the behavior of the energy characteristic, as shown in [10], where a pendulum is balanced with a curved beam. However, due to advantages in analysis and manufacturability this design uses initially straight beams for balancing the arm.

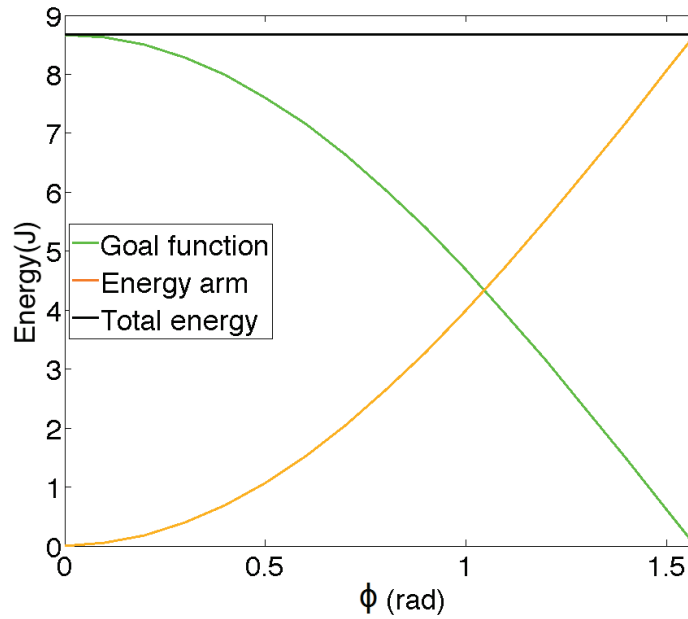


Figure 5.2: Energy-angle characteristic of the arm (yellow) and the goal function (green) needed to balance the arm. The total energy (black) is constant, which means that the whole system is in balance.

5.3.2. FINAL CONCEPT

Fig. 5.3 shows the final concept with respect to the arm. A beam is fixed at the trunk (B1) and at an interface to the arm (B2). The force exerted by the beam is acting through these points (F_{B1B2}). The interface at the arm is connected to the shoulder (S) with a wire and constraints B2 to rotate about S. The resultant force in the wire (F_S) and the beam (F_{B1B2}) is perpendicular to the wire and generates the moment about S to support the arm (F_{Supp}). During rotation the curvature in the beam changes. This means that also the supporting force and the moment about the shoulder changes.

5.3.3. SIMULATION

This final concept is simulated using an isogeometric analysis [11], an alternative to finite element analysis. In Fig. 5.4a it can be seen that the energy in the beam increases linearly when the beam is bending (distance B1-B2 decreases). The distance B1-B2 increases with a sinus shaped relation for an increasing angle if B1 is placed vertically below the shoulder (S) and B2 is rotating about S (Fig. 5.4b), where B1B2 denotes the length of the beam. The slope of the sinus shaped characteristic is dependent on the distance B1-S and the length of the beam (see next section for detailed explanation on this variable). The combination results in an energy characteristic for the beam that is equal to the goal function.

5.3.4. INFLUENCE OF VARIABLES ON ENERGY IN THE BEAM

The elastic strain energy (U) of planar Bernoulli-Euler beams is described as follows:

$$U = \frac{1}{2} \int [EA(\lambda - \lambda_0)^2 + EI(\kappa - \kappa_0)^2] dS \quad (5.1)$$

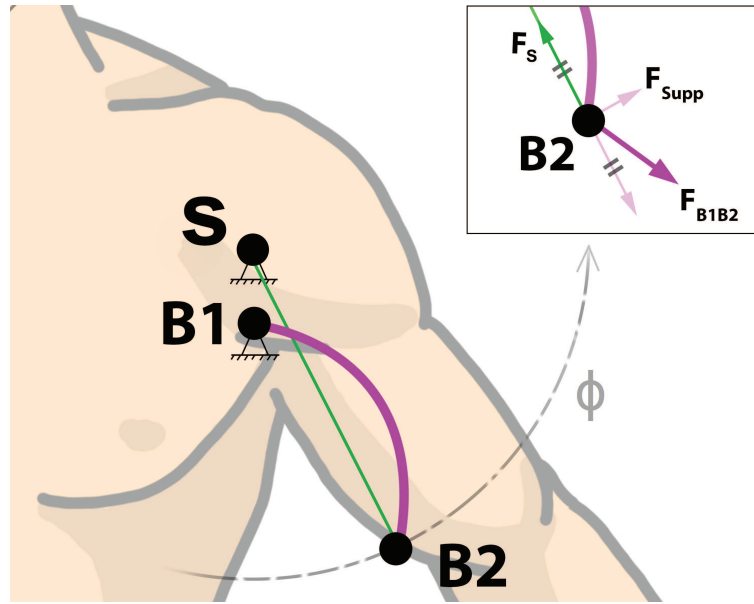


Figure 5.3: The final concept for the balancing mechanism. The arm is balanced with a beam (fixed at the trunk (B1) and at the arm (B2)) and a wire (fixed at the shoulder and the arm at (B2)). The resultant of F_S and F_{B1B2} is the force that generates a moment to support the arm (F_{Supp}).

5

$ S - B1 $ (m)	Deviation from goal function (Nm)	Max. F_S (N)	Thickness (m)	Width (m)
1	1	1	1	1
2	1.4	0.49	0.64	1.74
4	3.1	0.25	0.41	2.96

Table 5.1: Normalized results of the influence of distance S-B1 on parameters of the design.

where E , A , I , dS represent the elastic modulus, the cross-sectional area ($w \cdot t$), the area moment of inertia ($w \cdot t^3/12$) and the initial differential beam length respectively [12]. E , A and I are considered constant over the whole beam length. λ is the stretch and κ the curvature of the neutral axis which are defined by the shape of the beam.

As can be seen in Eq. 5.1, the energy linearly relates to the width of the beam. The thickness however is related to the energy to the third power. Another more complex variable is the distance S-B1, because this influences several parameters, including the curvature of the beam. To illustrate the effect of changing this variable, beams are considered to be straight at 1.1rad and contain a maximum strain of 1%. Table 5.1 shows the normalized results of the deviation from the goal function, the maximum force in the wire (F_S) and the width and thickness of the beam. Since the relations are independent of the exact dimensions of the device, the reference values for normalization are not important. For an increasing distance S-B1, the maximum deviation from the goal function and the width increases, while the thickness and F_S decreases.

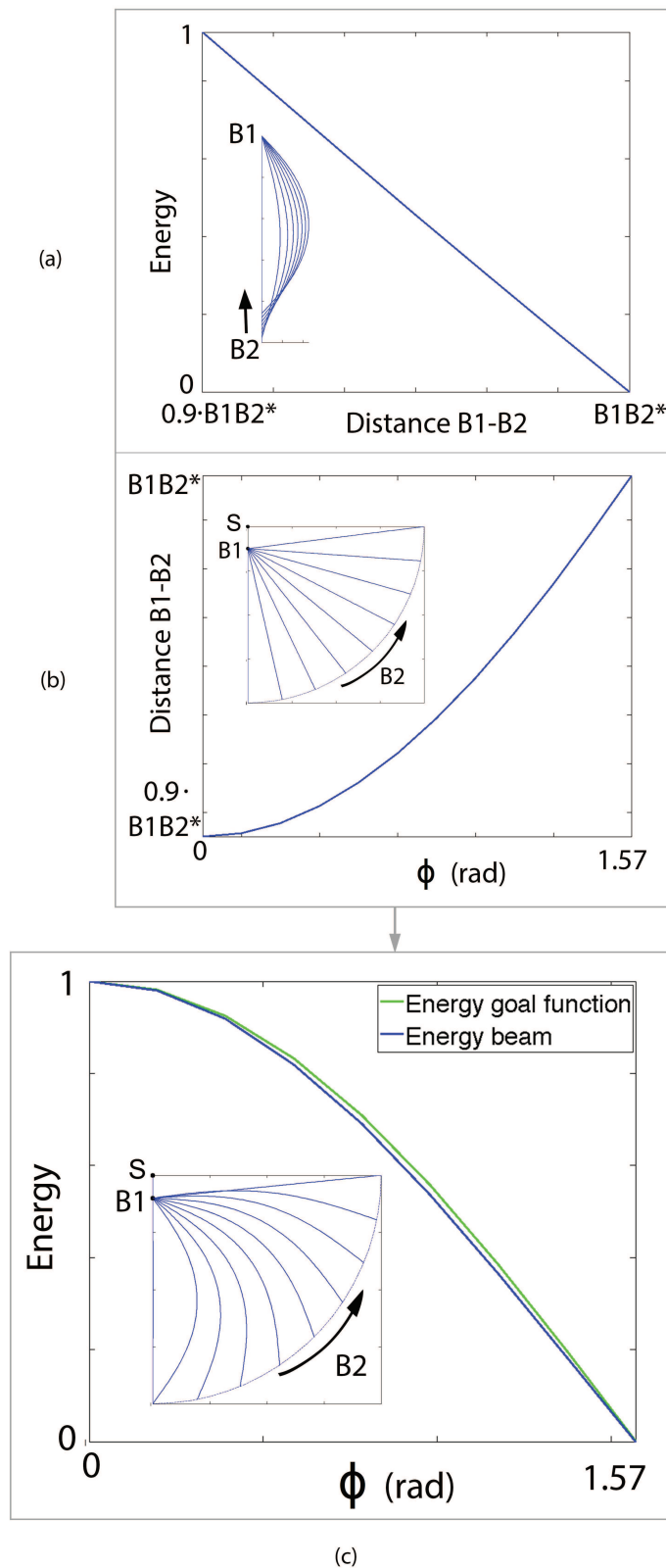


Figure 5.4: (a) The relation between the 'distance B1-B2' and 'energy in the beam'. (b) The relation between 'elevation of B2' about a shoulder joint (S) and 'distance B1-B2'. (c) The relation between the 'elevation of B2' and the 'energy in the beam', which shows that the energy in the beam during elevation is close to the goal function.

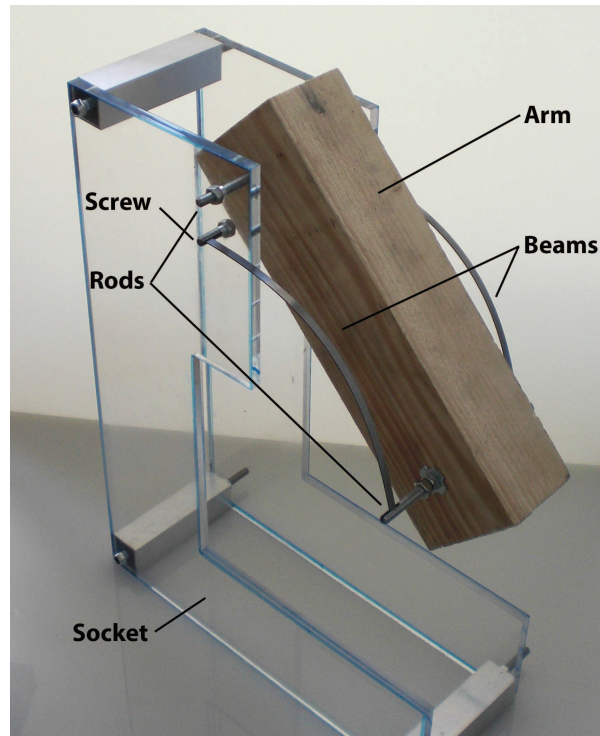


Figure 5.5: Photograph of the proof-of-principle prototype for evaluation of the supporting beams.

5.4. EXPERIMENTAL EVALUATION OF THE CONCEPT

IN this section the concept is converted into a simple proof-of-principle prototype and experimentally evaluated (Fig. 5.5). The arm is simplified to a piece of wood (0.57kg) with the CoM at 0.105m from the shoulder joint. The distance S-B1 is 0.025m with B1 vertically below the shoulder joint. The beams ($0.202 \cdot 0.05 \cdot 0.008m$ ($l \cdot w \cdot t$), $E = 180GPa$) at both sides of the arm are attached to the arm at 0.2m from the shoulder joint, and fixed to the axes B1 and B2 with notches in the rods (0.04kg).

The prototype was measured using the measurement setup shown in Fig. 5.6. A linear stage (Physik Instrumente M-505.4DG, resolution: $0.05\mu m$, travel range: 107mm) is connected to the prototype with a wire that runs over a pulley through a force sensor (FUTEK LSB200, resolution: 10mV, range: 0-44.5N). The data was read using an amplifier (ICP DAS 3016) and a data acquisition module (National Instruments USB6008), logged with the software Labview 12 and processed with MATLAB. A 100gr weight was attached to the prototype to ensure a pulling force on the force sensor. The effect of this weight was subtracted from the total moment.

The elevation up to 1.57rad was measured forwards and backwards to measure hysteresis. The prototype was measured with and without the beams. The results are shown in Fig. 5.7. Both the simulated and measured moment-angle characteristics of the arm without the balancing system are shown (green and blue line, respectively). The purple line shows the measurement of the arm with the balancing beams. This shows an almost flat line until 1.1rad. At 1.1rad the purple line intersects with the line that represents 87% balancing of the total moment of the arm (almost 0.1Nm).

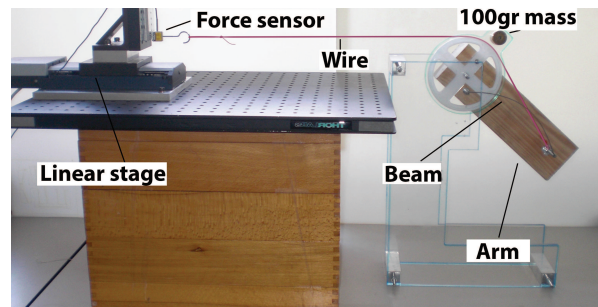


Figure 5.6: The setup for evaluation of the moment that is balanced by the proof-of-principle prototype.

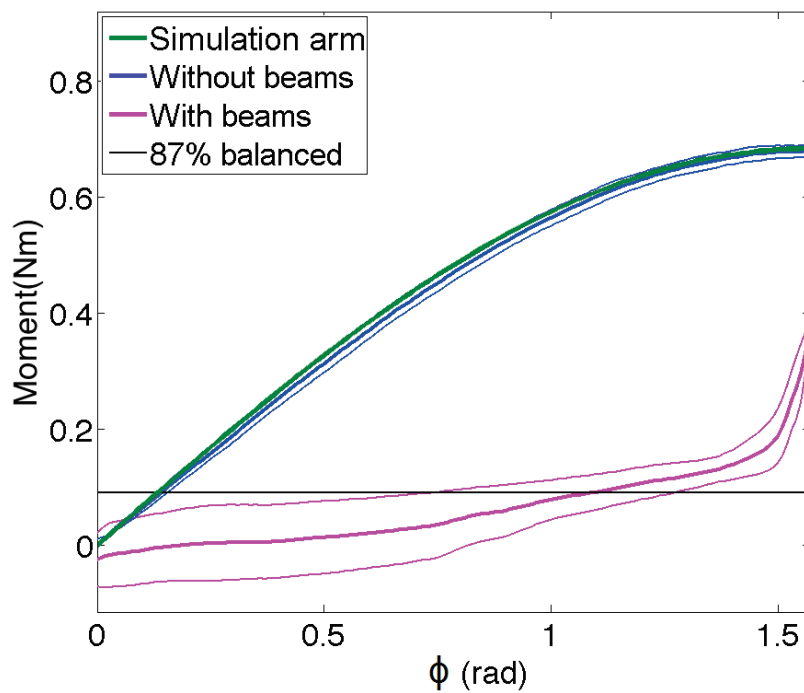


Figure 5.7: Moment-angle characteristics of the proof-of-principle prototype including hysteresis loops (thin lines) measured with and without beams (purple and blue, respectively). If the average (thick lines) of the up and down movement is taken as the remaining balancing moment, more than 87% of the moment (black) of the arm is balanced by the beams until 1.1rad.

5.5. PROTOTYPE

IN this section a prototype is shown to evaluate the proximity to the arm, the comfort of the device, and the behavior for 3D motions.

5.5.1. PROTOTYPE

Fig. 5.8a shows the prototype. A U-shaped structure represents the rigid trunk structure, providing a rotation point anterior and posterior of the shoulder. The beams (made of unidirectional CFRP, $0.22 \cdot 0.041 \cdot 0.027m$ ($l \cdot w \cdot t$), $E = 121GPa$, $\sigma_{max} = 2450MPa$ [13]) are connected to this structure at one end ($|S - B1| = 0.025m$), and at the other end connected to the arm through a cup that transfers the supporting force to the arm. The cup is connected to the shoulder joint with steel wires. In Fig. 5.8b it can be seen that the structure needed for balancing (wire + beam) is only 7.5mm width. For this prototype, the maximum distance from the device to the arm is 59mm. The mass of the upper arm support is only 0.11kg. During elevation of the arm, no movement of the cup with respect to the skin was measured.

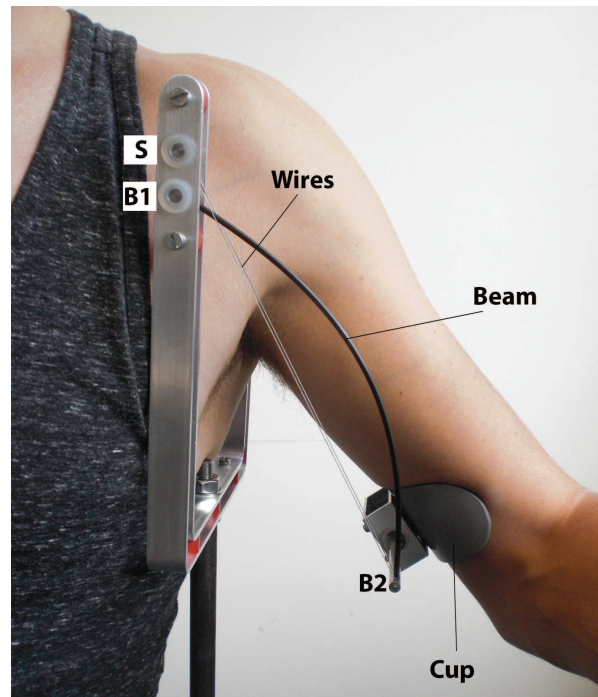
5.5.2. 3D BEHAVIOR

During the design of the balancing mechanism the focus was on balancing the arm in a single plane. This is also what was observed with the prototype. Due to the parallel beams at both sides of the arm, out-of-plane movements and shoulder rotation is not possible. Out-of-plane movements would be possible if the cup stays parallel to the base at the trunk (Fig. 5.9a), but this is very uncomfortable for the user because the cup rotates on the skin and introduces shear forces. Besides that, both balancing beams are in an unstable situation during arm elevation. The beams want to rotate the shoulder to reach a more stable position with almost straight beams (Fig. 5.9b).

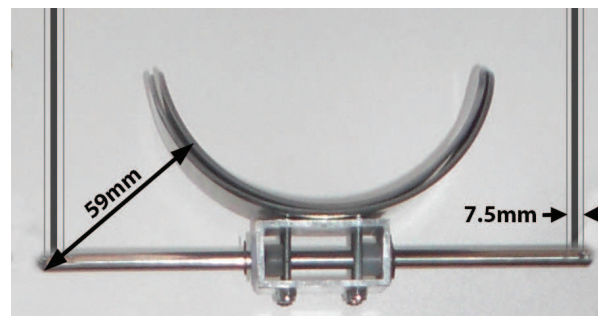
5.6. DISCUSSION

DURING the design of the concept, the arm is simplified to a single pendulum. The mass of the lower arm is represented as a point mass in the elbow. Since this research only focused on balancing the upper arm this was convenient. During different movements, also during the eating movement, the lower arm is moving with respect to the upper arm. Its contribution to the moment that has to be balanced is variable and also depending on the angle of the lower arm. For a future design, the balancing method should be extended to the lower arm, for in-plane movements, and the balancing principle should be evaluated on users.

The proof-of-principle prototype showed that the upper arm can be balanced for 87% up to 1.1rad. This can be increased to 100% by increasing the width or the thickness of the beams. The range of motion could also be increased if needed for other important ADL. By changing the length or the attachment points of the beam the range of motion can be changed. However, the balancing quality is very sensitive to tuning of these parameters. Besides that, it has to be kept in mind that for a larger range of motion the non-linear behavior of the beam increases and it will be harder to reach 100% balance. In a future prototype there can be looked into the adjustability options to tune the stiffness and the balancing quality more accurate.

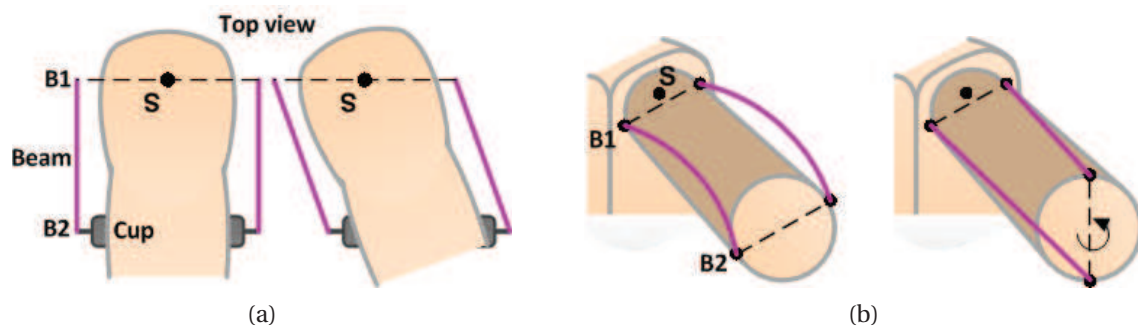


(a)



(b)

Figure 5.8: (a) Prototype in relation to the arm. The beams and wires are connected on one end to a cup (detail in (b)) that supports the arm. The other ends are connected to a U-shaped profile that facilitates the fixed rotation points anterior and posterior of the shoulder.



(a)

(b)

Figure 5.9: (a) For out-of-plane movements the cup wants to rotate and stays parallel to the base at the trunk. (b) The beams want to rotate the shoulder to reach a more stable position with almost straight beams (the steel wires are not shown)

The balancing quality decreases for an elevation larger than 1.3rad (Fig. 5.7). Theoretically, the characteristic of the mass combined with the balancing beams should be more continuous and be closer to zero. In reality, this behavior is caused by a slight curve in the unstressed situation of the beams caused by plastic deformation of the beams. When a material with higher yield strength is used, the behavior could be prevented. The hysteresis shown in Fig. 5.7 is mainly due to friction in the system. The small hysteresis in the measurements without the beams shows the friction in the rotational (shoulder) axis. This axis was not supported by bearings. The hysteresis in the measurements with the beams is larger. This is because the forces on the axes increase, which add more friction between the wood and the axes.

Another prototype was made to evaluate the comfort of the arm support and the proximity to the arm. It was observed that the cup did not move with respect to the skin of the user. This means that there are no uncomfortable shear forces that are noticeable for the user. Besides that, also no uncomfortable displacement was observed with a 20-30mm deviation of the shoulder joint of the prototype (S) from the human shoulder joint. This means that point S is not required to be accurately aligned with the human shoulder joint in order to have low shear forces. The absence of shear forces makes the device comfortable to wear during daily life. Although this is only evaluated on one user, the authors do not expect any differences when evaluating the device with more subjects. Only the comfort on the arm was evaluated. The connection to the trunk was considered rigid. This rigid connection could be made with an orthotic jacket. In the future, the comfort of such a jacket, and the connection of the prototype to the jacket should be evaluated.

The maximum distance to the skin for this prototype is 59mm. However, the structural elements needed to balance the upper arm are only 2x 7.5mm wide, which is 4 times smaller than the WREX arm support. With an arm cup with improved rotational axis, the arm support could fit within 20mm from the skin. This would meet the initial requirement to be close to the body. More research is required to evaluate how the system behave underneath clothing. The authors expect that if the wires are not too close to each other, wearing clothes over the device would not be a problem. The wires and beams can act as proposed without the clothes being stuck in between the wires and beam.

5.7. CONCLUSIONS

THE goal of this research was to propose a concept for a balancing mechanism, to balance the upper arm in a single plane needed to support the eating movement. The balancing mechanism should be able to fit within 20mm. The presented balancing mechanism is based on bending beams, which acts as compression springs to support the arm instead of tension springs. With this approach, no other structural elements than wires are needed to support the arm. A proof-of-principle prototype was build to experimentally evaluate the behavior of the mechanism. Simulations and measurements showed that two beams (one at each side of the arm) of CFRP with dimensions $0.22 \cdot 0.041 \cdot 0.027m$ ($l \cdot w \cdot t$) can store enough energy to balance the arm up to 87% until 1.1rad elevation. This is enough to support the eating movement. The structural elements (beam + steel wire) are only 7.5mm wide and can fit within 20mm from the body.

This is more than 4 times smaller than current arm supports. The device does not exert any shear forces to the skin, which is an important factor for comfort during daily life. From this research it can be concluded that using bending beams as a balancing mechanism can result in an inconspicuous and comfortable device that can support the arm in a single plane.

REFERENCES

- [1] A. E. H. Emery, *Population frequencies of inherited neuromuscular diseases - a world survey*, *Neuromuscular Disorders* **1**, 19 (1991).
- [2] T. Rahman, W. Sample, R. Seliktar, M. Alexander, and M. Scavina, *A body-powered functional upper limb orthosis*, *Journal of rehabilitation research and development* **37**, 675 (2000).
- [3] A. Kumar and M. F. Phillips, *Use of powered mobile arm supports by people with neuromuscular conditions*. *Journal of rehabilitation research and development* **50**, 61 (2013).
- [4] A. G. Dunning and J. L. Herder, *A review of assistive devices for arm balancing*, *International Conference on Rehabilitation Robotics* , 6650485 (2013).
- [5] T. Rahman, S. Stroud, R. Ramanathan, and M. Alexander, *Task priorities and design for an arm orthosis*, *Technology and Disability* **5**, 197 (1996).
- [6] L. F. Cardoso, S. Tomazio, and J. L. Herder, *Conceptual design of a passive arm orthosis*, *ASME International Design Engineering Technical Conferences* **5**, 747 (2002).
- [7] M. M. H. P. Janssen, A. Bergsma, A. C. H. Geurts, and I. J. M. de Groot, *Patterns of decline in upper limb function of boys and men with DMD: an international survey*, *Journal of neurology* **261**, 1269 (2014).
- [8] D. A. Winter, *Biomechanics and motor control of human movement*, 4th ed. (John Wiley & Sons, inc., 2009) p. 86.
- [9] C. J. van Andel, N. Wolterbeek, C. A. M. Doorenbosch, D. H. E. J. Veeger, and J. Harlaar, *Complete 3D kinematics of upper extremity functional tasks*, *Gait & posture* **27**, 120 (2008).
- [10] G. Radaelli and J. L. Herder, *Isogeometric Shape Optimization for Compliant Mechanisms with Prescribed Load Paths*, *ASME International Design Engineering Technical Conferences* , 1 (2014).
- [11] J. Austin Cottrell, T. J. R. Hughes, and J. Bazilevs, *Isogeometric Analysis: Toward Integration of CAD and FEA* (John Wiley & Sons, Inc., 2009) p. 360.
- [12] A. P. Nagy, M. M. Abdalla, and Z. Gürdal, *Isogeometric sizing and shape optimisation of beam structures*, *Computer Methods in Applied Mechanics and Engineering* **199**, 1216 (2010).
- [13] Hexcel, www.hexcel.com/Resources/Cont-Carbon-Fiber-Data-Sheets (2015).

6

DESIGN OF A COMPACT ACTUATED COMPLIANT ELBOW JOINT

Orinally appeared as:
J.G. Kleinjan, A.G. Dunning, J.L. Herder,
Design of a compact actuated compliant elbow joint,
International Journal of Structural Stability and Dynamics **14**, 1440030 (2014),
DOI:10.1142/S0219455414400306

As described in Chapter 4, another promising concept for gravity balancing and transferring forces in an inconspicuous arm support is the use of compliant joints. Compliant joints can be very compact, which is a valuable property in the design of assistive devices. Next to that, in a later stage of the disease, the patients need an active arm support. This chapter presents an explorative research to include compliant rotational joints in an arm support and actuate the device with shape-changing materials. A proof-of-principle prototype is designed and build. In addition, an overview and evaluation on newly introduced performance indicators of shape-changing-material-actuated large-deflection compliant rotational joints is given in this chapter.

For consistent use of terminology in this dissertation, the term 'lower arm' in the original paper is replaced by 'forearm'.

ABSTRACT

COMPACTNESS is a valuable property in designs of assistive devices and exoskeletons. Current devices are large and stigmatizing in the eyes of the users. The cosmetic appearance will increase by reducing the size. The users want a device that is small enough to be worn underneath the clothes, so it becomes unnoticeable. The goals of this paper are (1) to provide an overview of the shape-changing-material-actuated large-deflection compliant rotational joints, (2) provide new introduced performance indicators that evaluate the designs on performance with respect to volume or weight, and (3) design a compact active assistive elbow device as a case study. In order to reach these goals, two evolving fields of study are brought together that have great potential to reduce the size of exoskeletons: smart materials and compliant rotational joints. Smart materials have the ability to change their shape, which make them suitable as actuators. Compliant joints can be compact, since they are made out of one piece of material. An overview of shape-changing-material-actuated large-deflection compliant rotational joints is presented. Performance indicators are proposed to evaluate the existing designs and the prototype.

As a case study a compact actuated rotational elbow joint is presented. An antagonistic actuator made from shape memory alloy wires is able to carry an external load and to actuate to move the arm to different positions. The compliant joint is optimized to balance the weight of the arm and to auto-align with the rotational axis of the human elbow joint. A prototype is able to generate a volume specific stall torque of $5.77 \cdot 10^3 \text{ Nm/m}^3$, produces a work density of $7.27 \cdot 10^3 \text{ J/m}^3$ based on volumes including isolation covers and the half-cycle efficiency of the device is 3.6%. The prototype is able to balance and actuate a torque of 1.1 Nm .

6.1. INTRODUCTION

IN the design of exoskeletons, prosthetics and orthotics one of the three key requirements is cosmetics [1]. In recent years, many applications that focused on the arm were developed: passive arm supports based on cable pulley systems with weights [2] or based on spring mechanisms [3], robotic arms controlled by a joystick [4], and active arm supports with different kinds of actuators [5]. The current devices are rather large and stigmatizing in the eyes of the users [6]. What they want is a device that is compact and in the ideal case fits underneath their clothing. However, conventional (rotational) joints and actuators are too large to achieve this natural look. Therefore, this paper will combine two evolving fields of study which have great potential to reduce the size of exoskeletons: smart materials and compliant rotational joints.

Smart materials can change one or more of its properties (like their shape) when they are triggered by an external stimulus. Using smart materials, muscle-like actuators can be developed with high (specific) work densities generating high forces, while conventional actuators such as electric motors and combustion engines require complex transmissions to perform discontinues tasks [7, 8].

Compliant rotational joints gain their degree of freedom from the elastic deformation of the compliant segments. Therefore, the range of motion strongly depends on the topology and the yield strength of the material. They have different advantages over conventional joints: no backlash, no wear, no friction, no need of lubrication and a high accuracy. The most important advantages for this study is that they can be very compact since they are made out of one piece of material and do not need any assembling and they can store energy which can be regained to make the device more energy-efficient [9, 10].

When the advantages of both fields are combined, interesting designs will evolve with small sizes and low weights, generating high volume specific torques and have high (specific) work densities.

The goals of this paper are (1) to provide an overview of the shape-changing-material-actuated large-deflection compliant rotational joints, (2) provide performance indicators that evaluate the designs with respect to their volume or weight, and (3) design a compact active assistive elbow device as a case study. This overview will be useful for designers, who are designing in small volumes or who have weight restrictions on their designs.

6.2. METHOD

FROM literature, current designs that combine the two fields of study, shape-changing materials and compliant rotational joints, were classified and evaluated. Preliminary performances of the designs were calculated and a comparison study is done between two most promising designs for compact actuated joints. The most promising design is used in a case study to design a compact actuated compliant elbow joint.

6.2.1. CLASSIFICATIONS

With an overview of classified materials and joints, it can be seen which combinations of classes exist or do not (yet) exist. The shape-changing materials can be classified into

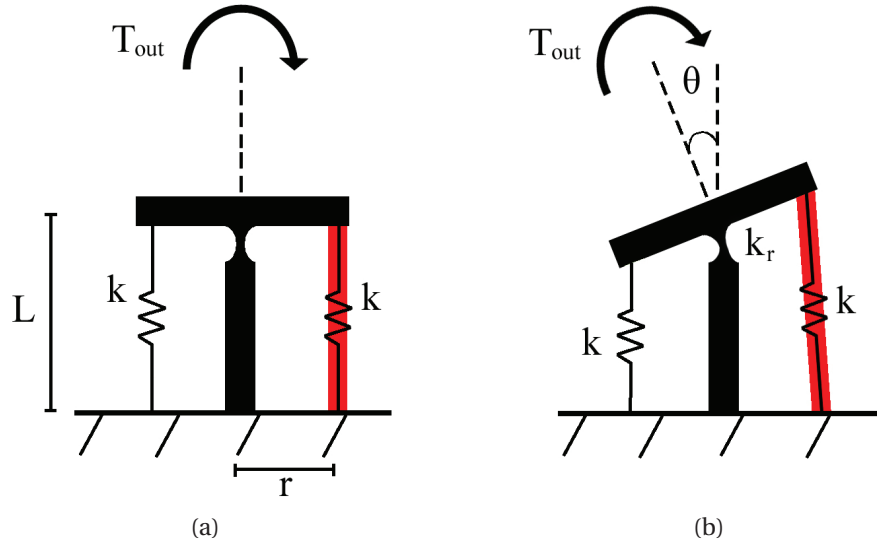


Figure 6.1: (a) Benchmark model based on [12]. (b) An external load T_{out} is displaced over θ by a configuration of shape-changing material (active part (red) and passive part) with a compliant rotational joint.

five classes based on the principle of actuation: (1) field activated Electro Active Polymers (EAP), (2) ionic EAP, (3) shape memory materials, (4) piezoelectric ceramics and (5) thermal expansion.

The compliant rotational joints can be classified into lumped compliance and distributed compliance. Lumped compliant structures gain their degree of freedom by the elastic deformation of small segments. On the other hand, with distributed compliance the elastic deformation is distributed over longer segments.

6.2.2. PROPERTIES OF SHAPE-CHANGING MATERIALS

With the properties of shape-changing materials preliminary calculations can be done on the performance of potential designs. Therefore, the ranges of values reported in different sources will be shown. The following properties are evaluated as described in [7, 11]: (1) maximum strain rate, (2) relative full cycle speed, (3) blocking stress, (4) maximum strain, (5) work density, (6) specific work density, and (7) efficiency.

6.2.3. BENCHMARK CALCULATIONS AND PERFORMANCE INDICATORS

The performance of a shape-changing material combined with a compliant rotational joint is evaluated using a benchmark model, performing a predetermined actuation. The benchmark model is based on a design with a dielectric elastomer of White [12], shown in Fig. 6.1. It consists of a compliant rotational joint with stiffness $k_r(\theta)$, active (red) and passive shape-changing material with stiffness $k(\theta)$ at both sides of the joint. A constant external load $T_{out} = 2Nm$ is displaced throughout a predefined range of motion (RoM) of $\theta = 30^\circ$. Additionally, length $L = 20mm$ and stiffness $k_r = 20Nm/rad$ are fixed.

The torques working on the design are the constant external load T_{out} , the torques generated by the material (active $T_{act} = \sigma Ar$ and passive $T_{pas} = \epsilon_l EAr - \epsilon_r EAr$, with A

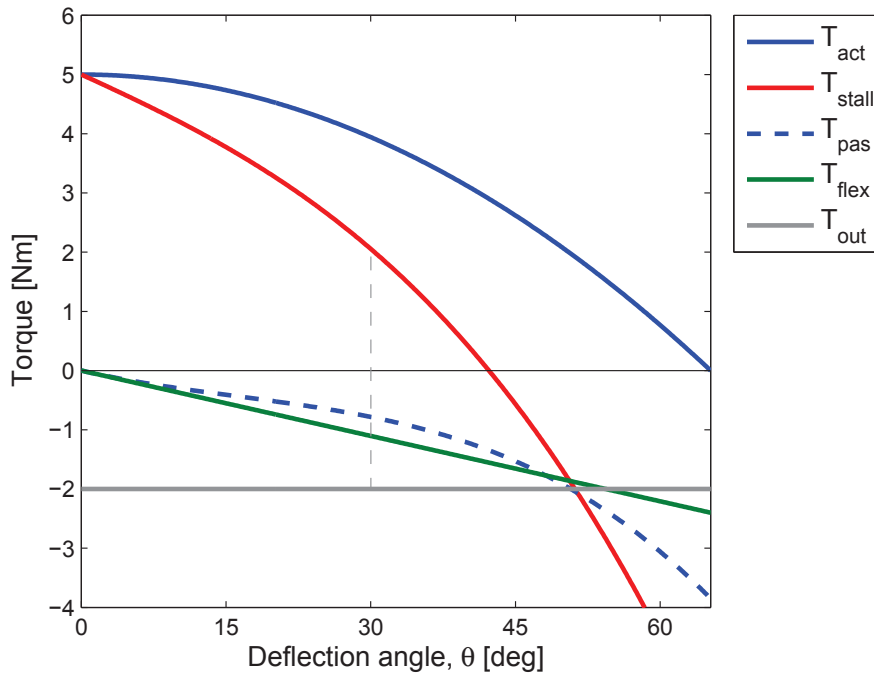


Figure 6.2: Example of an actuation curve. At 30° the sum of T_{stall} ($T_{act} + T_{pas} + T_{flex}$) and T_{out} equals zero and the system is in equilibrium.

as the cross sectional area, blocking stress σ , Young's modulus E , and transmission ratio r) [12] and the torque generated by the compliant joint $T_{flex} = k_r \theta$. The device is in equilibrium when the sum of these torques equals zero (Eq. 6.1).

$$\Sigma T|_{\theta=30^\circ} = 0 = T_{act} + T_{pas} + T_{flex} + T_{out} \quad (6.1)$$

An example of an actuation curve is shown in Fig. 6.2. In this figure the line T_{stall} represents the sum of T_{act} , T_{pas} , T_{flex} , and is the maximal torque that the system (actuator with compliant joint) is able to maintain position and to counteract the external load T_{out} .

For the preliminary calculations of the performances, the stall torques normalized by the volume $t_{sp, stall, vol}$ or weight $t_{sp, stall, m}$ and the work densities over half a cycle for $\theta = 30^\circ$ are evaluated. The work densities are calculated according to Eq. 6.2.

$$w_{sp, vol} = \int_{\theta=0^\circ}^{\theta=30^\circ} t_{sp, stall, vol} \cdot d\theta \left[\frac{J}{m^3} \right], \quad w_{sp, m} = \int_{\theta=0^\circ}^{\theta=30^\circ} t_{sp, stall, m} \cdot d\theta \left[\frac{J}{kg} \right] \quad (6.2)$$

where the definitions $t_{sp, stall, vol}$ and $t_{sp, stall, m}$ can be found in [12]. The benchmark model is designed for a certain external load, so the stall torque is considered when it equals the external load, $T_{stall} = T_{out}$ at the maximal RoM ($\theta = 30^\circ$). The volume optimized for this situation is the minimal volume needed to reach this maximal RoM.

For further evaluation of the shape-changing materials also the half-cycle efficiency is

evaluated (Eq. 6.3). This indicates how much input energy is required for half an actuation cycle. Since the input energy strongly depends on the type of shape-changing material and both the shape-changing material and the compliant rotational joint can store elastic energy, this may either have positive or negative effects on the required input energy.

$$\eta_{half} = \frac{W_{out}}{W_{in}} \cdot 100 = \frac{\int_{\theta=0^{\circ}}^{\theta=30^{\circ}} T_{out} \cdot d\theta}{W_{in}} \cdot 100 \quad [\%] \quad (6.3)$$

This coefficient only involves loading conditions, so the energy stored in elasticity, electricity or even heat can still be recovered during unloading which will increase the full-cycle efficiency with respect to the half-cycle. However, the hysteresis in the material cannot be recovered during unloading, so this will decrease the full-cycle efficiency with respect to the half-cycle efficiency.

6.2.4. CASE STUDY: A COMPACT ACTIVE COMPLIANT ELBOW JOINT

The goal of this case study is to design an elbow joint that is not stigmatizing and is still able to support activities of daily living. This gives some requirements for the design. First, a RoM of $140deg$ is required: $40deg$ to $125deg$ during eating movements and up to $180deg$ flexion during reaching tasks [13]. Second, the size of the device should be small enough to fit underneath clothing, which gives a space of $3cm$ between the skin and clothing [14]. Third, the external load is not a constant static torque for the forearm, but describes a sinusoid function with an amplitude of $3Nm$ and a half period of $180deg$. Since a compliant mechanism can store elastic energy prior to actuation, and regain this stored energy during actuation and increase the performance of the system, the compliant joint (T_{flex}) needs to generate $3Nm$ to balance the forearm including hand ($m = 1.84 kg, L_{CoG} = 0.166 m$). An additional static torque of $0.7Nm$ due to payloads of $200gr$, and a dynamic torque of $0.3Nm$ due to the an average speed of $70deg/s$ of the forearm needs to be generated by the actuator ($T_{act} + T_{pas}$). In total, this is a sinusoid torque of $1Nm$. The actuator is made of the shape-changing material that generates the largest volume specific stall torque and work density.

6.3. RESULTS

THIS section will show the results and highlight some interesting details. First, the results found in literature are shown for the smart materials and the compliant rotational joints, together with the preliminary performance calculations of the combined designs. Afterwards, a comparison study is performed based on simplified models of two promising configurations. Finally, one configuration is chosen and applied in the case study.

6.3.1. OVERVIEW FROM LITERATURE

Table 6.1 shows an overview of the different shape-changing materials and their properties. The properties in the table are based on different sources, so the range of the values is reported here. Different compliant rotational joint designs can be found in [15, 16]. The 26 designs that combined smart materials with a compliant rotational joint are listed

in Table 6.2. With the values of the smart materials, the preliminary performances of each configuration are calculated. In order to calculate the preliminary performances, T_{pas} is neglected, because the required information to calculate T_{pas} was not found in literature for every material. Each existing combination of material and joint can be seen, as well as the potential combinations. An Ionic Polymer Metal Composite (IPMC) is a special shape-changing material that can only be used in bender actuators. Eq. 6.1 cannot be applied on this type of actuators, so the performance is not calculated.

6.3.2. SIMPLIFIED MODELS OF TWO PROMISING CONFIGURATIONS

According to the preliminary performance calculations, the three most promising designs are based on a dielectric elastomer, a conducting polymer or a SMA configuration. However, conducting polymers require an electrolyte solution surrounding the shape-changing material. This will increase the volume and mass of the structure. Therefore, only the dielectric elastomer and the SMA are further analyzed with simplified models, including the passive effects.

DIELECTRIC ELASTOMER CONFIGURATION

A dielectric elastomer consists of a thin film with a compliant electrode at each side of the film. When a voltage is applied on the electrodes, the electrodes squeeze the thin film due to coulomb forces. This causes a strain in the thickness direction and the in-plane direction. The input energy to calculate the half-cycle efficiency can be calculated using Eq. 6.4, taken into account some simplifications and assumptions as described in [11].

$$W_{in} = \frac{1}{2} e_0 e_r w L \frac{V^2}{t} \quad (6.4)$$

where e_0 is the dielectric permittivity of free space, e_r is the relative dielectric permittivity, w is the width of the film, L is the length of the film, V is the Voltage and t is the film thickness.

SMA CONFIGURATION

SMA's are able to actuate due to a solid phase transformation from martensite to austenite, when it is heated above the transition temperature. SMA wires produce a recovery strain of maximal 8% and can reach recovery stresses over 500 MPa [51]. For the SMA configuration, the active shape-changing material in Fig. 6.1 is replaced to the left, because SMA wires can only exert pulling forces. For SMA, the input energy is found in the form of heat. According to [51], the input energy can be calculated using Eq. 6.5.

$$W_{in} = mc_p \Delta T + m \Delta H_{M \rightarrow A} \quad (6.5)$$

where m is the mass of the actuation material, c_p is the specific heat constant of the SMA, ΔT is the change in temperature between the two phases and $\Delta H_{M \rightarrow A}$ is the enthalpy change as described in [51].

RESULTS OF THE SIMPLIFIED MODELS

The performance indicators of the two configurations are calculated according to Eq. 6.2, 6.3, 6.4 and 6.5 and shown in Table 6.3. It shows that the SMA configuration has

Classification	Shape-changing material	Strain rate [%/s]	Relative full cycle speed	Strain [%]	Block stress [MPa]	Work density [J/cm ³]	Efficiency [%]	Density [kg/m ³]
Field activated EAP	Dielectric elastomer: acrylic based	450	Medium	158-380	2.4-8.2	0.15-3.4	30-90	960
	Dielectric elastomer: silicone based	34000	Fast	32-120	0.8-3.2	0.01-0.75	25-90	960
	Relaxor ferroelectric	>2000	Fast	3.5-10	20-45	0.32-1	80	1870
	Graft elastomer		Fast	4-5	24	0.48		1870
	Piezoelectric polymer		Fast	0.1	4.8	0.0024		1870
Field activated Piezoelectric ceramic	PZT	5-10000	Fast	0.1-0.2	15.7-100	0.003-0.1	>90	7700
	PZT-PT single cristal		Fast	1.7	131	1	>90	7700
Ionic EAP	Carbon nanotubes	0.6-19	Slow	0.2-1	1-27	0.002-0.04	0.1-1	615
	Conducting polymer	1-12	Slow	2-40	5-450	0.1-23	1-18	1000
	Ionic gel		Slow	>40	0.3	0.06	30	1000
	IPMC	0.001-3.3	Slow	0.5-40	0.3-30	0.0055	1-2.9	1500
Shape memory	SMA	300	Slow	4-8	100-700	1-100	<10	6450
	SMP		Slow	20-800	1-10	0.22-2	<10	1000
Thermal expansion	Aluminium with $\Delta T = 500^\circ C$		Slow	1	75	0.4	<10	2700
	Entropic elastomer	3-10	Slow	6	1	0.25	2.4	1000
Natural muscle	Human	>50	Medium	>40	0.35	0.07	>35	
	Peaks in nature		Slow-fast	100	0.8	0.04	40	

Table 6.1: Overview of the classes and properties of shape-changing materials (ranges reported from [7, 11, 17–31]).

Compliant rotational joints		Shape-changing materials										
		Dielectric elastomer	Relaxor ferroelectric	Graft elastomer	Piezoelectric polymer	Carbon nano tubes	Conducting polymer	Ionic gel	IPMC's	SMA NiTi	SMP	Piezoelectric ceramic
Lumped compliance	Notch-type	[12]								[32]		
Distributed compliance	Leaf spring		[30]				[33, 34]		[27, 29, 35–37]	[29, 31, 38]	[31, 39, 40]	[29]
	Leaf spring / Flex rod									[31, 41–46]		
	tape spring											
	curved beam									[47–49]		
	contact based										[50]	
Performance	$t_{sp, stall, vol} [\frac{Nm}{m^3}]$	10^9	10^8	10^8	10^5	10^7	10^9	10^7		10^9	10^8	10^7
	$t_{sp, stall, m} [\frac{Nm}{kg}]$	10^6	10^5	10^4	10^2	10^4	10^6	10^4		10^5	10^5	10^3
	$w_{sp, vol} [\frac{J}{m^3}]$	10^9	10^8	10^7	10^5	10^6	10^9	10^6		10^9	10^7	10^7
	$w_{sp, m} [\frac{J}{kg}]$	10^6	10^4	10^4	10^2	10^3	10^6	10^3		10^5	10^4	10^3

Table 6.2: Overview of existing designs together with preliminary calculated performances.

Performance indicator	Dielectric elastomer	Shape memory alloy
$t_{sp,stall,vol} [\frac{Nm}{m^3}]$	$4.1 \cdot 10^5$	$1.7 \cdot 10^7$
$t_{sp,stall,m} [\frac{Nm}{kg}]$	$0.43 \cdot 10^3$	$2.6 \cdot 10^3$
$w_{sp,vol} [\frac{J}{m^3}]$	$2.1 \cdot 10^5$	$8.7 \cdot 10^6$
$w_{sp,m} [\frac{J}{kg}]$	$0.22 \cdot 10^3$	$1.3 \cdot 10^3$
$\eta_{half} [\%]$	90.2	7.82

Table 6.3: Performance indicators for both configurations with a RoM of $\theta = 30^\circ$, calculated according to Eq. 6.2, 6.3, 6.4 and 6.5

significant larger volume specific stall torques and work densities and a significant lower half-cycle efficiency than the dielectric elastomer configuration.

6.3.3. CASE STUDY

Based on the comparison with the simplified models an SMA configuration is chosen to use in the case study. A compliant rotational joint is designed to balance the external load of the forearm, and an antagonistic pair of SMA wires are used to actuate the system. The prototype is shown in Fig. 6.3a, where the green lines represents the compliant beams, and the yellow lines represents the antagonistic SMA wires. The compliant rotational joint consists of thin flexible preloaded beams of stainless steel (HSfolien art.nr. 80010, batch nr. 1725, width: $10mm$, $E = 196GPa$, $\sigma_{yield} = 1468 - 1484MPa$). The beams are clamped at both ends. One side is rigidly connected to the upper arm at a distance r_1 (Fig. 6.3b). The other side is clamped to a disc with radius r_2 that is rigidly connected to the forearm. From a numerical optimization with the finite element package ANSYS with the objective functions (1) maximal torque amplitude and (2) average percentage error over four measurement points of the torque deflection characteristic with respect to the sinusoid function it appears that the thickness of the beams should be $0.1mm$ to keep the stresses below the yield strength. To reach the required $3Nm$ to balance the forearm, a stack of 23 leaf springs is needed, with a joint on both sides of the arm. The optimized dimensions are $L = 67.1mm$, $\alpha = 2.31rad$, $\beta = 0.05rad$, $r_1 = 26mm$, and $r_2 = 7.5mm$ (Fig. 6.3b). The SMA actuator is made of NiTi (INGpuls NiTi SMA-wire, diameter: $0.5mm$, state: straight annealed, surface: oxidlayer, transition temperature: $90 - 110^\circ C$). The dimensions according to Fig. 6.1 are: $L = 250mm$ and $r = 5mm$. With a maximal strain of 5%, an angular displacement of $105deg$ can be reached at an activation temperature of $95^\circ C$.

Due to the specifications of the available measurement setup a prototype is fabricated with less leaf springs, to be able to measure the torque characteristic of the compliant joint. For the measurements four stacks of 7 beams are used on each side of the arm. In Fig. 6.4 the results of the torque characteristics of the system are shown. As can be seen in the figure, the torque generated by the compliant joint (T_{flex}) is in the same



Figure 6.3: The prototype (a), with the antagonistic actuator (yellow) along the upper arm and the compliant rotational joint (green) attached at the elbow of an artificial arm and (b) a schematic representation of one preloaded leaf spring in the compliant rotational joint.

Specification	
Volume [m^3]	$1.905 \cdot 10^{-4}$
Work to displace T_{out} [J]	1.38
Input energy W_{in} [J]	38.7
Total weight device [g]	382
Performance indicator	
Volume specific stall torque [Nm/m^3]	$5.77 \cdot 10^3$
Work density [J/m^3]	$7.27 \cdot 10^3$
Half-cycle efficiency [%]	3.6

Table 6.4: Specifications and performances of the design, based on measurements.

direction as the torque generated by the actuator and in the opposite direction as T_{out} . In other words, the stored energy is regained during actuation to increase the performance of the system.

PERFORMANCE

The volume, weight and the performances of the prototype are presented in Table 6.4, taking into account the isolation covers to protect the user from the moving parts in the joint and the hot SMA wires. The performances are based on a sinusoid external load, T_{out} , with an amplitude of $1.1 Nm$.

6.4. DISCUSSION

THE data in Table 6.1 is based on different sources with varying measurement standards. Therefore, this table can only be used as preliminary evaluation and not as a

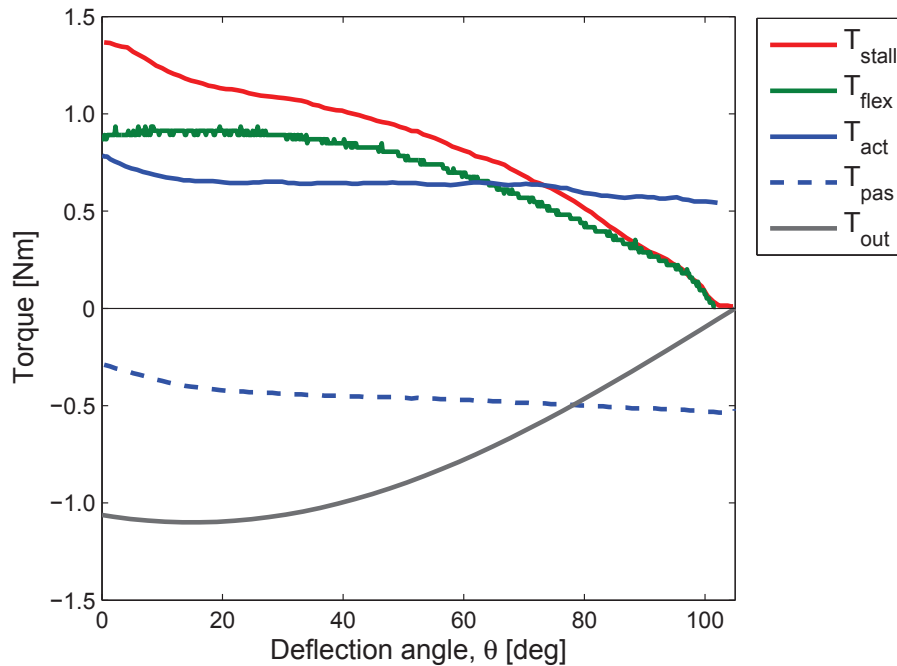


Figure 6.4: Results of the actuation curves of the prototype. The torque of the compliant joint (T_{flex}) is almost equal and opposite to the weight of the arm T_{out} , so it balances the arm. This results in a lower required actuation torque of the SMA actuator ($T_{act} + T_{pas}$).

qualitative analysis. Moreover, the values of strain rate, strain and block stress are based on maximally reported experimental data, so practical values may be lower [11].

The overview that combines the classes of the shape-changing materials and compliant rotational joints (Table 6.2) shows which interesting combinations of material and joints with high volume specific stall torques and high work densities will result in small and low-weight designs. The three materials with the highest preliminary performances are (1) dielectric elastomers, (2) conducting polymers and (3) SMA NiTi. Conducting polymers need a fluid to be actuated. This increases the volume and the mass of the actuator and it is not safe to use close to the body. In contrast to dielectric elastomers and SMA material, which can be actuated without additional material, although these materials (and especially the hot SMA wires) need to be isolated from the user.

The performances based on simplified models are lower than the performances based on assumptions and estimations. This indicates that the latter performances are not very accurate, and can only be used as rough estimation. For the simplified model calculations, several assumptions on the material properties are required. For example, the block stress and therefore the actuation torque T_{act} of the actuators is not constant over the range of motion and the passive effects of the actuator T_{pas} cannot be neglected. Therefore, it is more realistic to investigate these assumptions with detailed models of shape-changing materials, which is not considered in this study. Nevertheless, the results show a significant difference in performance between the two configurations, which indicates that there will be a significant difference in practice as well. The half-cycle efficiency, η_{half} , only considers the loading conditions of the system. However, it

does give an indication of the performance of the designs on a full cycle, although some energy stored in elasticity, heat or electricity can still be recovered.

As a case study to balance the forearm of a user, a compliant rotational joint is combined with an antagonistic SMA actuator. Due to the energy storage capacity of the compliant rotational joint, it is possible to use the joint to balance the weight of the arm. Because the center of rotation of the joint is not fixed it can passively auto-align itself with the elbow joint of the user. However, when a torque is generated the off-axial stiffness of the actuator will counteract the auto-alignment properties of the joint. The torque generated by the compliant joint of the prototype is less than the objective torque of $3Nm$, but has the right characteristic. The objective torque can be achieved by increasing the amount of stacked leaf springs up to 23. This will of course increase the volume of the joint, but it could stay within the $3cm$ available space. To reduce the number of stacked leaf springs other materials could be investigated. It should also be mentioned that the compliant joint is very sensitive to fabrication errors. But with the amount of stacked leaf springs the output torque can be altered. In addition, the antagonistic actuator does not yet generate the required torque of $1Nm$ either. The SMA wire is heated to $95^{\circ}C$ during measurements, which is within the transition temperatures. When the wires are heated above the transition temperature, they will be fully in the austenite phase and produce a significantly higher torque. However, the device should be very well isolated from the user. The low half-cycle efficiency of SMA wires should always be kept in mind. The amount of input energy should be sufficient during the period of use. In conclusion, with extra leaf springs in the joint and the SMA wires heated above the transition temperature, it seems possible to balance and actuate the forearm during activities of daily living.

6.5. CONCLUSIONS

THIS paper presents (1) an overview of the shape-changing-material-actuated large-deflection compliant rotational joints, (2) a benchmark model with new introduced performance indicators to evaluate the different actuation materials on performance with respect to volume or weight and (3) a case study for a design of an compact elbow joint actuated with SMA actuators.

The overview shows interesting unexplored areas of potential designs. The unexplored areas have become interesting by the benchmark model calculations, because they consist of designs that will have low-weights and low volumes based on estimations and assumptions.

Based on simplified models of SMA and a dielectric elastomer, it can be concluded that an SMA configuration has higher volume specific stall torques and work densities, while the dielectric elastomer configuration has a higher half-cycle efficiency based on a constant external load.

For a case study, the SMA configuration is combined with a compliant rotational joint for an assistive device. The property of a compliant joint to regain stored energy is used to counteract the torque of the forearm and balance its weight. Another advantage of the joint is its passive aligning properties with the elbow joint. When the strength in the arm is deteriorated too much for full passive support, the antagonistic SMA actuator is added for active support. Due to high transition temperature of the SMA wires it is im-

portant to isolate the device from the user very well. Due to the low half-cycle efficiency the amount of input energy should be sufficient for daily use. Furthermore, the positive off-axial stiffness of the antagonistic SMA actuator worsen the alignment properties of the device and a better alignment with the elbow joint is needed. Most importantly is that the device can be worn underneath the clothes. It is required to wear slightly larger clothes than the user normally do. Future work will focus on the control of the antagonistic SMA actuator. Furthermore, solutions need to be found for elbow alignment in combination with the antagonistic SMA actuator.

REFERENCES

- [1] D. H. Plettenburg, *Basic requirements for upper extremity prosthesis: the wilmer approach*, Annual International Conference of the IEEE Engineering in Medicine and Biology Society **20**, 2276 (1998).
- [2] S. help arm, <http://www.activeforever.com/swedish-help-arm>, (2013).
- [3] B. Mastebroek, E. De Haan, M. van den Berg, and J. L. Herder, *Development of a mobile arm support (armon): design evolution and preliminary user experience*, International Conference on Rehabilitation Robotics **24**, 1114 (2007).
- [4] Jaco of Focal Meditech, <http://www.focalmeditech.nl/in-dex.php/home/75-personal-robot-jaco>, (2013).
- [5] T. G. Sugar, J. He, E. J. Koeneman, J. B. Koeneman, R. Herman, H. Huang, R. S. Schultz, D. E. Herring, J. Wanberg, S. Balasubramanian, P. Swenson, and J. A. Ward, *Design and control of RUPERT: a device for robotic upper extremity repetitive therapy*, IEEE Transactions on Neural Systems and Rehabilitation Engineering **15**, 336 (2007).
- [6] A. G. Dunning and J. L. Herder, *A review of assistive devices for arm balancing*, International Conference on Rehabilitation Robotics , 6650485 (2013).
- [7] J. D. W. Madden, N. A. Vandesteeg, P. A. Anquetil, P. G. A. Madden, A. Takshi, R. Z. Pytel, S. R. Lafontaine, P. A. Wieringa, and I. W. Hunter, *Artificial muscle technology: physical principles and naval prospects*, IEEE Journal of Oceanic Engineering **29**, 706 (2004).
- [8] Y. Bar-Cohen and Q. Zhang, *Electroactive polymer actuators and sensors*, MRS bulletin **33**, 173 (2008).
- [9] L. L. Howell, *Compliant mechanisms* (Wiley-Interscience, New York, 2001) p. 459.
- [10] B. P. Trease, Y. M. Moon, and S. Kota, *Design of large-displacement compliant joints*, Journal of Mechanical Design **127**, 788 (2005).
- [11] Y. Bar-Cohen, *Electroactive polymer (EAP) actuators as artificial muscles: reality, potential, and challenges* (SPIE Press, 2001) p. 816.

- [12] P. J. White, S. Latscha, S. Schlaefer, and M. Yim, *Dielectric elastomer bender actuator applied to modular robotics*, IEEE/RSJ International Conference on Intelligent Robots and Systems, 408 (2011).
- [13] C. J. Van Andel, N. Wolterbeek, C. A. M. Doorenbosch, D. H. E. J. Veeger, and J. Harlaar, *Complete 3D kinematics of upper extremity functional tasks*, Gait & posture **27**, 120 (2008).
- [14] J. T. Smidts, *Heren vrijetijdsleding naar maat, vrijetijdsleding naar uw maat*, (2003).
- [15] D. Farhadi, N. Tolou, and J. L. Herder, *The scope for a compliant homokinetic coupling based on review of compliant joints and rigid-body constant velocity universal joints*, ASME International Design Engineering Technical Conference & Computers and Information in Engineering Conference **137**, 1 (2012).
- [16] S. Bi, T. Qiao, H. Zhao, and Y. Yao, *Analysis of annulus-shaped compliant pivot with series-parallel leaves*, Proceedings of the Institution of Mechanical Engineers, Part C: Journal of Mechanical Engineering Science **227**, 1090 (2012).
- [17] V. Giurgiutiu, C. A. Rogers, and Z. Chaudhry, *Energy-based comparison of solid-state induced-strain actuators*, Journal of intelligent material systems and structures **7**, 4 (1996).
- [18] R. Pelrine, R. Kornbluh, Q. Pei, and J. Joseph, *High-speed electrically actuated elastomers with strain greater than 100%*, Science **287**, 836 (2000).
- [19] P. Brochu and Q. Pei, *Advances in dielectric elastomers for actuators and artificial muscles*, Macromolecular rapid communications **31**, 10 (2010).
- [20] P. J. Cottinet, D. Guyomar, J. Galineau, and G. Sebald, *Electro-thermo-elastomers for artificial muscles*, Sensors and Actuators A: Physical **180**, 105 (2012).
- [21] R. Shankar, T. K. Ghosh, and R. J. Spontak, *Dielectric elastomers as next-generation polymeric actuators*, Soft Matter **3**, 1116 (2007).
- [22] J. Leng, X. Lan, Y. Liu, and S. Du, *Shape-memory polymers and their composites: stimulus methods and applications*, Progress in Materials Science **56**, 1077 (2011).
- [23] S. Rapp and H. Baier, *Determination of recovery energy densities of shape memory polymers via closed-loop, force-controlled recovery cycling*, Smart materials and structures **19**, 45018 (2010).
- [24] A. Price, A. Edgerton, C. Cocaud, H. Naguib, and A. Jnifene, *A study on the thermomechanical properties of shape memory alloys-based actuators used in artificial muscles*, Journal of intelligent material systems and structures **18**, 11 (2007).
- [25] M. Mertmann and G. Vergani, *Design and application of shape memory actuators*, The European Physical Journal Special Topics **158**, 221 (2008).

- [26] O. Benafan, J. Brown, F. T. Calkins, P. Kumar, A. Stebner, T. Turner, R. Vaidyanathan, J. Webster, and M. L. Young, *Shape Memory Alloy Actuator Design: CAsMART Collaborative Best Practices*, International Journal of Mechanics and Materials in Design **10**, 1 (2013).
- [27] M. Shahinpoor, Y. Bar-Cohen, J. O. Simpson, and J. Smith, *Ionic polymer-metal composites (IPMCs) as biomimetic sensors, actuators and artificial muscles—a review*, Smart Materials and Structures **7**, R15 (1999).
- [28] A. O’Halloran, F. O’Malley, and P. McHugh, *A review on dielectric elastomer actuators, technology, applications, and challenges*, Journal of Applied Physics **104**, 71101 (2008).
- [29] W. S. Chu, K. T. Lee, S. H. Song, M. W. Han, J. Y. Lee, H. S. Kim, M. S. Kim, Y. J. Park, K. J. Cho, and S. H. Ahn, *Review of biomimetic underwater robots using smart actuators*, International Journal of Precision Engineering and Manufacturing **13**, 1281 (2012).
- [30] F. Bauer, *Review on the properties of the ferrorelaxor polymers and some new recent developments*, Applied Physics A: Materials Science & Processing **107**, 567 (2012).
- [31] L. Sun, W. M. Huang, Z. Ding, Y. Zhao, C. C. Wang, H. Purnawali, and C. Tang, *Stimulus-responsive shape memory materials: a review*, Materials & Design **33**, 577 (2012).
- [32] V. A. Sujan, M. D. Lichter, and S. Dubowsky, *Lightweight hyper-redundant binary elements for planetary exploration robots*, IEEE/ASME International Conference on Advanced Intelligent Mechatronics **2**, 1273 (2001).
- [33] F. Carpi, R. Kornbluh, P. Sommer-Larsen, and G. Alici, *Electroactive polymer actuators as artificial muscles: are they ready for bioinspired applications?* Bioinspiration & Biomimetics **6**, 45006 (2011).
- [34] E. Smela, *Conjugated polymer actuators for biomedical applications*, Advanced Materials **15**, 481 (2003).
- [35] L. A. Hirano, M. T. Escote, L. S. Martins-Filho, G. L. Mantovani, and C. H. Scuracchio, *Development of artificial muscles based on electroactive ionomeric polymer-metal composites*, Artificial Organs **35**, 478 (2011).
- [36] G. Y. Lee, J. O. Choi, M. Kim, and S. H. Ahn, *Fabrication and reliable implementation of an ionic polymer–metal composite (IPMC) biaxial bending actuator*, Smart Materials and Structures **20**, 105026 (2011).
- [37] K. J. Kim and S. Tadokoro, *Electroactive Polymers for Robotic Applications: Artificial Muscles and Sensors* (Springer, 2007) p. 281.
- [38] S. Oehler, D. Hartl, and D. C. Lagoudas, *Analysis and optimization of improved hybrid SMA flexures for high rate actuation*, SPIE, Smart Structures and Materials **7979**, 797907 (2011).

- [39] X. Lan, Y. Liu, H. Lv, X. Wang, J. Leng, and S. Du, *Fiber reinforced shape-memory polymer composite and its application in a deployable hinge*, Smart Materials and Structures **18**, 24002 (2009).
- [40] D. Ratna and J. Karger-Kocsis, *Recent advances in shape memory polymers and composites: a review*, Journal of Materials Science **43**, 254 (2008).
- [41] M. Sreekumar, T. Nagarajan, and M. Singaperumal, *Experimental investigations of the large deflection capabilities of a compliant parallel mechanism actuated by shape memory alloy wires*, Smart Materials and Structures **17**, 65025 (2008).
- [42] K. Yang and C. L. Gu, *A novel robot hand with embedded shape memory alloy actuators*, Proceedings of the Institution of Mechanical Engineers, Part C: Journal of Mechanical Engineering Science **216**, 737 (2002).
- [43] J. H. Crews and G. D. Buckner, *Design optimization of a shape memory alloy-actuated robotic catheter*, Journal of Intelligent Material Systems and Structures **23**, 545 (2012).
- [44] S. J. Furst, R. Hangekar, and S. Seelecke, *Development, assembly, and validation of an SMA-actuated two-joint nozzle and six-channel power supply for use in a smart inhaler system*, Proceedings of SPIE - Active and Passive Smart Structures and Integrated Systems **7643**, 76430J (2010).
- [45] S. J. Furst and S. Seelecke, *Experimental validation of different methods for controlling a flexible nozzle using embedded SMA wires as both positioning actuator and sensor*, Proceedings of SPIE - Behavior and Mechanics of Multifunctional Materials and Composites **7978**, 79781K (2011).
- [46] Y. Fu, X. Li, S. Wang, H. Liu, and Z. Liang, *Research on the axis shape of an active catheter*, The International Journal of Medical Robotics and Computer Assisted Surgery **4**, 69 (2008).
- [47] J. H. Wang, C. H. Fan, and C. C. Lan, *A two-way flexural rotation manipulator using opposing shape memory alloy wires*, IEEE/ASME International Conference on Advanced Intelligent Mechatronics , 6 (2009).
- [48] E. Torres-Jara, K. Gilpin, J. Karges, R. J. Wood, and D. Rus, *Compliant modular shape memory alloy actuators*, Robotics & Automation Magazine **17**, 78 (2010).
- [49] P. Singh and G. K. Ananthasuresh, *A Compact and Compliant External Pipe-Crawling Robot*, IEEE Transactions on Robotics **29**, 251 (2013).
- [50] F. Auffinger, M. Fisher, and M. Maddux, *Shape memory polymer (SMP) actuation technology*, in *Proceedings of SPIE - Sensors and Smart Structures Technologies for Civil, Mechanical, and Aerospace Systems*, Vol. 7647 (2010) p. 76473A.
- [51] Y. Liu, *The work production of shape memory alloy*, Smart materials and structures **13**, 552 (2004).

II-A

CLOSE-TO-BODY SPRING SYSTEMS

This sub-part elaborates the concept to use normal or rubber springs as balancing mechanism, in combination with a serial linkages without auxiliary links. This concept is a combination of the rubber bands and rubber branches concepts that are described in Chapter 4. First, in Chapter 7, the theoretical background and technical analysis of such spring systems is described. With this analysis it is possible to design spring configurations that are close to the body. In this chapter, two springs configurations are described for an arm support: a 2-springs configuration (elaborated in Chapter 11), and a 2-parallel-springs configuration, with two bi-articular springs parallel to the upper arm running from the trunk to the forearm (the embodiment of the spring configurations can be seen in elaborated in Chapter 12). In Chapter 8, a spring configuration with three springs (one bi-articular spring from trunk to forearm, and two mono-articular springs from upper arm to trunk and forearm, respectively) is elaborated and evaluated (the embodiment of the spring configurations can be seen in elaborated in Chapter 12). In Chapter 9, the different spring configurations are compared to each other on the balancing quality and the tuning rules. A choice has been made for a spring configuration that is best to apply in a close-to-body arm support.

7

CARTESIAN BASED STIFFNESS MATRIX APPROACH & GRAPHICAL REPRESENTATION TO STATICALLY BALANCE SERIAL LINKAGES

Submitted as:

M.P. Lustig, A.G. Dunning, J.L. Herder,
*Cartesian based stiffness matrix approach and graphical
representation to statically balance serial linkages*,
Submitted to Mechanism and Machine Theory, march 2016.

A slightly shorter and altered version of this chapter appeared as:

M.P. Lustig, A.G. Dunning, J.L. Herder,
*Parameter analysis for the design of statically balanced serial linkages
using a stiffness matrix approach with cartesian coordinates*,
14th IFToMM World Congress (2015).

This chapter describes the theoretical background and technical analysis of statically balanced serial linkages. This part has two objectives. The first is to describe the design of such linkages based on the stiffness matrix approach, based on Cartesian coordinates. With this method is much more user friendly and results in less complex design equations. Contrary to current literature, the spring attachment points to the world can be chosen freely with this method and it is much easier to describe such an attachment point in the Cartesian coordinate system. The second objective is to show this method with two illustrative examples. The behavior of each spring configuration is elaborated and visualized.

ABSTRACT

A statically balanced system is in equilibrium in every pose, by maintaining a constant potential energy level. In classical solutions for balancing serial linkages, each DOF is balanced by an independent element (counter-mass or mono-articular spring). Disadvantages are increased mass and inertia for counter-mass elements, and the need for auxiliary links for spring solutions. Recent literature presents a method for balancing serial linkages without auxiliary links; using multi-articular springs. This method obtains constraint equations from the stiffness matrix. Downsides are different coordinate systems for describing locations and states, and set criteria constraining attachments to fixed lines. In the present paper the stiffness matrix approach is implemented using a consistent Cartesian coordinate system. Goal is to compare the use of this single coordinate system to the use of multiple coordinate systems for this method, and to obtain an increased insight and a visualization of the relations between different parameters. The Cartesian coordinates are implemented successfully, resulting in a simpler, more intuitive method for designing statically balanced serial linkages. Furthermore, obtained parameter relations are visualized in two examples providing knowledge about how systems parameters can be changed while balance is maintained. One example showed simplified relations, where the balancing conditions and adjustment rules are defined in two simple design equations. This also provides a building block to design balanced complex multi-articulated serial linkages.

7.1. INTRODUCTION

A system which is in equilibrium in every motionless state is called statically balanced. For such systems the potential energy level remains constant in every pose [1]. This constant energy level greatly reduces operational effort as only dynamic effects remain to be overcome during motion. Many applications for static balancing exist due to these benefits [1–4].

Different techniques exist to statically balance the rotation of a rigid pendulum. A simple option is adding a counter-mass [1], downside of which is the increased mass and inertia [5]. A second option is connecting a zero-free-length spring (ZFLS) between the link and fixed world [1]. For a ZFLS the spring force is proportional to its length. Other less common solutions use a non-circular cam [6] or compliant flexure elements [7]. These solutions are all designed to balance a single degree of freedom (DOF).

Solutions for balancing a serial linkage with multiple DOFs make use of counter-mass or ZFLSs. In the first case a counter-mass is added to each link [8, 9], additional auxiliary links allow counter-mass relocation [10]. Inertia increase becomes a greater problem as added weights of distal counter-masses must be balanced as well. Classical ZFLS solutions require a parallel beam construction providing a link with fixed orientation at each joint [1, 11, 12]. Each link is balanced by a single ZFLS that spans the joint of the respective link, a mono-articular spring. The disadvantage of parallel beams are an increased complexity and added inertia. In these systems each DOF is balanced by an independent balancing element.

Recent literature presents two methods in which ZFLSs can span multiple joints to balance serial linkages without parallel beams. The first method is the stiffness matrix approach by Lin et al. [12–15]. Energy equations are set up in a general form $U = \frac{1}{2} \mathbf{Q}^T \mathbf{K} \mathbf{Q}$, separating states \mathbf{Q} and parameters in a stiffness matrix \mathbf{K} . Off-diagonal elements of \mathbf{K} contain state dependent energy terms, constraining these terms equal to zero results in a statically balanced system [13]. The second method is an iterative method developed by Deepak and Ananthasuresh [16]. Balance is ensured link by link, in steps, starting at the most distal link. At each step, balance of a specific link is acquired by adding up to two ZFLSs between this link and fixed world. For each link only energy terms of the current and previous step links affect its constraint equations [16]. In these two methods each DOF is balanced by combined efforts of multiple ZFLSs.

Both methods can create statically balanced serial linkages and are based on an energy approach. Nevertheless, multiple differences exist in ease of implementation and capabilities. The first is that in Lin's method all constraints are obtained at once for a chosen spring configuration, whereas in Deepak's method only a selection of the constraints is evaluated at once. If no straightforward solution is found, Deepak's method explains which spring(s) can be added for a solvable system, Lin's method does not directly. However, information on which links are unbalanced and thus require additional springs can be extracted from the stiffness matrix [15]. Another difference is that all springs are connected to the fixed world in Deepak's method while in Lin's method springs can be attached in between any two links, i.e. additional constraints are provided considering these springs. Finally, Deepak's method allows planar placement of spring attachments while in Lin's method criteria are set up constraining attachments to be located on fixed straight lines [15].

In the present paper the stiffness matrix approach is selected for calculating balanced linkages as it provides all constraints at once and allows additional spring placement options. The exact implementation however is altered. Current literature describes locations on links using polar coordinate systems, while states are described using unit vectors (xy-components). In the present paper Cartesian (xy-) coordinates are used describing link locations as well as the states.

Three goals are formulated in the present paper. The first goal is to implement Cartesian coordinates in the stiffness matrix approach for balanced serial linkages to investigate its benefits over using a polar coordinate system. The second goal is to gain more insight in the relations between different parameters of this method in the design space, for instance it will be investigated if placement of springs outside the vertical straight lines is allowed. The third goal is to visualize these behavioral relations in two examples. The first example uses a new spring configuration with two bi-articular ZFLSs, both between the fixed world and the second link (Fig. 7.2b). The spring configuration is parameterized such that transparent design equations are obtained. The second example is based on the spring configuration as described in [12] (Fig. 7.2c).

The structure of this paper is as follows. First, in the second section the Cartesian coordinate stiffness matrix approach is derived. In the next section two examples of balanced linkages are presented of which the behavior is analyzed. Finally, the use of Cartesian and polar coordinates are compared and discussion and conclusions concerning the set goals are obtained.

7.2. METHOD

THIS paper proposes the use of Cartesian coordinates in the stiffness matrix approach for designing serial statically balanced linkages. This is in contrast to the polar coordinate system used in current literature on this method [12–15]. In the present paper, the locations of spring attachments, joints and centers of mass (CoMs) are described using (local) x- and y- coordinates on the respective links they are located on. In this section, the assumptions are explained first, followed by the full derivation of the stiffness matrix approach using xy-coordinates.

7.2.1. ASSUMPTIONS AND LIMITATIONS

The presented method is set up for planar linkages, the gravitational field acting in this plane has constant magnitude and direction. The links are connected to each other and/or the fixed world using revolute joints. All springs have linear ZFLS behavior and the mass of these springs is neglected. Mechanical limits of links/springs colliding with one another are not taken into account. The fixed world is assumed to be rigid and static.

7.2.2. DERIVATION OF STIFFNESS MATRIX

The stiffness matrix approach is derived in five steps. First all coordinate points are described as a function of the link states and parameter values. The second step is setting up potential energy equations for all spring and mass components and writing these equations in a generalized form. The third step is to combine the energy equations of the different components to obtain the total stiffness matrix. The fourth step is obtain-

ing the constraint equations for balance from the stiffness matrix. The fifth and final step is focused on how to solve the obtained equations. The equations are set up for an n link system where the fixed world is link 1, as a result the system has $n - 1$ moving links.

STEP 1: COORDINATE VECTORS

The state of link u is described by global unit vector \mathbf{q}_u (Fig. 7.1a). The fixed world vector \mathbf{q}_1 is constant, aligned with the global x -axis. For moving links ($u = 2 \cdots n$) vector \mathbf{q}_u is aligned with the local x_u -axis. The origin of each local coordinate system is located at the proximal joint J_{u-1} . The y_u -axis are orientated perpendicular to the respective x_u -axis. A unit vector in this y_u direction is obtained by rotating the state vector \mathbf{q}_u by 90° using rotation matrix \mathbf{R} . Combined state vector \mathbf{Q} holds the states of all n -links.

$$\mathbf{q}_1 = \begin{bmatrix} 1 \\ 0 \end{bmatrix} \quad (7.1a)$$

$$\mathbf{q}_u = \begin{bmatrix} q_{xu} \\ q_{yu} \end{bmatrix} \quad (7.1b)$$

$$\mathbf{Q} = \begin{bmatrix} \mathbf{q}_1 \\ \vdots \\ \mathbf{q}_n \end{bmatrix} \quad (7.1c)$$

$$\mathbf{I} = \begin{bmatrix} 1 & 0 \\ 0 & 1 \end{bmatrix} \quad (7.1d)$$

$$\mathbf{R} = \begin{bmatrix} \cos(90^\circ) & -\sin(90^\circ) \\ \sin(90^\circ) & \cos(90^\circ) \end{bmatrix} = \begin{bmatrix} 0 & -1 \\ 1 & 0 \end{bmatrix} \quad (7.1e)$$

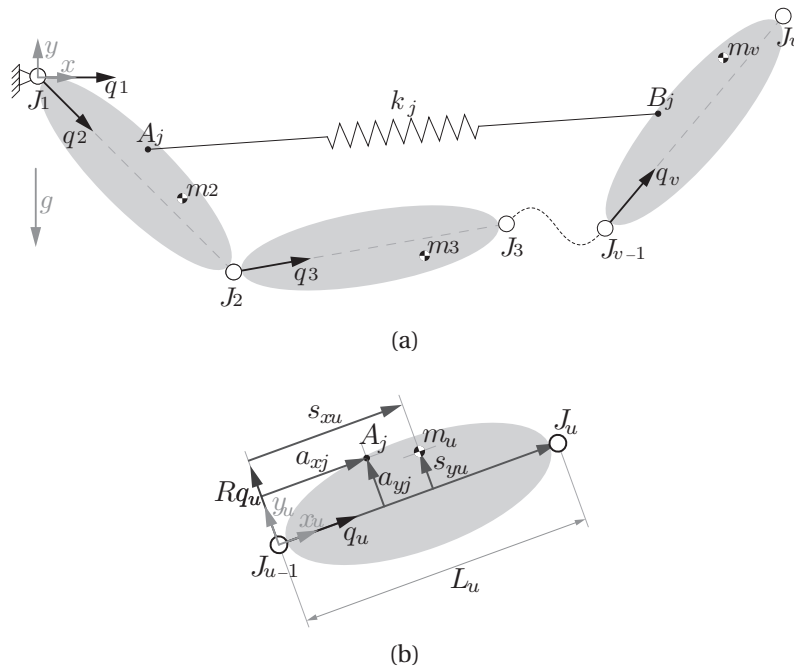


Figure 7.1: (a) Schematic representation of a serial linkage in a state defined by unit vectors \mathbf{q} , reproduced from [14]. (b) Parameterization of locations on link u in the Cartesian form.

Global coordinates of all point on the links are described as a linear combination of the state vectors and constant parameter values. Joint locations are described first. As said, fixed world joint J_1 is located in the global origin. The distal joint J_u of a link u is always located on the local x_u -axis at distance L_u from the local origin (Fig. 7.1b). Vector components of joint locations are set up in equation 7.2.

$$J_1 = \begin{bmatrix} 0 \\ 0 \end{bmatrix} \quad (7.2a)$$

$$J_u = L_2 \mathbf{I} \mathbf{q}_2 + L_3 \mathbf{I} \mathbf{q}_3 + \cdots + L_u \mathbf{I} \mathbf{q}_u = \sum_{i=2}^u L_i \mathbf{I} \mathbf{q}_i = J_{u-1} + L_u \mathbf{I} \mathbf{q}_u \quad (7.2b)$$

Spring attachment point locations for a spring j between link u to link v are A_j and B_j respectively. These locations are a linear combination of the proximal joint component J_{u-1} , the local x_u component ($a_{xj} \mathbf{I} \mathbf{q}_u$) and the local y_u component ($a_{yj} \mathbf{R} \mathbf{q}_u$) (Eq. 7.3). A schematic representation containing these components is given in Fig. 7.1b.

$$A_j = J_{u-1} + (a_{xj} \mathbf{I} + a_{yj} \mathbf{R}) \mathbf{q}_u \quad (7.3a)$$

$$B_j = J_{v-1} + (b_{xj} \mathbf{I} + b_{yj} \mathbf{R}) \mathbf{q}_v \quad (7.3b)$$

7

Similarly the CoM location of link u is set up (Eq. 7.4).

$$S_u = J_{u-1} + (s_{xu} \mathbf{I} + s_{yu} \mathbf{R}) \mathbf{q}_u \quad (7.4)$$

STEP 2: ENERGY EQUATIONS AND GENERALIZED FORM

This step is to write energy equations in the generalized form, separating the states \mathbf{Q} and the parameters in the stiffness matrix \mathbf{K} .

$$U = \frac{1}{2} \mathbf{Q}^T \mathbf{K} \mathbf{Q} \quad (7.5)$$

Spring energy is expressed in this form first. The vector describing spring length and orientation for spring j , going from link u to link v , is $\mathbf{B}_j - \mathbf{A}_j$. This is as a function of the states, because the locations of points \mathbf{B}_j and \mathbf{A}_j are state dependent as well. The expression for this spring vector is derived in equation 7.6. An expression is obtained where constants are separated for each state (Eq. 7.6e). The components \mathbf{C} holding these constant parameters are shown in matrix form (Eq. 7.7).

$$\mathbf{B}_j - \mathbf{A}_j = J_{v-1} - J_{u-1} - (a_{xj}\mathbf{I} + a_{yj}\mathbf{R})\mathbf{q}_u + (b_{xj}\mathbf{I} + b_{yj}\mathbf{R})\mathbf{q}_v \quad (7.6a)$$

$$J_{v-1} - J_{u-1} = J_u + J_{u+1} + \cdots + J_{v-1} = \sum_{n=u}^{v-1} L_n \mathbf{I} \mathbf{q}_n \quad (7.6b)$$

$$\mathbf{B}_j - \mathbf{A}_j = -(a_{xj}\mathbf{I} + a_{yj}\mathbf{R})\mathbf{q}_u + \sum_{n=u}^{v-1} L_n \mathbf{I} \mathbf{q}_n + (b_{xj}\mathbf{I} + b_{yj}\mathbf{R})\mathbf{q}_v \quad (7.6c)$$

$$= \underbrace{((L_u - a_{xj})\mathbf{I} - a_{yj}\mathbf{R})\mathbf{q}_u}_{\mathbf{C}_u} + \underbrace{\sum_{n=u+1}^{v-1} L_n \mathbf{I} \mathbf{q}_n}_{\mathbf{C}_{u+1} + \cdots + \mathbf{C}_{v-1}} + \underbrace{(b_{xj}\mathbf{I} + b_{yj}\mathbf{R})\mathbf{q}_v}_{\mathbf{C}_v} \quad (7.6d)$$

$$= \sum_{n=1}^v \mathbf{C}_n \mathbf{q}_n \quad (7.6e)$$

$$\mathbf{C}_u = \begin{bmatrix} L_u - a_{xj} & a_{yj} \\ -a_{yj} & L_u - a_{xj} \end{bmatrix} \quad (7.7a)$$

$$\mathbf{C}_i = \begin{bmatrix} L_i & 0 \\ 0 & L_i \end{bmatrix}, \text{ for } i = u+1, \dots, v-1 \quad (7.7b)$$

$$\mathbf{C}_v = \begin{bmatrix} b_{xj} & -b_{yj} \\ b_{yj} & b_{xj} \end{bmatrix} \quad (7.7c)$$

$$\mathbf{C}_i = \begin{bmatrix} 0 & 0 \\ 0 & 0 \end{bmatrix}, \text{ for } \begin{cases} i = 1, \dots, u-1 \\ i = v+1, \dots, n \end{cases} \quad (7.7d)$$

Knowing the spring length as a function of the states its potential energy can be calculated. The equation is set up for a ZFLS j with stiffness k_j (Eq. 7.8a) and rewritten in the generalized form (Eq. 7.8d). In this form the states (\mathbf{Q}) are separated from the parameters in the stiffness matrix of the spring ($\mathbf{K}_{s,j}$).

$$U_{s,j} = \frac{1}{2} k_j (\mathbf{B}_j - \mathbf{A}_j)^2 \quad (7.8a)$$

$$= \frac{1}{2} k_j \left(\sum_{u=1}^n \mathbf{C}_u \mathbf{q}_u \right)^2 \quad (7.8b)$$

$$= \frac{1}{2} k_j \begin{bmatrix} \mathbf{q}_1 \\ \vdots \\ \mathbf{q}_n \end{bmatrix}^T \begin{bmatrix} \mathbf{C}_1^T \mathbf{C}_1 & \cdots & \mathbf{C}_1^T \mathbf{C}_n \\ \vdots & \ddots & \vdots \\ \mathbf{C}_n^T \mathbf{C}_1 & \cdots & \mathbf{C}_n^T \mathbf{C}_n \end{bmatrix} \begin{bmatrix} \mathbf{q}_1 \\ \vdots \\ \mathbf{q}_n \end{bmatrix} \quad (7.8c)$$

$$= \frac{1}{2} \mathbf{Q}^T \mathbf{K}_{s,j} \mathbf{Q} \quad (7.8d)$$

$$\mathbf{K}_{s,j} = k_j \begin{bmatrix} \mathbf{C}_1^T \mathbf{C}_1 & \cdots & \mathbf{C}_1^T \mathbf{C}_n \\ \vdots & \ddots & \vdots \\ \mathbf{C}_n^T \mathbf{C}_1 & \cdots & \mathbf{C}_n^T \mathbf{C}_n \end{bmatrix} \quad (7.8e)$$

Next, the gravitational energy is expressed in the generalized form of equation 7.5. The height of the masses is found in the second element of vector \mathbf{S}_u , containing the global CoM y-coordinate of link u . The value for height is extracted by vector product: $height = [0 \ 1] \mathbf{S}_u$. This product is not yet expressed as in the generalized form because \mathbf{S}_u does not contain multiplications of states. By using state \mathbf{q}_1 , which is located on the fixed world, it is known that $(\mathbf{R}\mathbf{q}_1)^T = [0 \ 1]$, describing the gravitational field direction. Therefore the height of a mass is expressed as in the generalized form by product: $height = (\mathbf{R}\mathbf{q}_1)^T \mathbf{S}_u$. Based on this term the energy equations are first written for the mass of a single link u (Eq. 7.9) followed by a summed relation containing the masses of all links (Eq. 7.10). For this form the constant components \mathbf{D}_u that fill the stiffness matrix are described (Eq. 7.11), followed by the generalized form of the energy equation (Eq. 7.12).

$$U_{m_u} = m_u g (\mathbf{R}\mathbf{q}_1)^T \mathbf{S}_u \quad (7.9a)$$

$$U_{m_u} = m_u g \mathbf{q}_1^T \mathbf{R}^T \mathbf{S}_u \quad (7.9b)$$

$$U_{m_u} = m_u g \mathbf{q}_1^T \mathbf{R}^T [\mathbf{J}_{u-1} + (s_{xu}\mathbf{I} + s_{yu}\mathbf{R})\mathbf{q}_u] \quad (7.9c)$$

$$U_{m_u} = m_u g \mathbf{q}_1^T \mathbf{R}^T \left[\sum_{i=1}^{u-1} (L_i \mathbf{q}_i) + (s_{xu}\mathbf{I} + s_{yu}\mathbf{R})\mathbf{q}_u \right] \quad (7.9d)$$

Effect of combined mass of all links, for a linkage with n links (and thus $n - 1$ moving links) is given (Eq. 7.10).

$$U_{\Sigma m} = \sum_{u=2}^n U_{m_u} \quad (7.10a)$$

$$= \mathbf{q}_1^T \sum_{u=2}^n \left(\mathbf{R}^T m_u g \left[\sum_{i=1}^{u-1} (L_i \mathbf{q}_i) + (s_{xu}\mathbf{I} + s_{yu}\mathbf{R})\mathbf{q}_u \right] \right) \quad (7.10b)$$

$$= \mathbf{q}_1^T \sum_{u=2}^n \left(\underbrace{\mathbf{R}^T \left[\left(\sum_{i=u+1}^n m_i \right) g L_u \mathbf{I} + m_u g (s_{xu}\mathbf{I} + s_{yu}\mathbf{R}) \right]}_{\mathbf{D}_u} \mathbf{q}_u \right) \quad (7.10c)$$

The components \mathbf{D}_u are directly obtained from equation 7.10c and are rewritten in matrix form (Eq. 7.11).

$$\mathbf{D}_u = \mathbf{R}^T \left[\left(\sum_{i=u+1}^n m_i \right) g L_u \mathbf{I} + m_u g (s_{xu}\mathbf{I} + s_{yu}\mathbf{R}) \right] \quad (7.11a)$$

$$= \begin{bmatrix} m_u g s_{yu} & m_u g s_{xu} + \left(\sum_{i=u+1}^n m_i \right) g L_u \\ -m_u g s_{xu} - \left(\sum_{i=u+1}^n m_i \right) g L_u & m_u g s_{yu} \end{bmatrix} \quad (7.11b)$$

The generalized form $U_{\Sigma m}$ is obtained as states and parameters are separated.

$$U_{\Sigma m} = \frac{1}{2} \mathbf{Q}^T \mathbf{K}_m \mathbf{Q} \quad (7.12a)$$

$$\mathbf{K}_m = \begin{bmatrix} \mathbf{O} & \mathbf{D}_2 & \cdots & \mathbf{D}_n \\ \mathbf{D}_2^T & \mathbf{O} & \cdots & \mathbf{O} \\ \vdots & \vdots & \ddots & \vdots \\ \mathbf{D}_n^T & \mathbf{O} & \cdots & \mathbf{O} \end{bmatrix} \quad (7.12b)$$

When analyzing a new system it is possible to quickly set up the stiffness matrices without having to go through all derivations performed in this step. It is advised to directly substitute the component matrices for the springs \mathbf{C}_u (Eq. 7.7a-d) and the mass components \mathbf{D}_u (Eq. 7.11). By substituting these component matrices in equation 7.8e and 7.12b the stiffness matrix $\mathbf{K}_{s,j}$ and \mathbf{K}_m are obtained.

STEP 3: TOTAL STIFFNESS MATRIX

The combined energy U_t , containing all spring and mass terms is obtained by combining the spring and mass stiffness matrices (Eq. 7.13).

$$U_t = \frac{1}{2} \mathbf{Q}^T \mathbf{K}_t \mathbf{Q} \quad (7.13a)$$

$$\mathbf{K}_t = \left(\sum_{i=1}^{n_{springs}} \mathbf{K}_{s,i} \right) + \mathbf{K}_m \quad (7.13b)$$

STEP 4: CONSTRAINT EQUATIONS

In a balanced system, any state can be changed freely with respect to any other state without changing the overall potential energy level. For this to be the case, the effective stiffness between any two different states should be equal to zero. The effective stiffness terms for these relative rotations are found on the off-diagonal part of the stiffness matrix \mathbf{K}_t [14]. As a result, all off-diagonal parts of the \mathbf{K}_t matrix are constrained to be equal to zero for balance [13].

The number of constraint equations depends on the size of the \mathbf{K}_t matrix, which in turn depends on the number of links n . The matrices are symmetrical, thus all relations are found in the upper triangular part (Eq. 7.8e, 7.12b). Additionally, all relations in one of these triangular parts occur twice, once in each even and uneven row. Thus only every other row has to be examined to obtain all relations. Altogether the amount of constraint equations for an n -link system is equal to $n(n-1)$ [14].

STEP 5: OBTAIN BALANCE BY SOLVING CONSTRAINT EQUATIONS

The next step is solving the obtained constraint equations. In general, the minimal amount of variables to be calculated is equal to the number of equations. For example, for a three link planar system the number of constraint equations is equal to six and as a result at least six parameters should be left free while solving such a system. The remaining parameters can be selected to have constant values.

7.3. APPLICATION AND BEHAVIOR

IN this section two illustrative examples of balanced linkages are presented. The behavior of the balanced systems is analyzed, to gain a better understanding of how different parameters can be changed while maintaining the desired balance. Increased insight in the inner workings of the system will allow for a more efficient design process and a better overview of possible solutions. Found relations for varying parameters while maintaining balance are provided and visualized. The system studied in both examples has two moving links (Fig. 7.2a). It is balanced using two different spring configurations. In example 1 the spring configuration of Fig. 7.2b is used, having two bi-articular springs. In example 2 the configuration of Fig. 7.2c is used, having a mono- and bi-articular springs. The steps described in the methods section provide guidance in both examples.

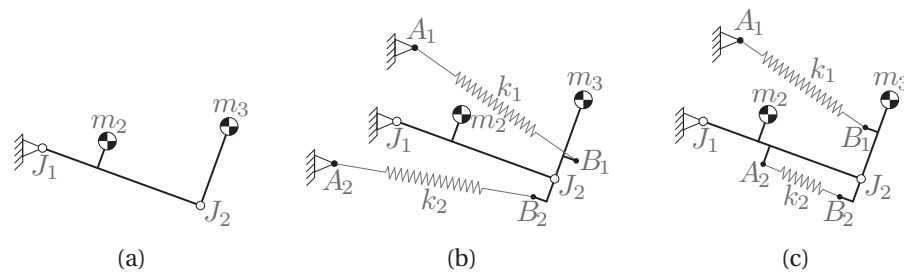


Figure 7.2: (a) Unbalanced linkage. (b) Spring configuration of example 1. (c) Spring configuration of example 2.

7.3.1. EXAMPLE 1

Two bi-articular springs are used to balance the system both connecting the fixed world to link 3 (Fig. 7.2b). In the first step the system locations in Fig. 7.2b are expressed in xy -coordinates as in Fig. 7.1b. The actual location vectors (Eq. 7.2-7.4) are not shown as their creation is not required for continuing in this method, nevertheless they are useful, for instance, to plot the system. In the second step the component matrices for the two springs C_1 and C_2 (Eq. 7.14a, 7.14b) and the mass terms D (Eq. 7.14c) are constructed based on equations 7.7 and 7.11. By substituting these component matrices in equations 7.8e and 7.12b the spring matrices K_{s1} , K_{s2} and mass stiffness matrix K_m are obtained (Eq. 7.15). The third step is to construct the total stiffness matrix by combining the spring and mass matrices (Eq. 7.15). In the fourth step the constraint equations are obtained from the K_t matrix (Eq. 7.16). The constraint equations to be satisfied for balance are the off-diagonal parts of the K_t matrix set equal to zero. Only terms in odd rows (1 and 3) are considered as the even rows hold exactly the same relations.

$$C_{1,1} = \begin{bmatrix} -a_{x1} & a_{y1} \\ -a_{y1} & -a_{x1} \end{bmatrix}; \quad C_{1,2} = \begin{bmatrix} L_2 & 0 \\ 0 & L_2 \end{bmatrix}; \quad C_{1,3} = \begin{bmatrix} b_{x1} & -b_{y1} \\ b_{y1} & b_{x1} \end{bmatrix} \quad (7.14a)$$

$$C_{2,1} = \begin{bmatrix} -a_{x2} & a_{y2} \\ -a_{y2} & -a_{x2} \end{bmatrix}; \quad C_{2,2} = \begin{bmatrix} L_2 & 0 \\ 0 & L_2 \end{bmatrix}; \quad C_{2,3} = \begin{bmatrix} b_{x2} & -b_{y2} \\ b_{y2} & b_{x2} \end{bmatrix} \quad (7.14b)$$

$$\mathbf{D}_1 = \begin{bmatrix} 0 & 0 \\ 0 & 0 \end{bmatrix}; \mathbf{D}_2 = \begin{bmatrix} m_2 g s_{y2} & m_3 g L_2 + m_2 g s_{x2} \\ -m_3 g L_2 - m_2 g s_{x2} & m_2 g s_{y2} \end{bmatrix};$$

$$\mathbf{D}_3 = \begin{bmatrix} m_3 g s_{y3} & m_3 g s_{x3} \\ -m_3 g s_{x3} & m_3 g s_{y3} \end{bmatrix} \quad (7.14c)$$

$$\mathbf{K}_{si} = \frac{1}{2} k_i \begin{bmatrix} \mathbf{C}_{i,1}^T \mathbf{C}_{i,1} & \mathbf{C}_{i,1}^T \mathbf{C}_{i,2} & \mathbf{C}_{i,1}^T \mathbf{C}_{i,3} \\ \text{sym} & \mathbf{C}_{i,2}^T \mathbf{C}_{i,2} & \mathbf{C}_{i,2}^T \mathbf{C}_{i,3} \\ & & \mathbf{C}_{i,3}^T \mathbf{C}_{i,3} \end{bmatrix}; \quad \mathbf{K}_m = \begin{bmatrix} \mathbf{O} & \mathbf{D}_2 & \mathbf{D}_3 \\ & \mathbf{O} & \mathbf{O} \\ \text{sym} & & \mathbf{O} \end{bmatrix};$$

$$\mathbf{K}_t = \mathbf{K}_{s1} + \mathbf{K}_{s2} + \mathbf{K}_m \quad (7.15)$$

$$\mathbf{K}_t(1,3) = 0 = -k_1 a_{x1} L_2 - k_2 a_{x2} L_2 + m_2 g s_{y2} \quad (7.16a)$$

$$\mathbf{K}_t(1,4) = 0 = -k_1 a_{y1} L_2 - k_2 a_{y2} L_2 + m_2 g s_{x2} + m_3 g L_2 \quad (7.16b)$$

$$\mathbf{K}_t(1,5) = 0 = -k_1 (a_{x1} b_{x1} + a_{y1} b_{y1}) - k_2 (a_{x2} b_{x2} + a_{y2} b_{y2}) + m_3 g s_{y3} \quad (7.16c)$$

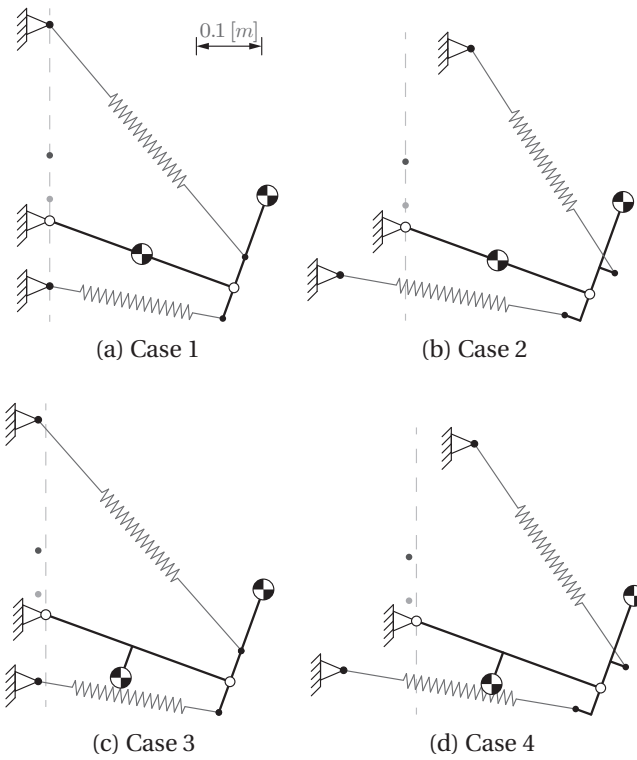
$$\mathbf{K}_t(1,6) = 0 = k_1 (a_{x1} b_{y1} - a_{y1} b_{x1}) + k_2 (a_{x2} b_{y2} - a_{y2} b_{x2}) + m_3 g s_{x3} \quad (7.16d)$$

$$\mathbf{K}_t(3,5) = 0 = k_1 b_{x1} L_2 + k_2 b_{x2} L_2 \quad (7.16e)$$

$$\mathbf{K}_t(3,6) = 0 = -k_1 b_{y1} L_2 - k_2 b_{y2} L_2 \quad (7.16f)$$

In the final step constraints are solved for four different cases, each showing different behavior (Fig. 7.3). Between these cases some general properties of the system are kept the same, specifically spring stiffness, mass and link length values. In each case, the constraints are solved for parameters a_{x1} , a_{y1} , a_{x2} , a_{y2} , b_{x1} and b_{y1} , describing spring attachment locations A_1 , A_2 and B_1 . Varied between cases are parameters b_{x2} and b_{y2} , describing the location of B_2 , while keeping the distance between joint J_2 and B_2 equal. Furthermore s_{x2} and s_{y2} are varied, describing the location of the CoM of link 2, while keeping the distances from joint J_1 to the CoM the same. Summarized parameter values of balanced configurations are found in Table 7.3e. Parameters on the first six rows (above the horizontal line) are calculated by solving the constraints, remaining parameter values (under the line) are chosen inputs.

Case 1 presents the general balanced configuration of this example (Fig. 7.3a). Here, spring attachment points, CoM locations and joints are aligned on each link. In case 2, spring attachment B_2 is rotated by an angle of -30° about joint J_2 with respect to the aligned orientation (Fig. 7.3b). Thus $b_{x2} = -0.05 \cos(-30^\circ) = -0.0433$ and $b_{y2} = -0.05 \sin(-30^\circ) = 0.025$ (Table 7.3e). When solved, it is observed that all other attachments follow the applied rotation (Fig. 7.3b). For case 3, the CoM location of link 2 is rotated by an angle of -20° around J_1 (Fig. 7.3c). Thus the constraints are solved with $s_{x2} = 0.15 \cos(-20^\circ) = 0.141$ and $s_{y2} = 0.15 \sin(-20^\circ) = -0.0513$ as inputs (Table 7.3e). For this case it is observed that both fixed world spring attachments shift to the left and down. In the final case 4, both offsets of spring attachment B_2 and the CoM of link 2 are applied to the system. As expected the solved configuration shows a combination of the behavior caused by the individual offsets of the previous cases (Fig. 7.3d).



	Case 1	Case 2	Case 3	Case 4	Units
a_{x1}	0	0.1	-0.0114	0.0886	[m]
a_{y1}	0.3	0.2732	0.298	0.2712	[m]
a_{x2}	0	-0.1	-0.0114	-0.1114	[m]
a_{y2}	-0.1	-0.0732	-0.102	-0.0752	[m]
b_{x1}	0.05	0.0433	0.05	0.0433	[m]
b_{y1}	0	-0.025	0	-0.025	[m]
b_{x2}	-0.05	-0.0433	-0.05	0.0433	[m]
b_{y2}	0	0.025	0	0.025	[m]
k_1	147.15	147.15	147.15	147.15	$[\frac{N}{m}]$
k_2	147.15	147.15	147.15	147.15	$[\frac{N}{m}]$
m_2	2	2	2	2	[kg]
m_3	2	2	2	2	[kg]
L_2	0.3	0.3	0.3	0.3	[m]
s_{x2}	0.15	0.15	0.141	0.141	[m]
s_{y2}	0	0	-0.0513	-0.0513	[m]
s_{x3}	0.15	0.15	0.15	0.15	[m]
s_{y3}	0	0	0	0	[m]

(e)

Figure 7.3: In scale balanced solutions for example 1, the dark and light grey dots near the first joint represent points Z_1 and Z_2 (described later on in this example). (e) Parameter values for the different cases.

7.3.2. BEHAVIOR EXAMPLE 1

The design equations for this spring configuration in this general form are difficult to solve and interpret. Therefore, the system is parameterized such that these equations can be written in an elegant form, providing insight in behavioral relations in the system. The used parameters for link and spring parameters are shown in Fig. 7.4a and 7.4b respectively. The corresponding design equations for static balance are given in Eq. 7.17. Proof that these equations describe all static balanced solutions and reasoning for defining the parameters as such, are elaborated hereafter.

$$m_1 g s_1 + m_2 g L = k d L \quad (7.17a)$$

$$m_2 g s_2 = k b c (1 - f) f \quad (7.17b)$$

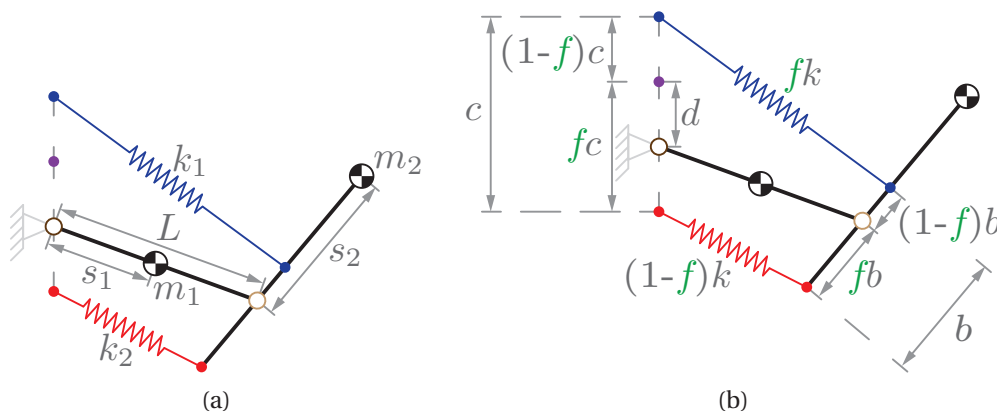


Figure 7.4: (a) Link parameters and (b) spring parameters of the spring configuration with 2 bi-articular springs.

Alongside parameters describing magnitudes for length, mass and stiffness, factor f is found in the design equations (Eq. 7.17). This factor describes the ratio between the spring stiffness of the upper and lower springs (Eq. 7.18).

$$f = \frac{k_1}{k_1 + k_2} = \frac{k_1}{k} = 1 - \frac{k_2}{k} \quad (7.18)$$

For a balanced system, this factor f is found between multiple system dimensions. To show where and why this factor is found, a force decomposition of the forearm is set up (Fig. 7.5a). The top and bottom spring forces are decomposed into two components. The first being dependent solely on the elbow joint location, the second only on the forearm orientation (Fig. 7.5a). Therefore, the effect of spring force on the upper arm and forearm can be examined separately.

The effect of the springs on the forearm is depicted in Fig. 7.5d, its force decomposition is shown in Fig. 7.5e. For static balance, the resultant force at the elbow joint must be independent of the forearm orientation. This is only the case when the force components aligned with the link, $F_{\parallel 1}$ and $F_{\parallel 2}$, have an equal magnitude and thus cancel each other out. These forces are a function of spring stiffness and the respective distance from joint to attachment (Eq. 7.19). It is found that these forces are equal only when the factor

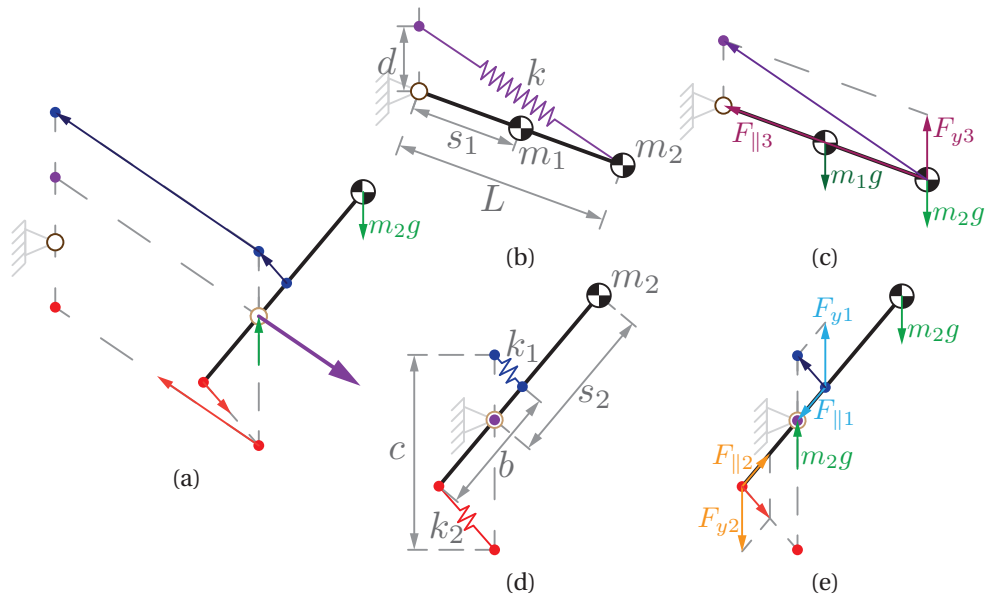


Figure 7.5: (a) Forearm force decomposition. (b) Representation of effect springs on upper arm. (c) Decomposition of forces dependent on upper arm orientation. (d) Representation of effect springs on forearm. (e) Decomposition of forces dependent on forearm orientation.

f is used to describe the ratio in distance b (Eq. 7.19c). Therefore b is parameterized using ratio f such that this requirement for balance is fulfilled consistently (Fig. 7.4b). The moment around the elbow, created by vertical force components F_{y1} and F_{y2} , balances the weight of the forearm.

7

$$F_{\parallel 1} = F_{\parallel 2} \quad (7.19a)$$

$$k_1 b_1 = k_2 b_2 \quad (7.19b)$$

$$f k(1-f)b = (1-f)kfb \quad (7.19c)$$

The force acting on the upper arm depends on the parallel force components of both springs (Fig. 7.5a). Their magnitudes depend on the location of the elbow joint. The force is equal to zero when the elbow is located at distance d above the shoulder joint. The location of point d is determined by factor f , with respect to the distance between the fixed world attachment c (Fig. 7.4b). When the elbow joint is moved from this force free point it behaves like a ZFLS with combined stiffness k . The effect of this virtual ZFLS on the upper arm is illustrated in Fig. 7.5b, the force decomposition is shown in Fig. 7.5c. The (purple) ZFLS, with stiffness k , can ensure static balance by providing a constant upward force (F_{y3}) at the elbow (Fig. 7.5c).

Each design equation in Eq. 7.17 describes the balance relation for a different link. Upper arm balance is ensured by Eq. 7.17a, it only contains parameters affecting the upper arm (Fig. 7.5b). Forearm balance is described by Eq. 7.17b, it only holds parameters affecting the forearm (Fig. 7.5d). In addition, the equations are written such that the left sides contain the effects of mass and the right sides the effects of the springs. Therefore, rules for adjusting parameters to balance a different mass, either of the upper arm or forearm, are directly described in these design equations (Eq. 7.17). Thus increasing

one of the spring parameters on the right side (k , b , c , d) will result in an increase in the upward balancing force acting on one (or both) of the links, in a linear manner (Eq. 7.17).

These adjustment rules can be used to balance a system of which the exact mass is unknown, like a human arm. For an arbitrary arm, it is assumed the arm dimensions are known and two ZFLSs are used, having known spring stiffness values. Thus arm parameters L , s_1 , and s_2 and spring parameters k and f are known. The springs are attached to the link, as in Fig. 7.4b and parameters are selected based on an estimate for the arm mass. However, the resulting system will, most likely, be unbalanced. For example, it is assumed the upper arm link is underbalanced and the forearm link is overbalanced. To balance the upper arm, a higher lifting force on this limb is required. According to Eq. 7.17a parameter d must be increased until this link is balanced. For forearm balance, a smaller lifting force is required. According to Eq. 7.17b, either the magnitude of b , c or both can be reduced until a balanced state is obtained.

The simultaneous rotation α , of the spring attachment points, can be added to the system. This does not affect the 2D in-plane balance (Fig. 7.6). For the fixed world attachments, the point of rotation is the (purple) point at a distance d above the shoulder joint. The forearm attachments rotate about the elbow joint. Distances between attachments, b and c , as well as factor f still apply and follow the same design equations for static balance (Eq. 7.17). For 3D balance, angle α must be equal to zero. At this angle, the system has a symmetry around the vertical axis through the shoulder joint. Therefore, it can rotate freely around this axis without changing spring length or CoM height. Additionally, at $\alpha = 0$, the forearm is balanced in every 3D pose. As at this angle, the system representing the forearm behavior (Fig. 7.5d), shows the same symmetry around the vertical axis. For any other α only motions in a single plane are balanced perfectly and the system has a tendency to fall out of this plane.

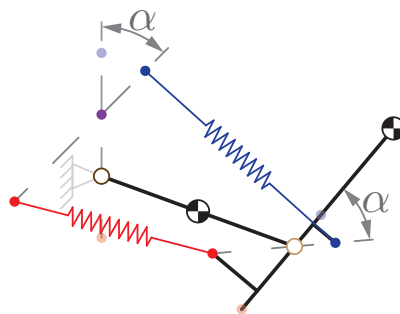


Figure 7.6: Rotation α does not affect 2D static balance behavior. Balance in the 3D space is affected by this rotation.

7.3.3. EXAMPLE 2

Two springs are used to balance the system, one bi-articular ZFLS connecting the fixed world to link 3 and one mono-articular ZFLS that connects links 2 and 3 (Fig. 7.2c). Constraint equations are set up similar to the first example, the steps are not shown for this example (steps 1 to 4). Next, these constraints are solved for four different cases (step 5) (Fig. 7.7), each showing different behavior. Finally, the relations between parameters

ensuring a balanced configuration are explained and illustrated.

Between these cases some general properties of the system remain the same. Specifically spring stiffness, mass and link length values. In each case the constraints are solved for parameters $a_{x1}, b_{x1}, b_{y1}, b_{x2}, b_{y2}$ and k_1 . Varied inputs between cases are parameters a_{x2} and a_{y2} , describing the location of attachment A_2 . Furthermore s_{y2} is varied, describing the location of the CoM of link 2. Obtained parameter values of balanced configurations are summarized in Table 7.7e.

In the first case all spring connections are aligned with the links (Fig. 7.7a). In case 2, the second spring is rotated about the second joint (Fig. 7.7b). In case 3, the CoM of link 2 is relocated (Fig. 7.7c). In the final case 4, the effects of case 2 and 3 are combined (Fig. 7.7d).

7.3.4. BEHAVIOR IN EXAMPLE 2

The four cases in example 2 are all statically balanced as they all fulfill the constraint equations. The unbalanced three link system is analyzed first in the orientation in which it has minimal gravitational energy (Fig. 7.8a). In this position link 2 is oriented at angle α with respect to the vertical. Angle α is now determined by setting the moment M_{J_1} around J_1 to be equal to zero as it should be when in equilibrium (Eq.7.20). The system shown in Fig. 7.8b is equal to the linkage of Fig. 7.8a only with redrawn links that give room for springs to be drawn later on.

$$M_{J_1} = 0 = m_2 s_{y2} \cos(\alpha) - m_2 s_{x2} \sin(\alpha) - m_3 L_2 \sin(\alpha) \quad (7.20a)$$

$$(m_2 s_{x2} + m_3 L_2) \sin(\alpha) = m_2 s_{y2} \cos(\alpha) \quad (7.20b)$$

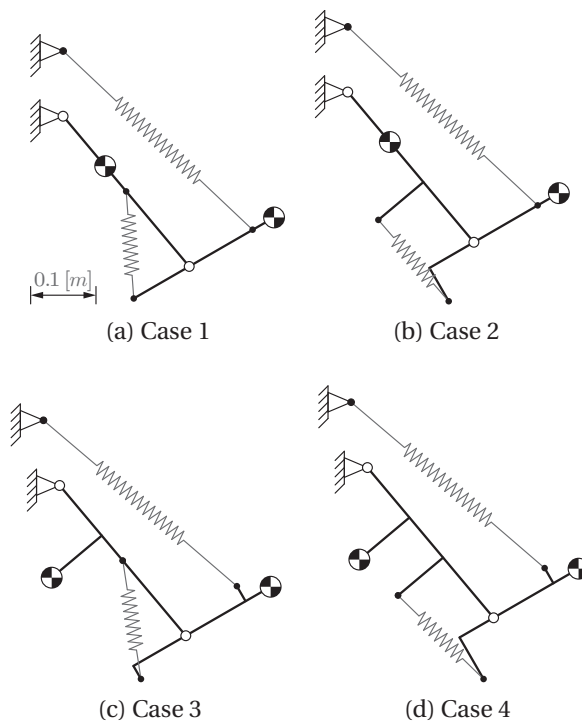
$$\frac{\sin(\alpha)}{\cos(\alpha)} = \tan(\alpha) = \frac{m_2 s_{y2}}{m_2 s_{x2} + m_3 L_2} \quad (7.20c)$$

$$\alpha = \tan^{-1} \left(\frac{m_2 s_{y2}}{m_2 s_{x2} + m_3 L_2} \right) \quad (7.20d)$$

Next, it is recognized that for balance a zero moment is required in all orientations. As this is already the case for the original system in the orientation of Fig. 7.8b neither of the added springs should apply a moment around any of the joints to keep this moment free condition. Spring 1 is located between the fixed world point A_1 and link 3 at point A_3 , and thus spawns both joints. As a result, spring connections A_1 and B_1 should be aligned with both joints J_1 and J_2 , exactly at the previously determined angle α (Fig. 7.8c). Spring 2 connects A_2 on link 2 and B_2 on link 3 and thus spawns only the second joint J_2 . Therefore, in this orientation with minimal potential the two connection points of this spring are to be aligned with J_2 (Fig. 7.8c).

Furthermore, as α is only dependent on parameters of the original linkage its value is unaffected by adjusting the other spring. For spring 2 the alignment of attachment A_2 depends on both angles α and β with respect to the local coordinate system of link 2. Attachment B_2 is dependent only on angle β with respect to the local coordinates of link 3. Therefore, by changing β spring 2 can be relocated anywhere on a ring shaped disk around J_2 , as partially visualized by dotted lines in Fig. 7.8c.

The locations of the spring attachments are now described based on a single position of the linkage where the gravitational energy is at a minimum. This does not directly



	Case 1	Case 2	Case 3	Case 4	Units
a_{x1}	0	0	-0.025	-0.025	[m]
b_{x1}	0.1125	0.1125	0.1059	0.1059	[m]
b_{y1}	0	0	0.0265	0.0265	[m]
b_{x2}	-0.0981	-0.0785	-0.0923	-0.06	[m]
b_{y2}	0	-0.0589	-0.0231	-0.0739	[m]
k_1	261.6	261.6	261.6	261.6	$[\frac{N}{m}]$
k_2	600	600	600	600	$[\frac{N}{m}]$
a_{y1}	0.1	0.1	0.1	0.1	[m]
a_{x2}	0.15	0.18	0.15	0.18	[m]
a_{y2}	0	-0.09	0	-0.09	[m]
m_2	2	2	2	2	[kg]
m_3	2	2	2	2	[kg]
L_2	0.3	0.3	0.3	0.3	[m]
s_{x2}	0.1	0.1	0.1	0.1	[m]
s_{y2}	0	0	-0.1	-0.1	[m]
s_{x3}	0.15	0.15	0.15	0.15	[m]
s_{y3}	0	0	0	0	[m]

(e)

Figure 7.7: In scale balanced solutions for example 2. (a) Case 1. (b) Case 2. (c) Case 3. (d) Case 4. (e) Parameter values for the different cases.

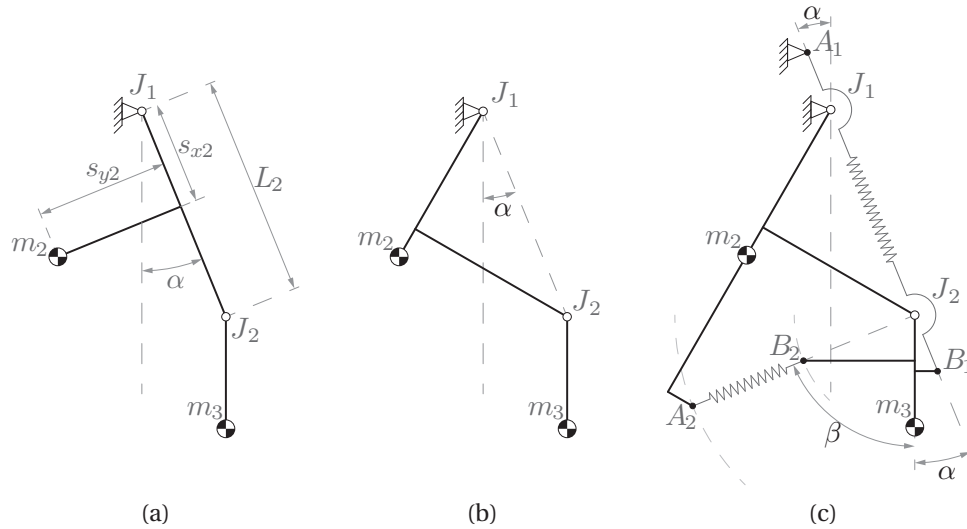


Figure 7.8: (a) and (b) Unbalanced linkage in equilibrium. (c) Relations between the location of spring attachment points required for a balanced system.

prove that the system is in balance in any pose as it is only clear that this one position is in equilibrium. However, the proof that the system can be balanced in any configuration is already given using the stiffness matrix approach. What the analysis of this single position does provide is insight in where the attachments can be placed and why they are constrained to lie on certain lines or positions. Additionally it can be reasoned that the system is capable of being balanced in all orientations as the energy behavior of all components is sinusoidal with respect to each rotation. These sinusoids have equal periods as these are equivalent to full rotations of a links, all having a minimum or maximum in the orientation of Fig. 7.8. The sinusoidal functions are either in phase or shifted by half a phase exactly and so can interfere with one another to cancel each other out.

The behavior described so far in this example is based on the orientations in which springs can be placed for the selected spring configuration (Fig. 7.8). However some additional interesting observations are made based on parameter magnitudes.

The first observation is that the location of spring attachment point \$B_1\$ (Fig. 7.8c) is a unique point depending solely on parameters of the original linkage, i.e. it is fixed independently of all other spring related parameters. Using the `solve` function in MATLAB the constraint equations are solved for parameters \$b_{x1}\$ and \$b_{y1}\$. These parameters describe the location of \$B_1\$, expressed as a function of the other parameters (Eq.7.21). The obtained equations consist solely of parameters describing link length, mass or CoM location.

$$b_{x1} = \frac{L_2^2 m_3^2 s_{x3} + L_2 m_2 m_3 (s_{x2} s_{x3} + s_{y2} s_{y3})}{(L_2 m_3 + m_2 s_{x2})^2 + m_2^2 s_{y2}^2} \quad (7.21a)$$

$$b_{y1} = \frac{L_2^2 m_3^2 s_{y3} + L_2 m_2 m_3 (s_{x2} s_{y3} - s_{x3} s_{y2})}{(L_2 m_3 + m_2 s_{x2})^2 + m_2^2 s_{y2}^2} \quad (7.21b)$$

For the spring attachment \$A_1\$ an additional constraint is found. It is found that the

distance from joint J_1 to this point A_1 is inversely related to its spring stiffness k_1 . This is by solving the constraint equations (Eq.7.16) for the parameters a_{x1} and a_{y1} which describe the location of A_1 (Eq.7.22a and 7.22b). Furthermore, the relation for α can again be extracted from these constraints by looking at the relative magnitudes of a_{x1} and a_{y1} (Eq.7.22c).

$$a_{x1} = \frac{m_2 g s_{y2}}{L_2} \frac{1}{k_1} \quad (7.22a)$$

$$a_{y1} = \frac{m_2 g s_{x2} + m_3 g L_2}{L_2} \frac{1}{k_1} \quad (7.22b)$$

$$\alpha = \tan^{-1} \left(\frac{a_{x1}}{a_{y1}} \right) = \tan^{-1} \left(\frac{m_2 s_{y2}}{m_2 s_{x2} + m_3 L_2} \right) \quad (7.22c)$$

For spring 2, an additional constraint is found as well, this is next to angle β which describes the springs orientation. When all other parameters are fixed, the product of its stiffness k_2 , distance from J_2 to A_2 and distance from J_2 to B_2 is constant ($k_2 \cdot |A_2 - J_2| \cdot |B_2 - J_2| = \text{constant}$). In other words, the two described lengths and the stiffness of this spring can be varied freely within these bounds without affecting any other parameter. This relation is affected by the location of A_1 and k_1 , however it is unpractical to take these into account in the same relation and much more convenient to fix these parameters before altering either A_2 , B_2 or k_2 .

7.4. DISCUSSION

BEHAVIOR found in the examples of this paper shows a number of simultaneous rotations of CoM locations and/or spring connection points that can be performed without affecting the balance of the system (Fig. 7.6 and 7.8). One could argue to use a polar coordinate system to describe this behavior as it is rotational. However, the centers of rotation for these simultaneous rotations can either be on the first joint, the second joint or a seemingly arbitrary point on one of the links. As the location of the center point is inconsistent it cannot be ensured that this point is always positioned on the origin of the local coordinate system. Furthermore, describing a rotation about a point other than the origin and the location of the springs on the links using polar coordinates, while describing the states with Cartesian coordinates is, according to the authors, unnecessarily complicated compared to describing the locations on the links, states and such a rotation as a sum of vector components in a Cartesian coordinate system. For this reason an xy-coordinate system is recommended when altering a system having planar offsets. Other benefits of using a Cartesian system is that the resulting constraint equations will be free of sinusoidal term, and describing coordinates on a link using xy-components is more intuitive compared to using an angle and magnitude.

The graphical representation of the behavior in example 1 provides a building block for creating complex balanced linkages. The building block is the linkage provided in Fig. 7.5a, 7.5d, which is the equivalent of a ZFLS. Any ZFLS in a balanced system can be replaced by this building block, resulting in a balanced linkage of higher order. In this manner complex multi-articulated linkages can be constructed, based solely on this

equivalence. Additionally, the minimal number of springs required to balance a n -link linkage can be established. When starting with a single balanced link (Fig. 7.5b), the ZFLS is replaced to obtain a two link balanced by two bi-articular springs by effectively adding one spring and one link. Replacing a spring can be repeated many times to obtain a n -moving link system balanced by n -ZFLSs. For this specific example, less and simpler design equations are obtained, providing more understanding of the system. For example, parameterizations according to Eq. 7.16 require six equations, on average containing 15 terms each, while after a simplification only two equations are required with an average of 8 terms per equation (Eq. 7.17). Moreover, the effect of the springs on different links is described in separate equations, providing useful adjustment rules. For creating custom parameters for larger linkages, it is advised to use factors between spring stiffness values as parameters and to describe virtual spring attachment locations, as in this paper.

7.5. CONCLUSIONS

IN this work the implementation of the stiffness matrix approach is altered such that states and link locations are expressed in the same coordinate system. The first goal was to implement Cartesian coordinates and comparing it to the use of polar coordinates in the stiffness matrix approach. The Cartesian coordinates were successfully implemented and in comparison they were found to be more intuitive in use, provide simpler constraint equations and be more convenient for altering parameters of balanced systems. The second goal was to gain more insight in the relations between parameters while the third goal was to illustrate these behavioral relations in two examples. These two goals were achieved simultaneously as in the examples two basic systems (both having two moving links) were analyzed. Relations were found between orientation, positioning and magnitude of springs and masses. These are described and illustrated providing a visual overview of the design space. Obtained relations provide knowledge in the possibilities to vary spring system parameters while maintaining static balance. For one spring configuration the relations could be simplified to two design equations. Adjustment rules are defined for altering the balancing forces acting on the upper arm and forearm. These rules define on how to balance a system with unknown mass and how to use the links as building blocks for balancing complex multi-articulated serial linkages.

REFERENCES

- [1] J. L. Herder, *Energy-free systems: theory, conception, and design of statically balanced spring mechanisms* (dissertation, 2001) p. 268.
- [2] S. K. Agrawal and A. Fattah, *Gravity-balancing of spatial robotic manipulators*, *Mechanism and machine theory* **39**, 1331 (2004).
- [3] A. H. A. Stienen, E. E. G. Hekman, G. B. Prange, M. J. A. Jannink, F. C. T. van der Helm, and H. van der Kooij, *Freebal: design of a dedicated weight-support system for upper-extremity rehabilitation*, *Journal of Medical Devices* **3**, 41009 (2009).
- [4] M. Carricato and C. Gosselin, *A statically balanced Gough/Stewart-type platform:*

- conception, design, and simulation*, Journal of Mechanisms and Robotics **1**, 31005 (2009).
- [5] K. Kobayashi, *Comparison between spring balancer and gravity balancer in inertia force and performance*, Journal of Mechanical Design **123**, 549 (2001).
- [6] G. Endo, H. Yamada, A. Yajima, M. Ogata, and S. Hirose, *A passive weight compensation mechanism with a non-circular pulley and a spring*, IEEE International Conference on Robotics and Automation, 3843 (2010).
- [7] C.-W. Hou and C.-C. Lan, *Functional joint mechanisms with constant-torque outputs*, Mechanism and Machine Theory **62**, 166 (2013).
- [8] R. Sapper, *Lamp with an articulated support*, patent **US3790773** (1974).
- [9] J. Wang and C. M. Gosselin, *Static balancing of spatial three-degree-of-freedom parallel mechanisms*, Mechanism and Machine Theory **34**, 437 (1999).
- [10] H. Hilpert, *Weight balancing of precision mechanical instruments*, Journal of Mechanisms **3**, 289 (1968).
- [11] S. K. Banala, S. K. Agrawal, A. Fattah, V. Krishnamoorthy, H. Wei-Li, J. Scholz, and K. Rudolph, *Gravity-balancing leg orthosis and its performance evaluation*, IEEE Transactions on Robotics **22**, 1228 (2006).
- [12] P.-Y. Lin, W.-B. Shieh, and D.-Z. Chen, *A theoretical study of weight-balanced mechanisms for design of spring assistive mobile arm support (MAS)*, Mechanism and Machine Theory **61**, 156 (2013).
- [13] P.-Y. Lin, W.-B. Shieh, and D.-Z. Chen, *A stiffness matrix approach for the design of statically balanced planar articulated manipulators*, Mechanism and Machine Theory **45**, 1877 (2010).
- [14] P.-Y. Lin, W.-B. Shieh, and D.-Z. Chen, *Design of statically balanced planar articulated manipulators with spring suspension*, IEEE Transactions on Robotics **28**, 12 (2012).
- [15] Y.-Y. Lee and D.-Z. Chen, *Determination of spring installation configuration on statically balanced planar articulated manipulators*, Mechanism and Machine Theory **74**, 319 (2014).
- [16] S. R. Deepak and G. K. Ananthasuresh, *Perfect static balance of linkages by addition of springs but not auxiliary bodies*, Journal of Mechanisms and Robotics **4**, 21014 (2012).

8

A CLOSE-TO-BODY 3-SPRINGS CONFIGURATION FOR GRAVITY BALANCING OF THE ARM

Orinally appeared as:
A.G. Dunning, J.L. Herder,
A Close-to-Body 3-Springs Configuration for Gravity Balancing of the Arm,
IEEE International Conference on Rehabilitation Robotics, 464 (2015),
DOI:10.1109/ICORR.2015.7281243

In the previous chapter, two spring configurations were elaborated. In this chapter, a 3-springs configuration is elaborated. The spring configuration is evaluated on the balancing quality and it is described how to springs can be located close to the body. In this chapter, the spring configuration is evaluated according to a model. The embodiment of this spring configuration is presented in Chapter 12.

ABSTRACT

A close-to-body arm support is needed to meet the need of patients for an inconspicuous arm support that is not stigmatizing. At the moment, these arm supports do not exist. All commercially available arm support use springs with a parallelogram structure that needs auxiliary links to balance the arm. Recent literature presents a 2-spring configuration without auxiliary links with multi-articular springs. A restriction to this spring configuration is that it cannot be attached close to the body. In this paper a new 3-springs configuration and a concept for attachment to the body is proposed. One bi-articular spring that spans the shoulder and elbow joint, one mono-articular spring that spans the elbow, and one mono-articular spring that spans the shoulder are used to balance the arm in its complete 3D workspace. The spring that spans the shoulder joint is rotated about the shoulder to bring the configuration closer to the body. To study the effect of this modification, the system was evaluated for the 9 most important positions for activities of daily life and the potential energy values of the whole system are compared. The energy values show no large difference as compared to the ideal 2-link system. We conclude therefore that the addition of an extra spring makes it possible to bring the spring configuration closer to the body. This extra spring does not introduce significant balancing errors, on top of the error of extra mass of the arm support and other alignment errors.

8.1. INTRODUCTION

MOST people use their arms a lot during activities of daily life (ADL). However, people with neuromuscular disorders have difficulties to use their arms. Due to decreasing muscle force, performing ADL become increasingly difficult. These people can have a large benefit from an arm support to help them to lift their arm and perform ADL [1–3]. Ideally, the arm is in equilibrium in every position of the workspace. In other words, the potential energy of the complete system (arm + arm support) is constant over the range of motion and the system is statically balanced [4]. When the arm is balanced, the user has to overcome only the inertia forces. The user does not have to lift the weight of the arm anymore. The use of a passive balancing system is also promising as a base for an active system. The motors do not have to be large to overcome the gravity forces acting on the arm.

In recent years, many types of arm supports are developed varying from rehabilitation devices [5] to devices for daily use [6, 7]. For many patients it is important to have an inconspicuous arm support that is not stigmatizing [7, 8]. In the ideal case, it could be worn underneath clothing.

In [9], a comparison is shown for 23 passive and active devices. It showed that all the arm supports cannot be worn underneath clothing and are therefore conspicuous and stigmatizing. Most of them do not support the complete range of motion of the arm. It was also shown that many arm supports need a parallelogram construction for maintaining balance over multiple serial links. Each parallelogram construction has its own single spring, spanning over 1 joint (mono-articular), to balance the weight of the distal links. The auxiliary links increase the mass and inertia of the arm support and limit the range of motion of the arm for several motions.

In [10], a spring configuration is presented that balances a serial 2-link system with 2 springs without using auxiliary links. One bi-articular springs (spanning over 2 joints) in combination with one mono-articular spring is used to balance the linkage in the complete 3D workspace. The main limitation of this spring system is that the position of the attachment points are constrained by the masses and length of the links. This is a promising concept, but as will be shown in this paper it does not fit underneath clothing. Furthermore, in [10] an ideal 2-link system is considered. It does not include the extra links of an arm support next to the arm, and where to attach the springs to the body. All the springs are perfectly aligned and attached to the axis of the links. For a human arm this is not possible, since the springs need to be next to the arm and cannot be attached to the axis of the arm.

In this paper, a spring configuration is proposed that can balance the complete workspace of the arm, and can be attached close to the body of the user.

In Section 8.2, the proposed close-to-body spring configuration and the method to evaluate the spring configuration is described. The results of this evaluation are shown in Section 8.3. This paper closes with a discussion of the results and the spring system, followed by the conclusion.

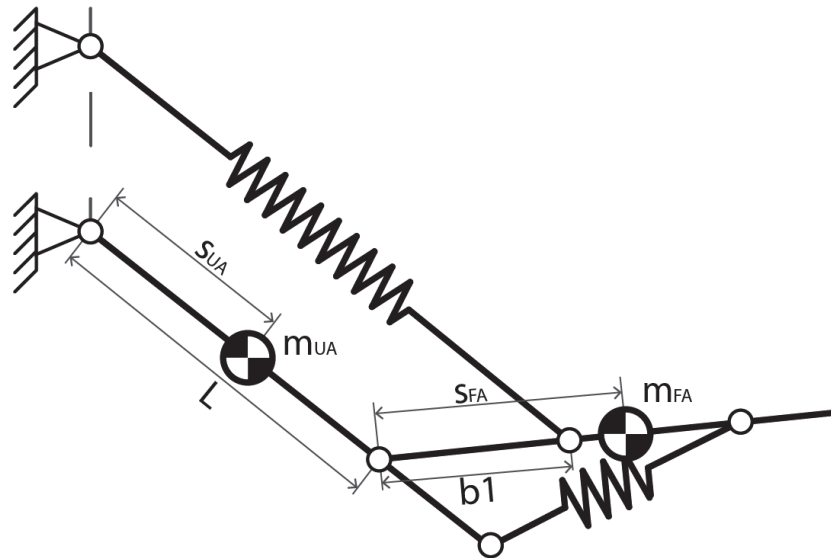


Figure 8.1: Spring configuration as presented in [10] (reproduced).

8.2. METHOD

THE spring configuration described in [10] is able to balance a 2-link system for its complete 3D workspace (Fig. 8.1). However, the spring system is constrained for certain parameters. The position of the bi-articular spring at the 'forearm' ($b1$) is constrained by the masses and lengths of the 'upper arm' and 'forearm' (Eq. 9.2) [10], and is too large to be close to the body and fit underneath clothing.

$$b1 = \frac{m_{FA}s_{FA}L}{m_{UA}s_{UA} + m_{FA}L} \quad (8.1)$$

To bring the whole system closer to the body and to make a real arm support, the mono-articular spring is repositioned and one extra spring is added to the system. The proposed spring configuration is shown in Fig. 8.2. All the springs are ideal zero-free-length springs [4]. The mono-articular spring that spans the elbow joint (further referred to as mono-articular elbow spring) is repositioned such that it runs almost parallel to the upper arm. The spring is also rotated about the elbow such that the behavior of the spring for elbow flexion/extension is similar [4]. In this way the spring can be placed in-plane with the links of the arm support and it does not obstruct the motions when the arm is on a table.

An extra mono-articular spring is added that spans the shoulder (further referred to as mono-articular shoulder spring). The spring is attached to the upper arm and the trunk. This spring is needed to be able to move attachment point $b1$ closer to the elbow. For complete balance of the arm, the stiffness k_1 need to increase. This increases the reaction force in the elbow. To counteract this reaction force, the extra spring is needed to pull the upper arm down for every movement. The mono-articular shoulder spring is also rotated about the shoulder. This brings attachment point $a3$ closer to the trunk, and attachment point $b3$ can be in-plane with the link or even below the upper arm. The rotation of the mono-articular shoulder spring affects the balancing quality in 3D space.

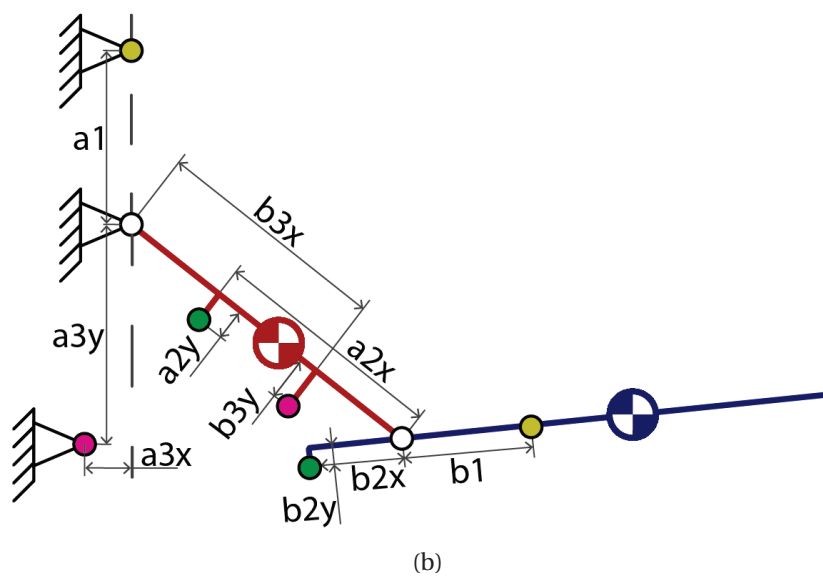
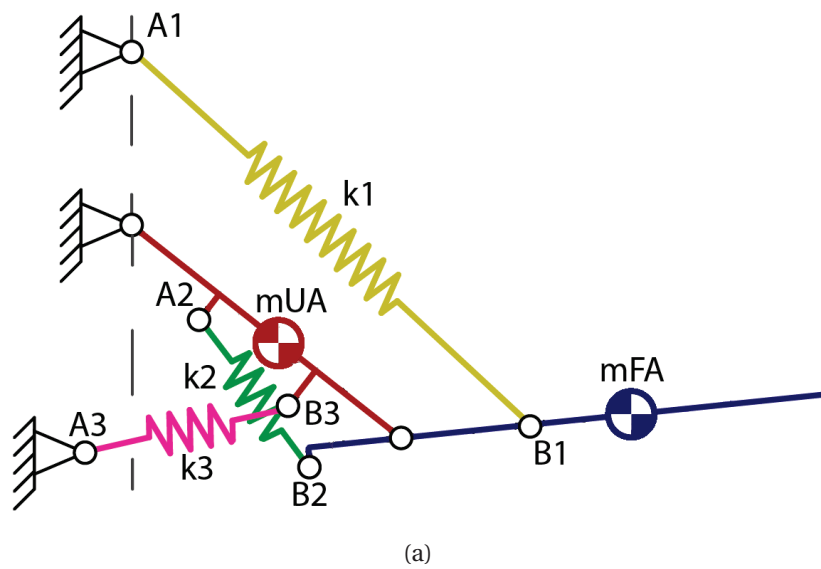


Figure 8.2: The proposed 3-springs configuration that can balance the arm in its complete 3D workspace, with the mono-articular elbow spring rotated about the elbow, and the mono-articular shoulder spring rotated about the shoulder.

Parameter	Value	Parameter	Value
m_{UA}	2.402kg	$a1$	0.09m
m_{FA}	2.1215kg	$b1$	0.06m
l_{UA}	0.3m	$a2x$	0.1m
l_{FA}	0.29m	$a2y$	0.025m
s_{UA}	0.147m	$b2x$	0.04m
s_{FA}	0.173m	$b2y$	0.005m
$k1$	666.75N/m	$a3x$	0.045m
$k2$	1477.1N/m	$a3y$	0.2m
$k3$	197.38N/m	$b3x$	0.2m
		$b3y$	0.045m

Table 8.1: Overview of the parameters of the spring configuration (as defined in Fig. 8.1 and 8.2).

This error will be investigated with an evaluation of the spring configuration. In Table 9.2 the values for each parameter are shown.

This spring configuration is implemented into a concept for an arm support (Fig. 8.3a). The arm support is simplified to three links. The first link runs along the trunk and is fixed to the world. The second link runs along the upper arm and is attached to the first link with a ball joint that coincides with the human shoulder joint. The third link runs along the forearm, with a revolute joint at the elbow. The bi-articular spring is split to each side of the forearm with $0.5 \cdot k_1$ at each side, to minimize interference with the body. The mono-articular shoulder spring has the attachment point at the trunk positioned $\frac{1}{2}\sqrt{2} \cdot 0.045m$ medial and posterior from the vertical through the shoulder joint (45deg rotation of the elevation plane [11]) and the attachment point at the upper arm positioned $\frac{1}{2}\sqrt{2} \cdot 0.045m$ medial and posterior of the upper arm (Fig. 8.3b). With these positions the upper arm can be positioned vertically down (resting on an arm rest) without interfering with the linkage and moves (according to the authors) the most in the plane wherein the arm is perfectly balanced.

To evaluate the balancing quality of the spring configuration, the error of the balancing quality in 3D space due to the rotated mono-articular shoulder spring and the error due to the extra linkages of the arm support next to the arm is evaluated. The model of the arm and the arm support was build in the MATLAB multibody simulation toolbox SimMechanics. For each element in the system the potential energy was calculated according to the force and length of the spring and the height of each mass. These values were determined with the SimMechanics model. The potential energy of the masses was calculated with the hip as reference point. To compare the situation with arm support to the ideal 2-link system, the extra potential energy of the splitted spring was compensated for the extra length.

The spring configuration was evaluated for 9 different positions. The positions were chosen to correspond with the most important ADL [12] (Fig. 8.4): (1) neutral (in rest), (2)

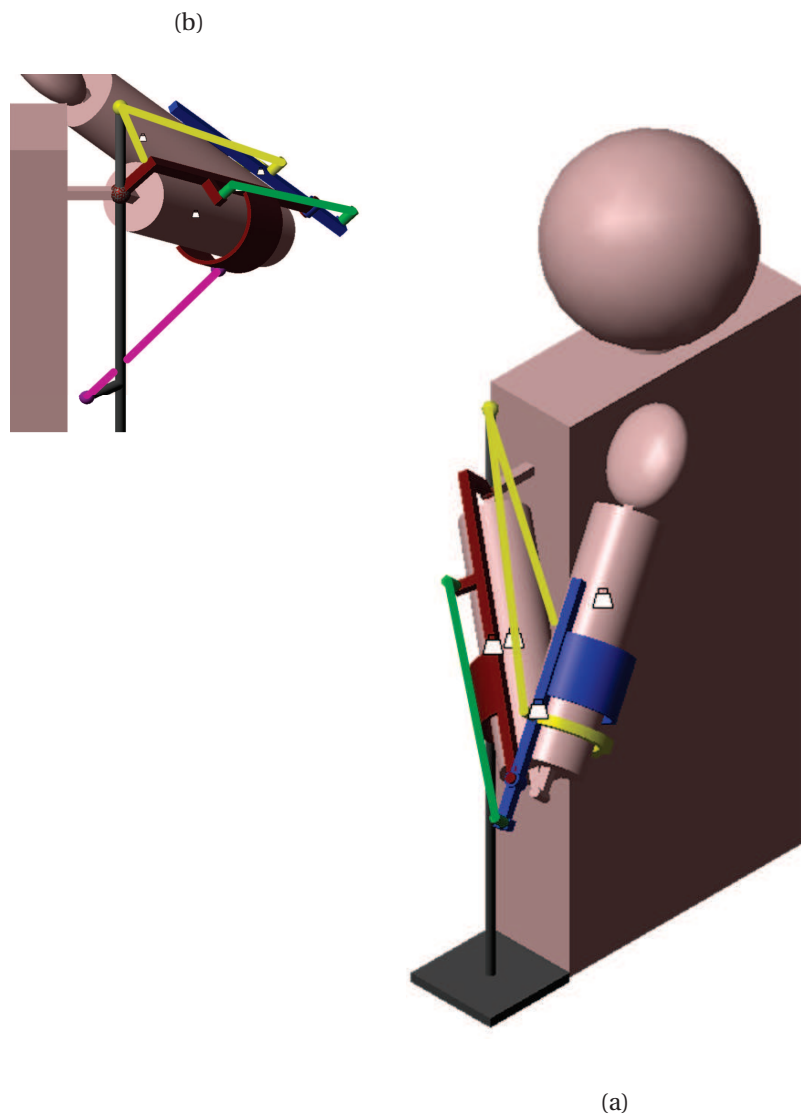


Figure 8.3: (a) SimMechanics model of the human arm with the arm support in eating position with (b) detailed posterior view with a bi-articular spring (yellow) that is split to both sides of the forearm, a mono-articular elbow (green) and shoulder (magenta) spring.

eating/drinking, (3) scratching the head, (4) control a keyboard, (4,5) open a package, (5) control a pc mouse, (6) reaching forward, (7) reaching sideways, (6,7) donning/doffing clothes, (8,9) hugging. The orientation of the arm support for each position is also shown.

8.3. RESULTS

FOUR different configurations of the spring system were evaluated. First, the ideal 2-link system as shown in Fig. 8.2, where the masses of the upper arm and forearm are positioned on the axes of the links, was evaluated for two situations: without (Fig. 8.5a) and with (Fig. 8.5b) a rotated mono-articular shoulder spring. The potential energy of each spring and the upper arm and forearm is shown. The grey area with the values at the right represents the lower and upper boundary of the total amount of energy. For the ideal 2-link spring configuration (without a rotated mono-articular shoulder spring) the value of total energy is constant for every position. The minimum and maximum value of the total energy for the 2-link system with a rotated mono-articular shoulder spring is $96.7J$ and $97.4J$, respectively.

In Fig. 8.6 the results of the evaluation with the arm support are shown. As can be seen in Fig. 8.3a, the extra links add extra mass to the arm, and the center of masses are not perfectly aligned with the axes of the upper arm and forearm anymore. This introduces an error as can be seen in Fig. 8.6a, which are the results for arm with arm support with a non-rotated mono-articular shoulder spring. The minimum and maximum value of the total energy is $96.9J$ and $97.2J$, respectively. In Fig. 8.6b the results are shown for the arm with arm support combined with the rotated mono-articular shoulder spring, as proposed. The minimum and maximum value of the total energy is $96.7J$ and $97.7J$, respectively.

8.4. DISCUSSION

FROM the previous section some interesting results can be seen. When comparing the ideal spring configuration (Fig. 8.5a) to the configuration with the rotated mono-articular shoulder spring (Fig. 8.5b), an error in total potential energy is found. This error is introduced because the spring is rotated about the shoulder joint. In one plane ($45deg$ rotation of the elevation plane) the arm is perfectly balanced. But for 3D movements out of the plane an error will be introduced. The maximum error for this system is only max. 0.5% of the total potential energy, when the hip is taken as a reference point for calculating the potential energy of the mass of the arm support, upper arm and forearm. But even if the potential energies of the masses (max. 25% of the total energy) are not taken into account, but the error is only compared to the energy in the springs, the max. error is still only max. 0.64% with respect to the energy in the springs.

Adding the arm support next to the human arm also introduces a small error (Fig. 8.6a). The combined center of masses of the upper arm and forearm are replaced a bit and are not positioned in the axis of the arm anymore, but lateral of the axis. For some shoulder movements this affects the potential energy of the system (e.g. reaching sideways, hugging). This error is only max. 0.6% of the total energy, when the hip is taken as a reference point. If this error is calculated with respect to the difference in potential energy of the mass, the max. error is 2%.

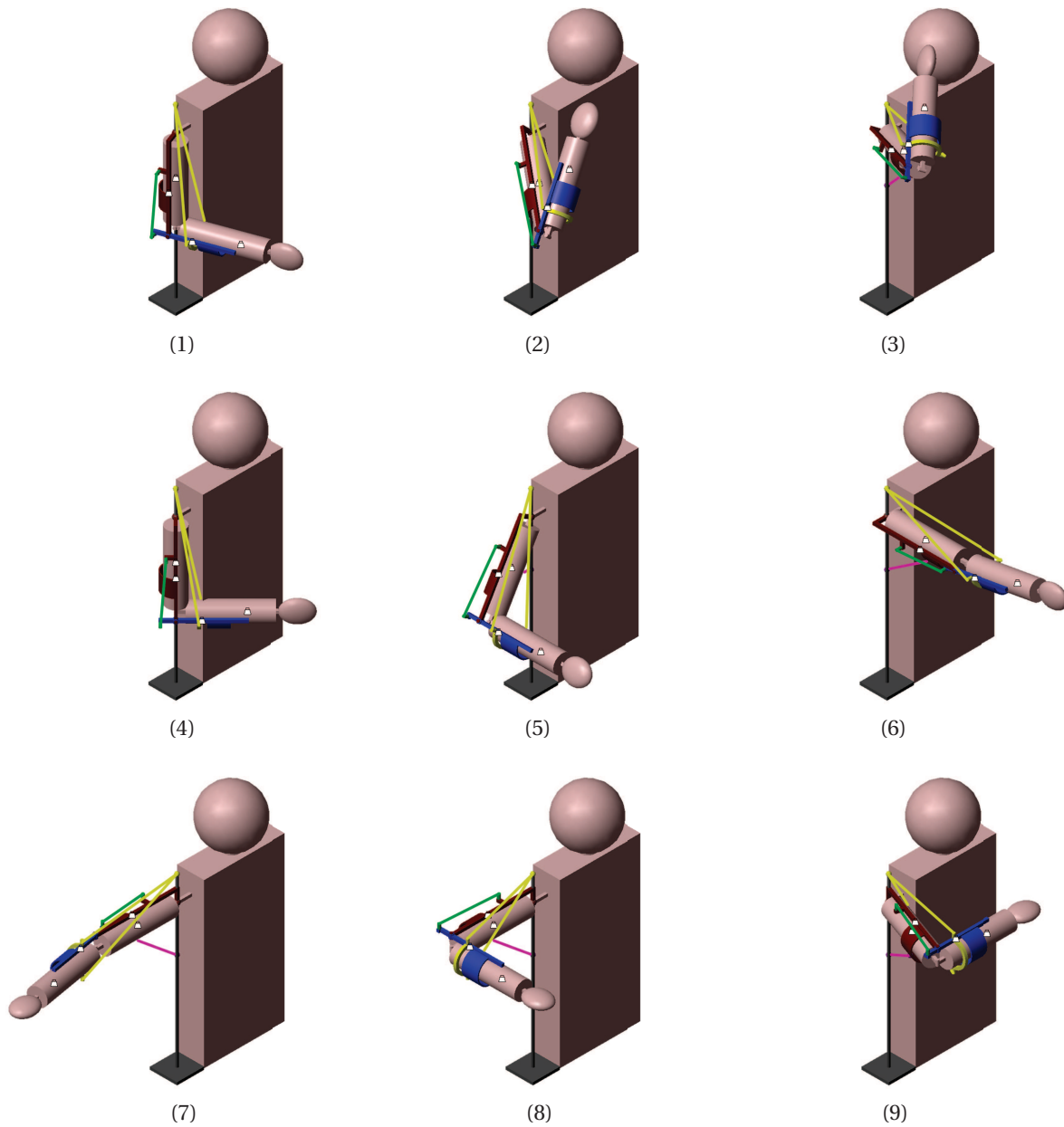
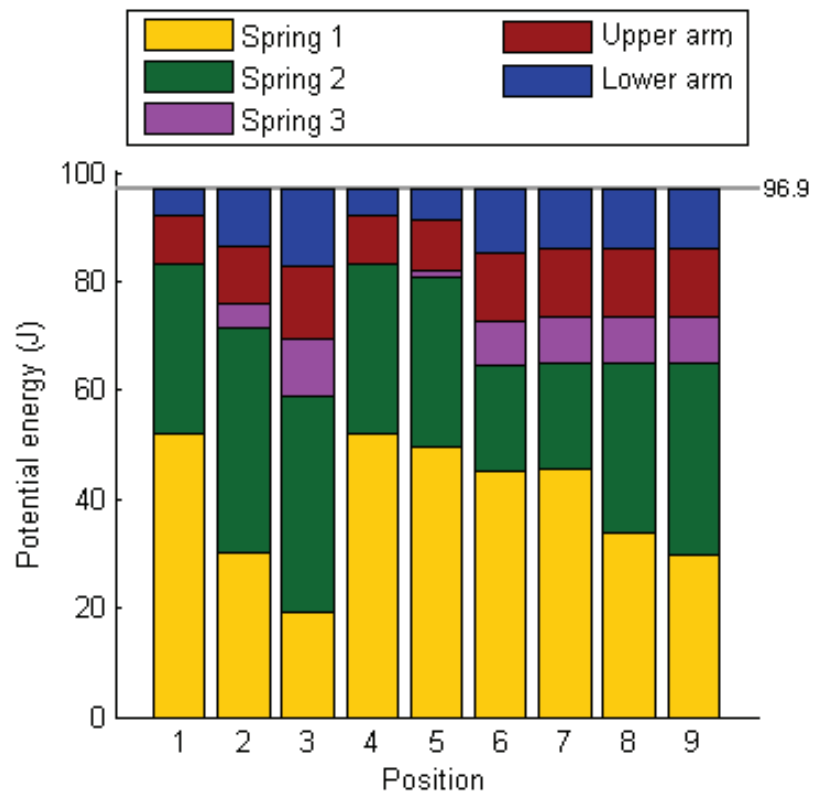
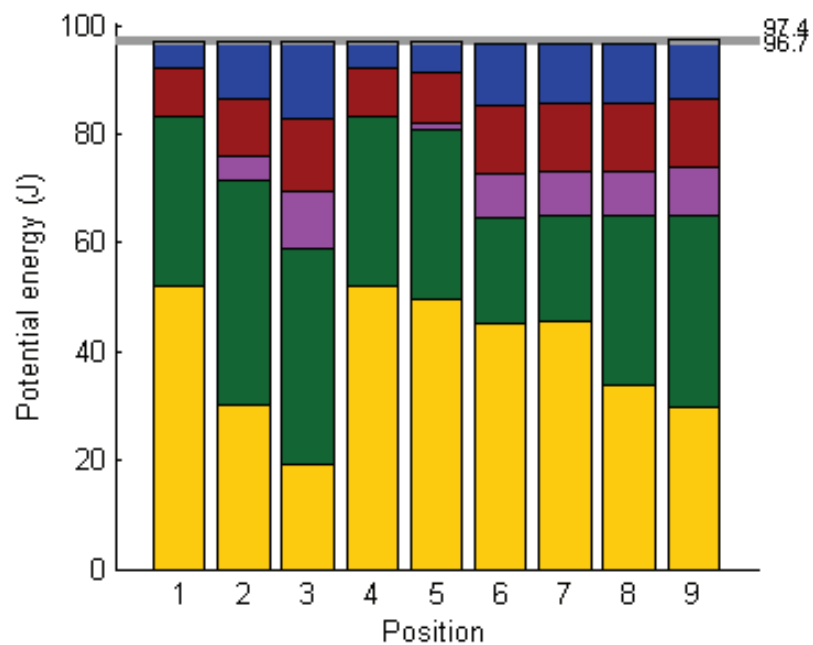


Figure 8.4: Evaluated positions: (1) neutral/rest, (2) eating/drinking, (3) scratching head, (4) control keyboard / open package, (5) control pc-mouse / open package, (6) reach forward / donning clothing, (7) reaching sideways / donning clothing, (8,9) hugging

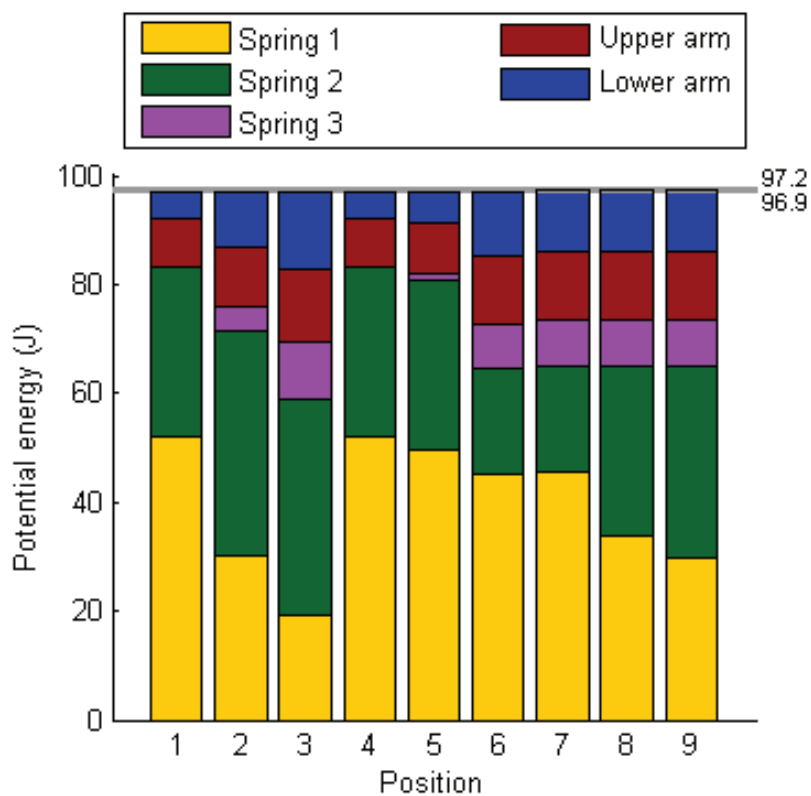


(a)

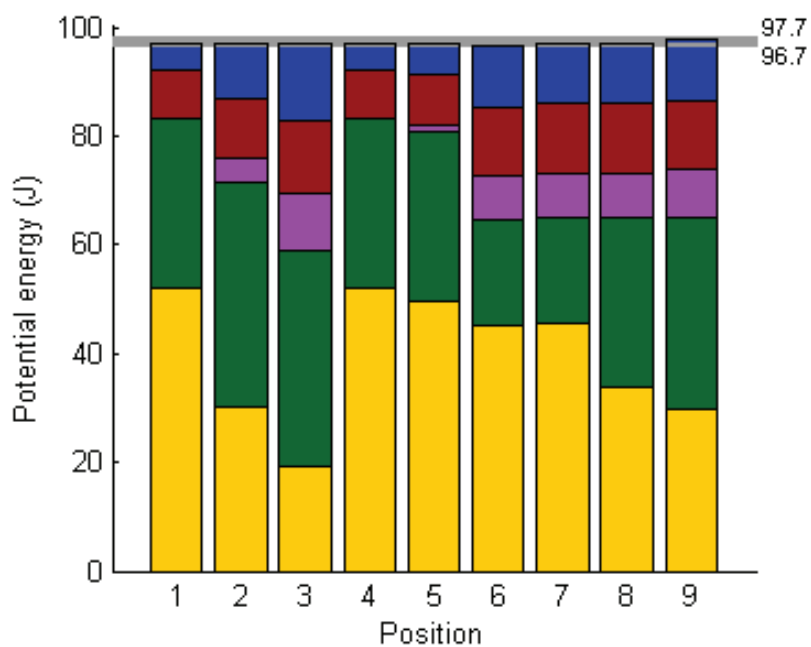


(b)

Figure 8.5: Results of the evaluation of the 2-link system, for (a) the ideal case that the mono-articular shoulder spring is not rotated ($Vp = 96.9J$ and constant) and (b) the case with the rotated mono-articular shoulder spring ($96.7J \geq Vp \leq 97.4J$).



(a)



(b)

Figure 8.6: Results of the evaluation of the arm support attached to the human arm, for (a) the case that the mono-articular shoulder spring is not rotated ($96.9J \geq Vp \leq 97.2J$) and (b) the case with the rotated mono-articular shoulder spring ($96.7J \geq Vp \leq 97.7J$).

When the mono-articular shoulder spring is rotated in the system with the arm support, one would expect that the error will be a sum of the error due to the rotated spring and the extra mass. However, the interesting result is that the error is actually smaller (max. 0.77%), when the hip is taken as a reference point. It seems like the error due to the extra linkage compensates for the error introduced by the rotated mono-articular shoulder spring. This can be explained by the fact that the attachment point of the spring on the upper arm is on the opposite side of the arm than the linkage. When the arm is rotated for example, the potential energy for the mass of the linkage increases while the energy of the spring decreases.

Although the error in total potential energy is small and decreasing when introducing an extra linkage and a rotated spring, it is hard to say what the effect on the behavior of the system is. Both the mass of the arm support and the rotated spring introduce a moment for movements out of the perfectly balanced plane. Nevertheless, the moment exerted by the spring is opposite to and somewhat compensating the moment exerted by the mass. The effect of the moments should be investigated in further research.

Furthermore, in the model it is assumed that the shoulder joint and elbow joint of the user are perfect ball and revolute joints, respectively. But in reality this is not the case. For example, the shoulder joint moves up and down during abduction/adduction. This results in improper alignment of the arm support, that introduces an error. What the effect of this alignment error is should be investigated in further research. According to the authors it is not necessary to design a perfectly balanced spring system in 3D workspace, while these errors still maintain. The error introduced by the extra spring and movements out of the perfectly balanced plane are that small, that it is not worth to design a perfectly balanced springs system, while errors due to misalignment are introduced always and hard to compensate.

Although this spring configuration uses 3 springs to balance the arm in its complete workspace, it is able to position every spring such that the whole system is close to the body and can fit underneath clothing. The bi-articular spring is split to each side of the arm to decrease interference with the arm and the be able to attach is on the right positions. The mono-articular shoulder spring is rotated such that it does not interfere with arm movements, and at the trunk it can be placed close to the waist, for example on a (slim-fit) orthotic jacket. Besides that, for this spring configuration it is possible to adjust the balancing force by tuning every position of the spring attachments.

8.5. CONCLUSIONS

THE goal of this research was to propose a new spring configuration that can balance the arm in its complete 3D workspace, and can be attached close to the body. A 3-springs configuration is proposed with one bi-articular spring that spans the elbow and shoulder joint, and two rotated mono-articular springs that span the elbow or the shoulder joint. With this configuration, every attachment point of the springs can be chosen such that the whole system can be attached close to the body of the user. The spring configuration is evaluated and the energy values of the whole system are compared for an ideal 2-link system and a system where extra links of an arm support are included. It was concluded that the balance error for 3D movements (out of the perfectly balanced plane) was only max. 0.5% of the total potential energy, and max. 0.64% with respect

to the spring energy. The error introduced by the extra mass of the arm support is only 0.6%, and max. 2% with respect to the spring energy. The combination of a system with an arm support and a rotated extra spring is only 0.77%, and smaller compared to the sum of each individual error. These errors are small enough to overcome by the user, since the errors due to misalignment of the arm support are probably larger. This new 3-springs configuration could be used in a close-to-body arm support that is able to support the arm for the most activities of daily living.

APPENDIX

As an elaboration on the 3-springs configuration, an idea is sketched to combine it with the concept of the upper arm balancer based on bending beams [13] (Chapter 5). In Fig. 8.7a, another 3-springs configuration is shown that balances the arm. Different with the 3-springs configuration described in this chapter is that the bi-articular spring is attached to the fixed world below the shoulder. A mono-articular spring runs from above the shoulder to the upper arm. As elaborated in [13] (Chapter 5), this mono-articular spring can be replaced by a bending beam that is positioned in the arm pit (Fig. 8.7b). This configuration balances the arm throughout the complete range of motion. The advantages are that this system is not conspicuous. The springs are positioned in areas where there is enough space (in the arm pit). There is also no interference with the shoulder mechanisms with this system. A disadvantage is that the bending beams are hard to tune to compensate errors.

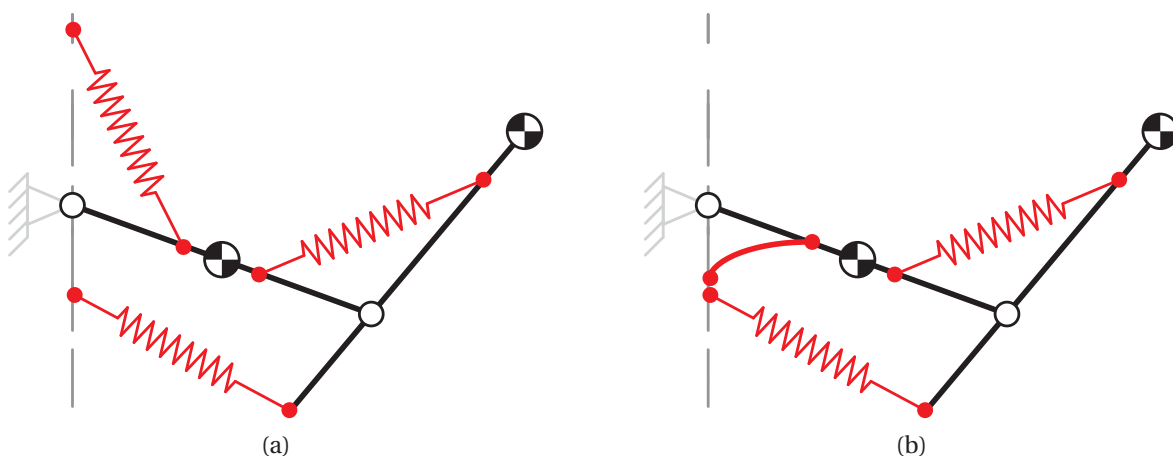


Figure 8.7: (a) A 3-springs configuration that balances the arm, where (b) the mono-articular spring from fixed world to the upper arm is replaced by a bending beam.

REFERENCES

- [1] S. Landsberger, P. Leung, V. Vargas, J. Shaperman, J. Baumgarten, Y. L. Yasuda, E. Sumi, D. McNeal, and R. Waters, *Mobile Arm Supports: History, Application, and Work in Progress*, Topics in Spinal Cord Injury Rehabilitation **11**, 74 (2005).
- [2] K. Lund, R. Brandt, G.-J. Gelderblom, and J. L. Herder, *A user-centered evaluation*

- study of a mobile arm support*, IEEE International Conference on Rehabilitation Robotics , 582 (2009).
- [3] M. Coscia, V. C. K. Cheung, P. Tropea, A. Koenig, V. Monaco, C. Bennis, S. Micera, and P. Bonato, *The effect of arm weight support on upper limb muscle synergies during reaching movements*. Journal of neuroengineering and rehabilitation **11**, 22 (2014).
- [4] J. L. Herder, *Energy-free systems: theory, conception, and design of statically balanced spring mechanisms* (dissertation, 2001) p. 268.
- [5] A. H. A. Stienen, E. E. G. Hekman, G. B. Prange, M. J. A. Jannink, F. C. T. van der Helm, and H. van der Kooij, *Freebal: Design of a Dedicated Weight-Support System for Upper-Extremity Rehabilitation*, Journal of Medical Devices **3**, 041009 (2009).
- [6] J. L. Herder, N. Vrijlandt, T. Antonides, M. Cloosterman, and P. L. Mastenbroek, *Principle and design of a mobile arm support for people with muscular weakness*, Journal of Rehabilitation Research and Development **43**, 591 (2006).
- [7] T. Rahman, W. Sample, R. Seliktar, M. Alexander, and M. Scavina, *A body-powered functional upper limb orthosis*, Journal of rehabilitation research and development **37**, 675 (2000).
- [8] A. Kumar and M. F. Phillips, *Use of powered mobile arm supports by people with neuromuscular conditions*. Journal of rehabilitation research and development **50**, 61 (2013).
- [9] A. G. Dunning and J. L. Herder, *A review of assistive devices for arm balancing*, International Conference on Rehabilitation Robotics , 6650485 (2013).
- [10] P.-Y. Lin, W.-B. Shieh, and D.-Z. Chen, *A theoretical study of weight-balanced mechanisms for design of spring assistive mobile arm support (MAS)*, Mechanism and Machine Theory **61**, 156 (2013).
- [11] L. F. Cardoso, S. Tomazio, and J. L. Herder, *Conceptual design of a passive arm orthosis*, ASME International Design Engineering Technical Conferences **5**, 747 (2002).
- [12] M. M. H. P. Janssen, A. Bergsma, A. C. H. Geurts, and I. J. M. de Groot, *Patterns of decline in upper limb function of boys and men with DMD: an international survey*, Journal of neurology **261**, 1269 (2014).
- [13] A. G. Dunning, J. L. Stroo, G. Radaelli, and J. L. Herder, *Feasibility Study of an Upper Arm Support based on Bending Beams*, International Conference on Rehabilitation Robotics , 520 (2015).

9

EVALUATION AND COMPARISON OF FIVE SPRING CONFIGURATIONS FOR BALANCING SERIAL LINKAGES WITHOUT AUXILIARY LINKS

To be submitted as:

A.G. Dunning, M.P. Lustig, J.L. Herder,

*Evaluation and comparison of five spring configurations for balancing serial linkages
without auxiliary links,*

Will be submitted to Mechanism and Machine Theory, 2016.

In this chapter, the spring configurations that are described and elaborated in the previous chapters (Chapter 7, 8) and applied into a prototype in Chapter 11 and 12 are evaluated and compared on their balancing quality and their tuning ability in order to make a choice for a good spring configuration to apply in a close-to-body arm support (Chapter 12).

ABSTRACT

PATIENTS with neuromuscular disorders often lose the leg and arm function. For regaining the arm function, an arm support can be used. Current state-of-the-art in arm supports do not meet the wishes of those patients, in terms of range of motion and inconspicuousness. Recent research showed arm supports that are based on a serial linkage without auxiliary links. With a springs configuration attached to the linkages, the arm is balanced throughout its range of motion. Different spring configurations have been elaborated.

In this paper, five different spring configurations are evaluated and compared to each other: a (1) 2-springs, (2) 2-asymmetric)-springs, (3) 2-parallel-springs, (4) 3-springs and (5) 3-asymmetric-springs configuration. This is done in order to choose a spring configuration to apply in a close-to-body arm support. An experimental setup was built to evaluate the spring configuration on their balancing quality. For this, the vertical force is measured at the elbow and center of mass of the arm. This force is compared to the vertical force that should be measured. Measurements are done for several states of the arm, to be able to measure to entire range of motion. Next to that, tuning rules are determined for each spring configuration in order to know how the balancing quality can be regained or improved by changing different parameters. The results of the vertical force showed that the measurements are very similar to the theoretical force for the 2-springs and 3-asymmetric-springs configuration. The tuning rules of the 3-(asymmetric)-springs configuration are the easiest to understand, and for these spring configurations a good balancing quality can always be achieved. Next to that, these spring configurations are the closest to the body. However, these spring configurations introduce an extra moment that is too large and patients with little muscle force in their arm cannot compensate for that. Therefore, the 3-springs configuration with a V-shaped mono-articular spring from the trunk to each side of the upper arm is proposed as a good spring configuration to apply in a close-to-body arm support.

9.1. INTRODUCTION

PATIENTS with a neuromuscular disorder (e.g., Duchenne muscular dystrophy), often lose the ability to walk and have insufficient strength to lift their arms [1]. This loss obstructs them in performing the most basic tasks of daily living. As a consequence, their quality of life is greatly reduced. Mobility can partially be regained by using a wheelchair. However, for arm related tasks, no adequate solution exists.

The state of the art of mobile arm supports consist of a variety of robotic and passive supporting solutions [2, 3]. In general, these solutions use a large volume and do not fit the human body in an elegant manner. Furthermore, most solutions constrain the natural range of motion of the human arm. They provide support, either only in a limited range of motion, or solely for the upper arm limb [2].

The most promising solutions make use of classical static balancing techniques to balance the arm [4, 5]. In a statically balanced system, the gravitational force acting on a mass is compensated for, independent of its pose [6, 7]. A simple example of static balance is balancing a mass, using the upward lifting force of a helium balloon. This system can be moved to different positions and remain motionless, without the need for any external force or energy source.

Most current arm support designs are based on classical balancing solutions for serial linkages, using mono-articular zero-free-length springs (ZFLS), where the spring force of a ZFLS is proportional to its length [6]. These solutions require a parallelogram linkage alongside the upper arm, to provide a link with fixed orientation at the elbow joint [6]. Disadvantage of using parallelogram linkages are the restricted planar motion, the increased number of parts and added mass, inertia and volume of the linkage.

In recent literature, a method for designing statically balanced serial linkages, using multi-articular ZFLSs, was presented [8, 9]. Obtainable systems have the advantage of not requiring a parallelogram linkage. Therefore, a 2-link system can be used, allowing spatial, out of plane rotations. These systems have the potential to balance the human arm in any natural pose. A spring configuration that is described in [10] makes use of two ZFLSs to balance a 2-link system. The first spring is a bi-articular ZFLS, between the fixed world and the forearm. The second spring is a mono-articular ZFLS, connecting the upper and forearm. In recent work this spring configuration was implemented in a dynamic arm support [11]. Using this spring system, the arm is balanced while maintaining the natural range of motion of the human, a great improvement compared to current solutions. Nonetheless, a downside of this configuration is that the forearm attachment point, for the spring connected to the fixed world, must be located on the combined center of mass (CoM) of the arm limbs (Chapter 7). This constrained point is located at an approximate distance of $0.1 m$ from the elbow joint, in line with the arm. A shorter distance would allow for a closer fit around the human body.

Two new spring configurations are developed in Chapter 7 and in [12]. In the first spring configuration, two bi-articular ZFLSs between the fixed world and the forearm balance the arm for the natural range of motion of the human arm. In the second configuration, 3 ZFLSs, one bi-articular between the fixed world and the forearm, and two mono-articular between the upper arm and forearm, and fixed world and upper arm, respectively, balance the whole arm. In both spring configurations, all spring attachment locations are adjustable, potentially allowing for a better fit to the human arm. Never-

theless, these attachment point locations cannot be selected independent of each other. Specific relations between these locations and other parameters must be fulfilled for the system to be statically balanced (Chapter 7).

The goal of this paper is to compare the different spring configurations to each other in order to make a choice for a spring configuration that is good to apply in a close-to-body arm support. They are compared on their balancing quality and their tuning ability. For evaluating the balancing quality the vertical force is measured. Next to that, tuning rules are determined for each spring configuration in order to know how the configuration can be tuned to regain or improve balancing quality.

9.2. METHOD

9.2.1. SPRING CONFIGURATIONS

THE balancing quality of five different springs configurations was measured. These spring configuration are described and elaborated in Chapter 7 and 8. A schematic view of the spring configurations is given in Fig. 9.1-9.3. For the 2-springs and 3-springs configuration, an asymmetric spring configuration is also measured. In this asymmetric spring configuration the bi-articular spring (from shoulder to forearm) is not splitted to each side of the forearm (as can be seen in Fig. 9.4b), but only attached at the lateral side of the forearm. For the 3-asymmetric-springs configuration, also the attachment point of the mono-articular spring (k_3) on the upper arm is positioned more lateral of the arm.

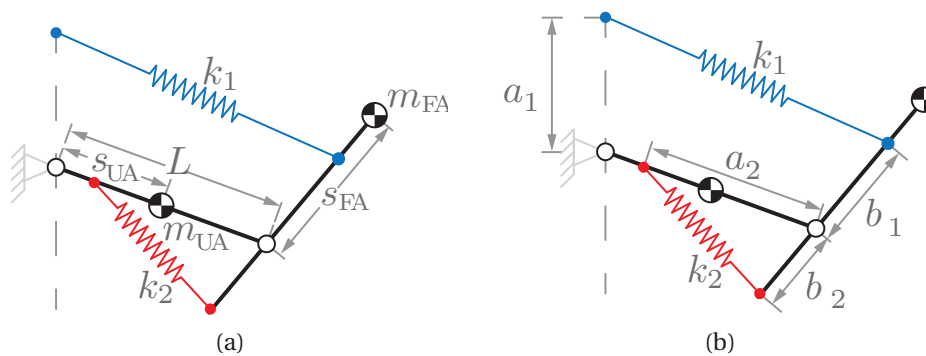


Figure 9.1: Schematic view and definition of parameters of the evaluated 2-springs (asymmetric) configuration, reproduced from [9].

9.2.2. EXPERIMENTAL EVALUATION

An experimental evaluation was set up to assess the balancing quality of the different spring configurations. A 2-link system, that has the same degrees of freedom (DoF) as the human arm (3DoF at the shoulder, and 1DoF at the elbow), was used to attach the spring configuration to (Fig. 9.4). It was rigidly attached to a frame that was connected to the world. This 2-link system is elaborated in [11] (Chapter 11), where this system is used as a prototype for an arm support.

Measurements were performed for different system states. The state of the system is defined by four DoFs, as described in [13] and Chapter 2. It defines a flexion angle (ρ_1),

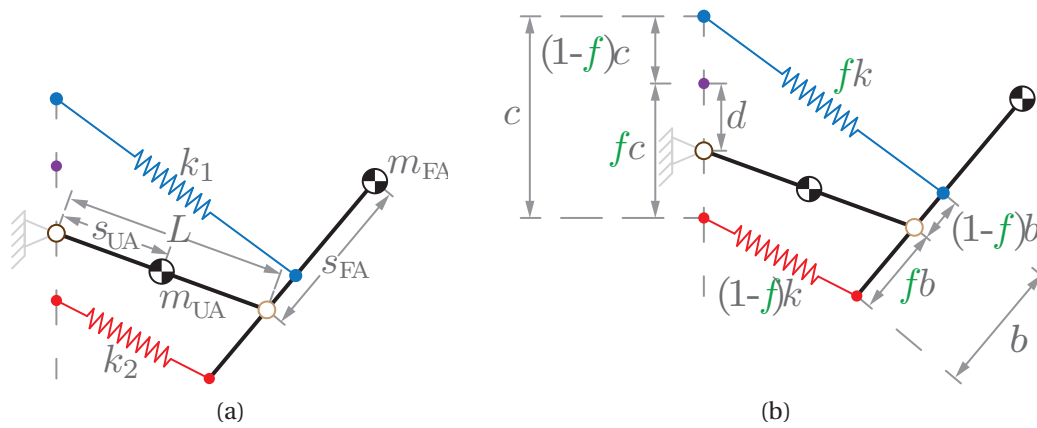


Figure 9.2: Schematic view and definition of parameters of the evaluated 2-parallel-springs configuration, extracted and reproduced from Chapter 7.

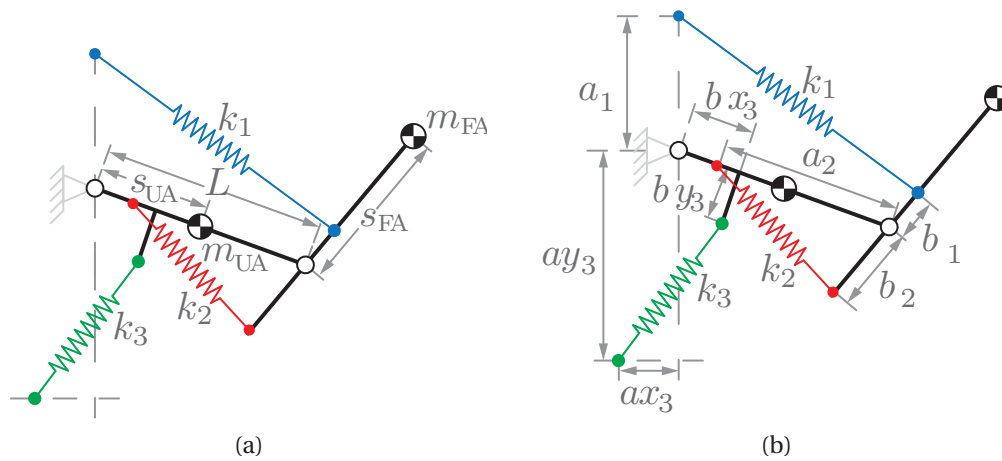


Figure 9.3: Schematic view and definition of parameters of the evaluated 3-springs (asymmetric) configuration, reproduced from [12].

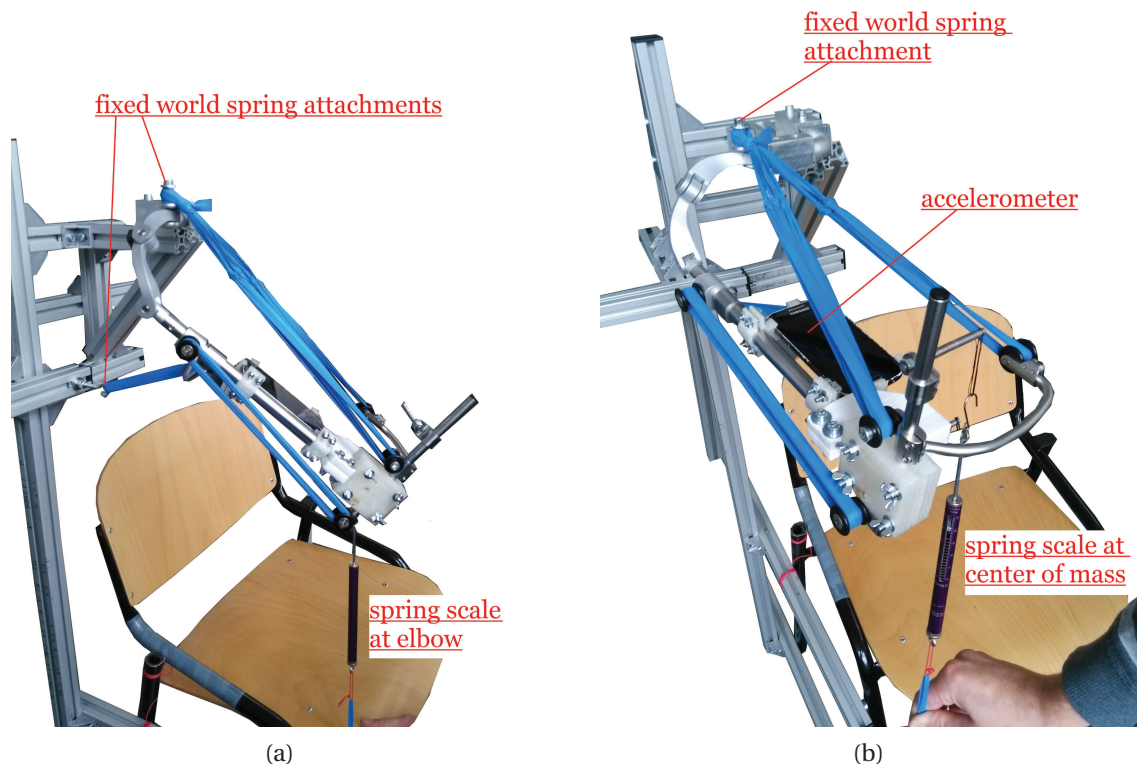


Figure 9.4: Pictures of the experimental setup with the 3-springs configuration (blue). The forces were measured with a spring scale (purple) at the (a) elbow, in the center of the arm, and (b) at the center of mass of the arm.

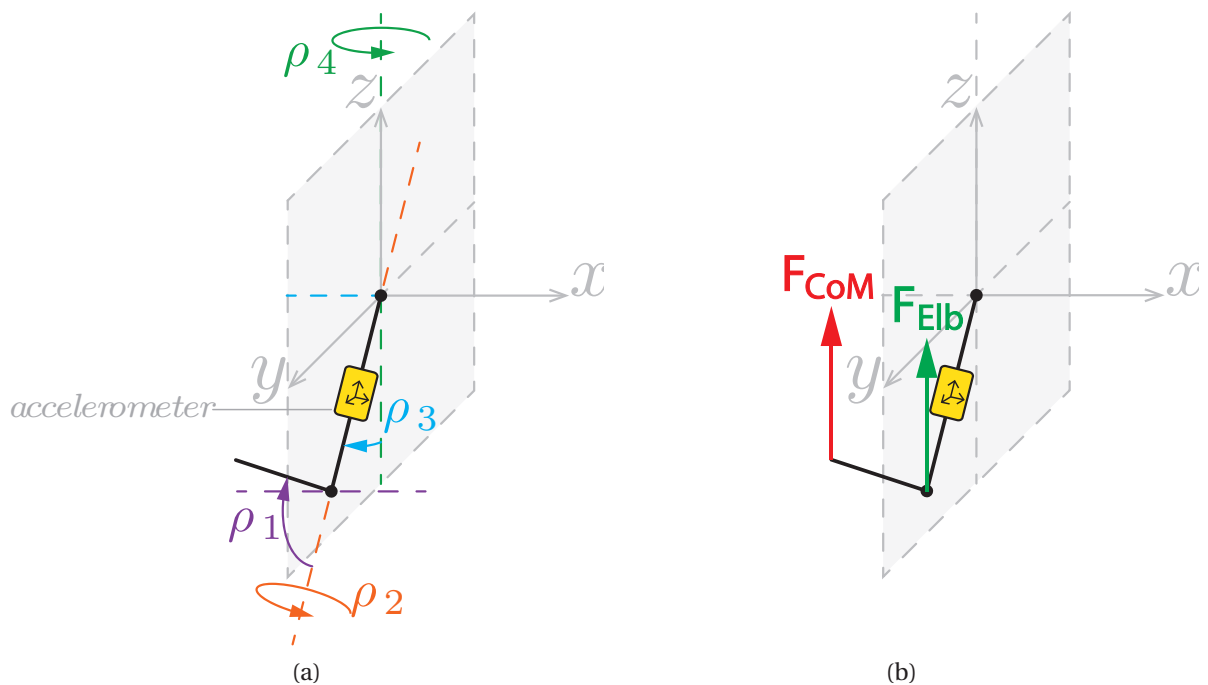


Figure 9.5: (a) Definition of state angles of the right human arm. The origin represents the shoulder. (b) Forces that were measured during the evaluation.

State	Description	Angle	Description specific state value	
φ_1	Flexion angle	45°	Partially extended elbow	
		90°		
		120°		Flexed elbow
φ_2	Orientation of flexion plane	0°	Arm in vertical plane	
φ_3	Elevation angle	30°	Lowest elevation upper arm	
		50°		
		70°		
		90°		Horizontal upper arm
		110°		Highest elevation upper arm
φ_4	Orientation of elevation plane	45°	Abducted plane	
		90°	Forward plane	

Table 9.1: States of measurements that were performed.

an elevation angle (ρ_3), and the orientation of the flexion and elevation planes (ρ_2, ρ_4 , respectively) (Fig. 9.5). Measurements were performed for all possible combinations of states listed in Table 9.1.

The spring parameters were calculated to balance a virtual arm and the 2-link system with the parameters shown in Table 9.2. This means that the resultant measured vertical force corresponds with the virtual mass of the upper arm ($m_{UA, virtual}$) and forearm ($m_{FA, virtual}$). For the 2-parallel-springs configuration the parameters that were used were slightly different: $m_{UA, virtual} = 1.55$ kg, $m_{UA} = 2.013$ kg, $s_{UA} = 0.154$ m, $m_{FA, virtual} = 0.593$ kg, $m_{FA} = 0.93$ kg, $s_{FA} = 0.12$ m. is used. the

During the measurements only the vertical forces at the elbow (F_{Elb}) and the CoM (F_{CoM}) of the arm were measured separately (Fig. 9.5b). This was performed with spring scales (Pesola, range: 0 – 25N, resolution: 0.5N) that were attached to the elbow, in the center of the arm, and at the CoM of the arm (Fig. 9.4). During a measurement, states φ_1 , φ_2 and φ_4 were kept constant while state φ_3 (elevation angle), was varied from $\varphi_3 = 110^\circ$ to $\varphi_3 = 30^\circ$, in steps of 20° . The measurements were done for the downwards movement and upwards movement, repeated twice, to be able to measure hysteresis and friction effects.

The experiment was set up to test the actual force output of the spring configuration, in multiple arm orientations. The difficulty of measuring the system is that there are four DOFs and only one output force. Because of this complexity, it is crucial to set up an experiment for which it is clear what the obtained measurements imply. Actions taken, to ensure clear measurements, consist of avoiding friction effects and measuring all forces in vertical direction.

For the used structure the friction in the elbow joint is large. The effect of this friction component on the measured output is of the same order of magnitude as the de-

Parameter	Value	Unit
m_{UA}	$1.463 (= 1 (m_{UA,virtual}) + 0.468 (m_{link,UA}))$	[kg]
s_{UA}	$0.155 (= 0.15 (s_{UA,virtual}) + 0.165 (s_{link,UA}))$	[m]
L	0.3	[m]
m_{FA}	$1.337 (= 1 (m_{FA,virtual}) + 0.337 (m_{link,FA}))$	[kg]
s_{FA}	$0.129 (= 0.15 (s_{FA,virtual}) + 0.068 (s_{link,FA}))$	[m]

Table 9.2: Link parameters of the 2-link system where the spring configurations were attached to.

sired output force. As the goal was to measure the effect of the spring system, the experiment was designed to avoid the effect of the elbow friction component. This was obtained by mechanically constraining the elbow joint at a fixed angle (φ_1) during the measurements. Other states (ρ_2 , ρ_3 and ρ_4) were manually maneuvered to have the specific values. The angles of these three states were measured by using an accelerometer of a smart phone, to determine its orientation with respect to the gravitational acceleration field. This sensor was fixated to the upper arm (Fig. 9.4). The angles were positioned with 2° accuracy.

For each measurement, F_{Elb} and F_{CoM} are not constant, but a function of the system states. This is because the ratio between moment arms, from shoulder to elbow or CoM, is not constant either (Figure 9.5b). In Eq. 9.1a and 9.1b, it is shown how the force that should be balanced by the spring configuration is calculated and where it acts on the links. Eq. 9.1c describes the theoretical force that should be measured at a certain place on the arm. This force is shown in the results of each spring configuration as a dotted line (Fig. 9.6-9.10).

$$F_{springs} = \left(m_{UA} \frac{s_{UA}}{L} + m_{FA} \right) g \quad (9.1a)$$

$$s_{springs} = \frac{m_{FA} s_{FA}}{m_{UA} \frac{s_{UA}}{L} + m_{FA}} \quad (9.1b)$$

$$F_{measured} = \frac{\left[F_{springs} (L \sin(\rho_3) + s_{springs} \sin(\rho_1 - \rho_3)) - m_{link,UA} \left(\frac{s_{link,UA}}{L} \right) g L \sin(\rho_3) - m_{link,FA} g (L \sin(\rho_3) + s_{link,FA} \sin(\rho_1 - \rho_3)) \right]}{(L \sin(\rho_3) + s_{measured} \sin(\rho_1 - \rho_3))} \quad (9.1c)$$

9.2.3. TUNING RULES

Next to the measurements of the balancing quality, tuning rules of each spring configuration are determined. This describes how each spring configuration can be tuned in order to reach a good balancing quality when the exact mass of the arm is unknown. Besides that, with the determined relations it can be seen which parameters should be changed to maintain the balancing quality if another parameter varies. With the measurements of the balancing quality and the tuning rules, a choice can be made for a spring system that is good to apply into a close-to-body arm support.

9.3. RESULTS

9.3.1. EXPERIMENTAL EVALUATION OF THE SPRING CONFIGURATIONS

FOR each spring configuration the vertical force measured at the elbow (F_{Elb}) and CoM (F_{CoM}) is plotted against the elevation angle (ρ_3), for the 2 sequential downwards and upwards movements. The dotted line in each plot shows the force that should be measured according to Eq. 9.1c. The results are only shown for measurements with parameters $\rho_1 = 90^\circ$, $\rho_2 = 0^\circ$ and $\rho_4 = 0^\circ$, because the other results show similar behavior. The results for each spring configuration are shown in Fig. 9.6-9.10. For each spring configuration, some observations that were seen during the measurements, but not directly in the results of the vertical force measurements are written down.

2-SPRINGS

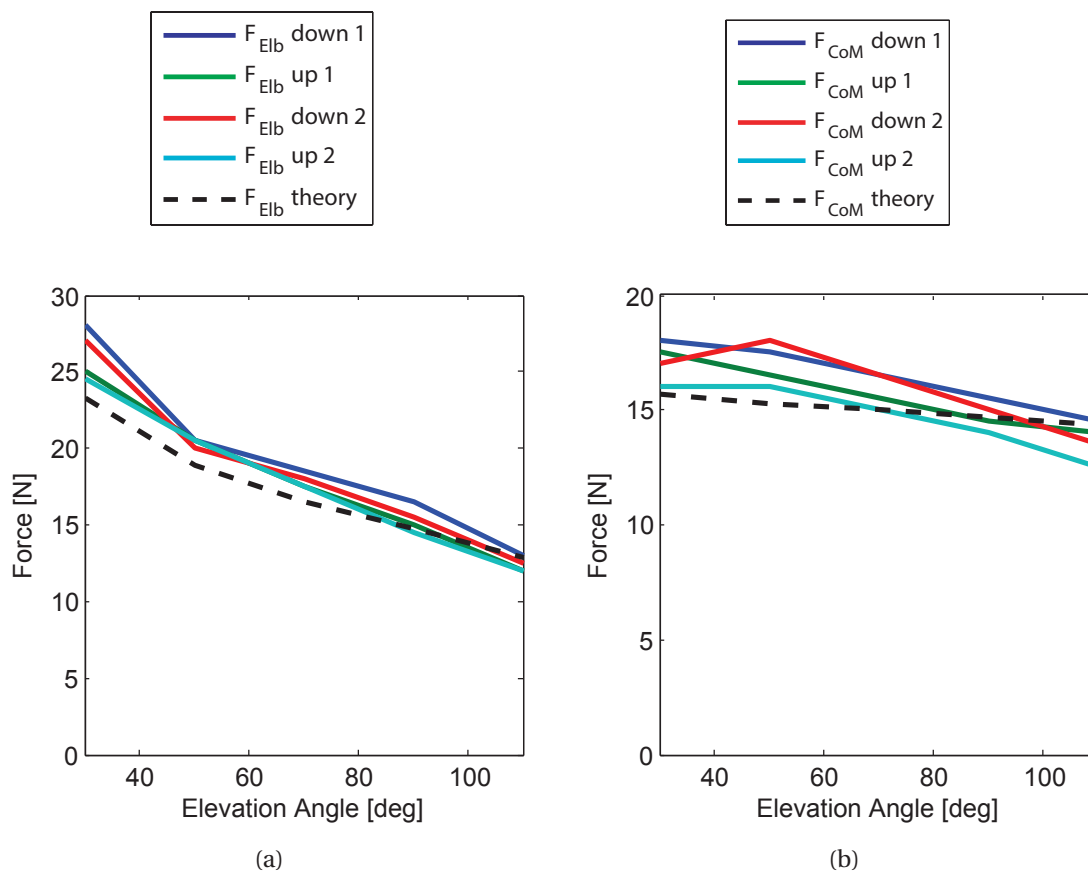


Figure 9.6: Measurement results of the 2-springs configuration for the force at the (a) elbow, and (b) center of mass (CoM). Each set consist of 2 sequential downwards and upwards measurements.

Observations: At $\rho_3 = 30^\circ$, the arm tends to make some exo-rotation of the shoulder.

2-ASYMMETRIC-SPRINGS

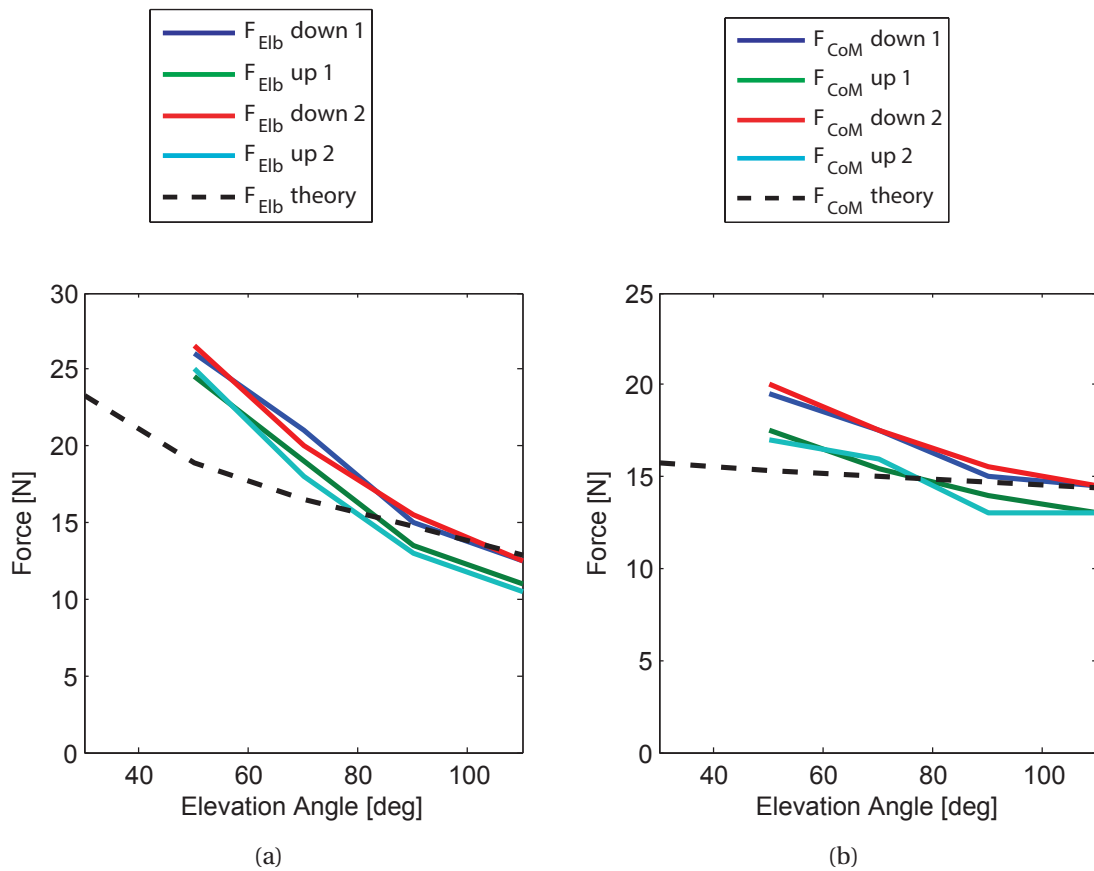


Figure 9.7: Measurement results of the 2-asymmetric-springs configuration for the force at the (a) elbow, and (b) center of mass (CoM). Each set consist of 2 sequential downwards and upwards measurements.

Observations: At $\rho_3 > 90^\circ$, the shoulder rotation tends to 0° and the force that is created due to the asymmetric spring system does not feel large. This force increases for decreasing ρ_3 , but feels low again at $\rho_3 = 0^\circ$. For $\rho_3 < 50^\circ$, the shoulder tends to make endo-rotation and abduction of the shoulder.

2-PARALLEL-SPRINGS

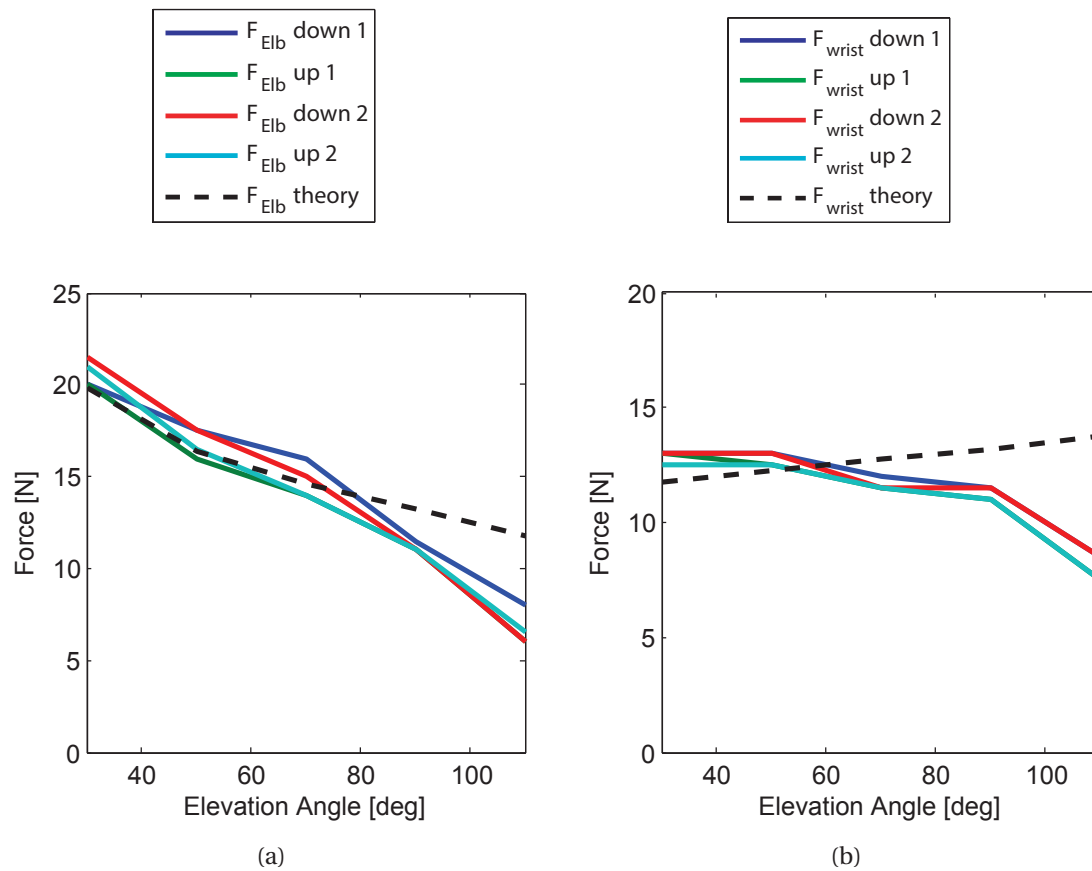


Figure 9.8: Measurement results of the 2-parallel-springs configuration for the force at the (a) elbow, and (b) wrist. Each set consist of 2 sequential downwards and upwards measurements.

Observations: At $\rho_3 < 30^\circ$, the lower spring (k_2) becomes very short and slack. At $\rho_3 = 110^\circ$ and $\rho_1 = 135^\circ$, the spring (k_1) becomes very short and almost slack.

3-SPRINGS

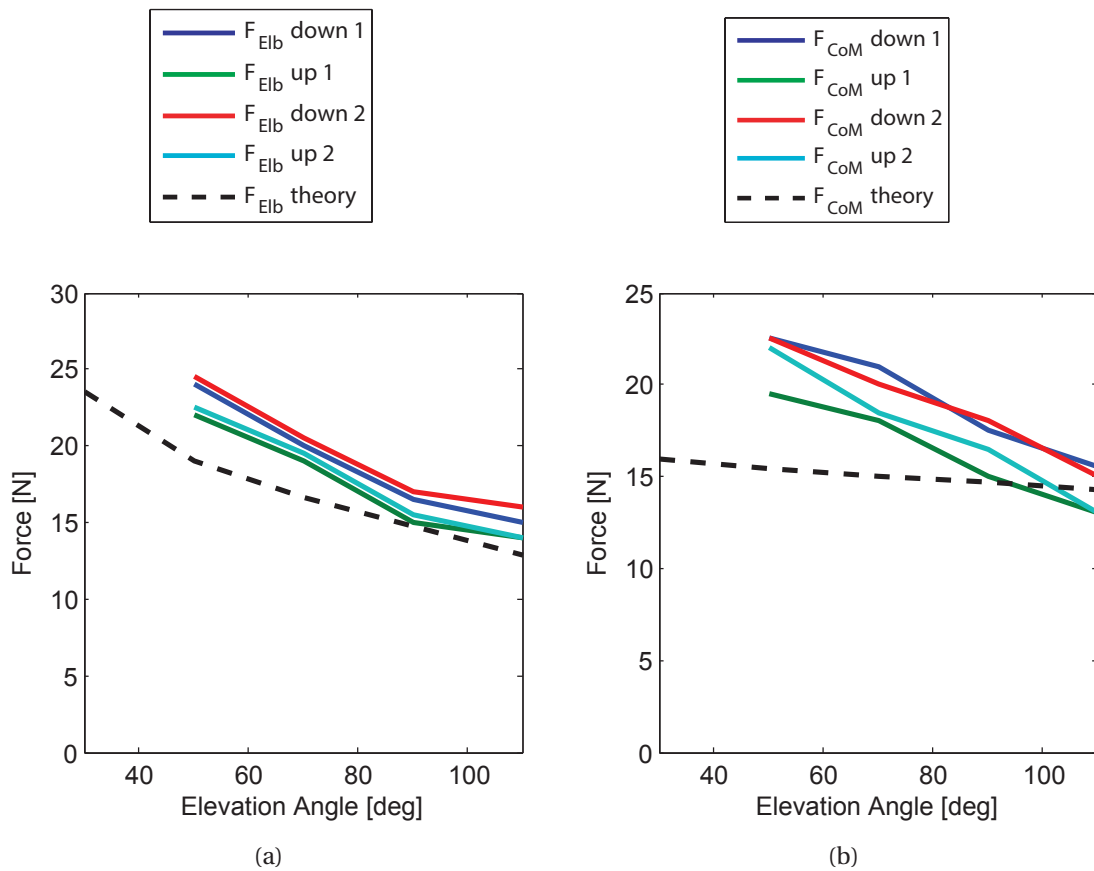


Figure 9.9: Measurement results of the 3-springs configuration for the force at the (a) elbow, and (b) center of mass (CoM). Each set consist of 2 sequential downwards and upwards measurements.

Observations: Same observations as with the 2-asymmetric-springs configuration. Next to those observations, at $\rho_3 = 0^\circ$ and $\rho_1 = 90^\circ$ (arm at armrest) the arm feels instable and has a preference to make endo- or exo-rotation. The third spring (k_3) introduces a moment and some endo-rotation and horizontal adduction of the shoulder. For smaller elevation angles, the third spring (k_3) becomes very short and almost slack.

3-ASYMMETRIC-SPRINGS

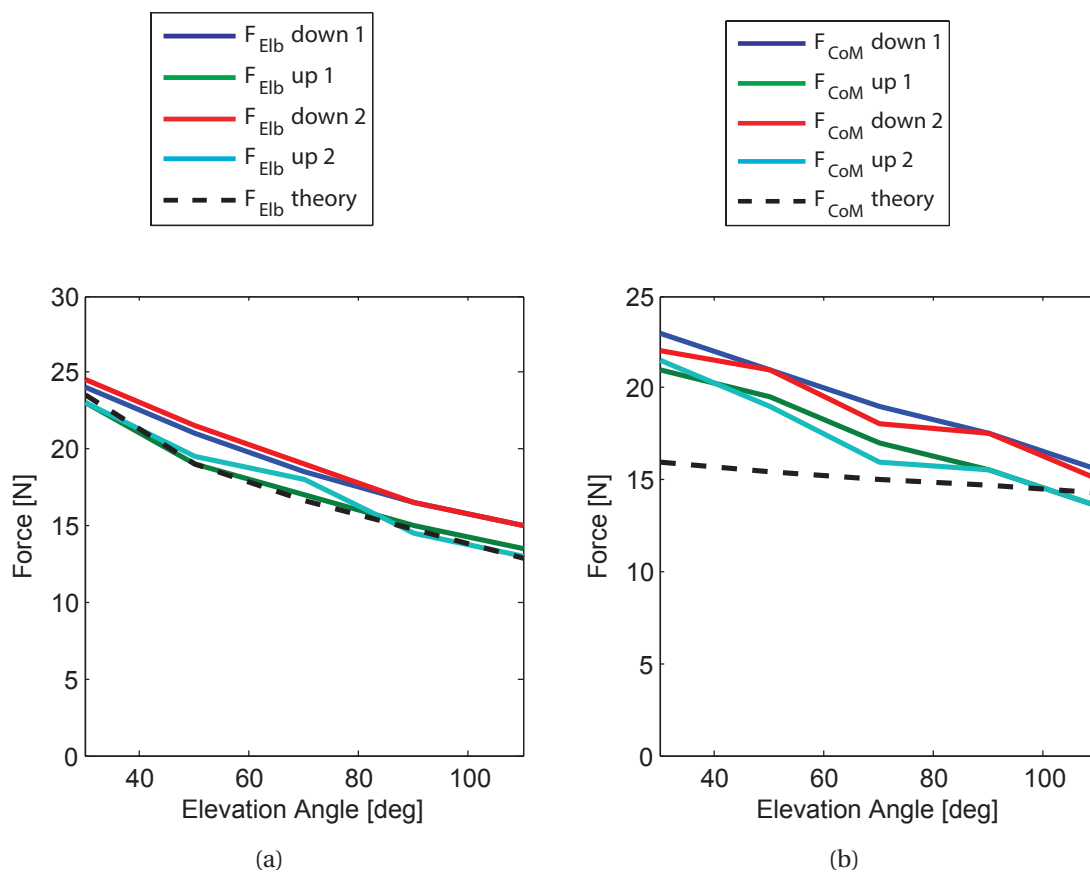


Figure 9.10: Measurement results of the 3-asymmetric-springs configuration for the force at the (a) elbow, and (b) center of mass (CoM). Each set consist of 2 sequential downwards and upwards measurements.

Observations: Same observations as with the 3-springs configuration, but the forces/moments due to the asymmetric springs feel lower.

9.3.2. TUNING RULES

In this section the tuning rules for each spring configuration are determined. These tuning rules can be used in order to reach a good balancing quality if the (center of) mass of the upper arm and forearm are unknown. For each spring configuration a short elaboration is given and the tuning rules (in correct order) are written down.

2-(ASYMMETRIC)-SPRINGS

In this spring configuration, the attachment points and the stiffness of the springs are determined according Eq. 9.2 [9, 11]. From these equation it can be seen that b_1 is constraint to the mass and length of the upper arm and forearm. In the equations it can be seen that every parameter relates to another parameter. This makes tuning very difficult

if the masses are unknown or if there is a slight error in a parameter.

$$b_1 = \frac{m_{FA}s_{FA}L}{m_{UA}s_{UA} + m_{FA}L} \quad (9.2a)$$

$$k_1 = \frac{g(m_{UA}s_{UA} + m_{FA}L)}{a_1L} \quad (9.2b)$$

$$\frac{k_1}{k_2} = \frac{a_2}{L} \frac{b_2}{b_1} \quad (9.2c)$$

Tuning steps:

1. Determine b_1 according to the equations, or try to find the CoM of the whole arm by balancing the arm on your finger and determine b_1 .
2. Choose a_1 close to the body.
3. Apply springs (k_1) until the whole arm is balanced.
4. Choose a_2 and b_2 close to the body.
5. Apply springs (k_2) according to the relations in Eq. 9.2c until the forearm is balanced.

2-PARALLEL-SPRINGS

As described in Chapter 7, there is a relation between the spring stiffness of each spring and the attachment points of the springs that includes a factor f (Fig. 9.2). In Eq. 9.3, the relations between all the parameters are shown.

$$kdL = m_{UA}gs_{UA} + m_{FA}gL \quad (9.3a)$$

$$kbc(1-f)f = m_{FA}gs_{FA} \quad (9.3b)$$

$$f = \frac{k_1}{k_1 + k_2} = \frac{k_1}{k} = 1 - \frac{k_2}{k}, \quad (9.3c)$$

$$\text{where } k_1 = fk, \text{ and } k_2 = (1-f)k$$

Tuning steps:

1. Choose b_1 , b_2 , c_1 and c_2 close to the body.
2. Apply springs (k_1 and k_2) according to the relations and factor f until the forearm is balanced.
3. Move attachments point c_1 and c_2 simultaneously up or down until the whole arm is balanced.

3-(ASYMMETRIC)-SPRINGS

For this spring configuration, the important difference with the 2-(asymmetric)-springs configuration is that b_1 can be chosen at any position and is inverse proportional to k_1 . The stiffness of the top spring (k_1) is also inverse proportional to a_1 . The relation between k_1 and k_2 (calculated according to Eq. 9.2c) does not change for a varying m_{UA} or m_{FA} . For example, if m_{FA} is 10% larger than expected, the moment about the elbow is 10% larger. This can be compensated by adjusting the moment created by the spring configuration, for example by increasing a_1 by 10% or by increasing k_1 and k_2 by 10% or increasing b_1 and b_2 by 10% or increasing k_1 and b_2 or increasing b_1 and a_2 , or a combination of these. It has to be kept in mind that due to these changing parameters, k_3 also needs to be changed. When m_{UA} is larger than expected, the balancing quality can be regained by decreasing b_3 , k_3 and/or a_3 . The varying m_{UA} does not affect the balance of the forearm.

Tuning steps:

1. Choose a_1 , a_2 , b_1 and b_2 close to the body.
2. Apply springs k_1 and k_2 according to the relations until the forearm is balanced.
3. Choose a_3 and b_3 close to the body.
4. Apply springs (k_3) until the whole arm is balanced.

9.4. DISCUSSION

FOR each spring configuration, the results of the experiments and tuning rules are shortly discussed.

Each spring configuration show the error that for smaller elevation angles the measured force is larger than expected, and for larger elevation angles the measured force is smaller than the theoretical value. This is because the springs that are attached to the fixed world above the shoulder are attached to a cylinder shaped axis and are bound together by wrapping a piece of rubber around them, creating a knot (Fig. 9.11). The effective location, from which the ZFLS behavior starts, changes for different orientations of the spring. For a small elevation angle (Fig. 5.6a), the effective attachment point is found to be higher up, compared to larger elevation angles (Fig. 5.6b). Height differences of approximately $0.012m$ are observed. That is an increase of 12.5% of the value of a_1 . Other attachment points have a different construction and do not shift as much. As can be seen in the equations and relations for each spring configuration (Eq. 9.2,9.3), this can have a large influence on the balancing quality. This means that for smaller elevation angles, the measured vertical force will be larger than the theoretical value, and for larger elevation angles the measured force will be smaller than expected. Next to that, it has to be mentioned that measuring the vertical force only was sometimes very difficult. Due to all kind of errors and introduces moments, some horizontal forces were also measured, especially for smaller elevation angles. This also resulted in a larger measured force.

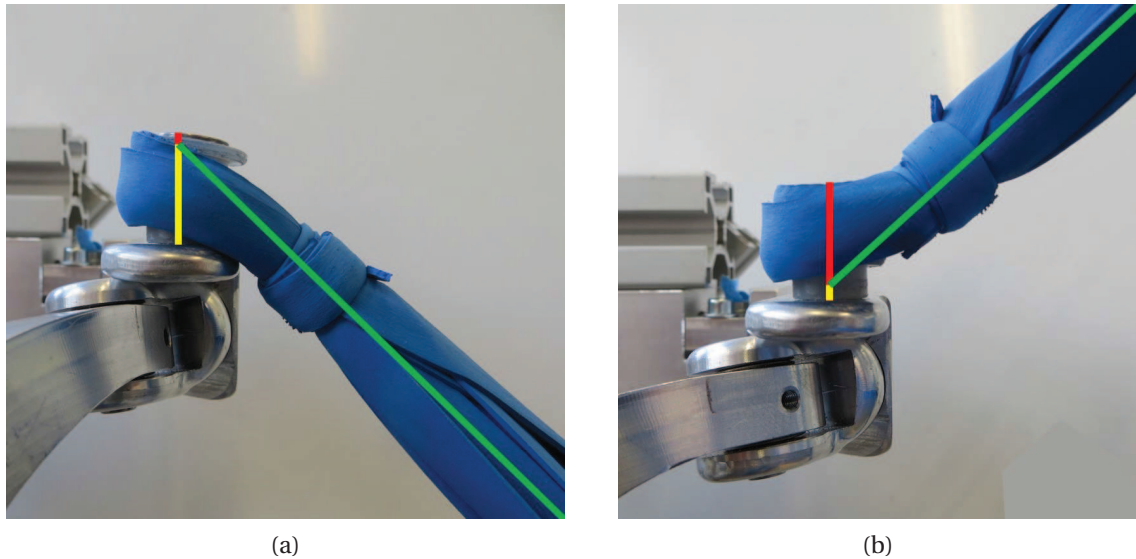


Figure 9.11: Representation of the varying spring attachment point above the shoulder. Dependent of the orientation of the spring the virtual attachment point is (a) above or (b) below the real attachment point.

In general, the hysteresis in the rubber bands is small. The effect on the balancing quality is small, compared to the errors that are introduced by the asymmetric springs or behavior of the spring configuration.

2-SPRINGS

The measured force for the 2-springs configuration is very similar to the theoretical force that should be measured. When measuring at the elbow (F_{Elb}) (Fig. 9.6a), no significant error can be found. For the 2-springs configuration, the distance a_1 is directly related to the stiffness k_1 and the balancing force. An increase in distance a_1 of 12.5% results in an increase of the measured force of 12.5%, which corresponds with the errors seen in Fig. 9.6.

2-ASYMMETRIC-SPRINGS

In the results of the 2-asymmetric-springs configuration, the errors for $\rho_3 < 70^\circ$ increase a lot, and the measured forces are much larger than they should be (Fig. 9.7). The forces were not measured for $\rho_3 = 30^\circ$, because at this position the shoulder rotation was too large to measure a useful vertical force, or the force was too large to be measured with the spring scale. The error is because the moment that the asymmetric bi-articular spring exerts on the arm results in a vertical force. The arm tends to make endo-rotation and abduction for smaller elevation angles (comparable with the arm during eating movement). Because the arm rotates about the center of mass, this extra force is larger for the measured F_{Elb} .

To calculate the order of magnitude of this moment, the moment about the shoulder for abduction is considered. In Fig. 9.12a, a force diagram of the arm is shown. The moment is calculated according to the moment arms of the decomposed spring force. The extra moment that is introduced by the asymmetric spring is shown Fig. 9.12b and

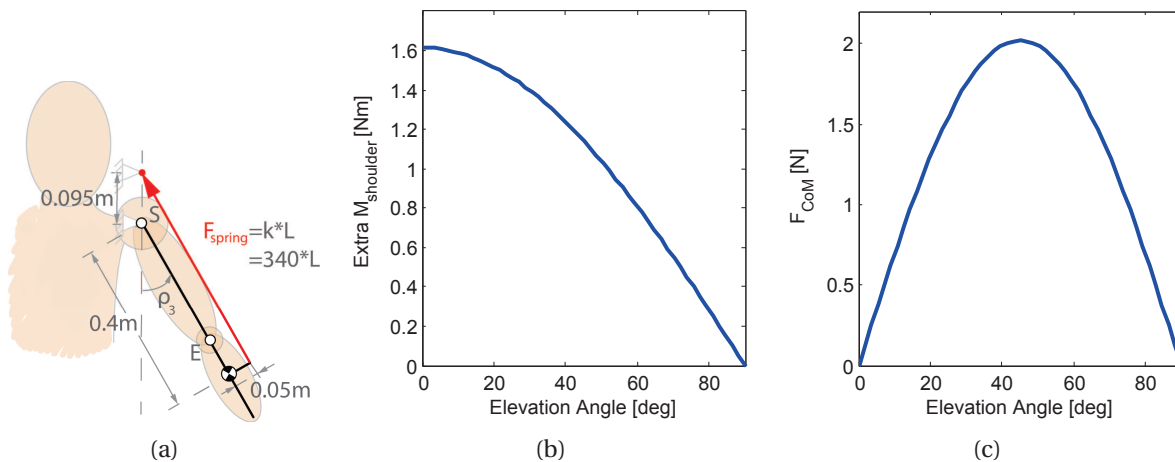


Figure 9.12: Force diagram of the top spring of the 2-asymmetric-springs configuration acting on the arm.

the vertical force that is measured at the CoM due to this moment is shown in Fig. 9.12c. This vertical force is 0 at $\rho_3 = 0^\circ$, because the moment does not introduce a vertical force on the shoulder. A max. vertical force of approximately 2N is measured at $\rho_3 = 45^\circ$. This explains the extra error that is measured for smaller elevation angles and also that it is observed that the force feels larger around $\rho_3 = 45^\circ$, and low again at $\rho_3 = 0^\circ$. It has to be noticed that this is the extra vertical force for the chosen parameters (Table 9.2). For a human arm, this moment and force will be larger, because the spring force needs to be larger to balance the arm. This extra moment will be too large to compensate for Duchenne patients with very little muscle force in their arms.

2-PARALLEL-SPRINGS

In Fig. 9.8, it can be seen that the measured forces matches the ideal balancing force quite well at small elevation angles ($\rho_3 < 70^\circ$). The forces were measured at the elbow and the wrist, instead of the CoM. This is taken into account to determine the theoretical force. For larger elevation angles ($\rho_3 > 90^\circ$), the measured force is clearly smaller than ideal. At these higher elevation, the top spring (k_1) reaches its shortest length. Approximately down to 150% of the original unloaded spring length, which is at the lower boundary of the linear stiffness range (Appendix A). Furthermore, at these small elongations the output spring force is relatively low. Therefore, absolute errors in spring force have a relatively high impact on its force output. Altogether, this reduced force in the top spring decreases the upwards moment acting on the linkage, resulting in a lower upwards force measurement. To quantify this effect, the found absolute errors at $\rho_3 = 110^\circ$ is examined. The difference of about 5N, between the ideal and measured force in this pose, corresponds to a force reduction in the top spring of approximately 20% of the ideal spring force. All in all, reduced force in the top spring is a plausible cause for errors in this high elevation region of the measurements.

The height difference of the top attachment affects parameter d . The location described by d is located in between the top and bottom attachments at the fixed world, at factor f of the distance between these points (Fig. 9.2b). Therefore, the resulting change in d is scaled by this same factor and is equal to 0.008m. The resulting error in force is the

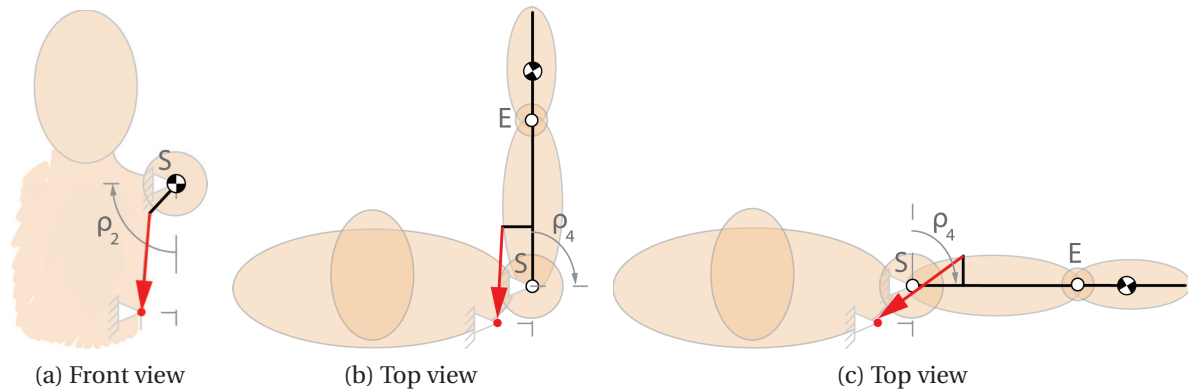


Figure 9.13: Force diagram of the third spring of the 3-springs configuration acting on the arm for an elevation angle $\rho_3 = 90^\circ$.

product of this height error and k (Eq. 9.3a). Between the lowest and highest measured elevations, this corresponds to an error in force of $3.8N$. This force is in the same order of magnitude as observed in the measurements.

3-SPRINGS

For the 3-springs configuration, the mono-articular spring that runs from the trunk to the upper arm [12] is connected to the trunk at a medial and posterior position from the vertical through the shoulder joint, and also medial and posterior from the upper arm. This spring exerts a moment on the arm (as was also observed during measurements), that tends the arm to make both endo-rotation and horizontal adduction. In Fig. 9.13, it is shown that the third spring of this spring configuration k_3 , exerts a moment about the shoulder for different positions of the arm. The extra moment that is exerted on the arm is difficult to calculate, because the direction of the moment changes for each position of the arm. Therefore, this configuration is also subjectively evaluated with a prototype to balance a human arm of a healthy subject. This extra moments felt large, and can definitely not be compensated by Duchenne patients with little muscle force in their arms.

The larger measured force for smaller elevation angles is a results of this extra moment and the measured horizontal forces that are introduced by the position of the arm, and is also a result of the slack third spring. This spring is almost acting in its non-linear stiffness range (Appendix A), and does not compensate the high forces introduced by the bi-articular spring (k_1) anymore.

For this spring configuration, the forces were also not measured for $\rho_3 = 30^\circ$, due to large forces and limitations of the spring scale.

3-ASYMMETRIC-SPRINGS

The 3-asymmetric-springs configuration seems to balance the arm much better than the 3-springs configuration. The F_{Elb} is equal to the theoretical value that should be measured (Fig. 9.10a). For the F_{COM} , a larger force is measured. This has the same reasons as with the 3-springs configuration (Fig. 9.10b). However, the third spring (k_3) is now attached to the upper arm more to the lateral side. This spring introduces a moment to the

upper arm for exo-rotation and horizontal abduction, which somewhat counteract the moments that are introduced by the asymmetric bi-articular spring. This is also what is observed during measurements. With the attachment point of this spring on the upper arm, this compensating moment can be tuned. Because the arm tends to rotate about the CoM, this compensation can be seen in the F_{Elb} , but not in the F_{CoM} . To feel this extra moment, this spring configuration is also build into a prototype and subjectively evaluated with a human arm of a healthy subject. The moment that is still in the system felt large, and can definitely not be compensated by Duchenne patients with little muscle force in their arms. The moment that is introduced by the asymmetric bi-articular spring can somewhat be compensated by the asymmetric third spring, but not enough and this is only for movements in one plane. For movements out of that plane, the moment increases.

TUNING RULES

The 3-(asymmetric)-springs configuration is the easiest to tune. Every parameter can be chosen. And more important, every slight error in one parameter can be compensated by adjusting another parameter (according to the relations given for this spring configuration). The advantage is that this spring configuration could be tuned by only adjusting the spring stiffnesses.

The 2-(asymmetric)-springs configuration is much harder to tune. Every parameter is related to other parameters. So an error in one parameter often results in adjusting multiple parameters according to the relations. Next to that, the parameter b_1 (Fig. 9.1) has to be calculated very precise to gain perfect balance of the arm. For example, if the parameter b_1 is $0.05m$ larger than calculated, the extra moment that is exerted on the shoulder and that the user feels is $M_{shoulder} = F_{balance} \cdot 0.05m = m_{CoM} \cdot g \cdot 0.05m = 3.75kg \cdot 9.81 \cdot 0.05m = 0.37Nm$, where m_{CoM} is the mass of the human arm including a serial linkage [11].

The 2-parallel-springs configuration is also hard to tune. Although an error in one parameter can be compensated by adjusting another parameter and a good balancing quality can always be achieved, the balancing quality is very sensitive for small errors in parameter d (Fig. 9.2). Another difficulty is that the parameters are related to each other with a factor f . Tuning would be possible by recalculating the other parameters taking this factor into account.

9.5. CONCLUSIONS

THE goal of this paper was to compare the different spring configurations to each other in order to make a choice for a spring configuration that is good to apply in a close-to-body arm support based on a serial linkage without auxiliary links.

To evaluate the balancing quality, the vertical force was measured. This vertical force was very similar to the theoretical force that should be measured for the 2-springs and 3-asymmetric-springs configurations. In the other spring configurations, moments were introduced due to asymmetric springs, or the force was very sensitive to small alignment errors. Due to all kind of errors, including misalignment of the attachment points and the use of non-linear rubber springs, none of the spring configurations balanced the arm perfectly. Next to that, the perception and wishes of every user is different. Therefore, it

is very important to have a close-to-body spring configuration that is very adjustable.

For each spring configuration, tuning rules are determined in order to know how the configuration could be tuned to regain or improve balancing quality. The 3-(asymmetric)-springs configuration is the easiest to tune by only adjusting the spring stiffnesses. For this spring configuration, each parameter can be chosen and a good balancing quality can always be achieved. For the other spring configurations, tuning is harder due to the sensitivity of the balancing quality to small errors in certain parameters, or that a certain parameter is constrained to the mass and length of the arm of the user and needs to be positioned very precise in order to achieve good balancing quality.

Because of the adjustability and the ease of tuning, the 3-(asymmetric-)springs configuration is proposed as a good spring configuration to apply in a close-to-body arm support. To limit the introduction of extra moments due to the asymmetric spring, it is proposed to split the third spring (from trunk to upper arm) into a V-shape with attachment points at the medial and lateral side of the upper arm. In this way, the virtual attachment point is at the axis of the arm.

REFERENCES

- [1] M. Kohler, C. F. Clarenbach, C. Bahler, T. Brack, E. W. Russi, and K. E. Bloch, *Disability and survival in Duchenne muscular dystrophy*, Journal of Neurology, Neurosurgery & Psychiatry **80**, 320 (2009).
- [2] A. G. Dunning and J. L. Herder, *A review of assistive devices for arm balancing*, International Conference on Rehabilitation Robotics , 6650485 (2013).
- [3] R. Gopura, K. Kiguchi, and D. S. V. Bandara, *A brief review on upper extremity robotic exoskeleton systems*, IEEE International Conference on Industrial and Information Systems **8502**, 346 (2011).
- [4] G. Kramer, G. R. B. Romer, and H. J. A. Stuyt, *Design of a Dynamic Arm Support (D AS) for gravity compensation*, IEEE International Conference on Rehabilitation Robotics , 1042 (2007).
- [5] T. Rahman, W. Sample, R. Seliktar, M. Alexander, and M. Scavina, *A body-powered functional upper limb orthosis*, Journal of rehabilitation research and development **37**, 675 (2000).
- [6] J. L. Herder, *Energy-free systems: theory, conception, and design of statically balanced spring mechanisms* (dissertation, 2001) p. 268.
- [7] H. Hilpert, *Weight balancing of precision mechanical instruments*, Journal of Mechanisms **3**, 289 (1968).
- [8] P.-Y. Lin, W.-B. Shieh, and D.-Z. Chen, *A stiffness matrix approach for the design of statically balanced planar articulated manipulators*, Mechanism and Machine Theory **45**, 1877 (2010).

-
- [9] P.-Y. Lin, W.-B. Shieh, and D.-Z. Chen, *A theoretical study of weight-balanced mechanisms for design of spring assistive mobile arm support (MAS)*, Mechanism and Machine Theory **61**, 156 (2013).
- [10] P.-Y. Lin, W.-B. Shieh, and D.-Z. Chen, *Design of statically balanced planar articulated manipulators with spring suspension*, IEEE Transactions on Robotics **28**, 12 (2012).
- [11] P. N. Kooren, A. G. Dunning, M. M. H. P. Janssen, J. Lobo-Prat, B. F. J. M. Koopman, M. I. Paalman, I. J. M. de Groot, and J. L. Herder, *Design and pilot validation of A-gear: a novel wearable dynamic arm support*, Journal of NeuroEngineering and Rehabilitation **12**, 1 (2015).
- [12] A. G. Dunning and J. L. Herder, *A Close-to-Body 3-Spring Configuration for Gravity Balancing of the Arm*, International Conference on Rehabilitation Robotics , 464 (2015).
- [13] L. F. Cardoso, S. Tomazio, and J. L. Herder, *Conceptual design of a passive arm orthosis*, ASME International Design Engineering Technical Conferences **5**, 747 (2002).

III

DESIGN AND APPLICATION

10

EVALUATION OF AN ARM SUPPORT WITH TRUNK MOTION CAPABILITY

Submitted as:

A.G. Dunning, M.M.H.P. Janssen, P.N. Kooren, J.L. Herder,

Technical brief: Evaluation of an arm support with trunk motion capability,

Submitted to Journal of Medical Devices, march 2016.

The first prototype that has been build in this project is explained in this chapter. The prototype is based on an existing arm support that scored rather well in the review presented in Chapter 3 in terms of volume and range of motion. The existing arm support (which is wheelchair-bound) is extended with a structure along the trunk, in order to make the device wearable and able to be worn underneath clothing, as well as increase the range of motion of the device with the opportunity to lean forwards and backwards. In this chapter, a comparison is made between the prototype with trunk motion capability and the existing wheelchair-bound arm support. The devices are evaluated on range of motion and balancing quality.

ABSTRACT

DUE to progressive muscle weakness, the arm function in boys with Duchenne Muscular Dystrophy (DMD) reduces. An arm support can compensate for this loss of function. Existing arm supports are wheelchair-bound, which restricts the ability to make trunk movements. To evaluate the function of a body-bound arm support, a prototype (based on the WREX arm support) that allows trunk movements is build. In order to examine the effect of this device and to compare it with the existing wheelchair-bound device, 3 healthy subjects performed single joint movement and activities of daily living with and without the devices. The range of motion of the arm and sEMG signals of 5 different arm muscles was measured. The range of motion increased when compared to the wheelchair-bound device, and the trunk motion was perceived as important to make some movements easier and more natural, especially the more extreme movements like reaching for a far object and reaching to the top of the head. The sEMG signal was comparable to that of the wheelchair-bound device. This means that an arm support with trunk motion capability can increase the range of motion of the user, while the amount of support to the arm is equal.

10.1. INTRODUCTION

DUCHENNE Muscular Dystrophy (DMD) is the most common form of muscular dystrophy in children, with an incidence of 1 in every 3500-5000 male live births [1, 2]. DMD is characterized by progressive loss of strength in the muscles, which leads to functional weakness. Around the age of 12, boys with DMD lose the ability to walk and the arm function also starts to deteriorate. Currently, the life expectancy is estimated at 30-35 years [3].

The loss of leg function can be compensated fairly well using a wheelchair. However, loss of arm function is much harder to compensate. An arm support can be used to lift the arm of the user and compensate for gravity. In recent years, much research is performed on arm supports [4–6]. This varies from robotic manipulators, which is basically an extra arm for the user, to powered and non-powered supports, which augment the arm muscle strength and motions. Requirements for assistive devices include comfort, functionality, and aesthetics. Many assistive devices are not used because they are too large or stigmatizing. Previous research [7] investigated powered and non-powered arm supports on the body interface, volume and workspace, in order to gain insight in the inconspicuousness and wearability of the devices. It was concluded that almost all arm supports were mounted to the wheelchair and conspicuous. As a result, the user is hindered in its movement when leaning forward, because the trunk could not move.

Within the project '*Flexension A-Gear*', one of the key assumptions is that users prefer an inconspicuous arm support. This is interpreted as a device that is body-bound and fits underneath clothing and still gives a natural support throughout the workspace of the arm. In order to achieve this, the complete structure of the arm support should fit underneath clothing, including the interface where the forces are transmitted to the fixed world. It is proposed to use an extra structure along the trunk to the upper legs for this, which also can increase the range of motion (RoM) of the user by allowing leaning with the trunk. This paper explores the effect of a body-bound arm support with trunk motion capability on the total RoM and balancing quality of the arm support.

10.2. METHOD

10.2.1. EXPERIMENTAL SETUP

IN order to design a body-bound arm support that fits underneath clothing and to increase the workspace, an experimental setup was made (Fig. 10.1). The Wilmington Robotic Exoskeleton, WREX [6]), was used as a basis for a prototype that allows trunk motion. An extra parallelogram mechanism from the shoulder to the hip was built and added to the WREX through some shoulder arcs. At the hips, the parallelogram was attached to a structure that fits around the upper legs and that transfers the forces to the chair. With this prototype, the user should be able to lean forward and backwards while still being able to perform the required arm motions.

10.2.2. PROCEDURES

Evaluation of the prototype was done by evaluating single joint movements (SJM) and activities of daily living (ADL) with Vicon motion analysis (Oxford Metrics, Oxford, UK) and surface electromyography (sEMG) measurements (Zerowire EMG, Aurion, Italy; Ag-

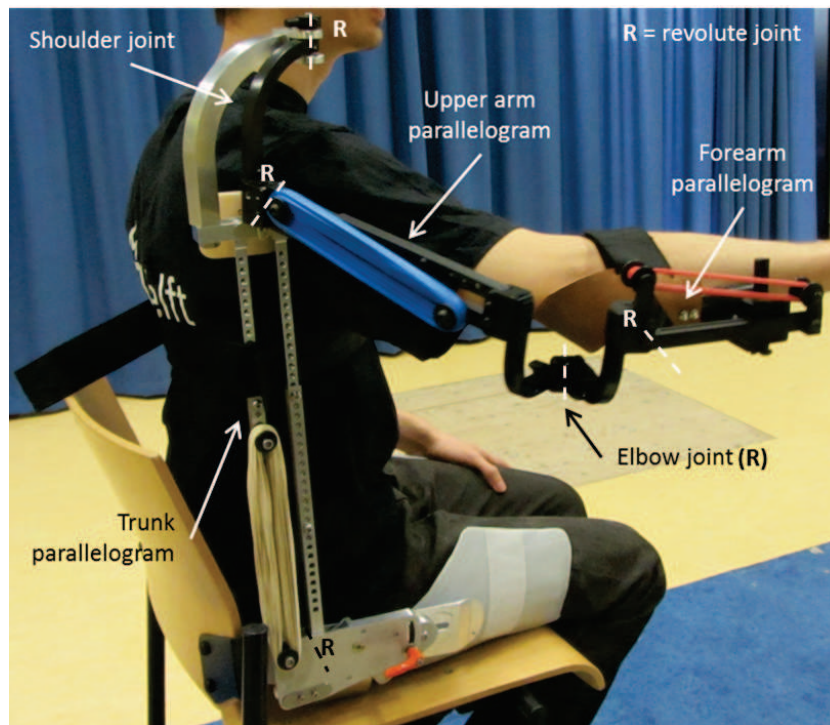


Figure 10.1: Prototype of a body-bound arm support with trunk motion capability: the existing WREX [6] combined with a trunk parallelogram).

AgCL, ARBO ECG electrodes, Tyco Healthcare, Neustadt, Germany) with 3 healthy subjects (24-28 years old, male). SJM performed were: shoulder flexion/extension, shoulder abduction, shoulder adduction in the horizontal plane, and shoulder internal/external rotation. The ADL performed were: reaching for high object, reaching for a far object at ipsilateral shoulder level, reaching for a far object at contralateral shoulder level, reaching for back pocket, reaching to front edge of the seat of the chair, hand to top of head, touching contralateral shoulder, open a zipper of a jacket, and drinking.

The subjects executed each movement simultaneously with the researcher. Each movement was done in approximately 3 seconds. The subject had to do the movement until the point they felt restrictions of the device or human anatomy, and was asked not to exert more force to reach the final position. Each movement was executed 3 times.

The movements were first performed without the arm support, then with the prototype and finally with the WREX. Before the measurements, the amount of balancing force was individually optimized to support the arm and the subjects had 5 minutes to get used to the arm support.

10.2.3. OUTCOME MEASURES

Range of motion: 3D hand motion was tracked during all movements with the Vicon system. With a marker on the hand, the RoM of the hand could be tracked and measured.

Normalized sEMG amplitude: sEMG signals were recorded during all movements. The sEMG activity of the following five muscles were measured during each movement: biceps brachii, deltoid, pectoralis major, triceps brachii and trapezius. They were normalized by using the maximal voluntary contraction (MVC) of each muscle, which was

recorded at the start of the measurements. Normalized sEMG amplitudes during the diverse movements were displayed as percentage of the MVC amplitude.

10.3. RESULTS

IN Fig. 10.2, the RoM of the user without the arm support, with the prototype, and with the WREX arm support is shown. It can be seen that the prototype has a larger RoM than the WREX. The RoM increases much for reaching forwards, and is almost equal to the RoM of a healthy arm. The prototype is more limited to reach positions in the area of the ipsilateral shoulder.

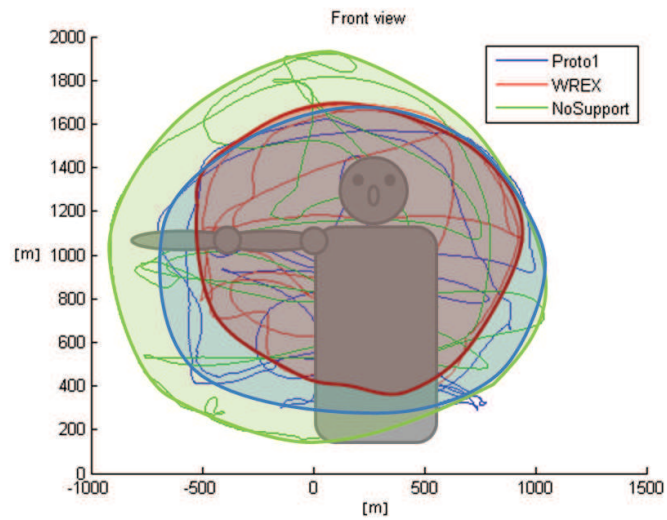
In Fig. 10.3, the normalized sEMG amplitudes of each muscle and each subject are shown for drinking and for an activity where the trunk movement is used (reaching far). Only the results for the triceps brachii are not shown, because this muscle is not very active for drinking and reaching for a far object. The results show the average with the standard deviation (SD) of the sEMG signal. The sEMG signal of the other ADL en SJM showed comparable results.

10.4. DISCUSSION

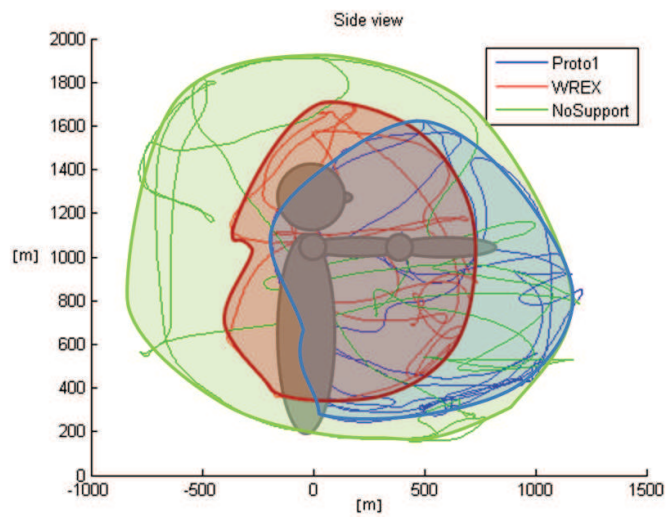
THE total RoM of the subjects with the prototype is increased 10% when compared to the wheelchair-bound arm support. This is measured by adding the areas of each view in Fig. 10.2 to each other. Especially for the more extreme movements, like reaching for a far or high object or touching the top of the head. The RoM mainly increases to the front of the subject, because the subject is able to lean forward. To user is able to reach 50% further anteriorly than with a wheelchair-bound device. To the side, the RoM is increasing slightly. This is because the trunk parallelogram is not fixed tightly to the trunk and can move a bit along the trunk. When reaching to the side, or when reaching for an object without leaning, the trunk parallelogram moved a bit in order to have a good alignment of the arm support with the human arm. This ensures a more natural feeling and is one of the reasons why the subjects perceived the trunk motion as important and comfortable. With the wheelchair-bound arm support, these movements would be less natural due to misalignment with the arm. The prototype has also been tested by DMD patients, and they also perceived free trunk motion as important. It allows for the use of compensatory movements of the trunk and shoulder, which is a mechanism that is often used by DMD patients to minimize the required energy to perform arm movements.

In Fig. 10.2, it can also be seen that the prototype has less RoM in the area of the shoulder. At these positions, the extra shoulder arc that connects the WREX arm support to the trunk parallelogram is interfering with the WREX. This limits the ability to reach positions close to the shoulder. Another remark is that the structure of the arm support limits the user to perform some movements. This is due to position of joints and the accompanying degrees of freedom (2DoF at the shoulder, and 2DoF at the elbow), while the human body has 3DoF at the shoulder, and 1DoF at the elbow. A recommendation for a future arm support would be to use the same DoF in the arm support as the human arm has. This allows for better alignment with the arm and results in a more natural behavior of the arm support.

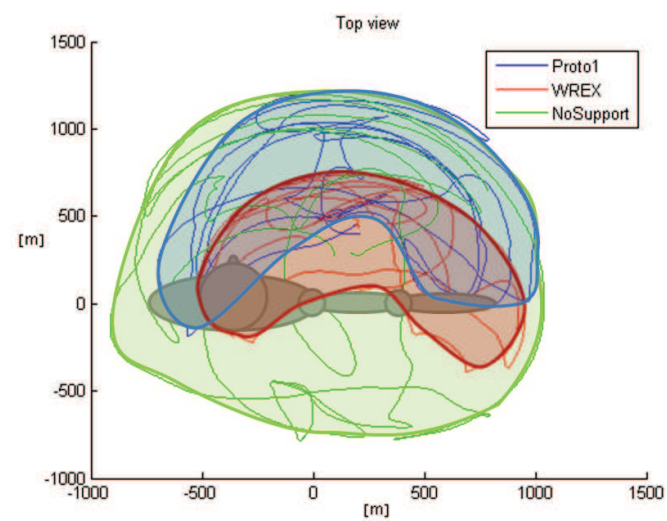
Fig. 10.3 shows the results of the sEMG signals of the healthy subjects for 2 ADL. The



(a)



(b)



(c)

Figure 10.2: Results of the range of motion of the hand of a healthy user without the arm support, with the prototype with trunk motion capability (proto1) and with the WREX arm support, shown from the (a) front, (b) side, and (c) top of the user.

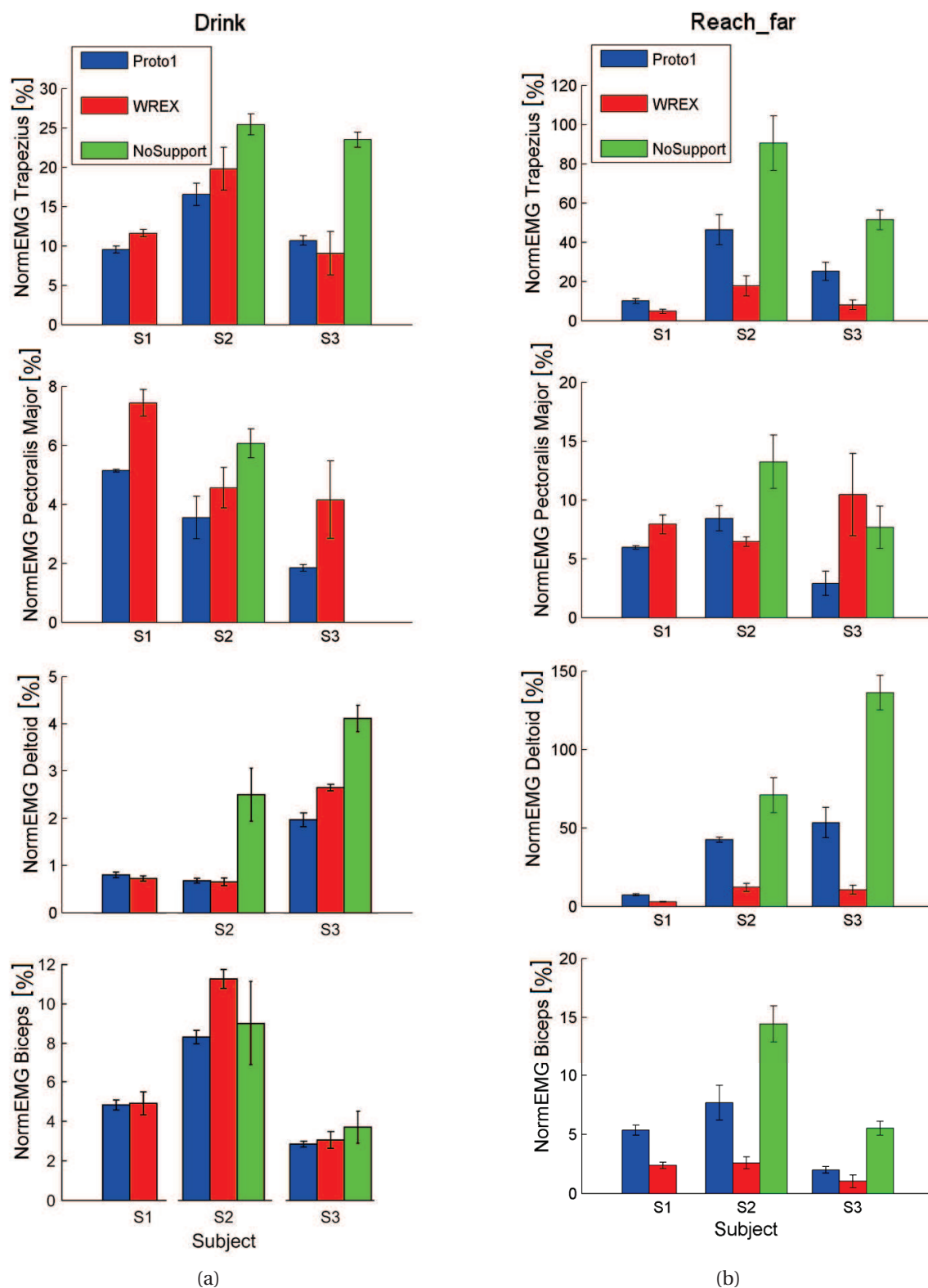


Figure 10.3: sEMG measurements (normalized to the MVC), including ± 1 SD from the average, of different muscles of three healthy subjects for drinking and reaching for a far object, without an arm support (green), with the prototype with trunk motion capability (proto1, blue) and with the WREX arm support (red).

other movements that were performed (both ADL and SJM) showed comparable results. The results are shown for the four muscles that are mainly active during shoulder and elbow movements. The results of the triceps brachii were not shown in the results. This is because this muscle is not really active during the performed movements, but also because the results were slightly influenced interference of the sEMG sensor with the prototype. It can be seen that the sEMG signals generally decrease when an arm support is used. The sEMG signals for using the prototype or the wheelchair-bound WREX are comparable. For some movements the prototype shows lower sEMG signals, while for other movements the WREX shows lower sEMG signals. This means that adding a trunk parallelogram to the arm support does not influence the balancing quality of the arm support and can give enough support to the arm. Since the goal of this research is to do an explorative study to the advantage of trunk motion capability, the results are not analyzed thorough with a statistical test. This would also be hard to do, since the amount of test subjects is small. Nevertheless, the results of the average and SD of the sEMG between the prototype and WREX are comparable, and clearly better than the results of the movements without an arm support.

Another advantage of the trunk parallelogram is that it could be used to give support to the trunk. Similar to the balancing mechanism at the upper arm and forearm, the springs in the trunk parallelogram can be used to create a balancing force to the trunk. This gives support to the body while leaning forwards and backwards. Next to supporting the trunk for leaning, the trunk structure can also support the trunk in the lateral direction.

10.5. CONCLUSIONS

THE goal of this paper was to explore the effect of trunk motion capability in an arm support that allows leaning forwards and backwards. This has been done by comparing a prototype with trunk motion capability with an existing wheelchair-bound arm support (WREX). The arm supports are evaluated for single joint movements and activities of daily living. Motion analysis with the Vicon motion system showed that the total range of motion increased by 10%, with an increase of 50% in reaching anteriorly. Especially the more extreme movements like reaching for high and far objects or touching the top of the head are allowed with the prototype. sEMG measurements of the prototype were similar to that of the WREX, the both showed that less muscle activity was needed to perform movements compared to the condition without an arm support. The effect of a body-bound device with trunk motion capability was perceived as important by both healthy subjects and patients. Movements were easier and more natural to perform and DMD patients mentioned that it also allowed for making compensatory movements. These compensatory movements are important to use for DMD patients in order to minimize the required energy for some movements.

REFERENCES

- [1] A. E. H. Emery, *Population frequencies of inherited neuromuscular diseases - a world survey*, Neuromuscular Disorders I, 19 (1991).

-
- [2] J. R. Mendell, C. Shilling, N. D. Leslie, K. M. Flanigan, R. Al-Dahhak, J. Gastier-Foster, K. Kneile, D. M. Dunn, B. Duval, A. Aoyagi, C. Hamil, M. Mahmoud, K. Roush, L. Bird, C. Rankin, H. Lilly, N. Street, R. Chandrasekar, and R. B. Weiss, *Evidence-based path to newborn screening for Duchenne muscular dystrophy*. *Annals of neurology* **71**, 304 (2012).
- [3] M. Eagle, S. V. Baudouin, C. Chandler, D. R. Giddings, R. Bullock, and K. Bushby, *Survival in Duchenne muscular dystrophy : improvements in life expectancy since 1967 and the impact of home nocturnal ventilation*, *Neuromuscular Disorders* **12**, 926 (2002).
- [4] L. F. Cardoso, S. Tomazio, and J. L. Herder, *Conceptual design of a passive arm orthosis*, *ASME International Design Engineering Technical Conferences* **5**, 747 (2002).
- [5] R. A. R. C. Gopura, K. Kiguchi, and D. S. V. Bandara, *A Brief Review on Upper Extremity Robotic Exoskeleton Systems*, *IEEE International Conference on Industrial and Information Systems* **8502**, 346 (2011).
- [6] T. Rahman, W. Sample, S. Jayakumar, M. M. King, J. Y. Wee, R. Seliktar, M. Alexander, M. Scavina, and A. Clark, *Passive exoskeletons for assisting limb movement*, *Journal of rehabilitation research and development* **43**, 583 (2006).
- [7] A. G. Dunning and J. L. Herder, *A review of assistive devices for arm balancing*, *International Conference on Rehabilitation Robotics* , 6650485 (2013).

11

DESIGN AND PILOT VALIDATION OF A-GEAR: A NOVEL WEARABLE DYNAMIC ARM SUPPORT

Orinally appeared as:

PN. Kooren, A.G. Dunning, M.M.H.P. Janssen, J. Lobo-Prat,
B.F.J.M. Koopman, M.I. Paalman, I.J.M. de Groot, J.L. Herder,
Design and pilot validation of A-Gear: a novel wearable dynamic arm support,
Journal of Neuroengineering and rehabilitation, **12**, 1 (2015),
DOI:10.1186/s12984-015-0072-y

ABSTRACT

BACKGROUND: Persons suffering from progressive muscular weakness, like those with Duchenne muscular dystrophy (DMD), gradually lose the ability to stand, walk and to use their arms. This hinders them from performing daily activities, social participation and being independent. Wheelchairs are used to overcome the loss of walking. However, there are currently few efficient functional substitutes to support the arms. Arm supports or robotic arms can be mounted to wheelchairs to aid in arm motion, but they are quite visible (stigmatizing), and limited in their possibilities due to their fixation to the wheelchair. The users prefer inconspicuous arm supports that are comfortable to wear and easy to control.

Methods: In this paper the design, characterization, and pilot validation of a passive arm support prototype, which is worn on the body, is presented. The A-Gear runs along the body from the contact surface between seat and upper legs via torso and upper arm to the forearm. Freedom of motion is accomplished by mechanical joints, which are nearly aligned with the human joints. The system compensates for the arm weight, using elastic bands for static balance, in every position of the arm. As opposed to existing devices, the proposed kinematic structure allows trunk motion and requires fewer links and less joint space without compromising balancing precision. The functional prototype has been validated in three DMD patients, using 3D motion analysis.

Results: Measurements have shown increased arm performance when the subjects were wearing the prototype. Upward and forward movements were easier to perform. The arm support is easy to put on and remove. Moreover, the device felt comfortable for the subjects. However, downward movements were more difficult, and the patients would prefer the device to be even more inconspicuous.

Conclusion: The A-Gear prototype is a step towards inconspicuousness and therefore well-received dynamic arm supports for people with muscular weakness.

11.1. INTRODUCTION

DUCHENNE Muscular Dystrophy (DMD) is the most common genetic neuromuscular disorder diagnosed in childhood, affecting approximately one in every 5000 live male births [1]. Due to the dystrophin gene being located on the X-chromosome, DMD primarily affects boys. DMD is caused by a mutation in the gene that encodes for dystrophin and results in progressive loss of muscle strength and muscle tissue [2].

People suffering from progressive muscular weakness, like those with DMD, can lose the ability to walk and stand and the ability to control the function of their arms. This hinders them from performing daily activities, participating socially and being independent. A wheelchair can overcome the loss of walking. However, for the loss of arm function there seem to be few efficient and well adopted aids. Currently used aids are powered and non-powered arm supports and robot arms mounted on the wheelchair. Overviews are given by van der Heide [3], Dunning [4] and Mahoney [5]. These overviews show for example the Armon (MicroGravity, NL), the WREX (Jaeco, US) and the Darwing (Focal, NL). The majority of the existing arm supports is mounted on the wheelchair, which limits the range of motion. Moreover, existing supports are quite visible [6] and can be experienced as stigmatizing.

In the case of boys with DMD, due to improved medical care and technical possibilities, life expectancy has increased rapidly [7, 8]. As a consequence, most of them will have no functional arm movements for more than half of their life, if unsupported.

A survey, in which 350 persons with DMD participated worldwide, stated that only a small percentage (8.5 %) of DMD patient uses an arm support. In addition, this survey describes which ADL tasks are most important for DMD patients [9]. Essential activities to perform with an arm support are eating, drinking, use of a phone and computers, personal hygiene, physical contact with others and dressing. Persons with DMD will use an arm support seated only, since they are in a wheelchair at the time they need an arm support. Wishes with respect to the arm support, apart from increased ability, are inconspicuousness, intuitive control, easy donning and comfort [6, 10]. The arm support preferably would be worn underneath clothing, e.g. sweater and pants.

Therefore, the objective of this study was to develop, and pilot test in persons with DMD, a novel wearable arm support. This paper describes a prototype design for an inconspicuous arm support for activities of daily living (ADL tasks) and presents the characterization and validation of this device.

The support is called A-Gear, where the A stands for ability. The A-Gear is a piece of equipment increasing the user's ability.

11.2. METHOD

11.2.1. DESIGN METHOD

TO generate design concepts the main function of the device, namely to support arm motion, is split into sub functions [11]. The sub functions are: 1) generating force to compensate for the weight of the arm, 2) transferring reaction forces through the arm support and 3) transferring forces to and from the user. First, solutions were generated for these sub functions by a team of medical specialists, technical specialists and a person with DMD, resulting in a morphological overview. By systematically combining the



Figure 11.1: The prototype arm support worn by a healthy user.

solutions for the sub functions about 700 possible concepts could be conceived. Seven concepts were intuitively selected from the morphological overview and elaborated to realistically dimensioned sketches. These drawings helped to evaluate them within the same team of specialists and choose the optimal concept to detail and manufacture. “Optimal” meant scoring best on the combination of these criteria: low balancing error, close to the body, technical feasibility, ease of donning and comfort. These criteria resulted from the user requirements, which arose from discussion with users, their relatives and their caregivers. The optimal concept uses rubber springs for storing energy and generating the supporting force. Reaction forces are transferred through a mechanism of rigid links with pivot joints nearly aligned the human joints. This near alignment results in a support that stays close to the body and that has a range of motion (ROM) resembling human ROM, so that ADLs can be performed. Ranges of motion of the human joints that correspond to important ADLs were found in literature [12, 13]. The arm support interfaces with the user through perforated pads under the forearm, upper arm and underneath the upper legs. See Figs. 11.1 and 11.2.

11.2.2. CHARACTERIZATION METHOD

The performance of the prototype is best characterized by the relative balancing error, E_b (Eq. 11.1).

$$E_b = \frac{Fz_{max} - Fz_{min}}{Fz_{max} + Fz_{min}} \cdot 100\% \quad (11.1)$$

where Fz_{max} and Fz_{min} represent the maximum and minimum upward forces exerted by the arm support on the virtual combined center of mass (CCOM) of the arm. To evaluate the balancing error of the arm support, a series of static measurements of the balancing forces and torques in eight functional poses have been performed. These poses, as shown in Fig. 11.10 in the Appendix, are in close correspondence with the

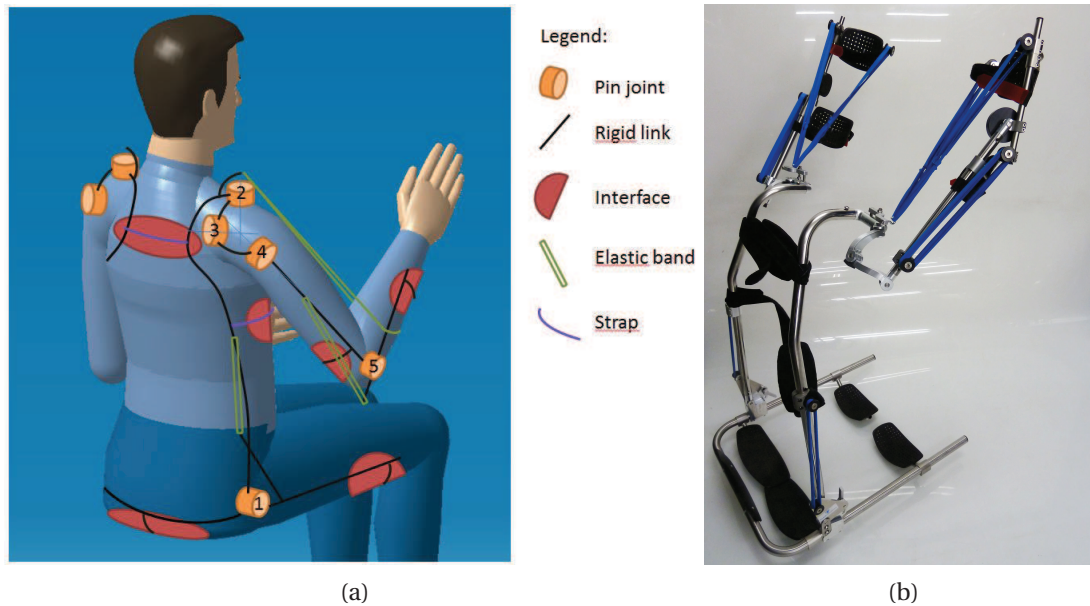


Figure 11.2: (a) A schematical representation of the kinematical architecture of the device. (b) A picture of the prototype.

most important ADL tasks as described by Janssen et al. [9]. The force/ torque measurements were performed attaching the forearm link of the arm support to a six Degree of Freedom (DoF) force/torque sensor (mini45, ATI Industrial Automation, USA) that was at the same time mounted to a position controlled robotic manipulator (UR5, Universal Robots, Denmark) that served as ground (Fig. 11.3). By switching the manipulator to a compliant state while repositioning manually, internal stresses between arm support and manipulator were minimized. Three measurements were performed at each position. A change of the force/torque sensor coordinate system was applied to the force/torque vectors in order to express the measurements at the arm coordinate system (Ψ_a), which is located at the CCOM of the arm. Furthermore, a rotation of this coordinate system was applied in order to express the force/torque signals in the global coordinate system (Ψ_g).

11.2.3. PILOT VALIDATION METHOD

For the validation of the prototype, three DMD patients with early functional limitations in their arms (Brooke scale 2 and 3. People in scale 2 can raise their arm above the head only by flexing the elbow. People in Brooke scale 3 cannot raise their arm above the head, but can raise a filled glass to the mouth) and one healthy subject, participated in testing the prototype (see Table 11.1 and Fig. 11.4). The healthy subject was included to establish reference values for the performance with and without the prototype. Participants were included through the Radboud UMC outpatient clinic and by advertising the study on the website of a Dutch patient organization. This study was approved by the medical ethical committee Arnhem-Nijmegen, the Netherlands, and subjects and their parents gave informed consent before participating in the study.

All participants performed standardized single joint movements of shoulder and el-

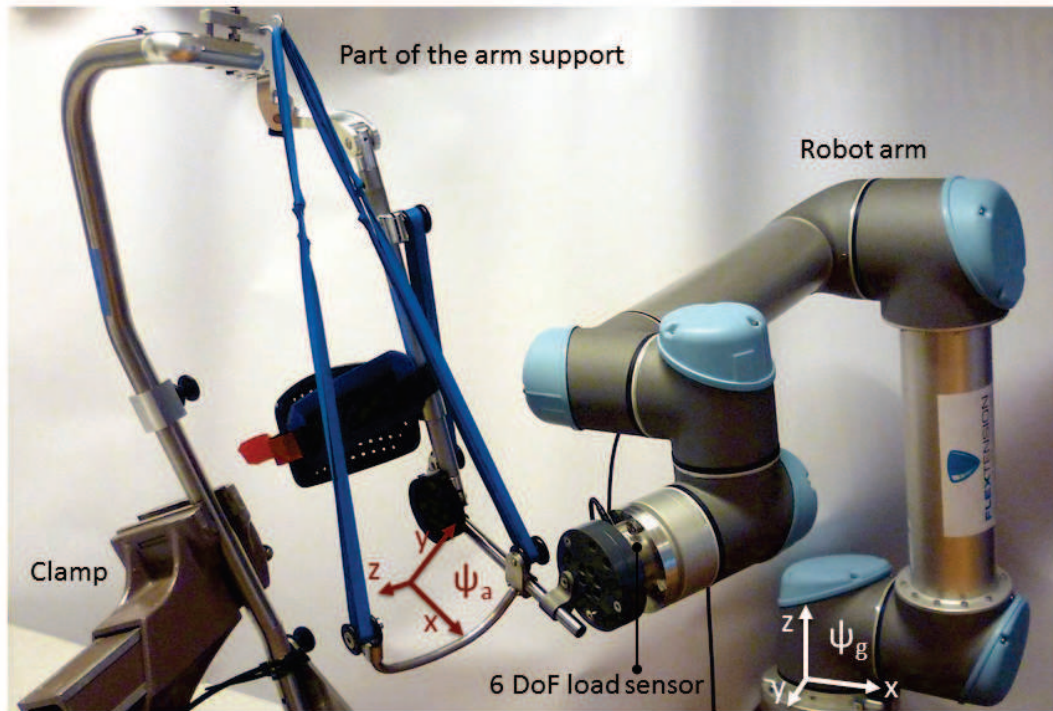


Figure 11.3: Setup for analyzing the balancing error. The balancing error of the prototype was verified by connecting it with a robot arm equipped with a six DoF load sensor.



Figure 11.4: Boy with Duchenne testing the prototype, while wearing electromyography and motion capturing devices.

Subject	Disease	Age [yrs.]	Sex	Weight [kg]	Brooke scale
1	DMD	15	M	63	2
2	DMD	14	M	70	3
3	DMD	17	M	82	3
4	Healthy	31	M	77	1

Table 11.1: Data of subjects in the pilot validation study.

bow (shoulder flexion, shoulder abduction, shoulder horizontal adduction, shoulder internal and external rotation and elbow flexion) and ADL tasks (extracted from the shoulder and elbow dimension of the “Performance of the Upper Limb (PUL) Scale” [14], which is used to measure upper limb performance in people with DMD) with and without wearing the prototype. Examples of the tasks are stacking cans, picking up coins and tearing paper. 3D motion analysis (VICON motion analysis system (Oxford Metrics, Oxford, UK)) was performed to gain insight in the ROM of the subject, by tracking the position of the hand marker during the single joint movements. The motion data was processed with Matlab (Mathworks, Natick, USA) coded algorithms. In addition, all participants filled out a questionnaire to gain more insight in functionality, comfort, aesthetics, safety, compatibility and donning and doffing.

11.3. RESULTS

11.3.1. DESIGN RESULTS

KINEMATIC ARCHITECTURE

THE arm support is supporting the forearm at the CCOM. In 3D space, the forearm of a user has six DoF’s. An assumption is made that a forearm supported by a curved interface can rotate within the skin when the user pro- or supinates the hand. Therefore, the mechanism of the arm support should provide the other five DoF’s. Intentionally, the arm support is only connected with the upper legs and forearm. In this manner, intermediate parts do not have to move synchronously with the human body and the joints do not have to be aligned perfectly. Still, near alignment is required, for the arm support to stay close to the body. An interface is placed against the upper arm, but this interface only supports the arm when the forearm is pointing upward. Without this interface the forearm would slip from the support when it is in vertical orientation with the hand upward.

Per arm, five revolute joints in series are used as kinematic chain. The first one is next to the hip. The second, third and fourth joint are pointing approximately towards the shoulder’s rotation point, and the fifth is next to the elbow (see Fig. 11.2). Revolute joints are simple and can be implemented with little friction. The advantage of having three joints in the shoulder region is that the arm support stays on the outer side of the arm. Therefore, the user can have direct contact with his arms on a table, and approach a table without bumping parts of the arm support against it.

Arc lengths between joint 2 and 3 and between 3 and 4 (Fig. 11.2) are chosen to be 56° such that the ROM of the human shoulder complex [15] is largely covered. The radius of the arcs is 70 mm. In this size, there is no interference of the arcs with the wheelchair's back- and headrest. Revolute joint 2 is tilted 10° posteriorly and 10° medially, to comply with the human shoulder motion, and also to make space for elastic bands. During arm motion, no singularities are encountered in the shoulder joint. The ROM of the individual revolute joints is limited with end stops.

The links between the joints, which are implemented as tubes, are custom made for the intended user.

INTERFACING WITH USER

The user is sitting on five pads (two below each upper leg, one against the user's bottom). The pads are flexible and can be formed to the body. The pads are clicked on metal tubes, which fixate their shape. The forearm link is attached to the users arm with a pad and a Velcro band. The upper arm pad is only to prevent the forearm from slipping from its pad when pointing upward. The pad against the forearm is the dominant contact point.

Since the user is sitting in the mechanism and it is only attached to the upper and lower arm, the complete mechanism is easy to put on and take off. Moreover, since the structure runs parallel to the users arm and trunk, it has the opportunity to be worn underneath clothing.

STATIC BALANCE

The balancing concept described by Lin et al. [16] was applied to the A-Gear. This concept provides a supporting force throughout the whole ROM of the human arm, combined with a slender mechanism consisting of few parts. A statically balanced system is in force equilibrium in all its possible postures. An arm that is statically balanced can therefore be moved with hardly any muscle force. In the concept of Lin, a two link mechanism with four DoF is balanced by only two springs. See Fig. 11.5. The first link (e.g. the upper arm) is connected with a spherical joint to a fixed point; the second link (e.g. the forearm) is connected to the first with a revolute joint. One biarticular spring running from a point above the spherical joint (e.g. the shoulder joint) to the second link, combined with a mono-articular spring running from the first link to the second link, provides a vertical force in the combined center of gravity of both links. This force is equal in size and opposite in direction to the gravitational force of both links. The springs that are used are zero-free-length springs. The balancing force is adjusted by varying the height of the spring attachment above the shoulder, a_1 . The prototype design allows for this adjustment.

In order to keep the structure close to the body and to avoid a structure below the elbow, the mono-articular spring is transferred to run along the upper arm, instead of the lower arm (Fig. 11.5). The parameters for the spring system are calculated as described in Lin et al. [16], and shown in Eqs. 11.2, 11.3, 11.4.

$$b_1 = \frac{m_3 s_3 L}{m_2 s_2 + m_3 L} \quad (11.2)$$

$$k_1 = \frac{g(m_2 s_2 + m_3 L)}{a_1 L} \quad (11.3)$$

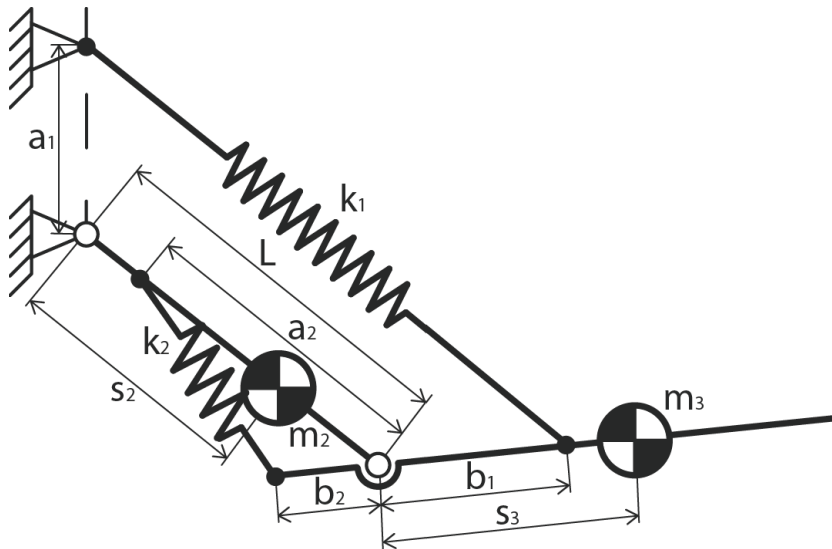


Figure 11.5: The principle of statically balancing the device. The principle and its parameters are described by Lin et al. [16].

$$k_2 = \frac{k_1 b_1 L}{a_2 b_2} \quad (11.4)$$

The distances a_1 , a_2 and b_2 were chosen to be practical in the device. When resulting stiffness k_1 and k_2 could not be implemented with the available elastic bands, then the nearest feasible stiffness was chosen and a_1 and b_2 adjusted to satisfy the balancing criteria.

The mass of the human upper arm is divided to the shoulder and the elbow according to the position of the center of mass of the upper arm. This means that in the equations from Lin et al. [16], to calculate the parameters of the spring system, m_2 is only the mass of the link of the prototype along the upper arm. The combined mass m_3 is the sum of the mass of the forearm, a part of the mass of the upper arm and the mass of the link of the prototype along the forearm (Eq. 11.5). According to this mass distribution the center of combined mass on the forearm is calculated using Eq. 11.6.

$$m_3 = m_{FA} + m_{UA} \cdot \frac{s_2}{L} + m_{link3} \quad (11.5)$$

$$s_3 = \frac{m_{FA}s_{FA} + m_{link3}s_{link3}}{m_3} \quad (11.6)$$

Rubber bands are chosen above metal springs, since a certain mass or volume of rubber that is axially stretched can store more elastic energy than the same mass or volume of metal in a helical spring [17]. Consequently, the arm support will be more lightweight and slender. To find springs matching the characteristics needed to balance the arm, we have compared the characteristics of different elastic bands. The rubber bands used in the arm support (Synthetic Polyisoprene, Jaeco Orthopedic, USA), almost behave like a zero-free-length spring between 150% and 400% strain, as is shown in Fig. 11.6. To verify whether the zero-free-length reference line is indeed related to the force/displacement

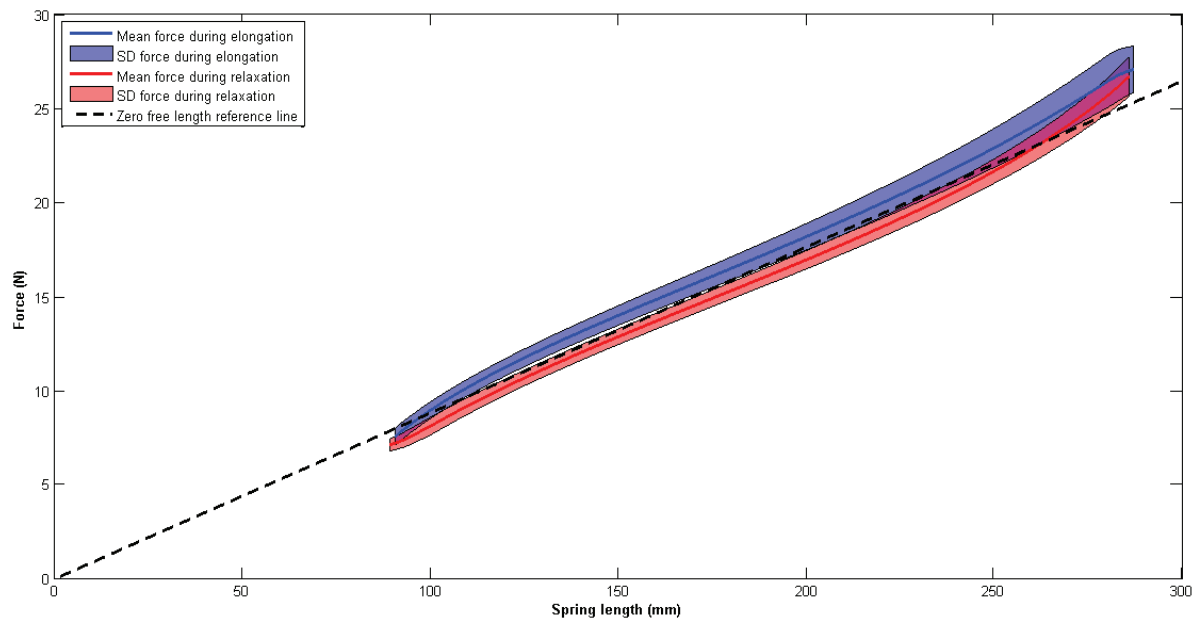


Figure 11.6: Characteristic of the rubber band with the zero-free-length spring behavior. In blue the mean and standard deviation of the force/displacement curve during elongation of the rubber band are shown. In red the same curve is shown during relaxation of the elastic band. The black dotted line shows the zero-free-length reference line.

curve, the intraclass correlation coefficient (Two-way mixed, average measure, ICC(3,k)) was calculated. The ICC between the reference line and the average force was 0.997, meaning that the spring characteristics match the zero-freelength reference line almost perfectly. This makes these elastic bands very suitable for this application. The stiffness can be varied stepwise by changing the amount of elastic bands.

PROTOTYPE

The manufactured prototype is shown in Figs. 11.1 and 11.2. The straight and bent tubes are made of steel, for convenient bending and welding. In future products, the tubes could be made of a composite material for weight reduction. A tube was designed, within the limits of the tube bending process, which follows the human shape as close as possible in order to be inconspicuous and fit between user and the wheelchair's backrest.

To interface with the user, polymer pads that have padding and perforation were used for comfort purposes (Fig. 11.2). In existing orthotics, this type of pads has been experienced as comfortable.

11.3.2. CHARACTERIZATION RESULTS: BALANCING ERROR

The balancing error test results (Fig. 11.7 and Table 11.2 in the Appendix) show that the gravity compensation force generated by the passive arm support is nearly constant across the eight poses (Fig. 11.10) with a mean vertical force of 12.4 N. By considering the lowest measured vertical force (12.0 N) and the highest measured vertical force (13.4 N), the arm support presents a vertical balancing error of 6 %, using Eq. 11.1. Additionally, the arm support presents the maximum non-vertical norm force of 4.9 N and a maximum norm torque of 1.14 Nm.

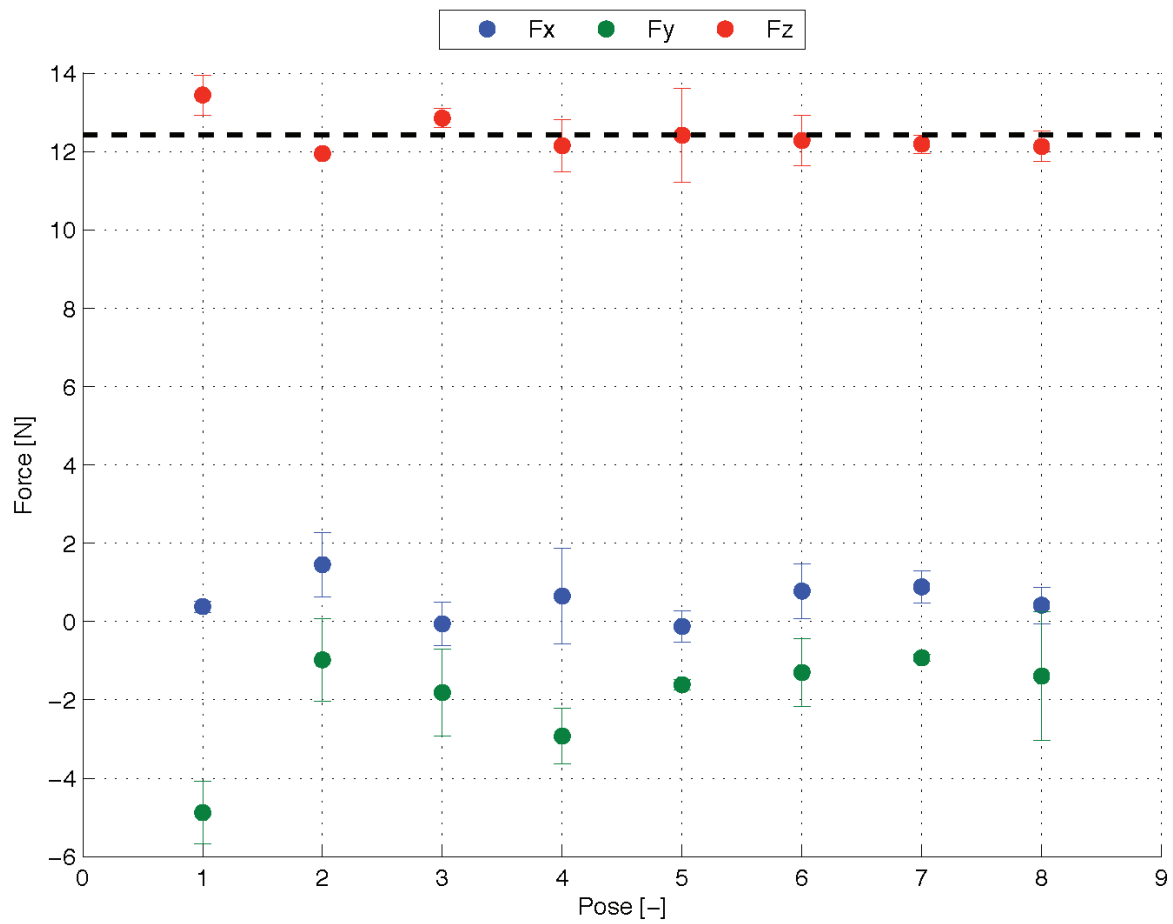


Figure 11.7: Plot of the mean measured forces exerted by the arm support with the 68 % confidence interval. The poses are shown in Fig. 11.10.

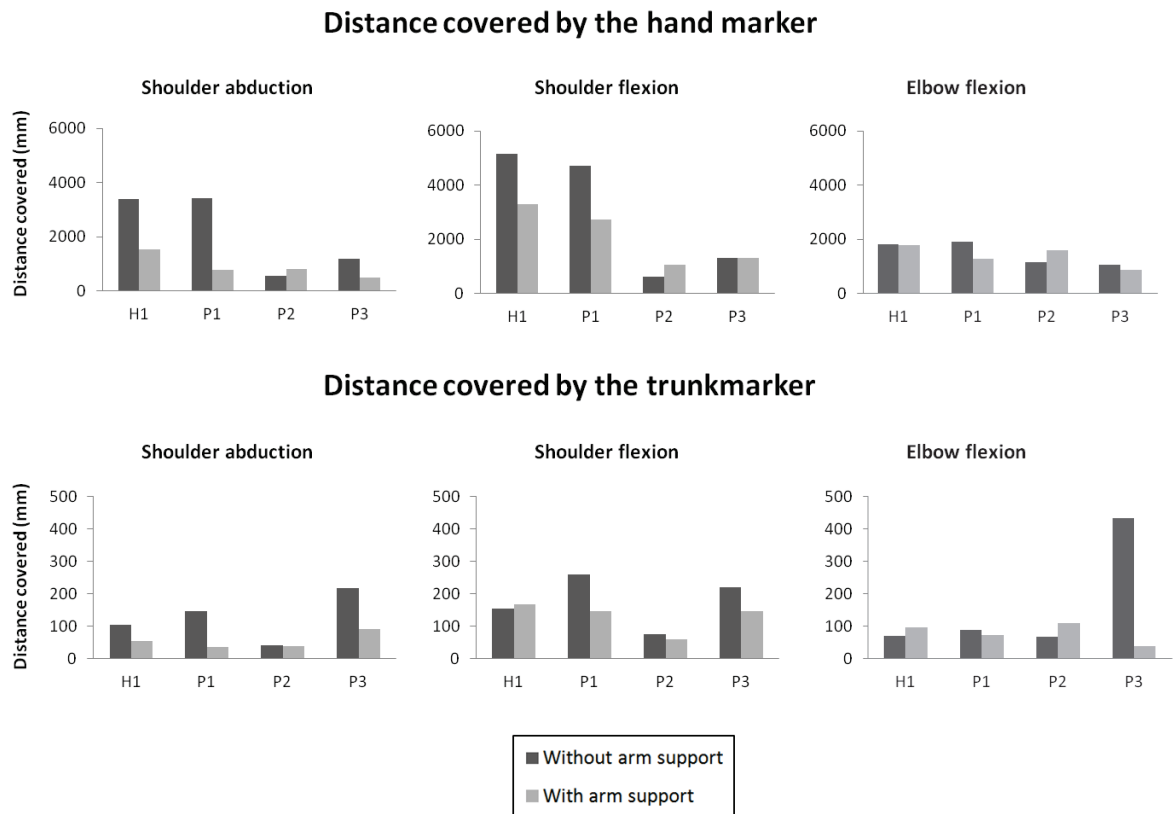


Figure 11.8: Range of motion displayed as the distance covered by the hand and trunk during single joint movements (shoulder abduction, shoulder flexion and elbow flexion), displayed for four different subjects with and without the passive arm support.

11.3.3. RESULTS PILOT VALIDATION

RANGE OF MOTION

ROM was calculated as the distance over which the hand moved during single joint movements of the shoulder and elbow. In addition, we calculated the distance over which the trunk moved during the single joint movements, to gain insight in compensatory movements of the subjects, as large trunk movements are often used to compensate for muscular weakness during daily activities. The distance, over which the hand and trunk moved during shoulder abduction, shoulder flexion and elbow flexion, are shown in Fig. 11.8.

The distance, over which the hand moved during shoulder abduction and shoulder flexion, when wearing the passive arm support, decreased in the healthy subject and in two out of three patients (Fig. 11.8). When looking at the movement of the trunk marker we saw that this movement was reduced in all patients when wearing the passive arm support. This indicated that less compensatory movements were used when wearing the passive prototype.

Elbow ROM did not change much when wearing the passive arm support, as participants were able to flex and extend the elbow over the entire passive ROM with and without the arm support. Therefore the active elbow ROM is not limited by the arm support, but by contractures in the elbow joint, which often occur in DMD patients. One subject

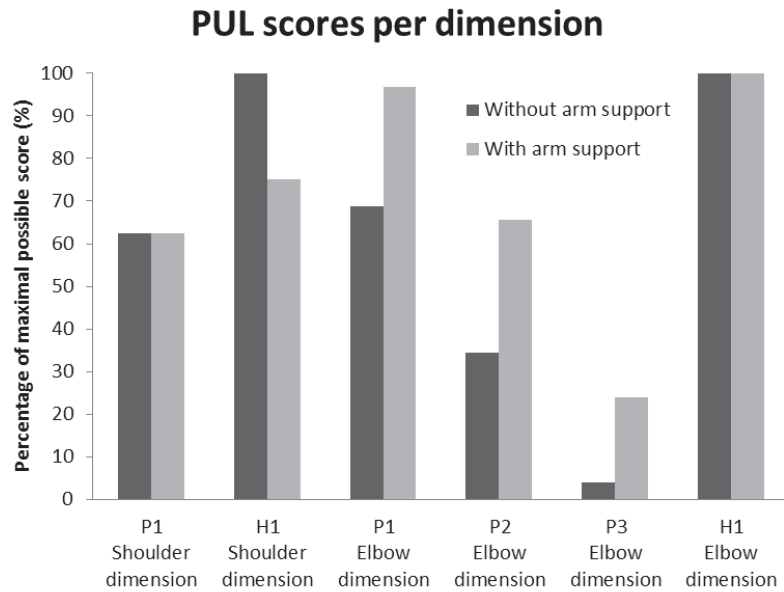


Figure 11.9: Performance of the Upper Limb scores per dimension as percentage of the maximal possible score of the dimension. P1, P2 and P3 are DMD patients, H1 is the healthy subject.

with minimal elbow contractures, however, experienced a bit limited elbow extension.

PERFORMANCE OF THE UPPER LIMB

To gain more insight in the subject's ability to perform ADL tasks with and without the passive arm support, the participants performed tasks from the shoulder and elbow dimension of the PUL scale [14]. The healthy subject and the subject with Brooke 2 performed the items from the shoulder and elbow dimension (dimension is meant in the clinical sense not in the technical) of the PUL. The subjects with Brooke 3 only performed the elbow dimension, since they were not able to execute the items from the shoulder dimension without the prototype. Fig. 11.9 shows the PUL scores per dimension as percentage of the maximal possible score on that dimension. The PUL scores of all patients improved for the elbow dimension, meaning that patients were able to perform more tasks and used less compensatory movements when wearing the arm support. The PUL score of the shoulder dimension of the healthy subject reduced, due to the limited shoulder ROM of the passive arm support.

QUESTIONNAIRE

The questionnaire consisted of question regarding: 'functionality', 'comfort', 'aesthetics', 'safety', 'compatibility' and 'donning and doffing'.

Upwards and forward movements are experienced easier while downward movements are experienced more difficult. On average, participants felt a little limited in their ROM by the prototype. However, the subjects stated that they were all still able to perform important activities, such as drinking and reaching for objects. In addition, the participants stated that the prototype fitted well and felt comfortable. However, sometimes the shoulder parts of the prototype interfere with the shoulder of the user or the wheelchair and sometimes the arm part collided with the table or wheelchair. The lower

arm interface felt comfortable to all participants. All participants stated that the arm support could not be worn underneath clothing. The opinions about the looks of the prototype differed between participants. One participant stated that he thought the visible parts of the prototype looked nice, while other participants stated that the appearance of the prototype should still be improved before they were willing to wear it in daily life. On the level of safety all patients were satisfied. The arm was steadily attached in the arm support. Furthermore, the prototype did not make unintended movements and was stable. One participant felt his skin getting pinched near the shoulder, while other participants did not have this experience. The prototype did not inhibit breathing. Donning the prototype was experienced harder than doffing the prototype, although most participants thought that the time it took to put on and off the prototype was reasonable.

Overall, all patients stated that they would like to use such an arm support in daily life, however they would also like to see some adaptations to prevent collisions with the body and surroundings and on the looks of the prototype.

11.4. DISCUSSION

THE results of the study show a prototype design that can be worn close to the body and permits more trunk movements, a quantification of the balancing performance and outcome of tests in which people with DMD used the arm support.

In comparison with current arm supports, the A-Gear is placed more naturally to the body. The device runs parallel to the arm, trunk and upper legs of the user and has mechanical joints nearly aligned with the human joints. The design makes motion more intuitive, free of singularities and the authors believe that, by optimizing the concept, the device will fit underneath clothing.

The vertical force generated by the arm support is largely constant across the measured poses. However, a balancing error of 6 % was found and the results do show non-vertical forces and torques in the system. There may be several reasons for the error and unintended forces and torques. Firstly, the springs compensate for the intrinsic mass of the device, but do not compensate for the fact that the mass is next to the human arm instead of in line with the human arm. To compensate this offset the balancing theory should be extended. Secondly, errors may arise from interaction forces between user and support on other locations than the forearm, e.g. the upper arm pad. This effect could be reduced by a forearm interface shape that prevents the forearm from slipping out and removing the upper arm pad.

One-hundred percent weight compensation is not always preferred by patients. One of the patients wanted less supporting force, which felt more comfortable to him.

In the pilot validation, all patients showed a functional improvement on the elbow dimension of the PUL scale. The improvement indicates that they were able to perform more items, or that they had to use less compensatory strategies, when wearing the passive arm support. The distance over which the trunk moved, which is a measure for the amount of compensatory movements used, also reduced in all patients, when they were using the passive arm support. The reduction of compensatory movements is very important, as compensatory movement consumes a lot of energy and therefore they restrict the endurance to perform daily activities.

The distance over which the hand marker moved reduced in three out of four subjects, when wearing the passive arm support. For the healthy subject and the patient with Brooke scale 2 (P1), this decrease in ROM was expected, because of the kinematics of the arm support, which restricted shoulder abduction beyond 90° and shoulder flexion beyond 120°. Since both the healthy subject and P1 were able to move the arm over the entire ROM without arm support, they were restricted in their shoulder movements by the passive arm support. For the patients with Brooke scale 3, we saw that the distance over which the hand moved during single joint movements increased in one patient (P2) and decreased in another patient (P3), when wearing the passive arm support. We would have expected an increase of the distance in both patients with Brooke scale 3. One possible explanation of a reduction of the distance, over which the hand was moved in P3, might lie in the amount of compensatory movements that were used by this patient, when he was not wearing the arm support. By using compensatory movements this patient was able to move the hand, but the movements were uncontrolled and not very functional, as can be seen by the lower PUL score without the arm support. Consequently, a large movement of the hand marker was seen. When this patient used the passive arm support less compensatory movements were used and much more control over the movement could be executed, therefore his functional score improved.

From the items as mentioned as essential activities to perform with an arm support (eating, drinking, use of a phone and computers, personal hygiene, physical contact with others and dressing) the vast majority can be met with the prototype according to the tests. The healthy subject already reached the maximal score of the elbow dimension without wearing the passive arm support and he was still able to do this with the passive arm support.

The results of the questionnaire indicated that patients were able to perform some activities with more ease, while other activities were more difficult. Some comments were expressed regarding comfort and safety, which should be improved in a future passive arm support.

Overall the passive arm support was especially beneficial for patients with a Brooke scale of 3, those that are not able to lift their hands above their head without support. These patients showed functional improvements and indicated that arm movements became less fatiguing. All patients stated that they would like to use such an arm support in daily life; however, some aspects of the arm support would still require improvement.

The practical implementation and clinical tests taught us which aspects need further development or should be included in a wearable arm support for people with muscular weakness. Firstly, the space between the wheelchair's arm supports is limited for the device. These arm supports are placed close to the user for sideways stability. Next to the hips the orthosis should be very slender to fit in the seat. Secondly, supporting only one arm causes a skew posture, since arm weight hanging from one shoulder is reduced. Two sided support is preferred. Thirdly, the possibility to lean forward is much appreciated. Lastly, the arm support preferably does not run between arm and trunk and does not add considerable volume underneath the forearm and elbow. Components between arm and trunk make it uncomfortable to have the arms relaxed along the trunk. Structures below the elbow clash with tabletops when moving over them.

11.5. CONCLUSIONS

IN this paper, a design of a passive dynamic arm support for persons with reduced functional abilities of their arms, more specifically, for people with Duchenne, is proposed. The architecture of the device follows human anatomy. According to the authors knowledge, the A-Gear was the first device that applied the principle for static balancing, proposed by Lin [16], in orthotics. Parameters were found so that elastics bands and attachment points stay close to the user. A step forward has been made to develop an inconspicuous arm support that can be worn underneath clothing.

Three persons with DMD tested the prototype and all showed an increased PUL score with less compensatory movements, compared with not using the support. The trunk has more freedom to move as well, due to hinges next to the hips.

Subjective feedback of the users tells that the arm support is easy to put on. Arm movements forward and up become easier, movements downward and tasks on a table top are still difficult. The users would prefer the device even more inconspicuous. The users felt wearing the device was comfortable, among others because it offers free breathing.

The shown prototype is a step towards well adopted dynamics arm supports that improve participation in society, that make people with muscular weakness more independent and more able to perform important activities in daily life.

APPENDIX

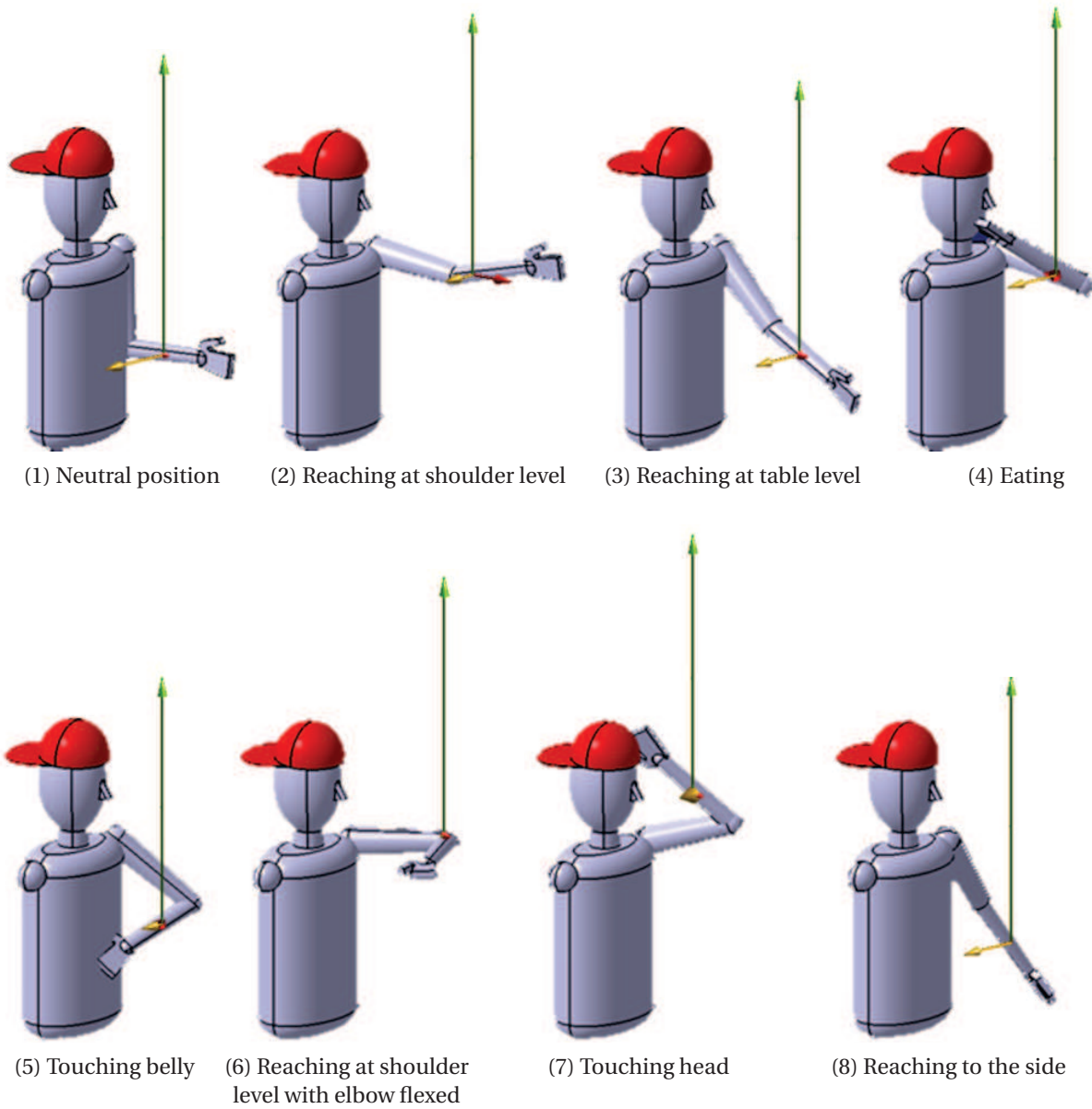


Figure 11.10: Forces exerted by the arm support displayed in context of the user. Moreover, the figure shows the poses, in which balancing error of the arm support was determined.

	Pose 1	Pose 2	Pose 3	Pose 4	Pose 5	Pose 6	Pose 7	Pose 8
Tx (Nm)	0.79 (0.18)	-0.59 (0.21)	-0.36 (0.69)	-0.09 (0.09)	-0.48 (0.06)	-0.75 (0.23)	-0.48 (0.03)	-0.07 (0.58)
Ty (Nm)	-0.56 (0.14)	-0.38 (0.02)	-0.73 (0.12)	0.40 (0.36)	-0.21 (0.29)	0.51 (0.29)	0.43 (0.03)	-0.88 (0.04)
Tz (Nm)	0.60 (0.04)	0.04 (0.46)	0.16 (0.36)	0.43 (0.35)	0.14 (0.04)	0.04 (0.04)	0.15 (0.01)	-0.02 (0.08)
Fx (N)	0.38 (0.14)	1.45 (0.82)	-0.06 (0.55)	0.65 (1.23)	-0.12 (0.40)	0.77 (0.70)	0.88 (0.40)	0.41 (0.46)
Fy (N)	-4.88 (0.79)	-0.98 (1.05)	-1.81 (1.11)	-2.93 (0.71)	-1.61 (0.13)	-1.30 (0.87)	-0.93 (0.09)	-1.39 (1.65)
Fz (N)	13.44 (0.51)	11.95 (0.04)	12.85 (0.25)	12.15 (0.66)	12.42 (1.19)	12.29 (0.65)	12.19 (0.23)	12.13 (0.39)
T (Nm)	1.14 (0.16)	0.81 (0.11)	1.05 (0.08)	0.75 (0.09)	0.59 (0.10)	0.92 (0.34)	0.66 (0.04)	1.00 (0.04)
F (N)	14.32 (0.46)	12.13 (0.23)	13.03 (0.05)	13.68 (1.46)	12.53 (1.19)	12.47 (0.86)	12.27 (0.25)	12.30 (0.49)

Table 11.2: Overview of the results of the balancing error tests. The forces and torques are exerted by the arm support (Fig. 11.3). The table gives the mean and 1 SD of the X, Y and Z forces and torques, expressed in the inertial frame, together with the mean and 1 SD of the corresponding norms. The poses of the measurements are shown in Fig. 11.10.

REFERENCES

- [1] J. R. Mendell, C. Shilling, N. D. Leslie, K. M. Flanigan, R. Al-Dahhak, J. Gastier-Foster, K. Kneile, D. M. Dunn, B. Duval, A. Aoyagi, C. Hamil, M. Mahmoud, K. Roush, L. Bird, C. Rankin, H. Lilly, N. Street, R. Chandrasekar, and R. B. Weiss, *Evidence-based path to newborn screening for Duchenne muscular dystrophy*. *Annals of neurology* **71**, 304 (2012).
- [2] A. E. H. Emery, *Population frequencies of inherited neuromuscular diseases - a world survey*, *Neuromuscular Disorders* **I**, 19 (1991).
- [3] L. A. Van der Heide, B. van Nijhuijs, A. Bergsma, G. J. Gelderblom, D. J. van der Pijl, and L. P. de Witte, *An overview and categorization of dynamic arm supports for people with decreased arm function*. *Prosthetics and orthotics international* **38**, 287 (2013).
- [4] A. G. Dunning and J. L. Herder, *A review of assistive devices for arm balancing*, *International Conference on Rehabilitation Robotics*, 6650485 (2013).
- [5] R. M. Mahoney, *Robotic Products for Rehabilitation : Status and Strategy*, *International Conference on Rehabilitation Robotics*, 12 (1997).
- [6] T. Rahman, W. Sample, R. Seliktar, M. Alexander, and M. Scavina, *A body-powered functional upper limb orthosis*, *Journal of rehabilitation research and development* **37**, 675 (2000).
- [7] M. Eagle, J. Bourke, R. Bullock, M. Gibson, J. Mehta, D. Giddings, V. Straub, and K. Bushby, *Managing Duchenne muscular dystrophy - The additive effect of spinal surgery and home nocturnal ventilation in improving survival*, *Neuromuscular Disorders* **17**, 470 (2007).
- [8] M. Kohler, C. F. Clarenbach, C. Bahler, T. Brack, E. W. Russi, and K. E. Bloch, *Disability and survival in Duchenne muscular dystrophy*, *Journal of Neurology, Neurosurgery & Psychiatry* **80**, 320 (2009).
- [9] M. M. H. P. Janssen, A. Bergsma, A. C. H. Geurts, and I. J. M. de Groot, *Patterns of decline in upper limb function of boys and men with DMD: an international survey*. *Journal of neurology* **261**, 1269 (2014).
- [10] L. A. van der Heide, G. J. Gelderblom, and L. P. de Witte, *Effects and Effectiveness of Dynamic Arm Supports*, *American Journal of Physical Medicine & Rehabilitation* **94**, 44 (2015).
- [11] G. Pahl, W. Beitz, J. Feldhusen, and K. H. Grote, *Engineering design: a systematic approach* (Springer, 2007) p. 629.
- [12] J. Aizawa, T. Masuda, T. Koyama, K. Nakamaru, K. Isozaki, A. Okawa, and S. Morita, *Three-dimensional motion of the upper extremity joints during various activities of daily living*. *Journal of biomechanics* **43**, 2915 (2010).

- [13] D. P. Romilly, C. Anglin, R. G. Gosine, C. Hershler, and S. U. Raschke, *A Functional Task Analysis and Motion Simulation for the Development of a Powered Upper-Limb Orthosis*, IEEE Transactions on Rehabilitation Engineering **2**, 119 (1994).
- [14] A. Mayhew, E. S. Mazzone, M. Eagle, T. Duong, M. Ash, V. Decostre, M. Vandenhauwe, K. Klingels, J. Florence, M. Main, F. Bianco, E. Henrikson, L. Servais, G. Campion, E. Vroom, V. Ricotti, N. Goemans, C. McDonald, and E. Mercuri, *Development of the Performance of the Upper Limb module for Duchenne muscular dystrophy*, Developmental medicine and child neurology **55**, 1038 (2013).
- [15] J. Rosen, J. Perry, N. Manning, S. Burns, and B. Hannaford, *The human arm kinematics and dynamics during daily activities - toward a 7 DOF upper limb powered exoskeleton*, International Conference on Advanced Robotics , 532 (2005).
- [16] P.-Y. Lin, W.-B. Shieh, and D.-Z. Chen, *A theoretical study of weight-balanced mechanisms for design of spring assistive mobile arm support (MAS)*, Mechanism and Machine Theory **61**, 156 (2013).
- [17] J. Cool, *Werktuigkundige Systemen* (VSSD, 1992) p. 344.

12

APPLICATION OF INNOVATIVE SPRING CONFIGURATIONS IN THE A-GEAR, A CLOSE-TO-BODY DYNAMIC ARM SUPPORT

To be submitted as:
A.G. Dunning, M.P. Lustig, J.L. Herder,
*Application of innovative spring configurations in the A-Gear -
a close-to-body dynamic arm support,*
Will be submitted to Journal of Medical Devices, 2016.

In this chapter, two close-to-body spring configurations that were elaborated in Chapter 7, 8 and 9 were applied to the linkage system of the A-Gear mobile arm support (Chapter 11). This chapter focuses on designing the spring configuration close to the body. Therefore, a technique is presented to split the springs and use hollow spring structures.

ABSTRACT

PEOPLE with neuromuscular disorders often lose their leg and arm functionality. For regaining the arm functionality, a suitable arm support that gives the required support and is inconspicuous is not readily available. In recent research the A-Gear is introduced as a novel wearable dynamic arm support. The spring configuration that was used in that device cannot be designed close to the body and inconspicuous. The goal of this paper is to apply two spring configurations that could be designed close to the body in a prototype and to provide technology to fit the spring configuration around the human body. This is done by splitting the spring into multiple springs, creating a web of springs in a V-shape or on X-shape. Hollow spring structures that correspond with a virtual spring has been created to be able to design spring around the human arm and shoulder. Subdividing the spring into multiple springs also allows for attaching the spring to multiple locations on the body. This gives more freedom to locate the springs at a feasible location that is close to the body. Next to that, the attachment points of the springs were located in the same plane as the arm links. This brings the whole system even closer to the body. With a shoulder cover the user and the spring are protected from getting pinched by the shoulder arc mechanism. An anatomically shaped forearm interface and sideways stabilization pads increase the comfort of the device. Next to that, the sideways stabilization pads give some support to the trunk to sit straight up.

12.1. INTRODUCTION

DUCHENNE Muscular Dystrophy (DMD) is a neuromuscular disorder that affects the arm and leg functionality of the patient [1]. Focusing on the arm, patients progressively lose their arm function and have difficulties to perform activities of daily living (ADL), including eating, drinking, personal hygiene and social contact. The arm function can be regained by using an arm support. For patients it is important that such a device is inconspicuous and not stigmatizing [2, 3]. In [4] (Chapter 11), it is stated that it is preferable to wear such a device underneath clothing.

Current solutions for arm supports range from robotic arms to passive supports [5, 6]. In [5], it is shown that these devices have a large volume, are not close to the body and limit the range of motion of the arm. In [4] (Chapter 11), the A-Gear mobile arm support is introduced. This is a novel wearable dynamic arm support, that uses a spring configuration that allows arm balancing throughout the complete workspace of the arm without the use of auxiliary links. However, this spring configuration is not close to the body and is constrained in such a way that it is not possible to bring it closer to the body.

In recent research (Chapter 9), a comparison has been performed between different spring configurations that could be designed close to the body and it is proposed to use a new spring configuration in a close-to-body arm support. Two spring configurations could be designed very close to the body. The first is a spring configuration with two bi-articular springs between the fixed world and the forearm, parallel to the upper arm (Chapter 7) (Fig. 12.1a). The second is a 3-springs configuration with one bi-articular spring from the fixed world to the forearm, and two mono-articular springs from the upper arm to the trunk and forearm, respectively [7] (Chapter 8) (Fig. 12.1b). These spring configurations are only described in a theoretical way with ideal attachment points of the springs.

The main goal of this paper is to implement and evaluate these two spring configurations in a prototype of a mobile arm support. This paper describes technology to make it possible to fit the spring configuration around the human body.

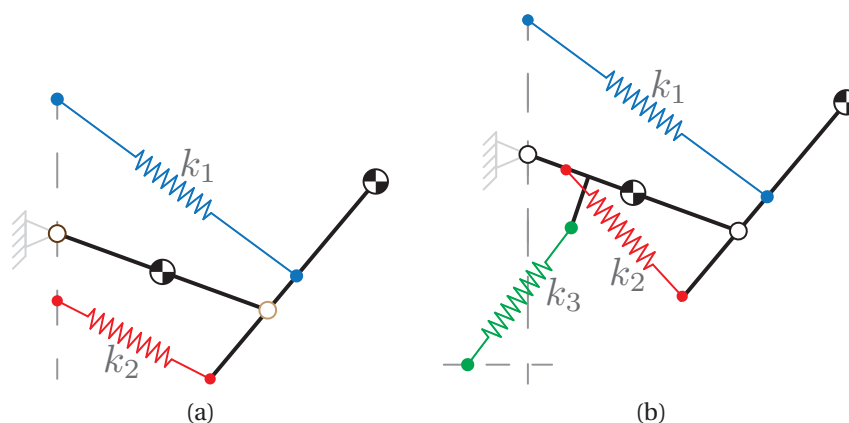


Figure 12.1: Schematic view and the proposed close-to-body spring configurations: the (a) 2-parallel-springs configuration and (b) 3-springs configuration, reproduced from [7] and Chapter 7.

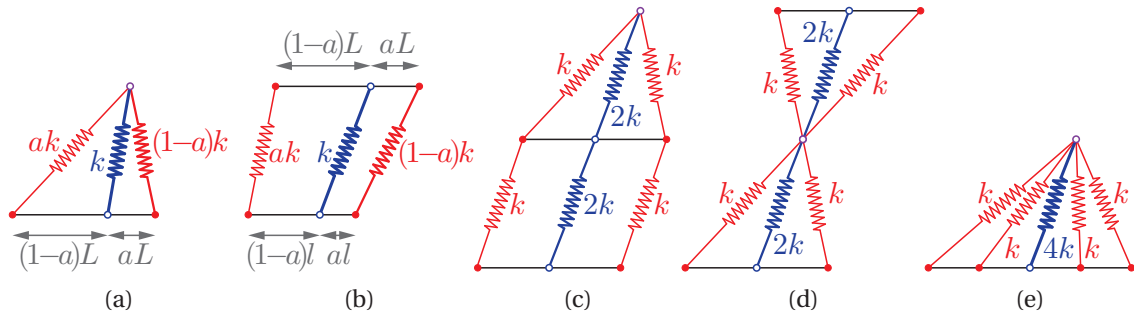


Figure 12.2: Subdivision schemes for ZFLSs, for creating equivalent virtual springs. (a) v-shaped configuration. (b) Parallel configuration. (c) Serial placements of two virtual springs, total stiffness value is k . (d) Serial x-shaped configuration, total stiffness value is k . (e) Parallel placement of two v-shaped configurations, summed stiffness value.

12.2. METHOD

12.2.1. SUBDIVIDING SPRINGS IN 2D

IN order to bring the springs closer to the body, a method is shown to slit and subdivide the springs.

Zero-free-length springs (ZFLS) can be subdivided such that a virtual ZFLS is created [8]. In this way, ZFLS behavior can be obtained for positions and configurations that are sometimes impossible to obtain. A V-shaped orientation of two ZFLSs (as can be found in [4]), act as a single virtual ZFLS with the summed stiffness value (Figure 12.2a) [8, 9]. The location of the virtual attachment depends on the ratio in stiffness between the split spring, represented by factor a (Figure 12.2a). An alternative option of subdividing a ZFLS is connecting two ZFLSs to two links (Figure 12.2b). When the two links are kept parallel to each other, a virtual ZFLS is created. The virtual attachment points are located in between the original attachments, at a location following from ratio a between the spring stiffness values (Figure 12.2b). A rotation of one of the links will result in the same rotation of the second link. The virtual springs can be combined with other virtual springs, by placing them in series or parallel to each other. In Fig. 12.2c, the V-shaped springs (Fig. 12.2a) and the parallel spring (Fig. 12.2b) are combined into a spring configuration with 2 virtual ZFLSs in series. Another option could be to combine two V-shaped springs with each other (Fig. 12.2d). This creates an X-shaped configuration. The center point of the springs is free to rotate. This way, both virtual spring can rotate independent of each other and the orientation of the top and bottom link are free. A parallel combination is shown in Fig. 12.2e, where four springs act as a single virtual spring. This configuration is a web of spring that act like a ZFLS.

12.2.2. SUBDIVIDING SPRINGS IN 3D

Subdividing ZFLSs is now extended to 3D. First, a cross section of a 2D spring subdividing scheme, perpendicular to the spring elongation direction, is shown in Fig. 12.3a. The virtual ZFLS is split into two springs. A 3D spring configuration is obtained by subdividing both springs into another pair, where each pair is in a rotated plane (Fig. 12.3b). The 3D subdivided spring act like the virtual ZFLS. When each spring is connected to each

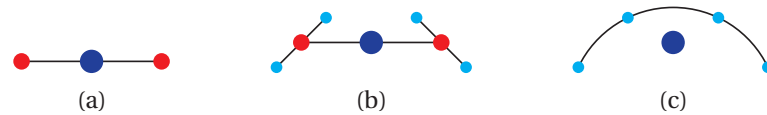


Figure 12.3: (a-c) Cross-section of 3D split up schemes, the blue dot represents the original zero-free-length spring, the two red dots and the four cyan dots are equivalent to the original blue spring, and the stiffness is equivalent to the surface area of the dots.

other with a circular shaped rigid structure, a hollow spring is created (Fig. 12.3c). Such hollow springs allow for close to body spring configuration, because they can follow body contours and can be designed around the body.

12.2.3. DESIGN AROUND THE HUMAN BODY

The two spring configurations are now fitted on the human arm. Ideally, the springs would be attached at the axes of the upper arm and forearm, which is impossible. Next to that, for a close-to-body spring configuration, the top bi-articular spring in each configuration will interfere with the shoulder, or the allowable poses of the arm as limited. Previously described techniques for splitting the springs are applied on both configurations, in order to prevent these conflicts and to increase the allowable poses of the human arm.

2-PARALLEL-SPRINGS CONFIGURATION

The top spring (k_1 , Fig. 12.1) attachments are located above the shoulder joint and on the forearm, in-between the elbow and wrist. The bottom spring (k_2) is located underneath the shoulder joint, going to the forearm at a location behind the elbow and at the axis of the forearm.

In Fig. 12.4a it can be seen how the top spring (k_1 , Fig. 12.1a) intersects the shoulder area of the human arm, for the pose of resting the arm on a table or armrest. Section A is the arm cross section in which the top spring acts. The cross section is illustrated in Fig. 12.4b. The green surfaces represent the upper arm and forearm sections, the blue crosses are the desired spring attachment point locations. When a spring is placed directly in-between these points, both the upper arm and forearm are clearly intersected by this spring (Fig. 12.4c). The conflict at the forearm can be resolved by using a V-shaped spring configuration, placing attachments on both sides of the forearm, separated by a circular link fitted around the surface of the forearm (Fig. 12.4d). Nevertheless, the upper arm is still intersected. A serial V-shaped and parallel spring resolves this issue (Fig. 12.4e). An additional spatial circular arc is used to separate the springs at shoulder height. This arc connects the springs on both sides of the arm and runs in front of it, effectively creating a hollow spring structure. The V-shaped spring is split several times to create a web of springs to reduce to stiffness of the each spring (Fig. 12.4f), up to a final extend where a single thin sheath of spring material is used (Fig. 12.4g). The embodiment of such a hollow spring configuration is shown in Fig. 12.4h. The circular arc separating the springs is shown in Fig. 12.5).

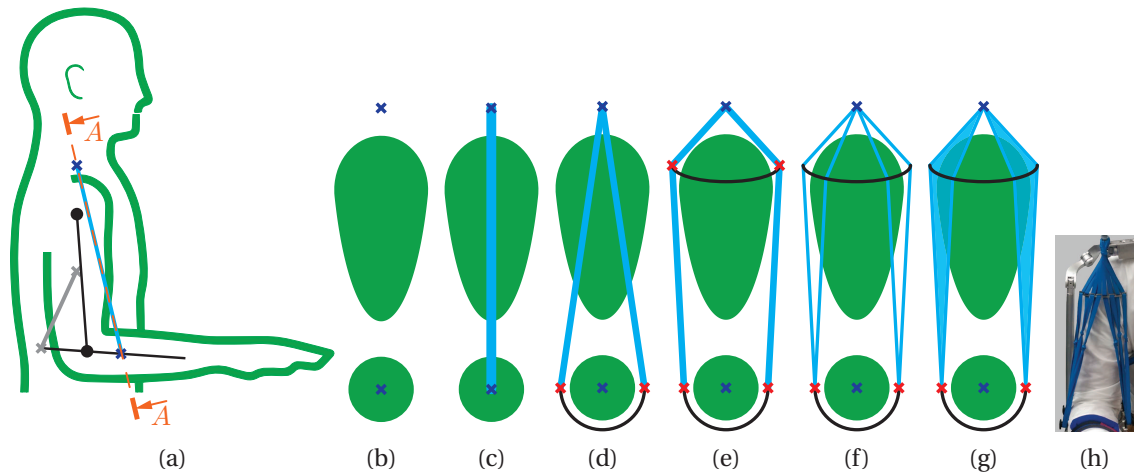


Figure 12.4: (a) Definition of section A. (b-g) Subdivision schemes in section A of the 2-parallel-springs configuration. The two green surfaces represent the cross sections of the human upper and forearm. (h) Top spring embodiment of the 2-parallel-springs.



Figure 12.5: Circular arc, for spring separation.

The lower spring (k_2 , Fig. 12.1a) is connected to the fixed world, underneath the shoulder, and to the forearm behind the elbow. The conflicts experienced by this spring are more difficult to capture in a single image.

The first critical area is that the attachment on the forearm should be located on the axis through the forearm. When the forearm is fully extended, this virtual point will interfere with the upper arm. To avoid this intersection the spring is split to both sides of the forearm. A circular link around the arm connects these points.

The second critical area is at the fixed world attachment. The spring attachment should be located directly underneath the shoulder joint, in the users arm pit. A physical component at this location is undesirable, as it would inhibit the upper arm to be positioned vertically besides the body and very uncomfortable because the arm pit is very sensitive. Instead, a virtual spring is realized at this point, by splitting this attachment to be on the chest (Q) and behind the shoulder (P) (Fig. 12.6a, 12.6b, 12.6c).

Both attachment points of the lower spring are subdivided. This results in an X-shaped spring in between these points (Fig. 12.6d). A rotation point appears at the intersection of the springs. The location of this point (h) can be varied by changing the spring stiffnesses.

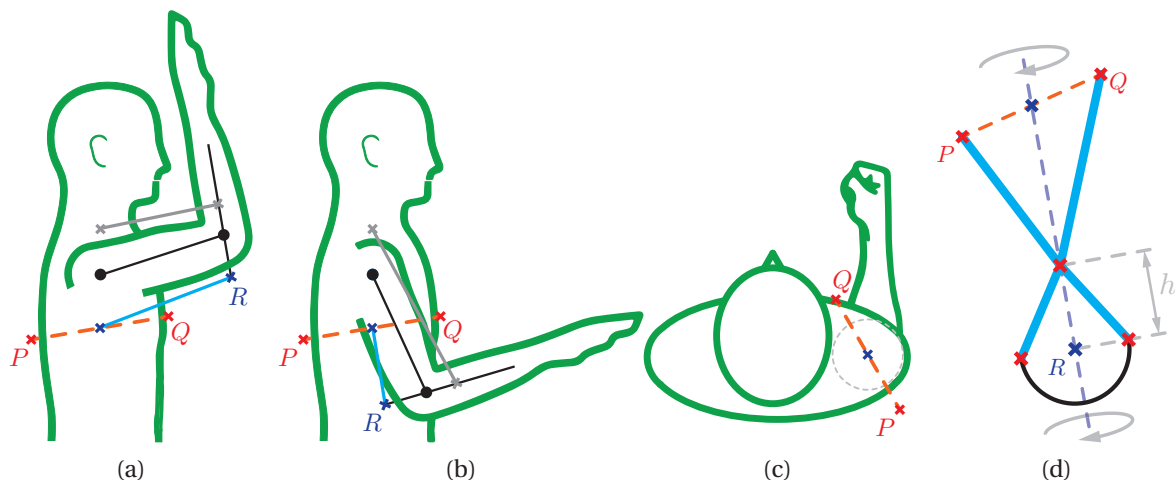


Figure 12.6: (a-c) Splitting the lower spring attachment points of the 2-parallel-springs configuration for a better fit around the human body results in a (d) X-shaped spring configuration.

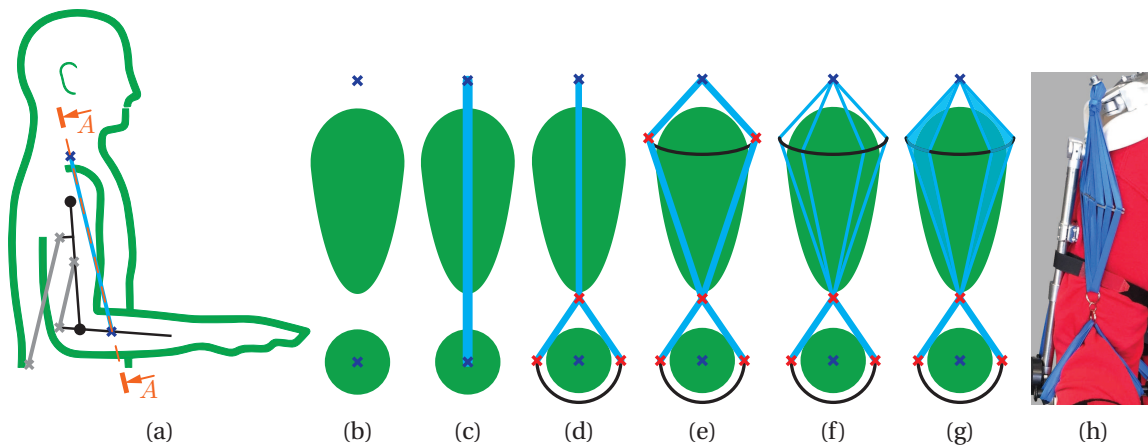


Figure 12.7: (a) Definition of section A. (b-g) Subdivision schemes in section A of the 3-springs configuration. The two green surfaces represent the cross sections of the human upper and forearm. (h) Top spring embodiment of the 3-springs configuration.

3-SPRINGS CONFIGURATION

The top spring of the 3-spring configuration (k_1 , Fig. 12.1b) intersects the shoulder area similar to the 2-parallel-springs configuration (Fig. 12.7a). The top spring is first split close to the forearm into a V-shaped spring (Fig. 12.7d). The single spring that runs to the shoulder is split into two V-shaped springs (Fig. 12.7e-12.7g). This results in an X-shaped spring in between the shoulder arc and the forearm, where the rotation is free at the intersection. The embodiment of the complete spring configuration is shown in Fig. 12.7h

The attachment point of the spring that runs from the trunk to the upper arm (k_3 , Fig. 12.1b) can be located far below the shoulder and the arm pit. Therefore, splitting the attachment point at the trunk (like it is done for the 2-parallel-springs configuration) is not needed. The spring has only to be split at the attachment to the upper arm. This is done the same way as shown in Fig. 12.7d, with a V-shaped spring close to the upper arm, and a single spring running to the trunk.

12.3. RESULTS

BOTH spring configuration are build into a prototype to be evaluated on comfort volume by healthy users. The linkage that is described in [4] (Chapter 11) is used to attach the spring configurations to. For each spring configuration, the complete system is shown in different poses of the arm.

12.3.1. 2-PARALLEL-SPRING CONFIGURATION

In Fig. 12.8, the prototype that is build for the 2-parallel-springs configuration is shown. The split lower and top spring are clearly shown in Fig. 12.8a and 12.8c, respectively.



Figure 12.8: (a-d) Prototype of the 2-parallel-springs configuration, with the (a) split lower spring, and (a) split top spring.

12.3.2. 3-SPRING CONFIGURATION

Next to the spring configuration, an attempt has been made to improve the appearance, safety and comfort of the prototype. In Fig. 12.9b,c, it can be seen that the attachment points of the springs are in the same plane as the links. Especially the second spring, that runs from the upper arm to the forearm, is much closer to the body. In the figures a shoulder cover is also shown. This shoulder cover is placed in between the human body and the shoulder arc mechanism, and also over the shoulder mechanism. This protects the user or clothes from getting pinched by the shoulder mechanism, and it also decreases the interference of the springs with the shoulder mechanism. For sideways stability, a comfortable pad is connected to the trunk link on both sides of the user. This stabilizes the user and prevent the user to fall sideways. And for more comfort, an anatomically shaped forearm interface, made with 3D scanning and 3D printing techniques, is used.

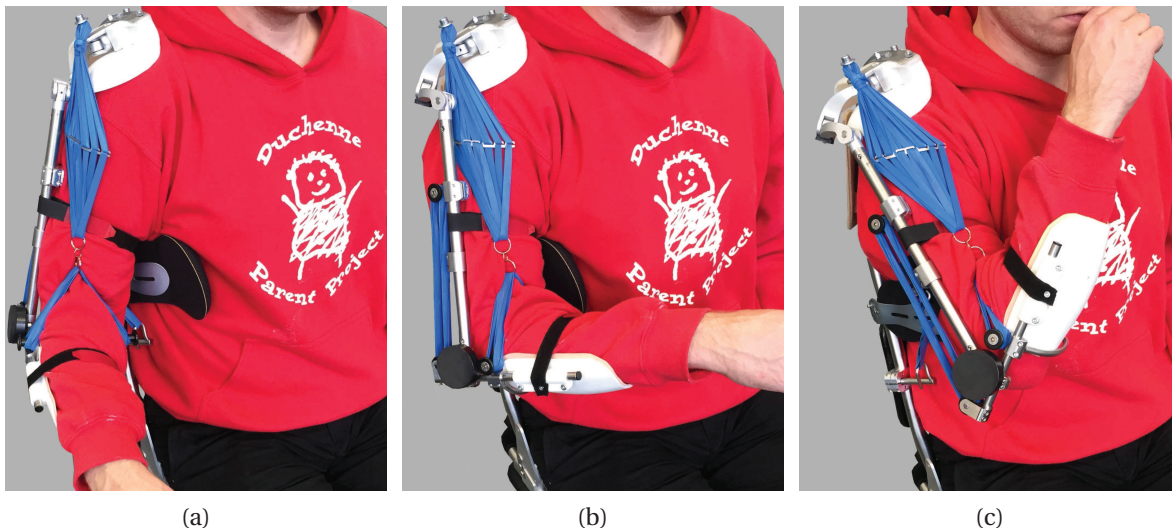


Figure 12.9: Front view of the prototype of the 3-springs configuration for the (a) neutral/resting pose and the (b,c) eating pose. The split top spring can be seen clearly.

12.4. DISCUSSION

FOR the 2-parallel-springs configuration, a good fit around the body was observed for poses with a low elevation angle (Fig. 12.8c). The benefits of the 3D hollow spring structure become clear, as the spring arc of the top spring fits well around the upper arm in these poses. For higher elevation angles, the space between the springs and the arm increases (Fig. 12.8d). This space can be decreased by lowering the spring attachment point above the shoulder. However, this point cannot be lowered much, because otherwise the balancing quality that is needed to balance a human arm cannot be obtained. Next to that, the spring attachment point P at the back of the trunk is located far from the body. For an inconspicuous arm support, this point needs to be closer to the body. Due to the V-shaped top spring, the arc that separates the spring will always align with the orientation of the forearm. As can be seen in Fig. 12.8b, for high elevation angles



Figure 12.10: Side view of the prototype of the 3-springs configuration. In (b) and (c), the split third spring from trunk to the upper arm can be seen clearly.

and shoulder rotation of 90° , this arc is not aligned with the upper arm anymore and sticks out. This is the reason that in the 3-springs configuration the top spring is split into an X-shaped and a V-shaped spring (Fig. 12.9a). The intersection of the X-shape is a rotation point for the springs. This allows the arc at the shoulder to align itself to the upper arm. The arc at the shoulder can even be positioned in between the user and the shoulder arc mechanism (Fig. 12.11a)). The shoulder arc mechanism moves over the springs and the interference with the springs is decreased. However, this has an effect on the balancing quality of the spring configuration for higher elevation angles. At higher elevation angles, the spring interfere with the shoulder mechanism and the virtual attachment point above the shoulder is relocated to another position (Fig. 12.11b). This affects the balancing quality.

Because the spring is so close to the body, and the limited space that is available at the V-shaped part of the top spring close to the forearm, it is difficult to don and doff the device. For better donning and doffing, the springs should be attached after the human arm is inserted in the device.

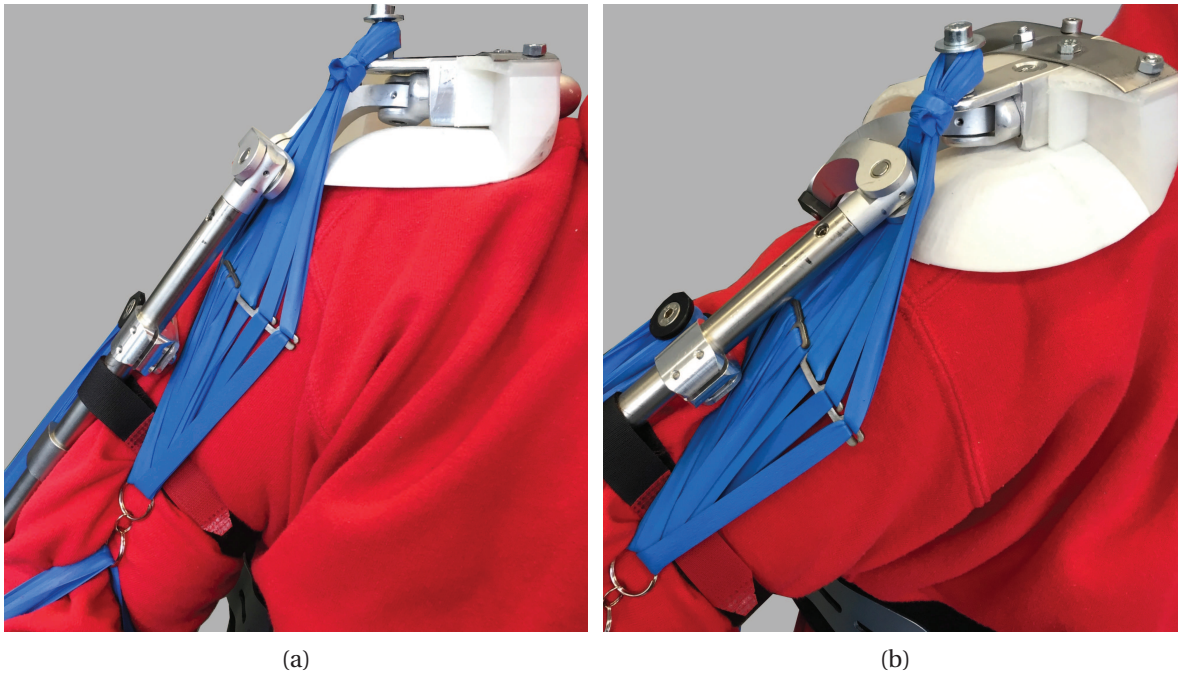


Figure 12.11: Detailed view of the top spring. When the spring is positioned below the shoulder arc mechanism, the abduction movement is limited, because the balancing quality is affected by the interference of the shoulder mechanism with the springs (b).

The extra attempts that were made to improve the appearance, safety and comfort (the in-plane attachment points, shoulder cover, sideways stability pad, and the anatomically shaped forearm interface) worked good. Due to the attachment points that were in-plane with the links, the whole system was closer to the body. The sideways stability pad and the anatomically shaped forearm interface were comfortable and prevented the user to fall to the side, or prevented the forearm to fall out of the device. The sideways stability pad even gave some support to the user to sit in straight up. The shoulder cover protected to user from getting pinched by the shoulder arc mechanism. However, because it is important that the (virtual) top spring can run in a straight line from the attachment point above the shoulder to the forearm, a cover at the front of the shoulder is not allowed. For some poses of the arm, the shoulder arc mechanism still interfere with the springs. This affect the balancing quality of prevent the user to make a smooth movement to that pose. The effect on the balancing quality needs be measured and validated with DMD patients.

Because the spring configuration is very close to the body, the forces that are introduced by the spring on the structure are also large. This introduces large stresses in the structure. For this particular prototype, the shoulder attachment point was rotated due to the large forces. For a correct balancing quality, it is important that the shoulder attachment point is horizontally aligned (as shown in Fig. 12.11a).

Evaluation of this prototype on comfort was only done by a healthy subject, who was wearing the device for one hour. Due to time limitations, this prototype was not evaluated in a lab environment, where the balancing quality could be measured with sEMG

activity and range of motion measurements. For a profound validation of the spring configuration, the arm support with the spring configuration should be tested in a lab environment to test the balancing quality and the range of motion, and in a home situation, where a patient can test the device during activities of daily living.

12.5. CONCLUSIONS

THE goal of this paper was to implement and evaluate two close-to-body spring configurations in a prototype of a mobile arm support. The spring configurations were: 1) a 2-parallel-springs configuration, with two bi-articular springs that run from the trunk to the forearm, parallel to the upper arm, and 2) a 3-springs configurations, with a bi-articular spring from the shoulder to the forearm, and two mono-articular springs running from the upper arm to the trunk and forearm, respectively. With a technique to split the springs into multiple springs, hollow spring structures were created, that correspond with a virtual spring. These hollow spring structures were used to design the spring configurations around the upper arm and shoulder. Splitting the springs into V-shaped and X-shaped springs resulted in multiple attachment points that were located at feasible locations on the trunk and the forearm. To make the mobile arm support even more close to the body, the attachments points on the arm links were placed in the same plane as the links. A shoulder cover and, an anatomical forearm interface and sideways stabilization pads were used to increase safety and comfort and give more support to the body.

REFERENCES

- [1] M. Kohler, C. F. Clarenbach, C. Bahler, T. Brack, E. W. Russi, and K. E. Bloch, *Disability and survival in Duchenne muscular dystrophy*, Journal of Neurology, Neurosurgery & Psychiatry **80**, 320 (2009).
- [2] T. Rahman, W. Sample, R. Seliktar, M. Alexander, and M. Scavina, *A body-powered functional upper limb orthosis*, Journal of rehabilitation research and development **37**, 675 (2000).
- [3] A. Kumar and M. F. Phillips, *Use of powered mobile arm supports by people with neuromuscular conditions*. Journal of rehabilitation research and development **50**, 61 (2013).
- [4] P. N. Kooren, A. G. Dunning, M. M. H. P. Janssen, J. Lobo-Prat, B. F. J. M. Koopman, M. I. Paalman, I. J. M. de Groot, and J. L. Herder, *Design and pilot validation of A-gear: a novel wearable dynamic arm support*, Journal of NeuroEngineering and Rehabilitation **12**, 1 (2015).
- [5] A. G. Dunning and J. L. Herder, *A review of assistive devices for arm balancing*, International Conference on Rehabilitation Robotics , 6650485 (2013).
- [6] R. Gopura, K. Kiguchi, and D. S. V. Bandara, *A brief review on upper extremity robotic exoskeleton systems*, IEEE International Conference on Industrial and Information Systems **8502**, 346 (2011).

- [7] A. G. Dunning and J. L. Herder, *A Close-to-Body 3-Spring Configuration for Gravity Balancing of the Arm*, International Conference on Rehabilitation Robotics , 464 (2015).
- [8] J. L. Herder, *Energy-free systems: theory, conception, and design of statically balanced spring mechanisms* (dissertation, 2001) p. 268.
- [9] B. M. Wisse, W. D. van Dorsser, R. Barents, and J. Herder, *Energy-free adjustment of gravity equilibrators using the virtual spring concept*, International Conference on Rehabilitation Robotics , 742 (2007).

IV

DISCUSSION AND CONCLUSIONS

13

DISCUSSION AND CONCLUSIONS

In this chapter, the accomplishments of this dissertations, as described in previous chapters, are evaluated and discussed. The general results are discussed and conclusions are drawn and directions for future research are proposed.

13.1. DISCUSSION

THE main goal of this dissertation was to develop a wearable, passive dynamic arm support that is inconspicuous and provides range of motion that is needed to perform important activities of daily living (ADL). Considering the individual requirements of the arm support, it can be stated that this goal is almost achieved, but very hard to achieve completely.

It was found that most important factor for the design of a close-to-body arm support is adjustability. Every user has different wishes and perception on comfort and the amount of support that is needed. For example, not every user wants perfect balancing of the arm. Sometimes this is perceived as uncomfortable and not intuitive. Another key issue is that errors are introduced by misalignment of the spring attachment locations and hysteresis and almost linear behavior of the rubber bands that are used, as well as the interference with the body or clothes. Therefore, designing a generic device that fits a large group of patients is very hard. The patients group of Duchenne muscular dystrophy (DMD) is small and only a few subjects are available to perform experiments. This makes it hard to perform statistical analysis and to design a generic device that does not need adjustment. Therefore, it is important to design an arm support and a spring configuration that is highly adjustable to the needs of the user. With a highly adjustable spring configurations and arm support, the needs of every user can be satisfied, and the errors in the system can be reduced. The 3-springs configuration developed in this dissertation is highly adjustable and allows for close-to-body placement. The balancing force can easily be adjusted to the preferences of the user during the day. This can be done by adjusting the spring attachment locations, but easier is to adjust the stiffness of the springs (number of rubber bands) in the device.

During evaluation of the Passive A-Gear prototypes it was observed that a trade-off between all the requirements of an arm support is needed. The different aspects of this trade-off are now discussed.

The inconspicuousness of the arm support is hard to achieve at certain locations in the workspace. This is particularly due to the amount of space consumed by the device right above the shoulder of the wearer. For the proposed spring system, a spring attachment vertically above the shoulder is needed. Also some space is needed for the shoulder arc mechanism to provide the required range of motion. To prevent the spring from interfering with the shoulder arc mechanism and with the human shoulder, the spring attachment should be at least about 30mm above the shoulder. Locating it closer to the body results in reduced balancing quality. In general, it was observed that a design that is closer to the body causes more difficulties in aligning the device to the body of the user, while at the same time comfort is maintained. Closer to the body also means that more errors are introduced by the spring system. Springs are forced into certain position that do not correspond with the pose of the arm, or springs interfere with the body. A trade-off must be made by the designer and the end-user between an arm support that has good balancing quality and range of motion, but which is not inconspicuous at certain locations (mainly above the shoulder), and an arm support that is more inconspicuous with less range of motion and less balancing quality.

Another trade-off that was made is on the structure of the device. Since the users with DMD have little muscle force in their arms, they need good balancing quality in order to

encourage them to use the arm support. Therefore, it is important that the spring configuration does not exert large moments and forces to the body except for the balancing force. To reach this, it is important that the spring attachment points are located in-line with the axis of the upper arm and forearm. The springs were split to each side of the arm. At the forearm, this is not a problem as it was designed in the prototype. For the upper arm however, the spring attachments should be attached on the upper arm link. To prevent the spring attachment next to the upper arm link from protruding too much, it is necessary to design the upper arm link such that it creates space for the spring attachments. This can be done by bending the upper arm link. However, when combining the passive arm support with actuators to create an active arm support, the actuators to drive the elbow joint and one shoulder joint are hard to locate inside a curved upper arm link. A trade-off should be made between the amount of inconspicuousness and the balancing quality when a straight upper arm link is required for the actuators. In this dissertation, the trade-off was made to use straight upper arm links to allow the placement of actuators (towards an Active A-Gear), and consequently be less inconspicuous.

A trade-off was also observed in the use of compliant structures. A feasible design of compliant structures as force transmission structure and as spring elements was not found. Although the prototypes were very promising in terms of balancing quality and inconspicuousness, the tuning possibilities and the range of motion of the arm fitted with these devices was limited. As a first concept, bending beams were used to balance the upper arm. The main limitation of these bending beams was that the arm can only be balanced in a single vertical plane. For some ADL it is sufficient to have support in a single vertical plane. But to be able to perform different ADL, it is necessary to have support in planes that are orientated differently. When the compliant structure is extended to the forearm, more limitations are introduced. Although a compliant structure can compensate for gravity of the forearm in a single plane, it is limited in compensating for gravity in different planes. For example, when a compliant elbow joint is able to balance the forearm for elbow flexion and extension in the vertical plane, the same compliant elbow joint would also exert a moment on the elbow when the forearm acts in a horizontal plane and the elbow would be flexed. In addition to the limited range of motion of the arm, compliant structures are hard to adjust for manufacturing errors or to tune to the preference of the user. These limitations are the cause that the use of compliant structures, as designed in this dissertation, were found not applicable in an arm support without the need of extra mechanisms (and volume) to overcome these limitations. A trade-off can be made for the different advantages and disadvantages of compliant structures. For example, it is possible to design a device that is very inconspicuous, but only balances the arm in a certain plane. To apply compliant structures in an arm support with the required range of motion, a different approach is needed. The current approach of 2D compliant structures that bend in a single plane is not sufficient. Therefore, a 3D approach where the compliant structure bends in multiple planes, with a predefined characteristic of the moment that will be exerted on the human joints, is valuable to investigate. This approach is elaborated in the *Shellmech* project of Flexension.

The use of rubber bands as spring elements is another trade-off that was made. The application of rubber bands is needed to be able to balance the arm with the spring

configurations applied in the Passive A-Gear prototypes that were developed in this dissertation. Other than steel helical springs, rubber bands allow strain rates up to 350% with almost linear and zero-free-length behavior between 150% and 350%, with hysteresis of less than 10%. The rubber bands are used in the almost linear range. For some of the springs in the developed spring configurations this meant that a couple of bands needed to be knotted to each other. This knot has influence on the stiffness of the rubber band. Therefore, it would be better and also more elegant to have rubber bands or sheets with the right length and material properties. The hysteresis and the nearly linear behavior also cause small error in the balancing quality.

Hollow spring structures were created by splitting the springs. These hollow structures were formed around the body of the user, while the spring characteristics were maintained. This makes the spring more compliant and comfortable when it interferes with the body, and it is also very inconspicuous for most of the movements of the arm. However, for some movements (like open or close a zipper), the hollow structure did not fully align with the body. For some extreme positions of the arm this hollow structure is protruding from the body. This has not been evaluated underneath clothing. Underneath clothing, it could be that the structure is forced to stay aligned with the body. On the other hand, it could also be that the balancing quality is affected by the clothes, since the spring is forced into a position that does not correspond with the pose of the arm.

Although a trade-off should be made between mainly the inconspicuousness of the device and the balancing quality, the second and third version of the Passive A-Gear fulfills the requirements of wearability and range of motion. The device is wearable and allows for wearability underneath clothing. The arm support is easy to don and doff, it is possible to change chairs, and it is comfortable to wear the device during the day. The dynamic range of motion of the arm support is enough to be able to perform the most important ADL. The important activities that the user is able to perform with the device are: eating and drinking, using a keyboard, mouse, or a game controller, opening a package, getting dressed, managing a wheelchair, washing the body and face, writing, reading books, lifting heavy object (if they have enough residual muscle force), scratching top of the head, hugging somebody, and reaching for a high object (up to 90° elevation angle). Activities where the arm needs to go to the back, like reaching the back pocket of jeans, cannot or not completely be performed.

Opportunities for future research are to apply 3D compliant structures in the arm support to replace the spring configuration and possibly some joints that are voluminous in the current design. More research can also be done to find or develop rubber bands or sheets with the right characteristics. It could be very interesting to apply this developed knowledge in other types of assistive devices, like a support for the legs to support patients (with DMD) during walking or standing. Besides that, the developed arm support could also be used by other users that could benefit from a passive arm support, like patients with stroke, spinal cord injury, or SMA. Even people with Parkinson can benefit from an arm support. The friction in the device and the hysteresis in the rubber can damp the shaking effects. Even healthy persons can benefit from a passive arm support. For example, people who perform a lot of work with their arms above their head. Lifting the arms with an arm support reduces the physical load. Increasing the balancing force helps to lift heavy objects.

13.2. CONCLUSIONS

- None of the current dynamic arm supports are wearable and passive, support the arm in its complete range of motion and fit underneath clothing.
- Three prototypes for passive arm supports (named as Passive A-Gear in this dissertation) were built and evaluated.
- Passive A-Gear version 1 introduced trunk motion capability. This was perceived by DMD patients as very important. The balancing quality was similar to an arm support that is mounted to a wheelchair. The total range of motion increased with 10%, and the user is able to reach 50% further anteriorly.
- Passive A-Gear version 2 introduced a new kinematic architecture and a new spring configuration. The kinematic architecture follows the body contour, and has the same degrees of freedom as the human arm (3DoF at the shoulder, 1DoF at the elbow). It has only 2 links next to the arm, and less mass. This architecture results in less singular positions of the device and is visually closer to the body. A new spring configuration with only 2 rubber springs balances the arm in its complete range of motion. A quantitative measurement protocol was developed and showed only 6% error with respect to the required balancing force.
- Passive A-Gear version 3 showed a new spring configuration with 3 rubber bands. This spring configuration is fully adjustable and can be located very close to the body. Additionally, it has a similar balancing quality as the spring configuration in the Passive A-Gear version 2. The device fits within 30mm from the body, where the device is not optimized to the dimensions.
- The 3-springs configuration is adjustable to the preferences and wishes of the user. The balancing force can be adjusted easily to different preferences during the day.
- Rubber bands are used as springs. These rubber bands have zero-free-length and linear behavior in the range between 150% and 350% strain. The hysteresis in the rubber bands is not larger than 10%.
- With the close-to-body Passive A-Gear (version 2 and 3), the users are able to perform most of the important activities of daily living. Those are: eating, drinking, using a keyboard / mouse / game controller, opening a package, getting dressed, managing a wheelchair, washing body and face, writing, reading books, lifting heavy object (if they have enough residual muscle force), scratching top of the head, hugging somebody, and reaching for a high object (up to 90° elevation angle). Activities where the arm needs to go to the back, like reaching the back pocket of jeans, cannot or not completely be performed.

V

APPENDIXES

A

CHARACTERISTICS OF RUBBER BANDS

A.1. INTRODUCTION

IN the prototypes described in this dissertation (Chapter 10, 11, 12), rubber bands are used as elastic elements in stead of metal springs. The arm support can be more lightweight, more slender, and the elastic bands also give some compliancy when they interfere with the user. To provide a good balancing quality, the rubber bands need to be zero-free-length springs, where the spring force is proportional to the length [1] (Fig. A.1).

Different rubber bands were tested to determine the force-elongation behavior of the spring. The rubber bands that had the least hysteresis, approached the zero-free-length behavior the best, and were readily available on the market were Synthetic Polyisoprene rubber bands (Jaeco Othopedic, USA). As stated in Chapter 11, this rubber band behaves like a zero-free-length spring between 150% and 400% elongation. In this appendix the behavior of the rubber bands is elaborated in more detail.

A.2. EXPERIMENTAL SETUP

IN Fig. A.2, the tensile test bench is shown. The rubber bands were attached to a force sensor (FUTEK LSB200, resolution: 10mV, range: 0-44.5N) with both sides and wrapped around a rod that was positioned 40mm (half of the length of the rubber band) from the force sensor. With a linear stage (Physik Instrumente M-505.4DG, resolution: 0.05 μ m, travel range: 107mm), the spring was elongated to 280mm total length (350%). To measure the hysteresis in the rubber bands, each measurement was done 3 times forwards and backwards (elongation and relaxation).

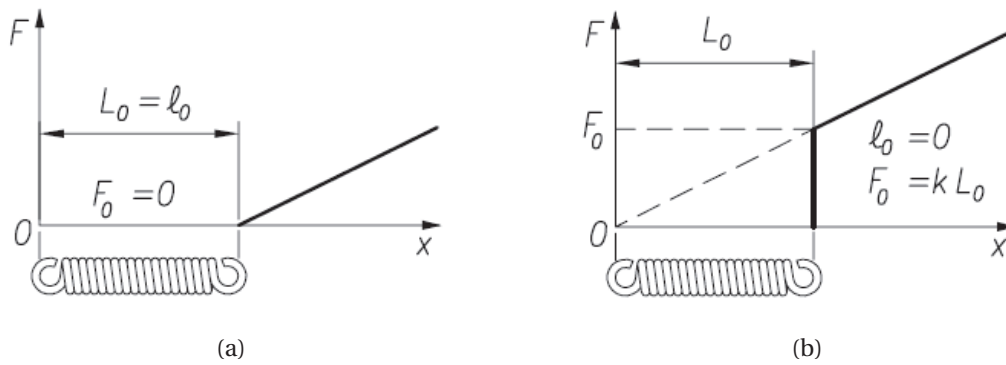


Figure A.1: (a) A normal spring, where the spring force is proportional to the elongation. (b) A zero-free-length spring, where the spring force is proportional to the length, extracted from [1] (with permission).

A.3. EVALUATION

THE behavior of the rubber bands was evaluated during time, and for different preloading conditions. The springs were preloaded to 150%, 250%, 350% and 450%. For each preloading condition, the spring was measured after 1 hour, 3, 4, 5, 22, and 26 hours. The intraclass correlation coefficient (ICC) (two-way mixed, average measure, ICC(3,k)) was determined for rubber band for each condition. The ICC indicates correlation between different sets of measurements. The higher the value, the more the measurements are consistent and correspond to each other. The ICC was determined for the relation between the average force-elongation characteristic and a linear reference line that corresponds with ZFLS behavior ($ICC_{refline}$), and for the correlation in between the repetitions ($ICC_{betweenreps}$).

A.4. RESULTS

IN Fig. A.3 - A.6, the results of the measurements (average and standard deviation) and the values of the ICCs are shown for the four different preloading conditions.

In Fig. A.7, the results are shown for the measurements of four preloading conditions after 3 hours of preloading. Only these results are shown, because the results for a longer preloading time are similar.

A.5. DISCUSSION AND CONCLUSIONS

THE results show very high values of the ICC for both the correlation between repetitions and the correlation between the average force-elongation characteristic and a linear reference line that corresponds with ZFLS behavior. This means that the characteristic of the rubber bands does not change for different preloading conditions and during time. The behavior of the rubber bands is very consistent during time and the amount of preloading does influence the behavior. It also means that the force-elongation characteristic is very similar to the linear reference line, with a stiffness between 84N/m and 91N/m for a range between 150% and 350% elongation. The creep and hysteresis in this range is small. The hysteresis is not larger than 10%. The rubber bands have ZFLS

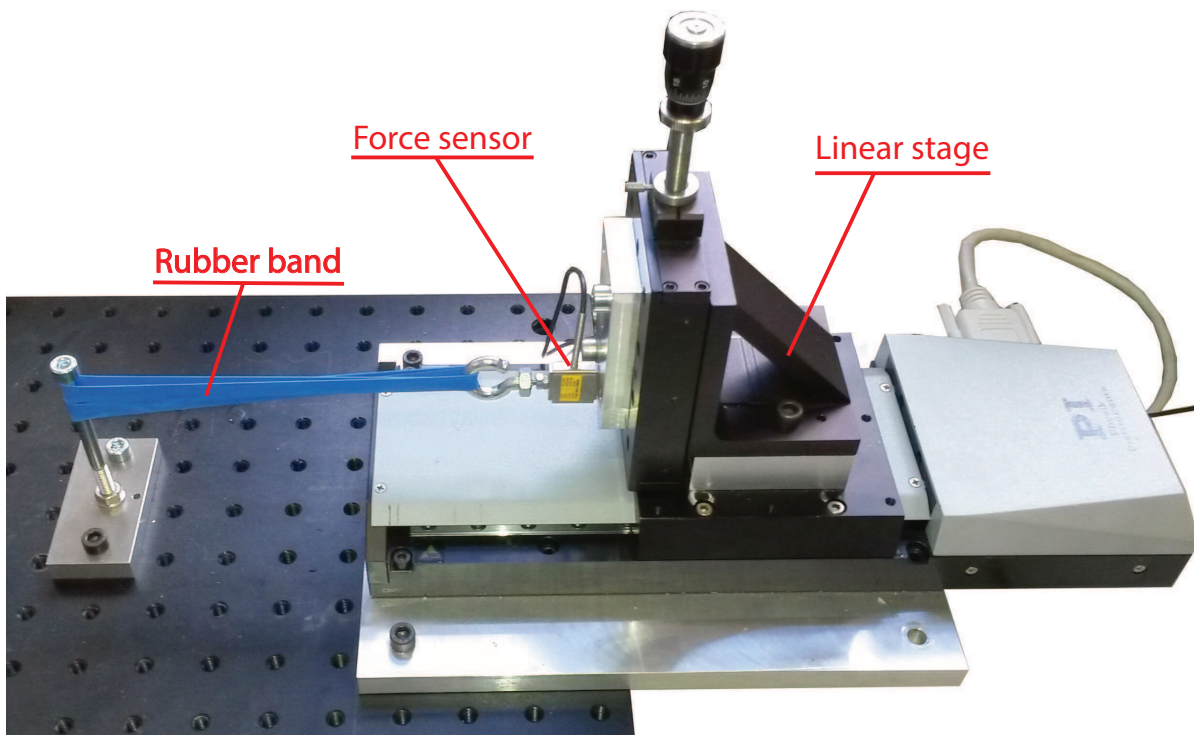


Figure A.2: Experimental setup for tensile tests of rubber bands.

behavior and can be used to provide good balancing quality to spring systems where such springs are required.

REFERENCES

- [1] J. L. Herder, *Energy-free systems: theory, conception, and design of statically balanced spring mechanisms* (dissertation, 2001) p. 268.

A

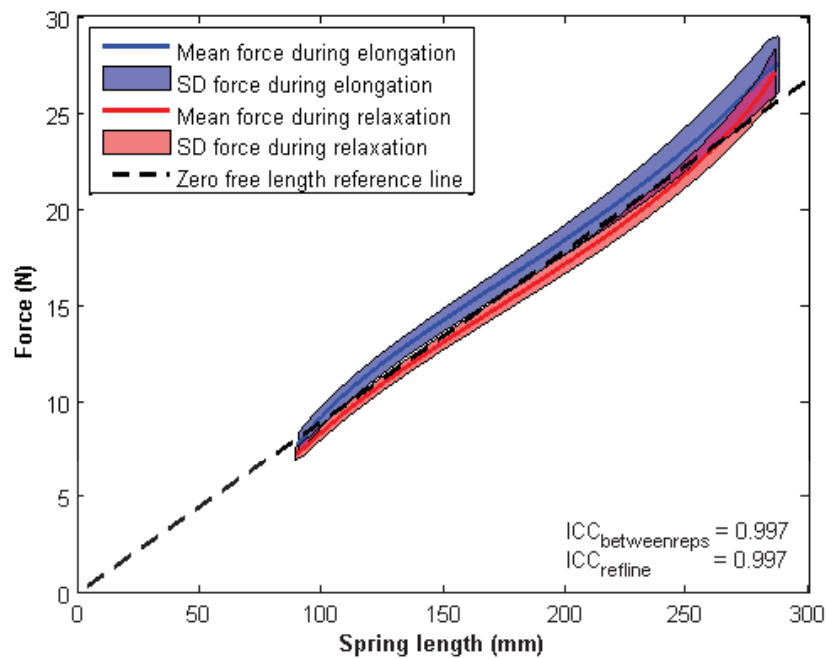


Figure A.3: Characteristics of the rubber bands with 150% preloading, measured after different preloading times. The mean and standard deviation of the force during elongation (blue) and relaxation (red) are shown. The black dotted line indicates the linear reference line that corresponds with ZFLS behavior.

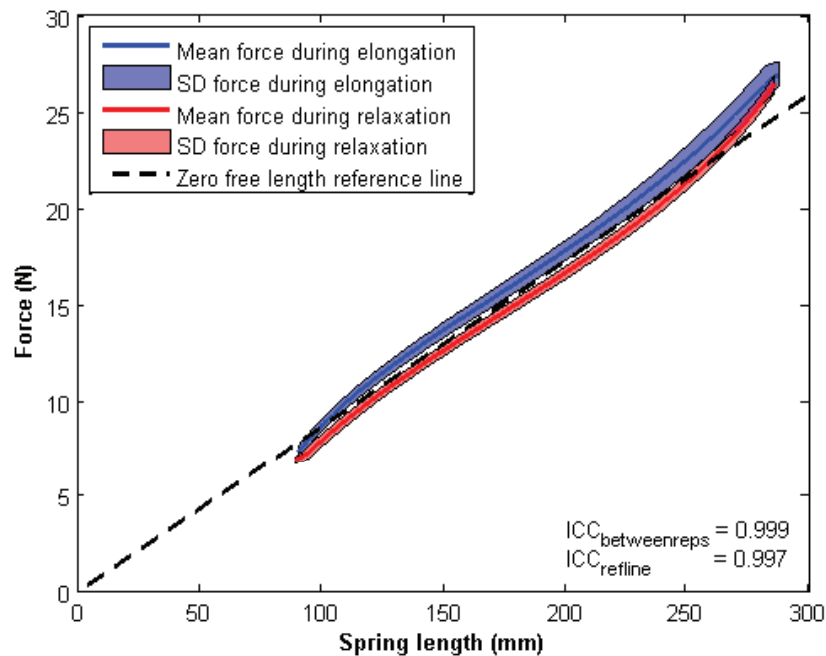


Figure A.4: Characteristics of the rubber bands with 250% preloading, measured after different preloading times. The mean and standard deviation of the force during elongation (blue) and relaxation (red) are shown. The black dotted line indicates the linear reference line that corresponds with ZFLS behavior.

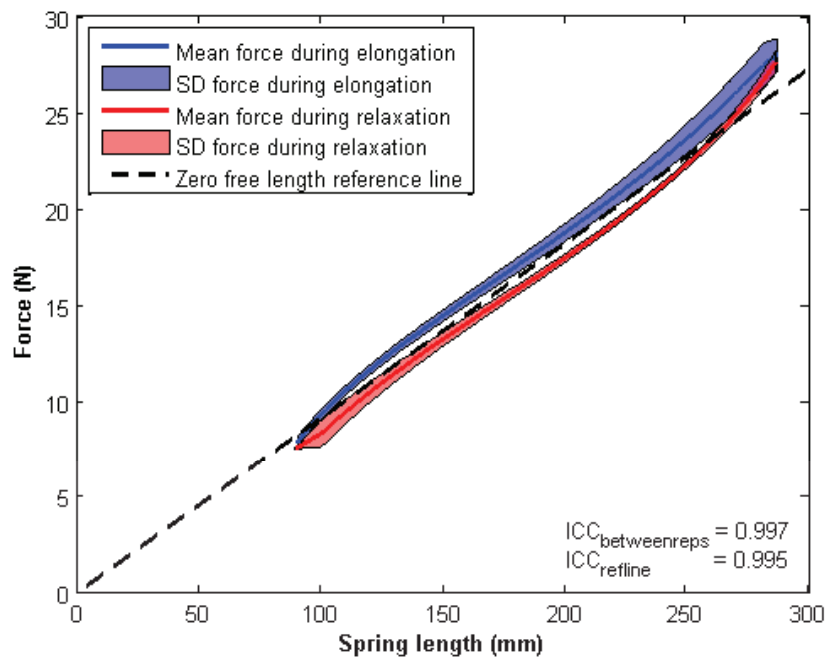


Figure A.5: Characteristics of the rubber bands with 350% preloading, measured after different preloading times. The mean and standard deviation of the force during elongation (blue) and relaxation (red) are shown. The black dotted line indicates the linear reference line that corresponds with ZFLS behavior.

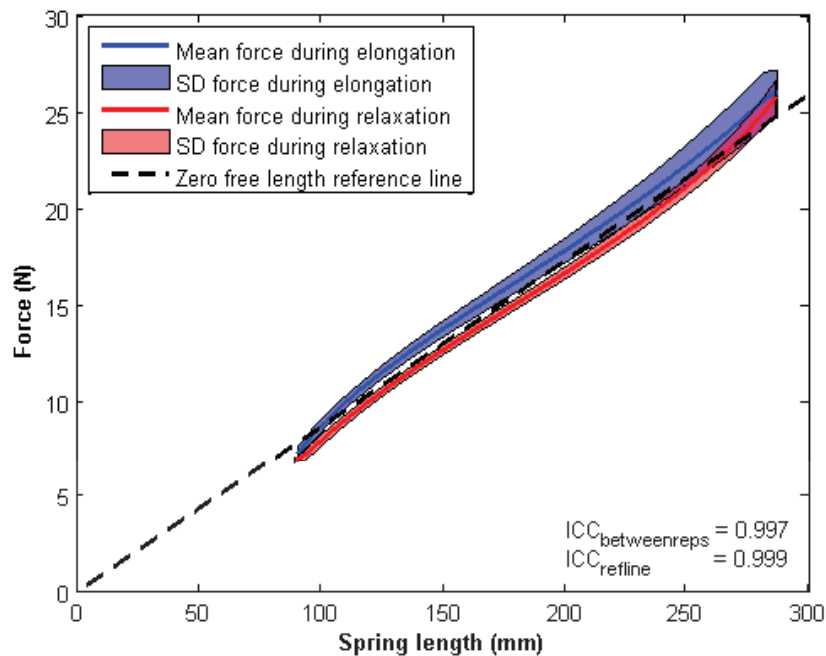


Figure A.6: Characteristics of the rubber bands with 450% preloading, measured after different preloading times. The mean and standard deviation of the force during elongation (blue) and relaxation (red) are shown. The black dotted line indicates the linear reference line that corresponds with ZFLS behavior.

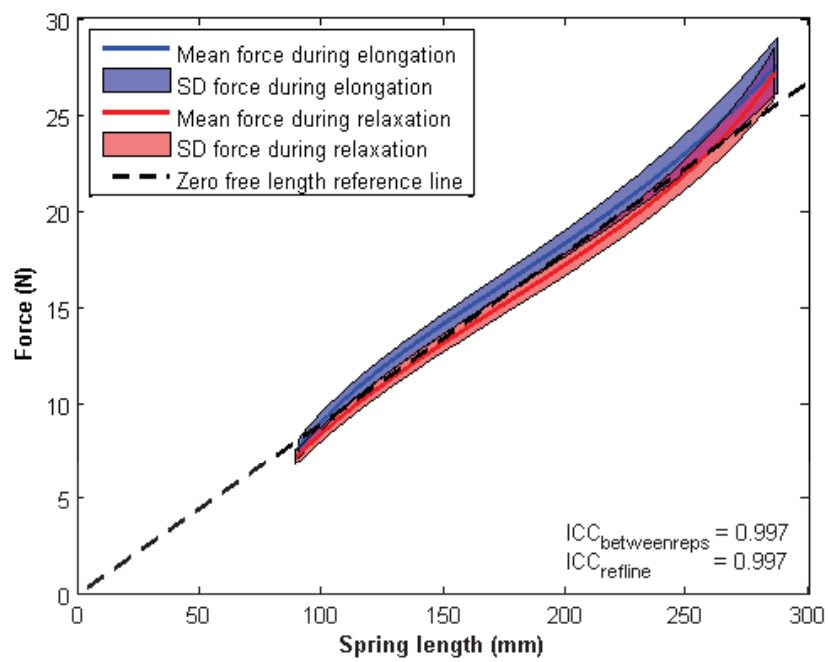


Figure A.7: Characteristics of the rubber bands with different preloading conditions, after a preloading time of 3 hours. The mean and standard deviation of the force during elongation (blue) and relaxation (red) are shown. The black dotted line indicates the linear reference line that corresponds with ZFLS behavior.

B

SHOULDER ARC MECHANISM

B.1. INTRODUCTION

THE shoulder arcs as described in [1] have an angle of 56° . The joint above the shoulder (joint 1, Fig. B.1) is tilted 10° posteriorly and medially. This is done to allow the human shoulder motion and to allow enough space for the elastic bands. However, the shoulder mechanism do not allow motion up to 90° elevation angle.

In this appendix the effect of changing the angle of the shoulder arcs and relocating of the joint 1 is investigated in order to find a better solution for the shoulder mechanism that allows for more range of motion and less singular positions.

B.2. VARYING THE ARC ANGLES

THE shoulder mechanism is elaborated in more detail. The shoulder mechanism is shown in Fig. B.1. When joint 1 is tilted posteriorly over and angle β (where β is the difference between the arc angles $\alpha_2 - \alpha_1$ plus an additional 10° to allow enough space for the shoulder arcs to not interfere with each other), joint 3 can be aligned vertically above the shoulder and even move further. This allows for elevation angles larger than 90° . For this research, it is considered that an elevation angle of 100° is required to perform the most important activities of daily living (Chapter 2) without reaching the limitations of the device. In order to relocate joint 1 posteriorly to allow larger elevation angles and to prevent singular positions of the shoulder mechanism, the angle of arc 2 (α_2) should be larger than the angle of arc 1 (α_1). This is also important to allow for horizontal abduction without having interference of arc 2 with the upper arm link (Fig. B.1c). The structure of the shoulder arcs gives a constraint to β . If β is too small, the shoulder arcs interfere with each other when joint 3 is positioned vertically above the shoulder (Fig. B.1a,b). Elevation angles up to 100° are not possible. In order to have enough space

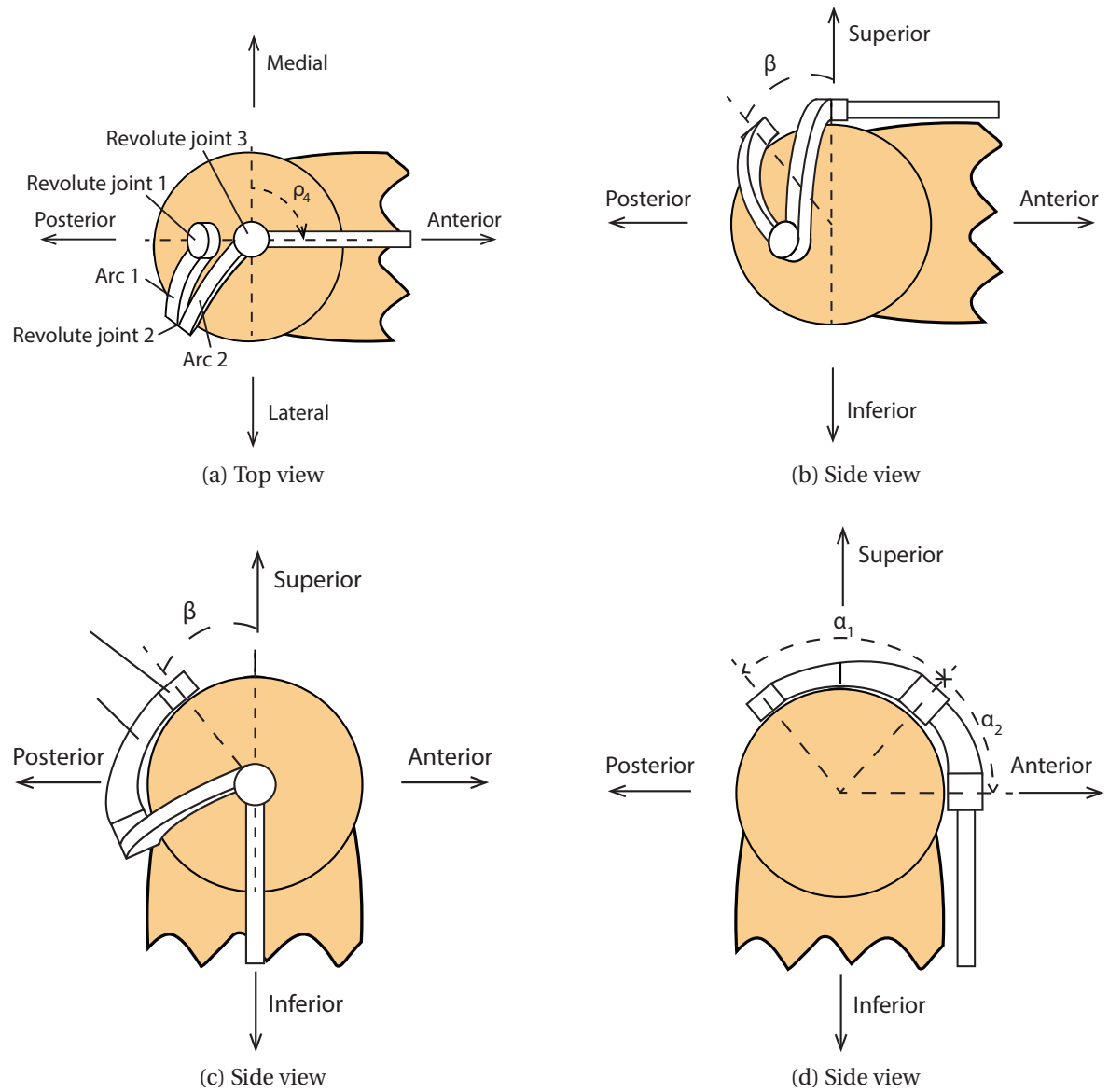


Figure B.1: View of different poses of the arm, with different orientations of the shoulder mechanism.

to allow this, joint 1 needs to be located more than 30° posteriorly.

To reach a position of the arm with an elevation angle of 0° (arm vertically down) and a shoulder rotation of $\rho_4 = 90^\circ$ (joint 3 is anterior of the shoulder) (Fig. B.1d), the sum of the arc angles ($\alpha_1 + \alpha_2$) needs to be larger than the $90^\circ + \beta$. Otherwise, the shoulder arcs are too short to reach this position without singularities. From this constraint and the previous constraint, it follows that α_1 needs to be larger than 50° but smaller than or equal to 60° and α_2 needs to be smaller than or equal to 80° .

Furthermore, for an angle of the arcs larger than 90° , the arcs interfere with the shoulder or upper arm. So the arc angles should always be smaller than 90° . This also limits the location of joint 1. When the sum of α_1 and β is larger than 90° , arc 1 can also interfere with the shoulder. Next to that, when α_1 is large it becomes more difficult to cover this arc and protect the user from getting pinched by the shoulder mechanism.

The constraint rules are summarized below:

- $\alpha_2 > \alpha_1$
- $\alpha_1 + \alpha_2 > 90^\circ + \beta (= \alpha_2 - \alpha_1 + 10^\circ) \rightarrow \alpha_1 > 50^\circ$
- $\alpha_1 + \beta \leq 90^\circ \rightarrow \alpha_2 \leq 80^\circ$
- $\beta \geq 30^\circ \rightarrow \alpha_1 \leq 60^\circ$
- $\alpha_1 \leq 90^\circ$
- $\alpha_2 \leq 90^\circ$

In Table B.1, an overview is shown for different angles of both shoulder arcs. The angles for each arc were varied from 10° to 90° , in steps 10° . The constraint rules that were determined were applied to the table. Were the constraint rules were not satisfied, an x is marked as an impossible solution. It can be seen that only one solution is possible within the constraint rules.

		α_1								
		10°	20°	30°	40°	50°	60°	70°	80°	90°
α_2	10°	x	x	x	x	x	x	x	x	x
	20°	x	x	x	x	x	x	x	x	x
	30°	x	x	x	x	x	x	x	x	x
	40°	x	x	x	x	x	x	x	x	x
	50°	x	x	x	x	x	x	x	x	x
	60°	x	x	x	x	x	x	x	x	x
	70°	x	x	x	x	x	x	x	x	x
	80°	x	x	x	x	x	o	x	x	x
	90°	x	x	x	x	x	x	x	x	x

Table B.1: Overview of the combinations of arc angles for the first angle (α_1) and second angle (α_1). The determined constraint rules are applied, and only one combination is feasible to satisfy the constraint rules.

B.3. CONCLUSIONS

THE goal of this research was to vary the arc angles and relocate the joint that connects the shoulder arc mechanism with the fixed world, in order to find a shoulder arc mechanism that allows for elevation of the arm up to 100° and is able to perform the most important activities of daily living without singularities. There is only one feasible combination of shoulder arc angles that allows this. The angle of the first arc (that is connected to the fixed world) needs to be 60° . The angle of the second arc (that is connected to the upper arm link) needs to be 60° . The location of the joint that connects the first arc to the fixed world is tilted 30° posteriorly with respect to the vertical axis through the shoulder joint.

REFERENCES

- [1] P. N. Kooren, A. G. Dunning, M. M. H. P. Janssen, J. Lobo-Prat, B. F. J. M. Koopman, M. I. Paalman, I. J. M. de Groot, and J. L. Herder, *Design and pilot validation of A-gear: a novel wearable dynamic arm support*, Journal of NeuroEngineering and Rehabilitation **12**, 1 (2015).

CONTRIBUTION TO EACH CHAPTER

Below, a short description of the contributions of the author is given for each chapter or article that is included in this dissertation.

Chapter 1: Introduction

The general goal and sub-goals of the A-Gear project were formulated in the project grant proposal. From the sub-goals, author focused and formulated the goal of this dissertation and wrote the body of this chapter.

Chapter 2: DMD, most important ADL and arm kinematics

Author wrote the body of this chapter. The figures about the range of motion were made by M.M.H.P. Janssen (Radboud medical center, Nijmegen, The Netherlands).

Chapter 3 (published article): State-of-the-art in arm supports

First author. Author wrote the article.

Chapter 4: Conceptual design

The content of this chapter is established in close collaboration with a multidisciplinary team, including DMD patients, project managers, physicians and developers of assistive devices. The concepts were elaborated by P.N. Kooren (VU medical center, Amsterdam, The Netherlands) and the author. Author wrote the body of the chapter.

Chapter 5 (published article): Bending beams for upper arm balance

First author. This article is the result of the MSc research of J.L. Stroo. Author was the daily supervisor of the student. After an extensive review, author elaborated the design in more detail and improved the body of the article.

Chapter 6 (published article): Compliant elbow joint actuated with shape memory alloy

Second author. This article is the result of the MSc research of J.G. Kleinjan. The initial concept idea was from the author. Author was the daily supervisor of the student and reviewed the article extensively.

Chapter 7 (1 published + 1 submitted article): Spring systems - technical analysis

Second author. This article is the result of the MSc research of M.P. Lustig. Author was the daily supervisor of the student and reviewed the article extensively.

Chapter 8 (published article): Spring systems - 3-springs configuration

First author. Author wrote the article.

Chapter 9 (to be submitted article): Spring systems - comparison of different spring configurations

First author. Author wrote the main body of the article. A part of the MSc research of M.P. Lustig, a MSc student of which the author was the daily supervisor, is included in this article.

Chapter 10 (submitted article): A-Gear Passive version 1

First author. Author did research into the conceptual design, the spring configuration to achieve the balancing quality, and validation of the prototype. Author wrote the main body of the article.

Chapter 11 (published article): A-Gear Passive version 2

Second author. Author did research into the conceptual design, the spring configuration to achieve the balancing quality, and validation of the prototype. Author partially wrote the design and discussion section.

Chapter 12 (to be submitted article): A-Gear Passive version 3

First author. Author did research into the application of the 3-springs configuration. The application of the 2-springs-parallel configuration was elaborated in the MSc research of M.P. Lustig, a MSc student of which the author was the daily supervisor. Author wrote the main body of the article.

ACKNOWLEDGEMENTS

This dissertation and this research would not have been finished without the help of others. I would like to thank all who contributed to this work and all that I worked or spend my time with the last couple of years. I would like to mention some people in particular.

I would like to start to thank Just Herder, my promotor and daily supervisor. I had the privilege to work with you for more than my PhD. I admired your supervision and advice. It was in such a positive way, that I always continued with more enthusiasm. I hope that we will do more projects and work together in the future. I would also like to thank Dick Plettenburg. I enjoyed the sessions with the DIPO lab. And Tariq Rahman, for hosting me at your lab in the A.I. duPont children hospital and providing me the opportunity to do research abroad and to see the great impact assistive devices have on very young children.

I would like to thank Peter, Joan and Mariska. I liked to work with you in a team on a daily base. Sometimes there were some ups and down, but at the end we always managed to deal with all issues. In addition, I have to thank Flextension with all their members. You gave me the opportunity to work on this project. I am happy that I got to know so many enthusiastic and dedicated people.

Many of the research was performed in cooperation with the students I supervised: Johan, Josella, Maarten, Jeanne, Thijs, Milos. I appreciate that I could be involved in your final year of your study. I think I can say that we both enjoyed our cooperation, and that we encouraged each other to perform at our best.

During my daily work at the university, I had the privilege to share the office with many great people. Next to the enjoyable working hours, we had great fun in during coffee breaks, competing each other with Meander or table football, drinks, and other lab outings. Thanks Nima, Juan, Guiseppe, Davood, Partice, Milton, Teun, Jos, Pieter, Lodewijk, Toon, Maarten, Rik, Jan, Sybren, Wout, Tom, Sjoerd, Josella, Asthor, Johan, and the others I probably forget.

A special thanks goes to Louise and Kevin Shaw. You made my time in the USA great. I am very happy that I could stay with you and be part of your family. Thanks for your hospitality, keep on doing that. I am sure we will meet again.

Finally, thanks to the people that I love most. My parents and family, for your endless support. And dad, after having 'ir' in front of my name and 'ing' at the end, this is it for the time being. To Marieke, for your support and feedback on me as a person. I hope that eventually we can enjoy our extra longs weekends again. And above all to the Lord, for giving me these blessings in life and the ability to work on this project.

CURRICULUM VITÆ

Alje Geert DUNNING

September 1, 1985

Born in Noordoostpolder, The Netherlands

1997-2003

VWO at Greijdanus College, Zwolle, The Netherlands

Profile: Nature & Technology and Nature & Health

2003-2011

B.Sc. Mechanical Engineering and M.Sc. Biomechanical Engineering at Delft University of Technology, Delft, The Netherlands

B.Sc. thesis: Rotational stiffness of the eye for redistribution of the orbital fat determined with Optical-Flow and MRI analysis.

M.Sc. thesis: Design of a zero stiffness six degrees of freedom compliant precision stage.

The graduation project was performed at Mapper lithography, Delft, The Netherlands.

2011-2015

Ph.D. candidate at Delft University of Technology, Delft, The Netherlands

Faculty of Mechanical Engineering, dept. of Biomechanical Engineering and Precision & Microsystems Engineering.

Topic: Slender spring systems, for a close-to-body dynamic arm support for people with Duchenne muscular dystrophy.

LIST OF PUBLICATIONS

JOURNAL ARTICLES

12. **A.G. Dunning**, M.P. Lustig, J.L. Herder, *Application of innovative spring configurations in the A-Gear, a close-to-body dynamic arm support*, Journal of Medical Devices, to be submitted (2016).
11. M.P. Lustig, **A.G. Dunning**, J.L. Herder, *Cartesian based stiffness matrix approach and graphical representation to statically balance serial linkages*, Mechanism and Machine Theory, to be submitted (2016).
10. **A.G. Dunning**, M.P. Lustig, J.L. Herder, *Evaluation and comparison of five spring configurations for balancing serial linkages without auxiliary links*, Mechanism and Machine Theory, submitted (2016).
9. **A.G. Dunning**, M.M.H.P. Janssen, P.N. Kooren, J.L. Herder, *Technical brief: Evaluation of an arm support with trunk motion capability*, Journal of Medical Devices, submitted (2016).
8. P.N. Kooren, **A.G. Dunning**, M.M.H.P. Janssen, J. Lobo-Prat, B.F.J.M. Koopman, M.I. Paalman, I.J.M. de Groot, J.L. Herder, *Design and pilot validation of A-gear: a novel wearable dynamic arm support*, Journal of Neuroengineering and rehabilitation **12**, 1 (2015).
7. M. Plooiij, **A.G. Dunning**, T. van der Hoeven, M. Wisse, *Statically Balanced Brakes*, Precision Engineering, in press (2015).
6. J.G. KleinJan, **A.G. Dunning**, J.L. Herder, *Design of a compact actuated compliant elbow joint*, International Journal of Structural Stability and Dynamics **14**, 1440030 (2014).
5. **A.G. Dunning**, N. Tolou, J.L. Herder, *A compact low-stiffness six degrees of freedom compliant precision stage*, Precision Engineering **37**, 380 (2013).
4. **A.G. Dunning**, N. Tolou, P.J. Pluimers, L.F. Kluit, J.L. Herder, *Bi-stable compliant mechanisms: correction for finite element modeling, preloading incorporation and tuning the stiffness*, Journal of Mechanical Design **134**, 084502 (2012).
3. **A.G. Dunning**, N. Tolou, J.L. Herder, *Review Article: Inventory of platforms towards the design of a statically balanced six degrees of freedom compliant precision stage*, Mechanical Sciences **2**, 157 (2011).

2. **A.G. Dunning**, A.M. van Ditten, K. de Vries, S. Ladde, S. Schutte, C.P. Botha, P. Wielopolski, H.J. Simonsz, *High-Resolution MRI of Horizontal Gaze Position for Improved Optical Flow Analysis*, *Investigative Ophthalmology & Visual Science* **50**, 661 (2009).
1. K. de Vries, A.M. van Ditten, **A.G. Dunning**, S. Ladde, S. Schutte, C.P. Botha, P. Wielopolski, H.J. Simonsz, *Validation of the Delft Finite Element Model of Orbital Mechanics*, *Investigative Ophthalmology & Visual Science* **50**, 658 (2009).

PEER-REVIEWED CONFERENCE ARTICLES

5. M.P. Lustig, **A.G. Dunning**, J.L. Herder, *Parameter analysis for the design of statically balanced serial linkages using a stiffness matrix approach with cartesian coordinates*, 14Th IFToMM World Congress (2015).
4. A.T. Steinþórsson, M. Aguirre, **A.G. Dunning**, J.L. Herder, *Review, Categorisation, and Comparison of 1DOF Static Balancers*, ASME International Design Engineering Technical Conferences & Computers and Information in Engineering Conference, DETC2015-47217 (2015).
3. **A.G. Dunning**, J.L. Stroo, G. Radaelli, J.L. Herder, *Feasibility Study of a Balanced Upper Arm Orthosis based on Bending Beams*, International Conference on Rehabilitation Robotics, 520 (2015).
2. **A.G. Dunning**, J.L. Herder, *A Close-to-Body 3-Spring Configuration for Gravity Balancing of the Arm*, International Conference on Rehabilitation Robotics, 464 (2015).
1. **A.G. Dunning**, J.L. Herder, *A review of assistive devices for arm balancing*, International Conference on Rehabilitation Robotics, 6650485 (2013).

PATENTS

- **A.G. Dunning**, J.L. Herder, J. Peijster, *Support structure for lithography system*, patent US20150014510 A1, WO 2013039401 A4 (2011).

BOOK CHAPTER CONTRIBUTION

- Entries to “Part Four: Library of Compliant Mechanisms,” in *Handbook of Compliant Mechanisms*, edited by L.L. Howell, S.P. Magleby, and B.M. Olsen, John Wiley & Sons (2012).

AWARDS

- Heidenhain Scholar, International Conference of the European Society for Precision Engineering and Nanotechnology, Stockholm, Sweden (2012).

OTHER ACADEMIC ACTIVITIES

- Visiting scholar, Nemours Alfred I. duPont Children Hospital, Wilmington, DE, USA (Apr-Jun 2015).

- Invited talk: **A.G. Dunning**, J.L. Herder, *Innovative spring configurations for close-to-body arm support*, International Conference on Rehabilitation Robotics, Singapore (2015).
- Invited talk: F.C.T. van der Helm, **A.G. Dunning**, H. Vallery, *Passive and active exoskeletons to enhance patients with neuromuscular diseases*, European Polio Conference, Amsterdam, The Netherlands (2014).
- Invited talk: **A.G. Dunning**, N. Tolou, J.L. Herder, *A Novel Constant Force Compliant Precision Stage to Balance a Load in Six Degrees of Freedom*, International Conference of the European Society for Precision Engineering and Nanotechnology, Stockholm, Sweden (2012).

Propositions

accompanying the dissertation

SLENDER SPRING SYSTEMS

FOR A CLOSE-TO-BODY DYNAMIC ARM SUPPORT
FOR PEOPLE WITH DUCHENNE MUSCULAR DYSTROPHY

by

Alje Geert DUNNING

1. Variability in wishes and perception of users is causing tension with a generic scientific approach (this dissertation).
2. Perfect balancing oftentimes is too much of a good thing (this dissertation).
3. Designing a dynamic arm support is like dealing with more equations than unknowns (this dissertation).
4. Designers should be more focused on the adaptability of assistive devices than that of the human.
5. Unlike rehabilitation exoskeletons do exoskeletons for daily use need to be anthropomorphic and anthropometric.
6. Engineers have to put that amount of effort in a design that they are unnecessary after completion of the product.
7. PhD research should not be routed by product development.
8. Perfection is oftentimes too much of a good thing.
9. Similar to arm supports, a passive bicycle is better to maintain fitness and health than a motorized bicycle.
10. As designer of compliant mechanisms, you should be more flexible than your design.

These propositions are regarded as opposable and defensible, and have been approved as such by the promotor prof. dr. ir. J.L. Herder.

Stellingen

behorende bij het proefschrift

SLENDER SPRING SYSTEMS

FOR A CLOSE-TO-BODY DYNAMIC ARM SUPPORT
FOR PEOPLE WITH DUCHENNE MUSCULAR DYSTROPHY

door

Alje Geert DUNNING

1. Variabiliteit in wensen en perceptie van gebruikers staat op gespannen voet met een generieke wetenschappelijke aanpak (dit proefschrift).
2. Perfecte balans is vaak te veel van het goede (dit proefschrift).
3. Het ontwerpen van een mobiele arondersteuning is als het omgaan met meer vergelijkingen dan onbekenden (dit proefschrift).
4. Ontwerpers moeten zich meer richten op het aanpassingsvermogen van hulpmiddelen dan dat van de mens.
5. Ingenieurs moeten zoveel inspanning in het ontwerp steken dat ze na oplevering van het product niet meer nodig zijn.
6. Anders dan revalidatie-exoskeletten moeten exoskeletten voor dagelijks gebruik antropomorf en antropometrisch zijn.
7. Promotieonderzoek moet niet worden opgejaagd door productontwikkeling.
8. Perfectie is vaak te veel van het goede.
9. Net als voor mobiele arondersteuning is een passieve fiets beter voor het behoud van conditie en gezondheid dan een gemotoriseerde fiets.
10. Als ontwerper van elastische mechanismen moet je flexibeler zijn dan je ontwerp.

Deze stellingen worden opponeerbaar en verdedigbaar geacht en zijn als zodanig goedgekeurd door de promotor prof. dr. ir. J.L. Herder.